Nitric oxide reactivity of copper(II) complexes with N-donor ligands: Development of NO sensors

A dissertation submitted to the
Indian Institute of Technology Guwahati as
partial fulfillment for the degree of
Doctor of Philosophy in Chemistry

Submitted by

Pankaj Kumar
(Roll No. 08612218)

Supervisor

Dr. Biplab Mondal

Department of Chemistry
Indian Institute of Technology Guwahati

February, 2013

Dedicated to my sister

Parvati

Statement

I hereby declare that this thesis entitled "**Nitric oxide reactivity of copper(II) complexes with N-donor ligands: Development of NO sensors**" is the outcome of research work carried out by me under the supervision of Dr. Biplab Mondal, in the Department of Chemistry, Indian Institute of Technology Guwahati, India.

In keeping with the general practice of reporting scientific observations, due acknowledgement has been made whenever work described here based on the findings of other investigators.

February, 2013 **Pankaj Kumar**

Certificate

This is to certify that Mr. Pankaj Kumar has been working under my supervision since December, 2008 as a regular Ph. D. student in the Department of Chemistry, Indian Institute of Technology Guwahati. I am forwarding his thesis entitled "**Nitric oxide reactivity of copper(II) complexes with N-donor ligands: Development of NO sensors**" being submitted for the Ph. D. degree.

I certify that he has fulfilled all the requirements according to the rules of this Institute regarding the investigations embodied in his thesis and this work has not been submitted elsewhere for a degree.

February, 2013 **Biplab Mondal**

Acknowledgements

First and foremost, I would like to thank my supervisor, a creative and outstanding scientist, Dr. Biplab Mondal for his numerous discussions, guidance and provided me the opportunity and resources to work on one of the most interesting field of the chemistry, nitric oxide reactivity and sensing. He always helped me to learn the chemistry, inspired me to do my best and I also appreciate his encouragement and confidence in me, making sure I am progressing along the forward path.

I would like to acknowledge my sincere gratitude to all my doctoral committee members Dr. Gopal Das, Dr. Shubhendu Sekhar Bag, Dr. Debasis Manna and former member, Dr Boomi Shankar, R. for their insightful advices and valuable suggestions. I am also grateful to the entire faculty and staff of the Department of Chemistry, Indian Institute of Technology Guwahati for providing a wonderful work atmosphere throughout this period.

I would like to thank my labmates Amardeep da, Moushumi didi, Rajib da, Apurba, Aswini, Vikash, Kanhu, Somnath, Hemanta, Kuldeep, Soumen, Sayantani and former labmates Neeraj, Satish, Madhav, Soham, Najmul, Narayani, Ivy, Pritam, Tulika, Debabrata, Gorachand and Pokhraj whom I had an opportunity to work with. No words can express my thankfulness for giving me their time and companionship, which made the time spent in the laboratory and outside pleasant and memorable.

I would like to give my special thanks to my friends Subhojit Das, Munendra Yadav, Sumit Chaturvedi, Rajesh Sharma, Anil Kumar and Abhijit Saha for their timely help, support and for the wonderful time we shared during this period.

The financial support from Council of Scientific and Industrial Research (CSIR), New Delhi for the research fellowship is duly acknowledged.

Finally, I would like to thank my parents, without their love and support this work would not have been completed. I am also thankful to my brothers, Khemkaran Koli and Mahesh Kumar Koli for their love and moral support during my research work.

I would like to thank my sister, Mrs. Puspa for her encouragement and support during my research work.

Finally, I would like to give my special thanks to my sister, Mrs. Parvati, she has been always a source of encouragement to me whenever I am in any problem. She is no more, but her memories always support me and give the strength to do my best.

February, 2013 **Pankaj Kumar**

CONTENTS

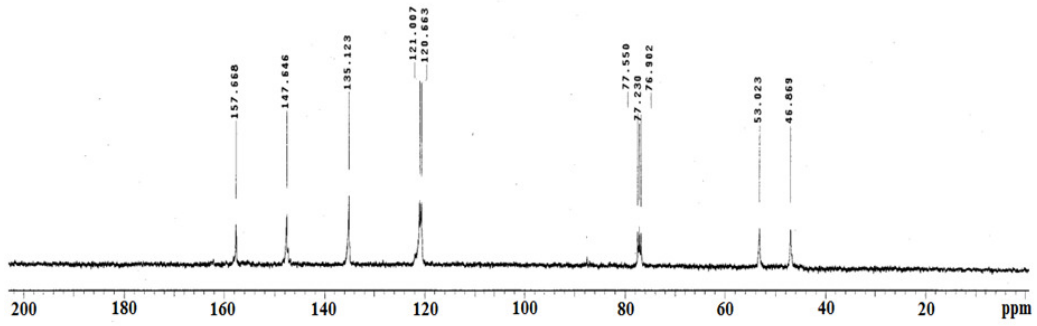

Figure A1.3 ^{13}C-NMR spectrum of $\mathbf{L_1}$ in $CDCl_3$.

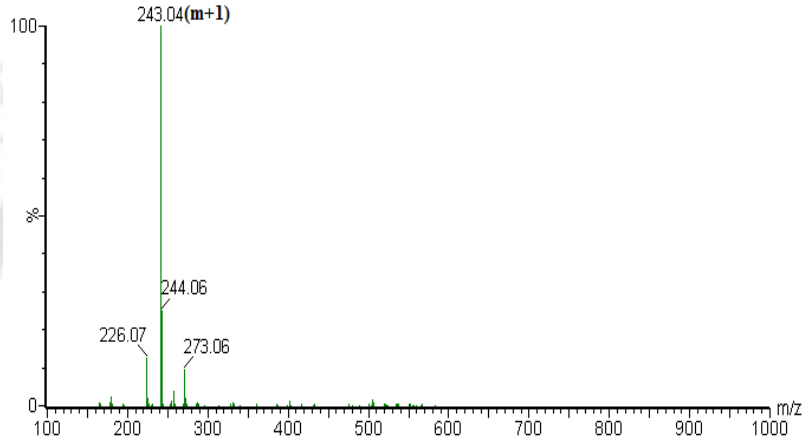

Figure A1.4 ESI-Mass spectrum of $\mathbf{L_1}$ in methanol.

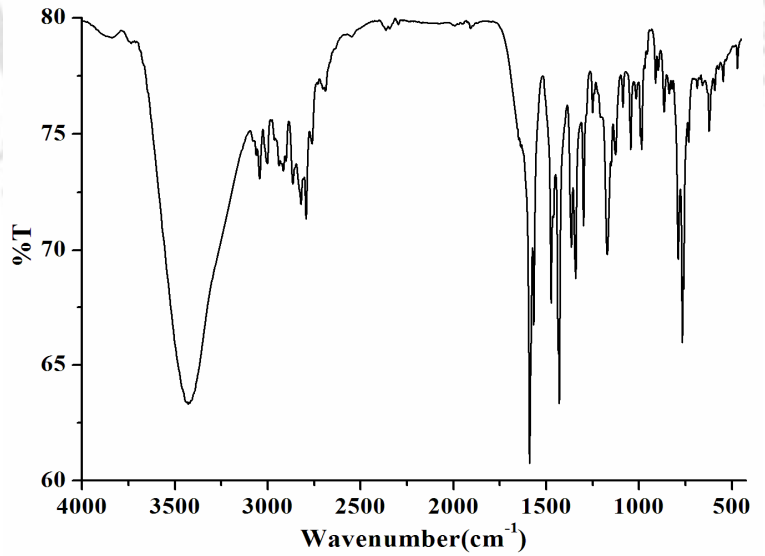

Figure A1.5 FT-IR spectrum of $\mathbf{L_2}$ in KBr pellet.

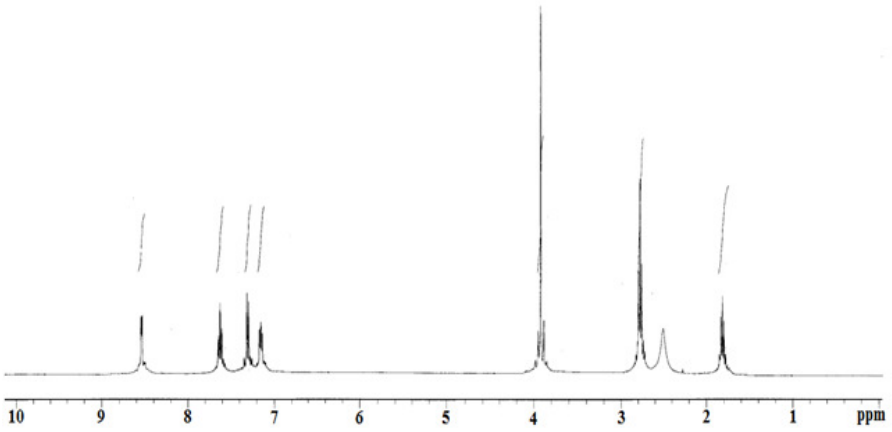

Figure A1.6 ^{1}H-NMR spectrum of **L_2** in $CDCl_3$.

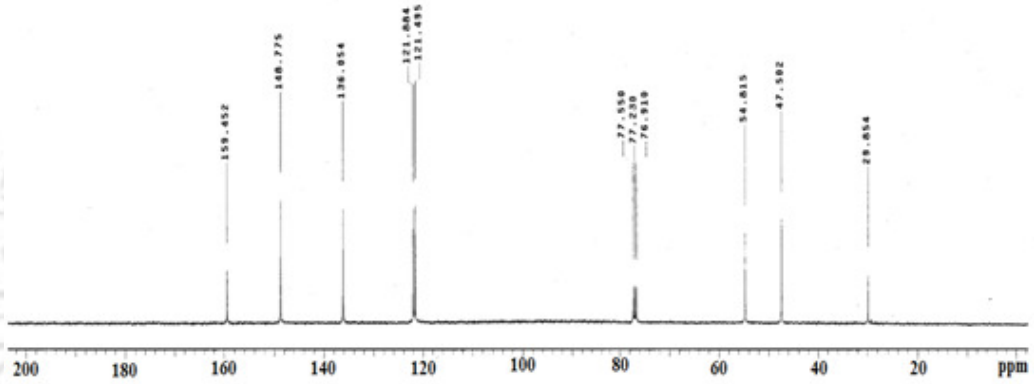

Figure A1.7 ^{13}C-NMR spectrum of **L_2** in $CDCl_3$.

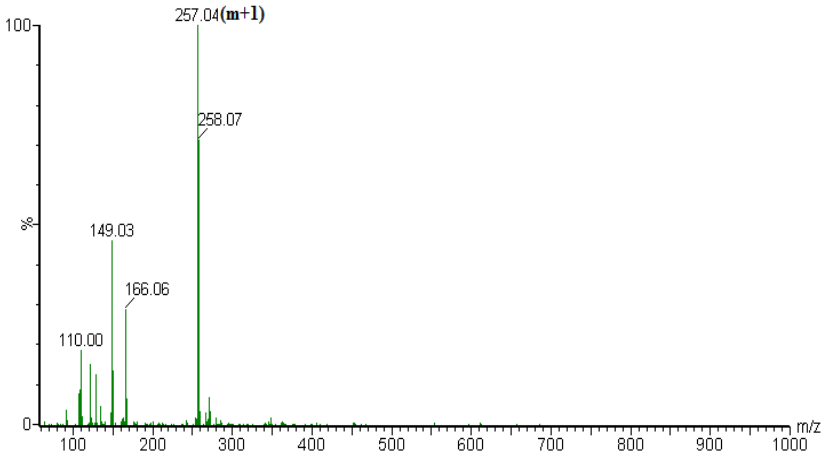

Figure A1.8 ESI-Mass spectrum of **L_2** in methanol.

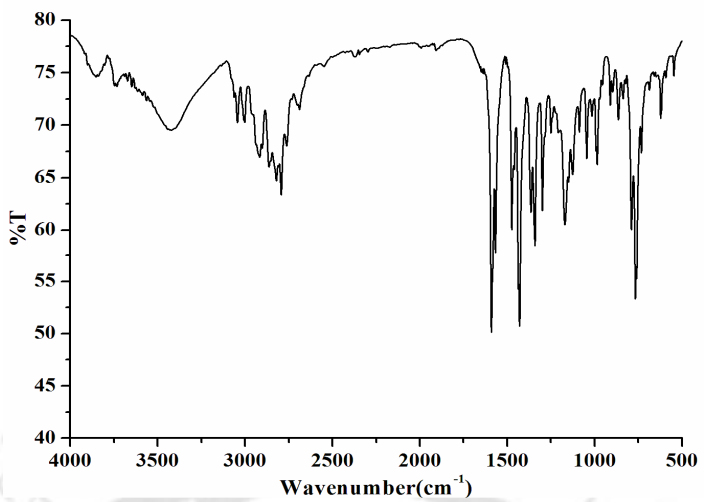

Figure A1.9 FT-IR spectrum of **L_3** in KBr pellet.

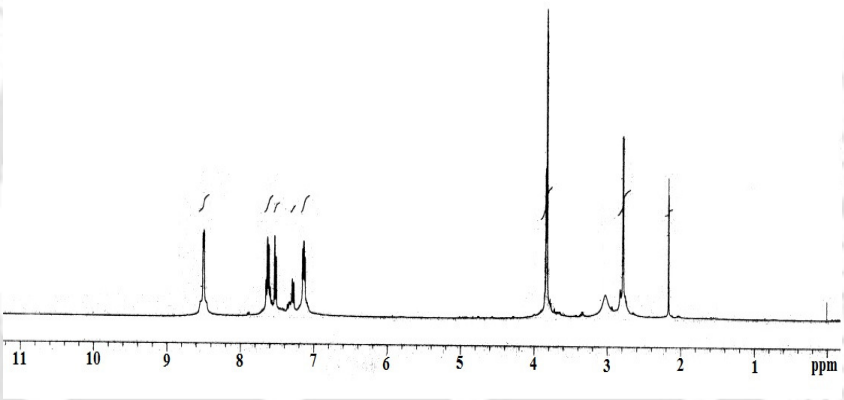

Figure A1.10 ^{1}H-NMR spectrum of **L_3** in $CDCl_3$.

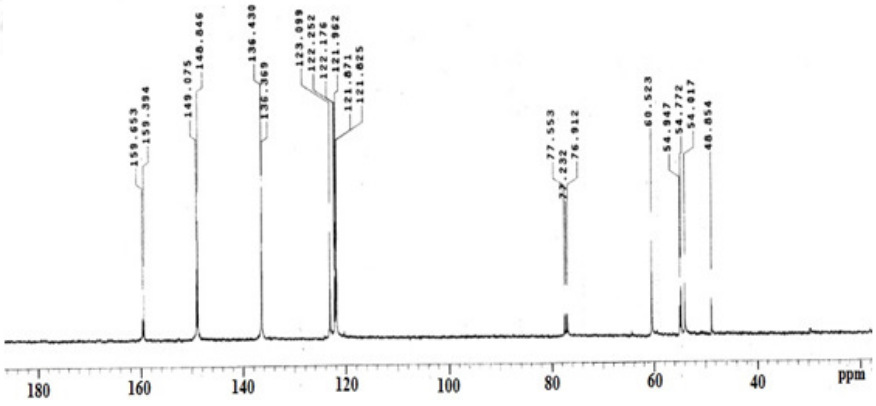

Figure A1.11 ^{13}C-NMR spectrum of **L_3** in $CDCl_3$.

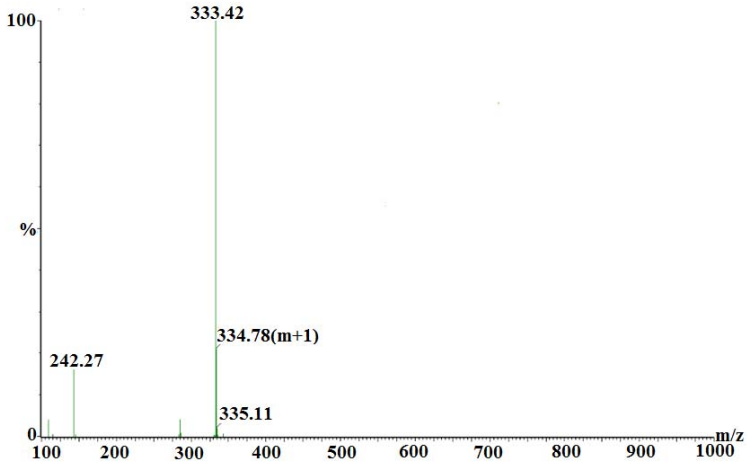

Figure A1.12 ESI-Mass spectrum of **L_3** in methanol.

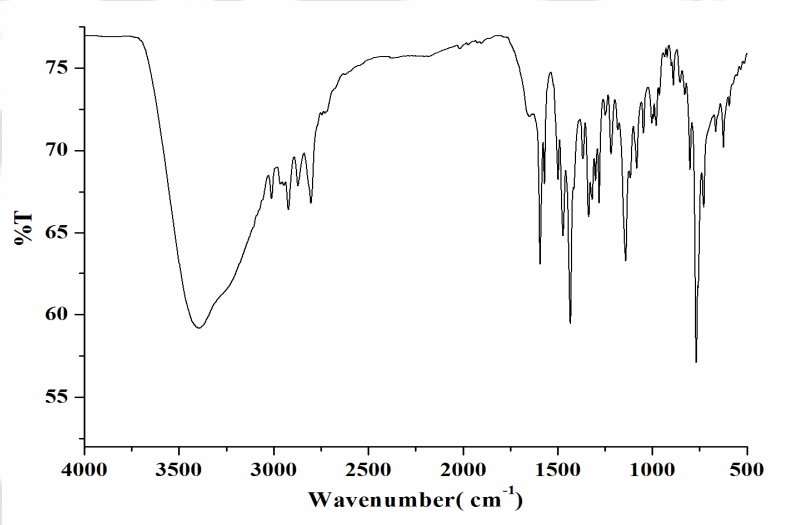

Figure A1.13 FT-IR spectrum of **L_4** in KBr pellet.

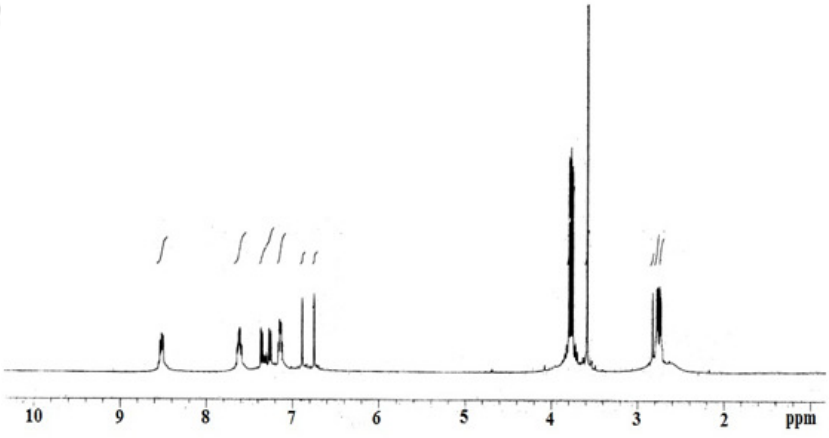

Figure A1.14 ^{1}H-NMR spectrum of **L_4** in $CDCl_3$.

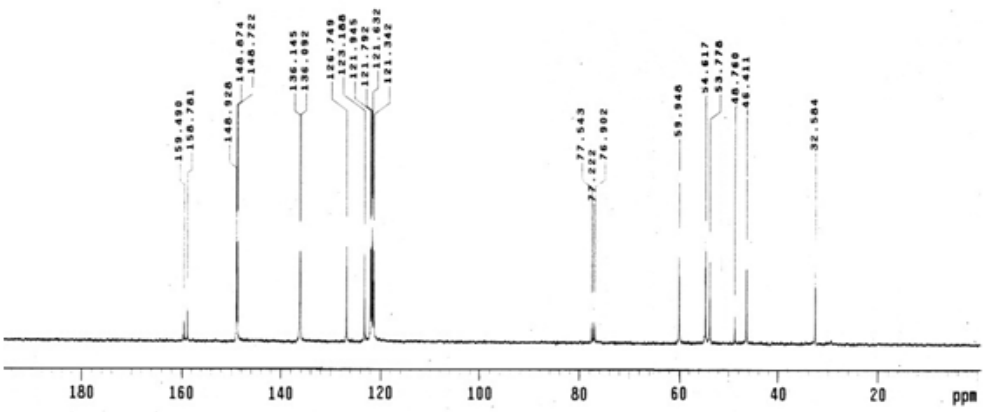

Figure A1.15 ^{13}C-NMR spectrum of **L$_4$** in $CDCl_3$.

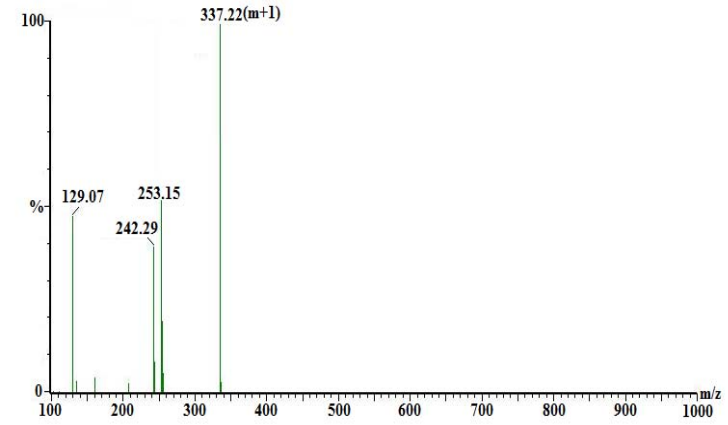

Figure A1.16 ESI-Mass spectrum of **L$_4$** in methanol.

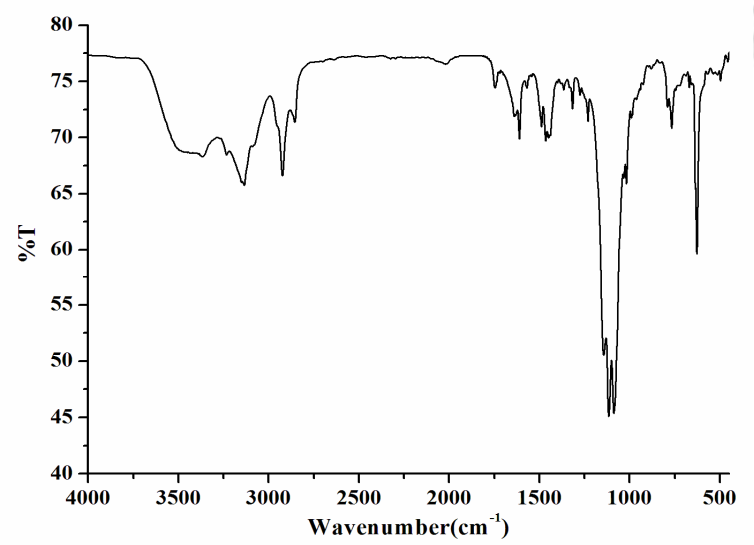

Figure A1.17 FT-IR spectrum of complex **2.1** in KBr pellet.

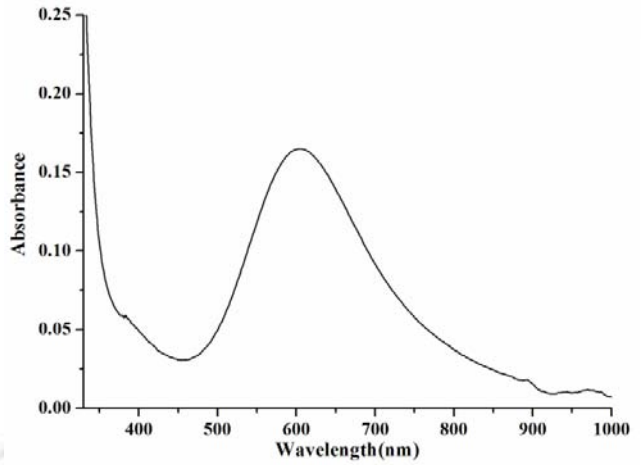

Figure A1.18 UV-visible spectrum of complex **2.1** in methanol.

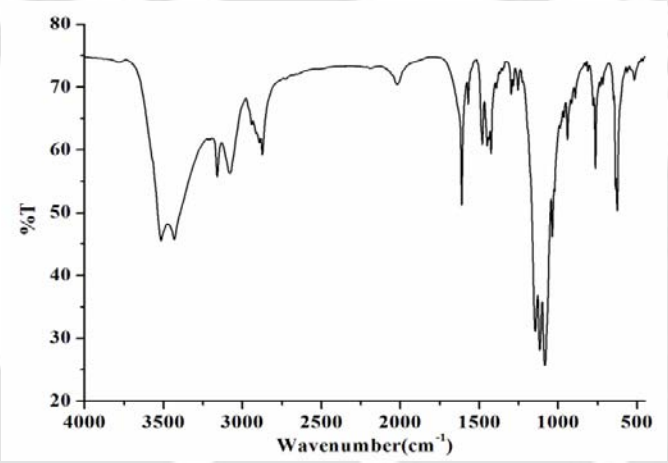

Figure A1.19 FT-IR spectrum of complex **2.2** in KBr pellet.

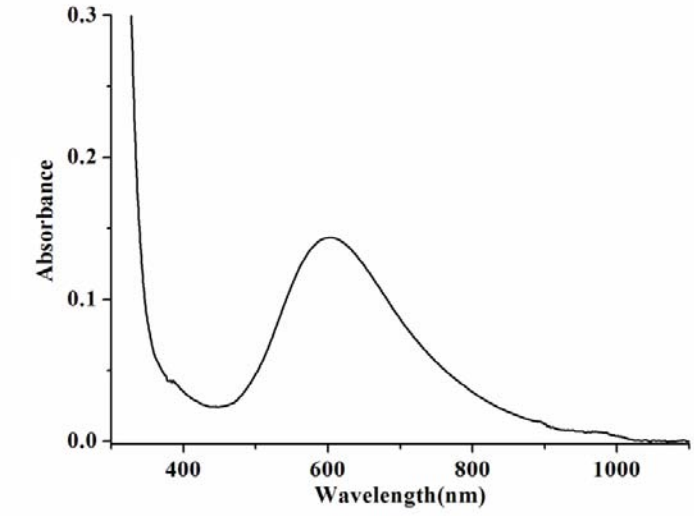

Figure A1.20 UV-visible spectrum of complex **2.2** in methanol.

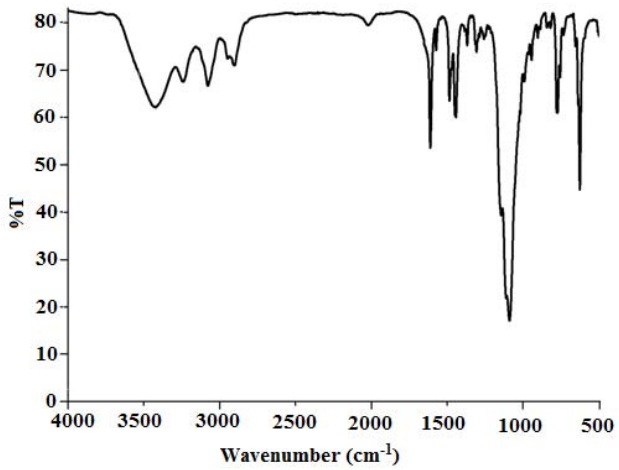

Figure A1.21 FT-IR spectrum of complex **2.3** in KBr pellet.

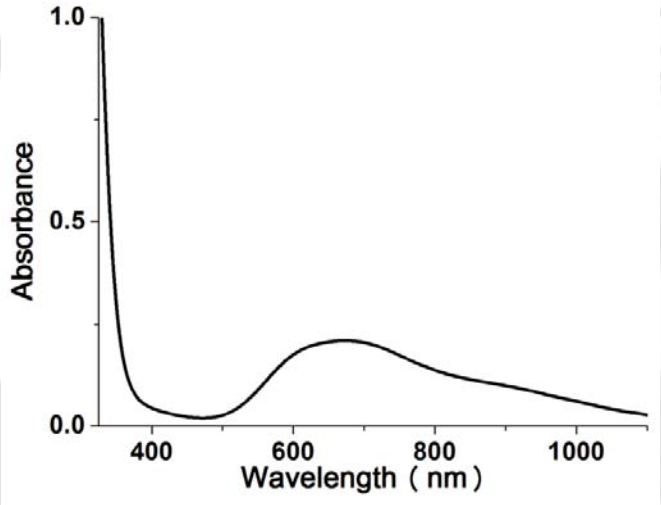

Figure A1.22 UV-visible spectrum of complex **2.3** in methanol.

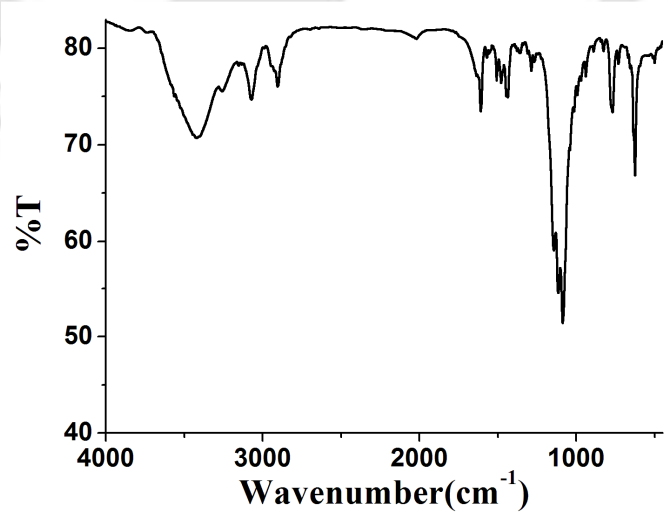

Figure A1.23 FT-IR spectrum of the complex **2.4** in KBr pellet.

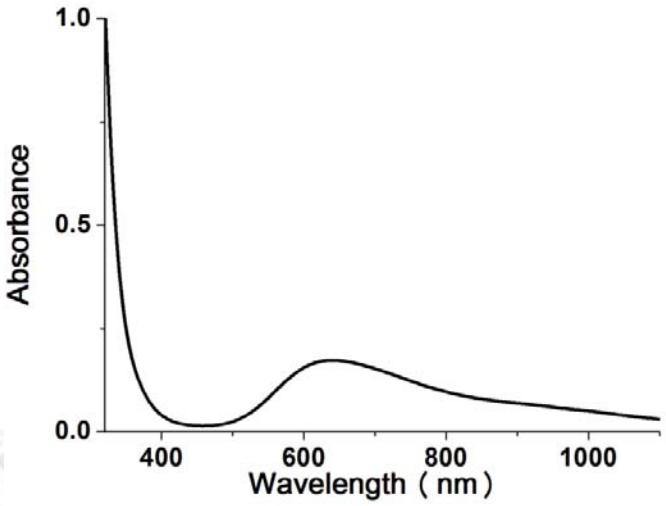

Figure A1.24 UV-visible spectrum of complex **2.4** in methanol.

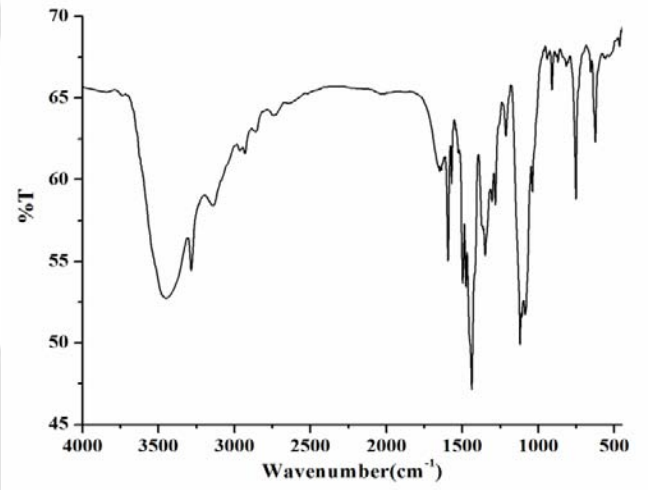

Figure A1.25 FT-IR spectrum of complex $\mathbf{L_1'}$**-ClO$_4$** in KBr pellet.

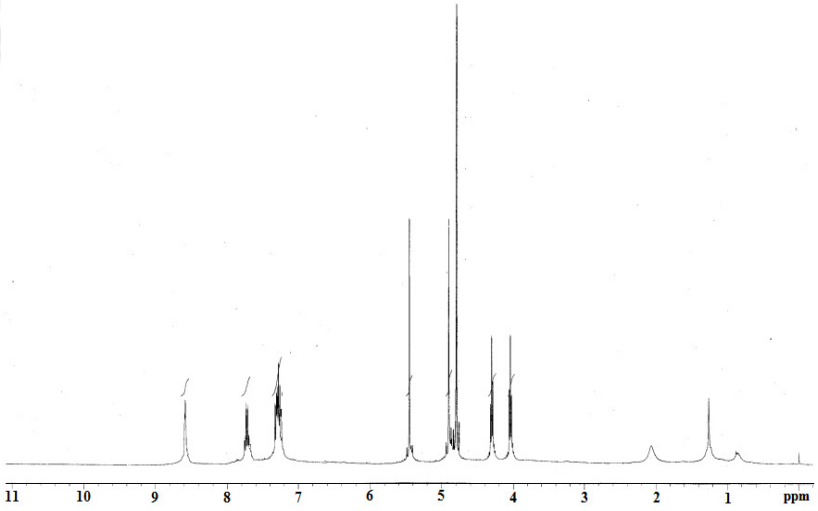

Figure A1.26 ^{1}H-NMR spectrum of $\mathbf{L_1'}$**-ClO$_4$** in D_2O.

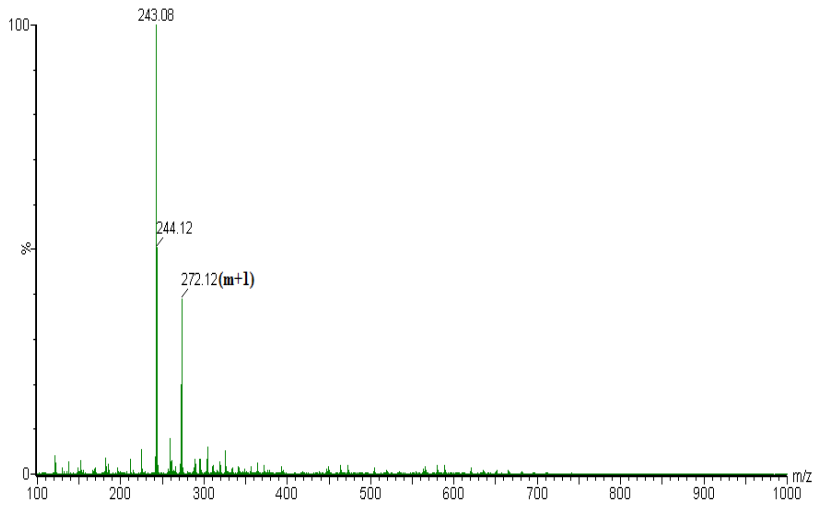

Figure A1.27 ESI-Mass spectrum of **L_1'-ClO_4** in methanol.

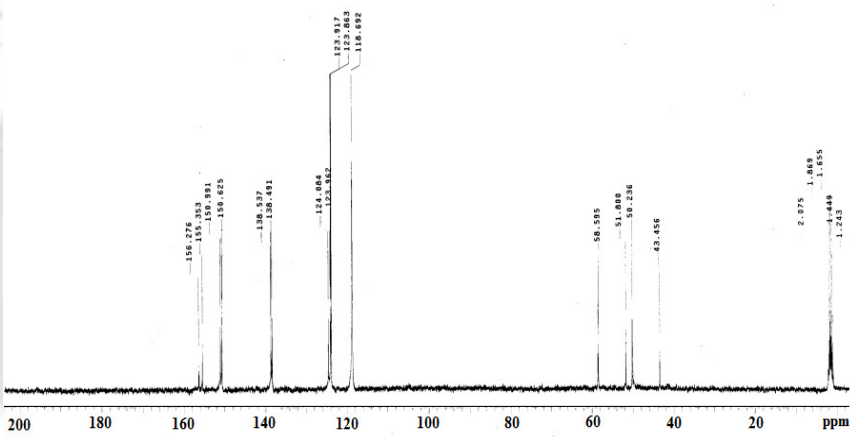

Figure A1.29 ^{13}C-NMR spectrum of **L_1'-ClO_4** in D_2O and CD_3CN mixture.

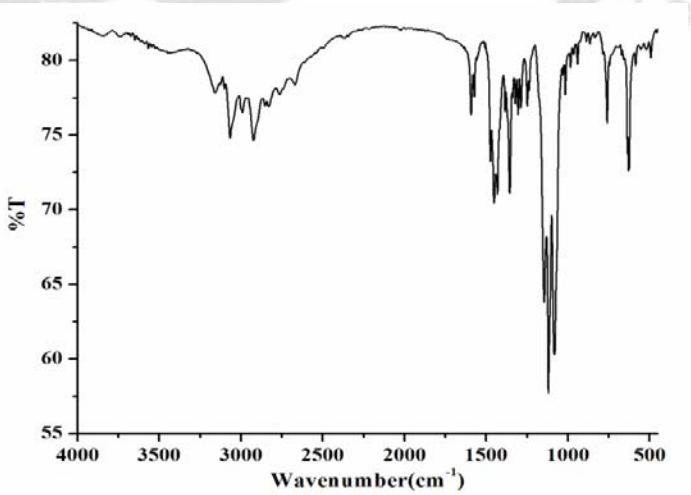

Figure A1.30 FT-IR spectrum of **L_2'-ClO_4** in KBr pellet.

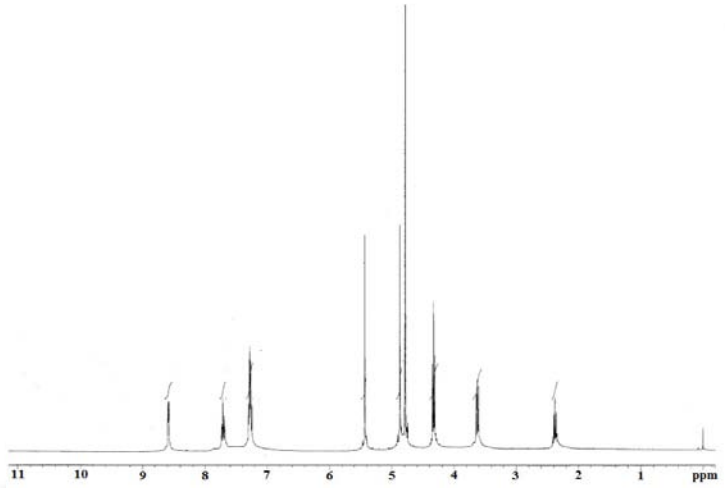

Figure A1.31 ^{1}H-NMR spectrum of $\mathbf{L_2'\text{-}ClO_4}$ in D_2O.

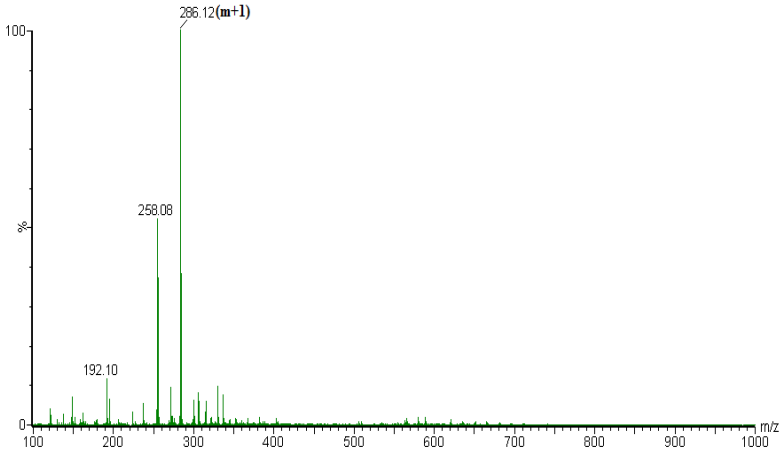

Figure A1.32 ESI-Mass spectrum of $\mathbf{L_2'\text{-}ClO_4}$ in methanol.

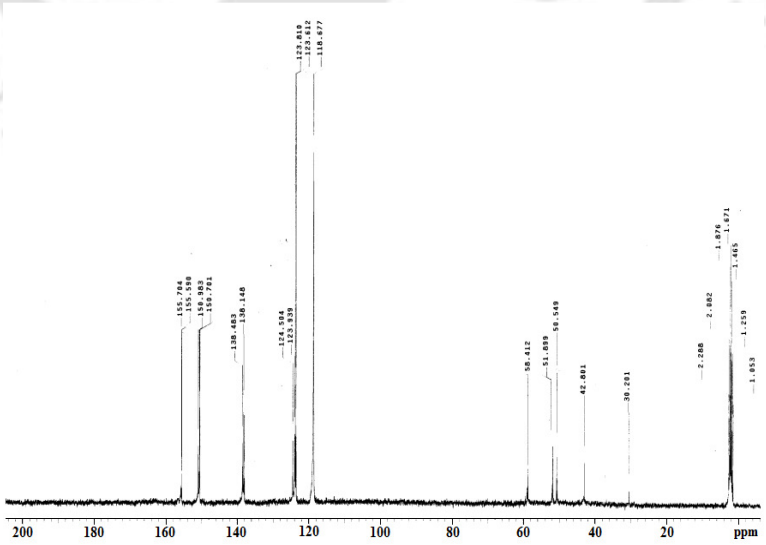

Figure A1.33 ^{13}C-NMR spectrum of $\mathbf{L_2'\text{-}ClO_4}$ in D_2O and CD_3CN mixture.

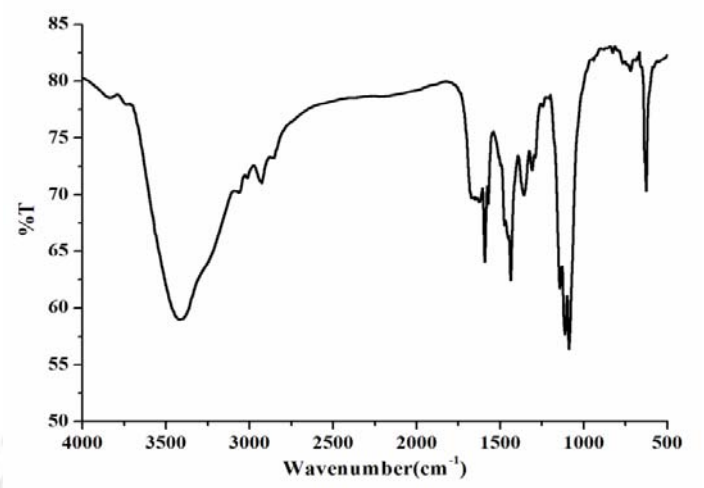

Figure A1.34 FT-IR spectrum of complex **L_3'-ClO_4** in KBr pellet.

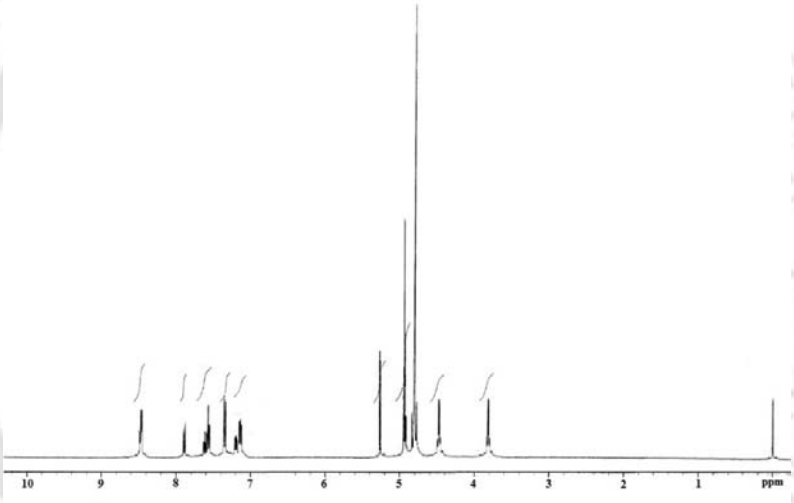

Figure A1.35 ^{1}H-NMR spectrum of **L_3'-ClO_4** in D_2O.

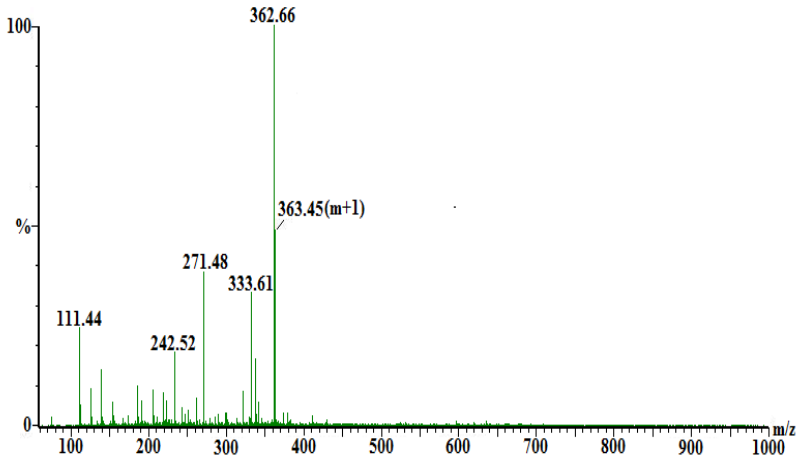

Figure A1.36 ESI-Mass spectrum of **L_3'-ClO_4** in methanol.

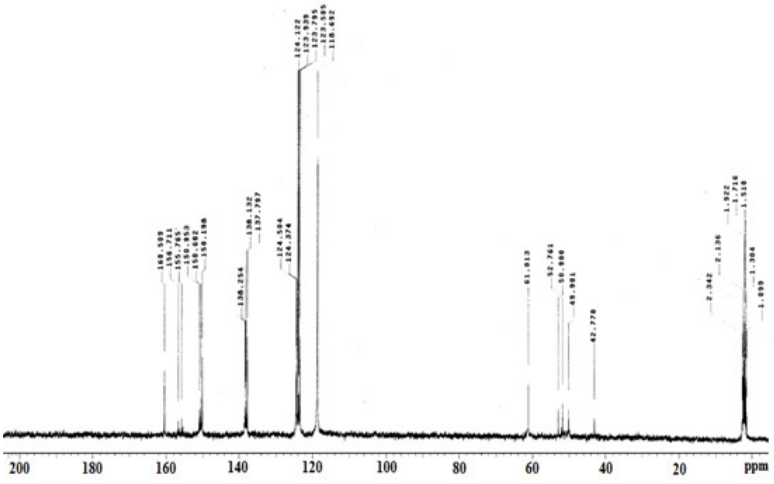

Figure A1.37 ^{13}C-NMR spectrum of **L_3'-ClO_4** in D_2O and CD_3CN mixture.

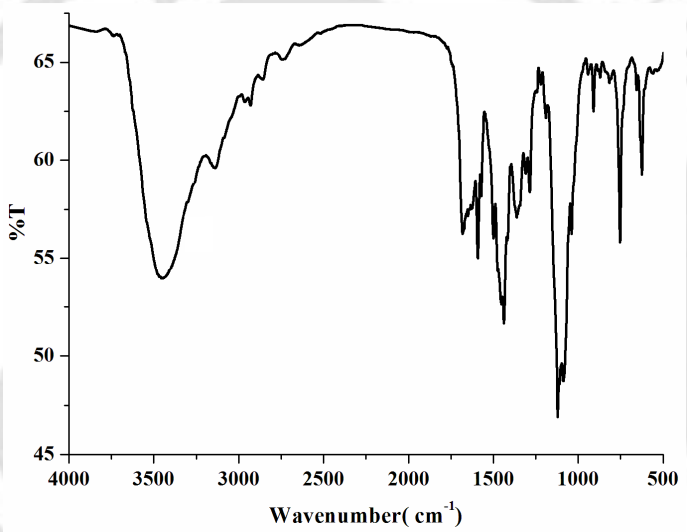

Figure A1.38 FT-IR spectrum of **L_4'-ClO_4** in KBr pellet.

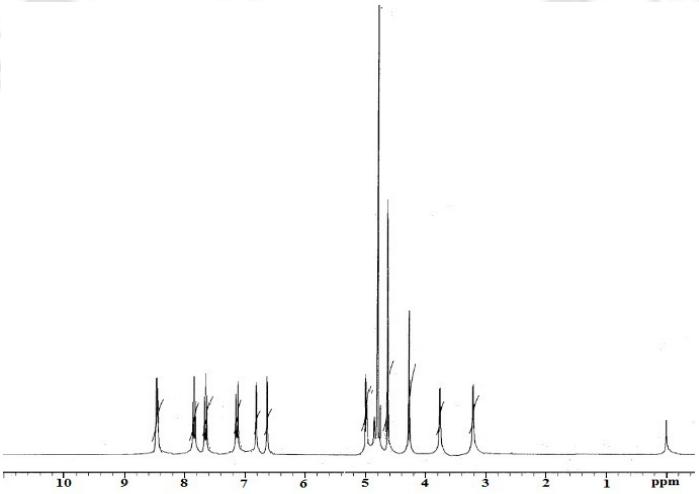

Figure A1.39 ^{1}H-NMR spectrum of **L_4'-ClO_4** in D_2O.

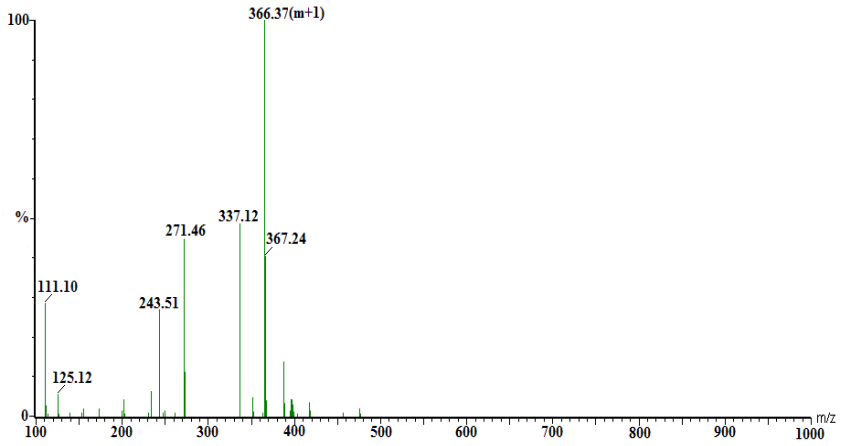

Figure A1.40 ESI-Mass spectrum of $\mathbf{L_4'}$**-ClO$_4$** in methanol.

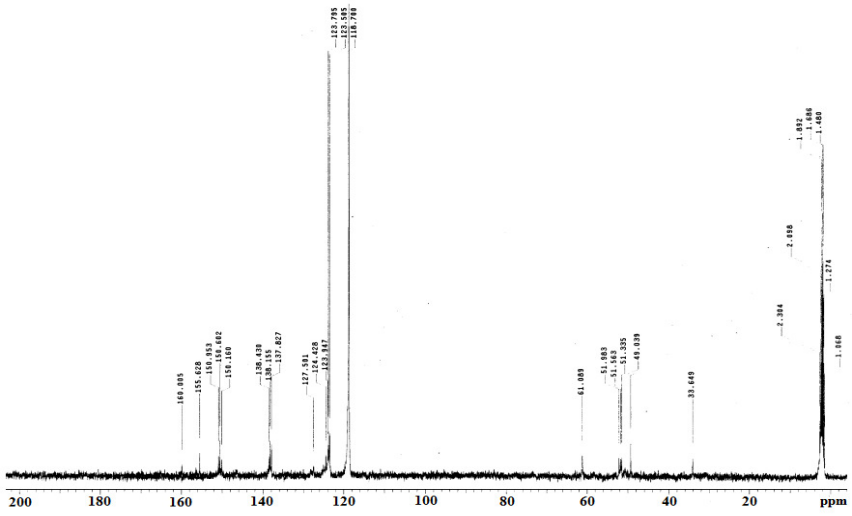

Figure A1.41 ^{13}C-NMR spectrum of $\mathbf{L_4'}$**-ClO$_4$** in D_2O and CD_3CN mixture.

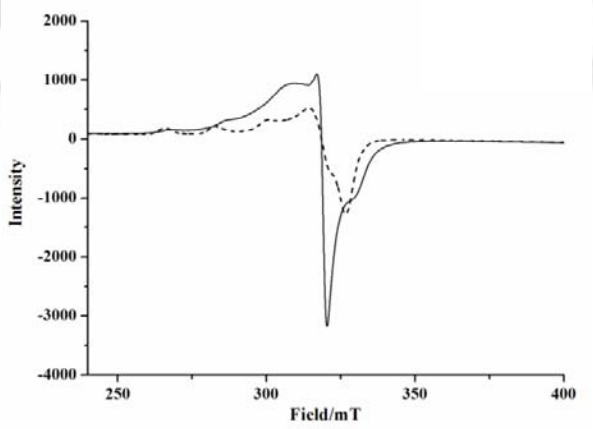

Figure A1.42 X-Band EPR spectra of complex **2.1** before (solid line) and after (dashed line) one equivalent of NaOEt in methanol medium at 77K.

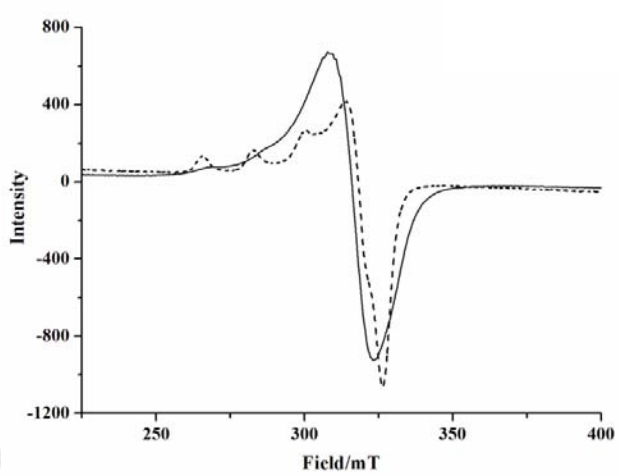

Figure A1. 43 X-Band EPR spectra of complex **2.2** before (solid line) and after (dashed line) one equivalent of NaOEt in methanol medium at 77K.

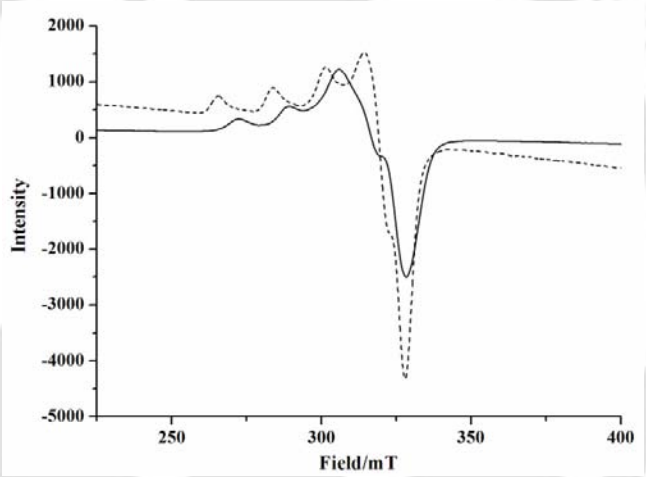

Figure A1.44 X-Band EPR spectra of complex **2.3** before (solid line) and after (dashed line) one equivalent of NaOEt in methanol medium at 77K.

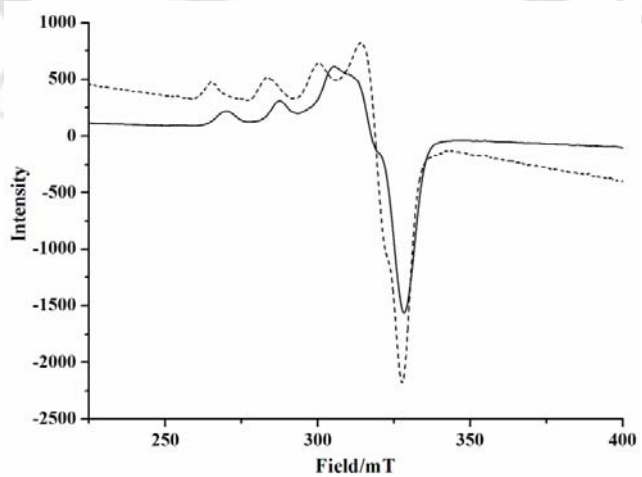

Figure A1.45 X-Band EPR spectra of complex **2.4** before (solid line) and after (dashed line) one equivalent of NaOEt in methanol medium at 77K.

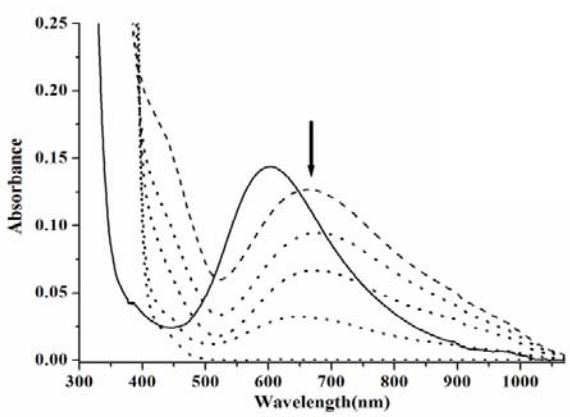

Figure A1.46 UV-visible spectra of complex **2.2** in methanol before (solid line), after (dash line) addition of one equivalent of sodium ethoxide and after (dotted line) purging nitric oxide.

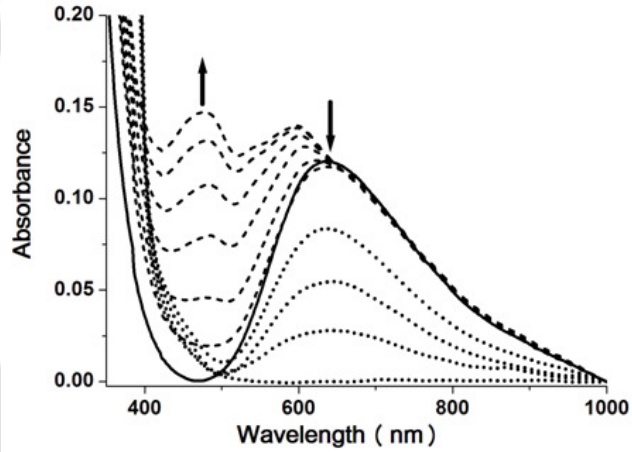

Figure A1.47 UV-visible spectra of complex **2.4** in methanol before (solid line), after (dash line) addition of one equivalent of sodium ethoxide and after (doted line) purging nitric oxide.

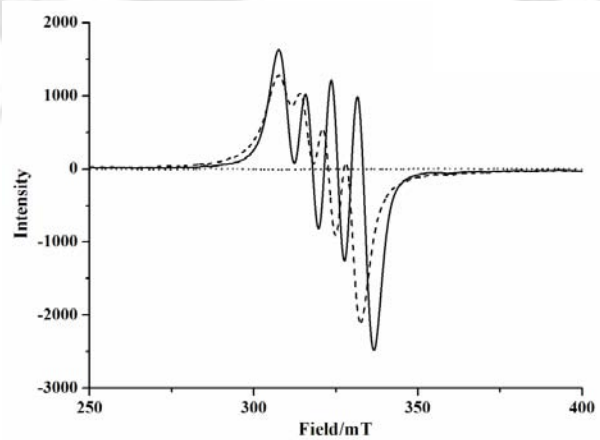

Figure A1.48 X-Band EPR spectra of complex **2.2** in methanol before (solid line), after (dash line) addition of one equivalent of sodium ethoxide and after (dotted line) purging nitric oxide.

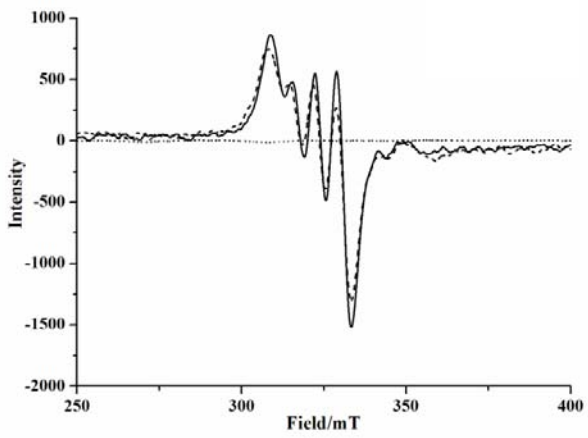

Figure A1.49 X-Band EPR spectra of complex **2.3** in methanol before (solid line), after (dash line) addition of one equivalent of sodium ethoxide and after (dotted line) purging nitric oxide.

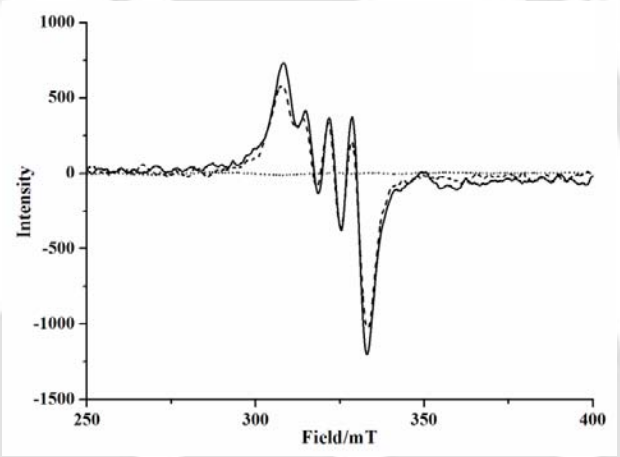

Figure A1.50 X-Band EPR spectra of complex **2.4** in methanol before (solid line), after (dash line) addition of one equivalent of sodium ethoxide and after (dotted line) purging nitric oxide.

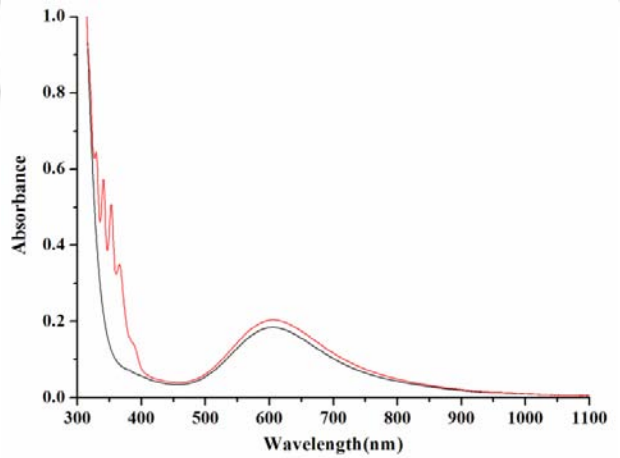

Figure A1.51 UV-visible spectra of complex **2.1** in methanol before (black line), after (red line) purging excess nitric oxide in absence of NaOEt.

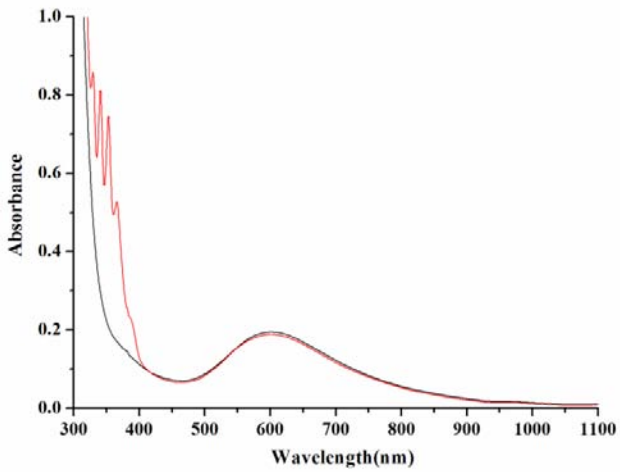

Figure A1.52 UV-visible spectra of complex **2.2** in methanol before (black line), after (red line) purging excess nitric oxide in absence of NaOEt.

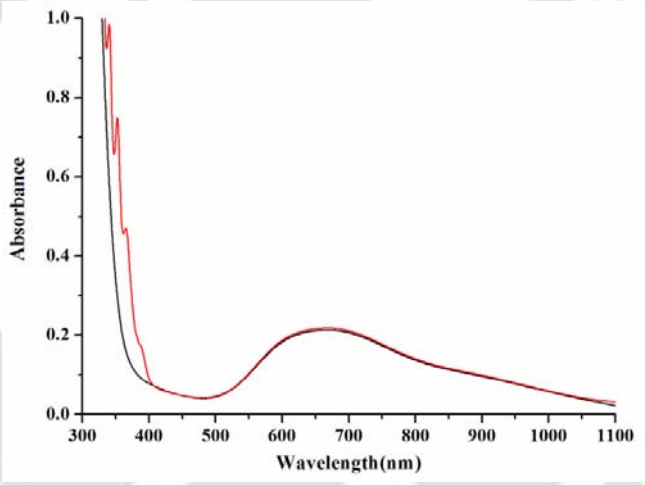

Figure A1.53 UV-visible spectra of complex **2.3** in methanol before (black line), after (red line) purging excess nitric oxide in absence of NaOEt.

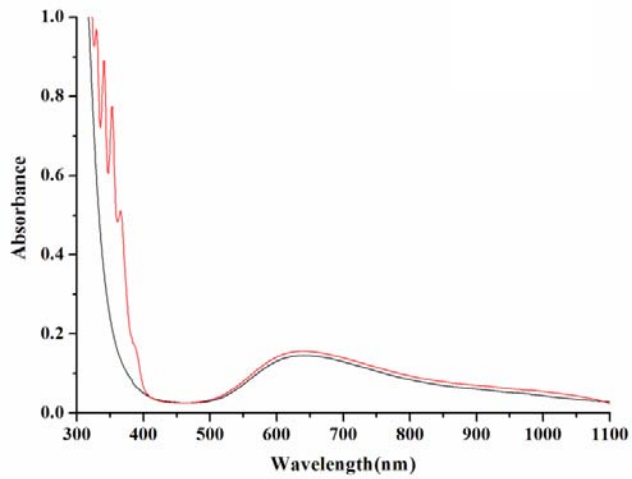

Figure A1.54 UV-visible spectra of complex **2.4** in methanol before (black line), after (red line) purging excess nitric oxide in absence of NaOEt.

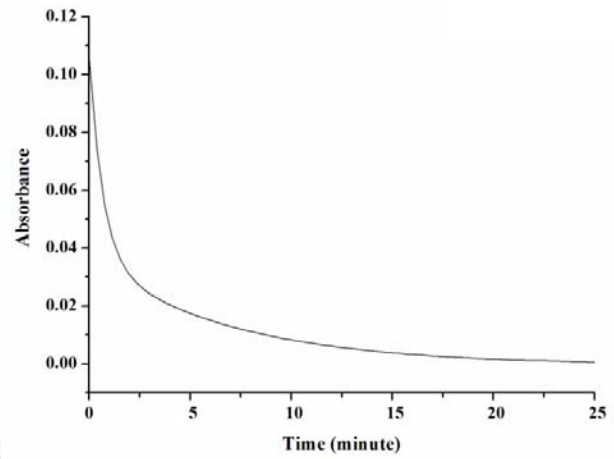

Figure A1.55 Time scan plot of complex **2.1** (λ_{max}= 642 nm) after reaction with nitric oxide in presence of one equivalent NaOEt at room temperature.

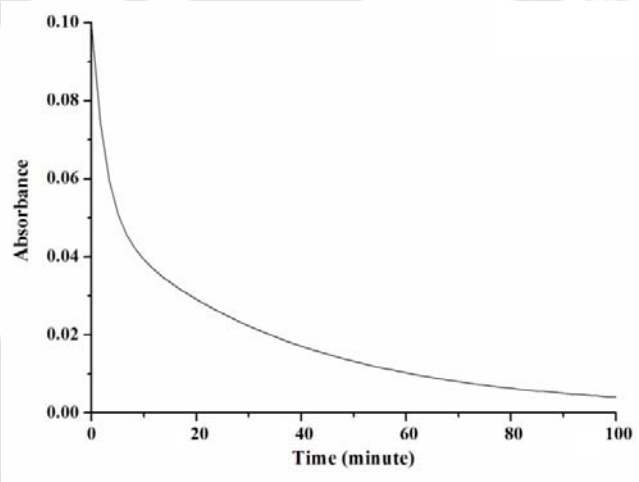

Figure A1.56 Time scan plot of complex **2.2** (λ_{max}= 664 nm) after reaction with nitric oxide in presence of one equivalent NaOEt at room temperature.

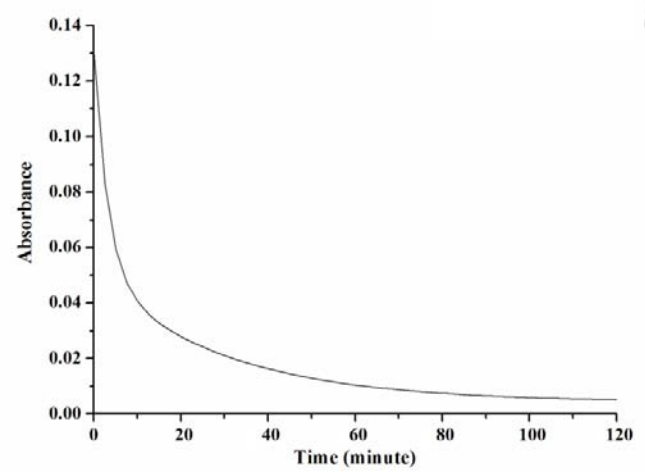

Figure A1.57 Time scan plot of complex **2.3** (λ_{max}= 668) after reaction with nitric oxide in presence of one equivalent NaOEt at room temperature.

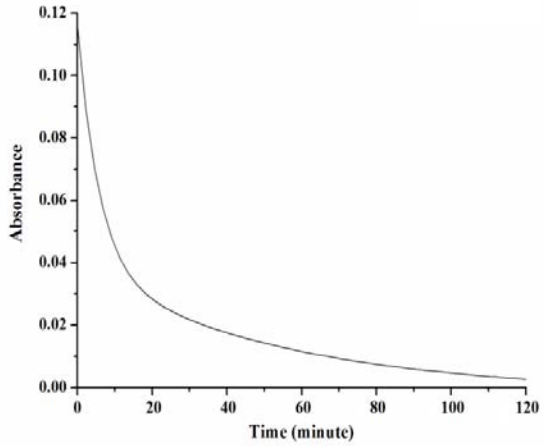

Figure A1.58 Time scan plot of complex **2.4** (λ_{max}=640) after reaction with nitric oxide in presence of one equivalent NaOEt at room temperature.

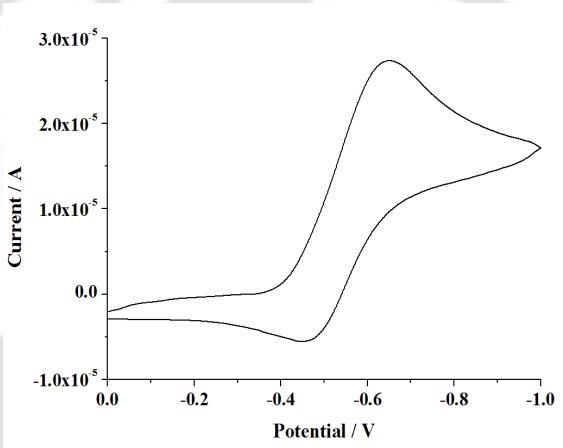

Figure A1.59 Cyclic voltammogram of complex **2.1** in methanol solvent. Working electrode, Pt; Reference electrode, Ag/Ag+; TBAP supporting electrolyte; scan rate 50 mv/s.

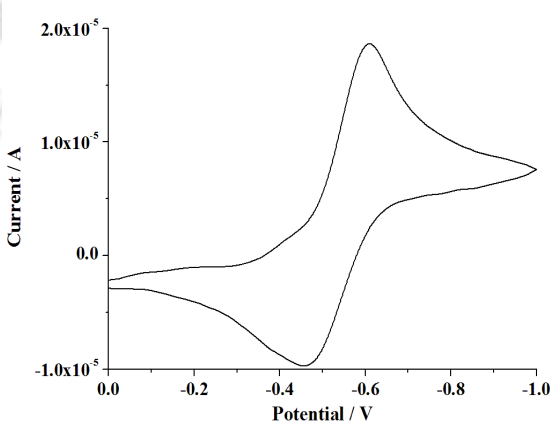

Figure A1.60 Cyclic voltammogram of complex **2.2** in methanol solvent. Working electrode, Pt; Reference electrode, Ag/Ag+; TBAP supporting electrolyte; scan rate 50 mv/s.

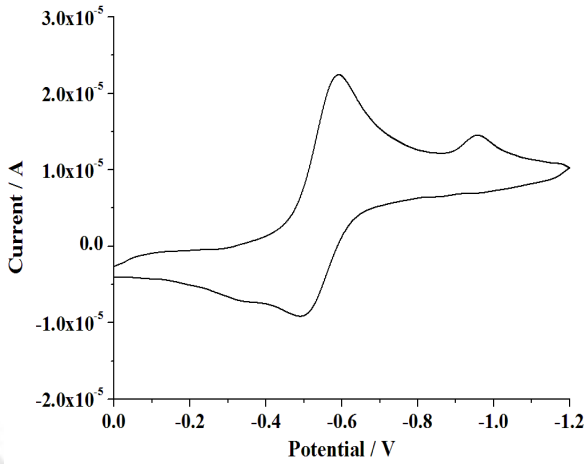

Figure A1.61 Cyclic voltammogram of complex **2.3** in methanol solvent. Working electrode, Pt; Reference electrode, Ag/Ag+; TBAP supporting electrolyte; scan rate 50 mv/s.

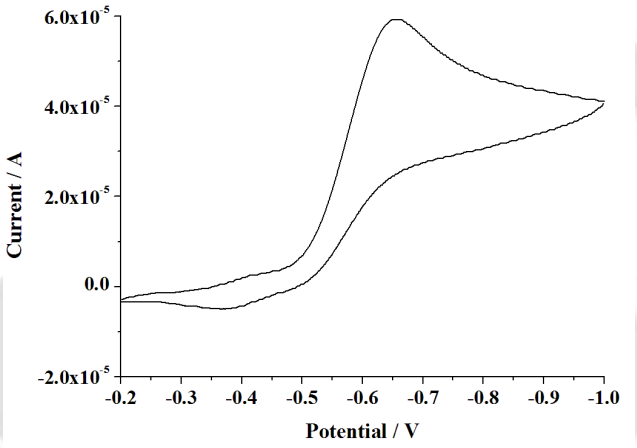

Figure A1.62 Cyclic voltammogram of complex **2.4** in methanol solvent. Working electrode, Pt; Reference electrode, Ag/Ag+; TBAP supporting electrolyte; scan rate 50 mv/s.

Appendix II

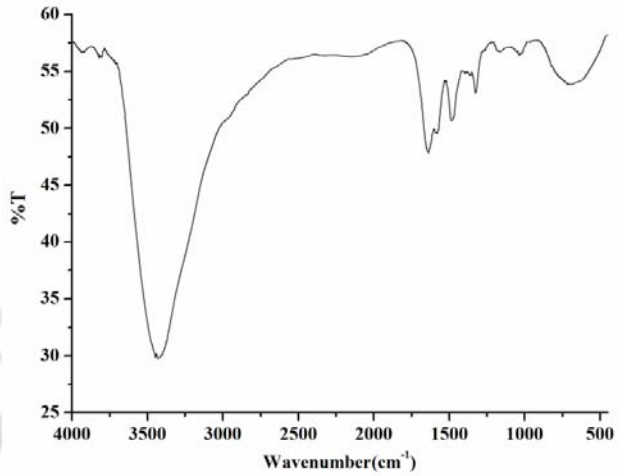

Figure A2.1 FT-IR spectrum of **L_5** in KBr pellet.

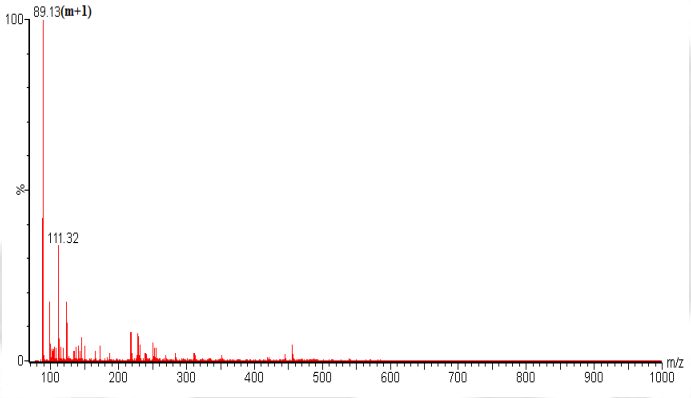

Figure A2.2 Mass spectrum for **L_5** in methanol.

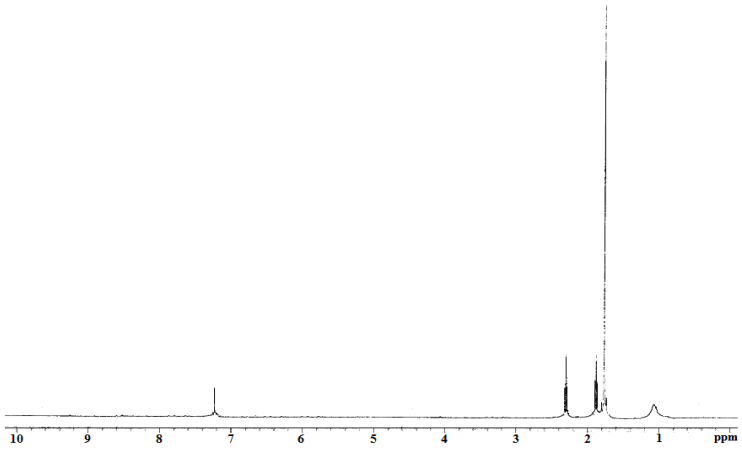

Figure A2.3 ^{1}H-NMR spectrum of **L_5** in $CDCl_3$.

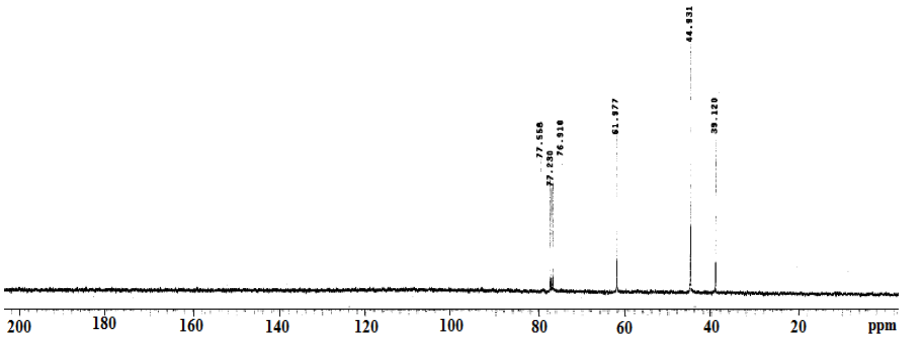

Figure A2.4 ^{13}C-NMR spectrum of $\mathbf{L_5}$ in $CDCl_3$.

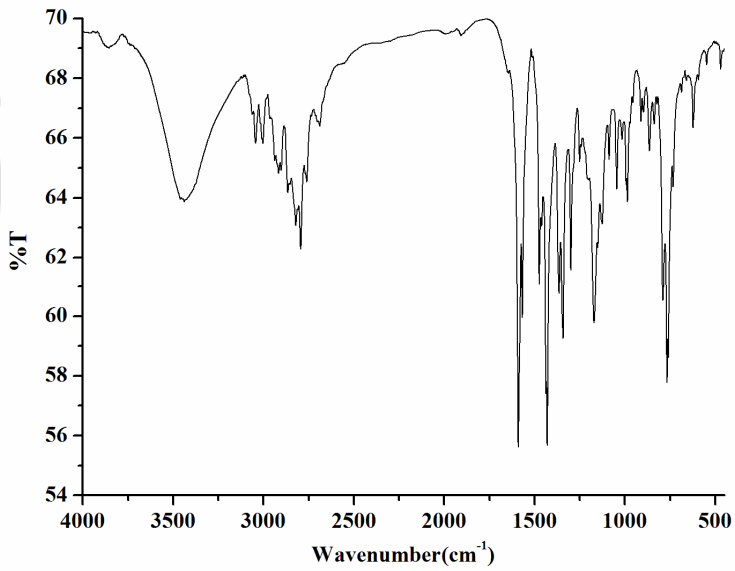

Figure A2.5 FT-IR spectrum of $\mathbf{L_6}$ in KBr pellet.

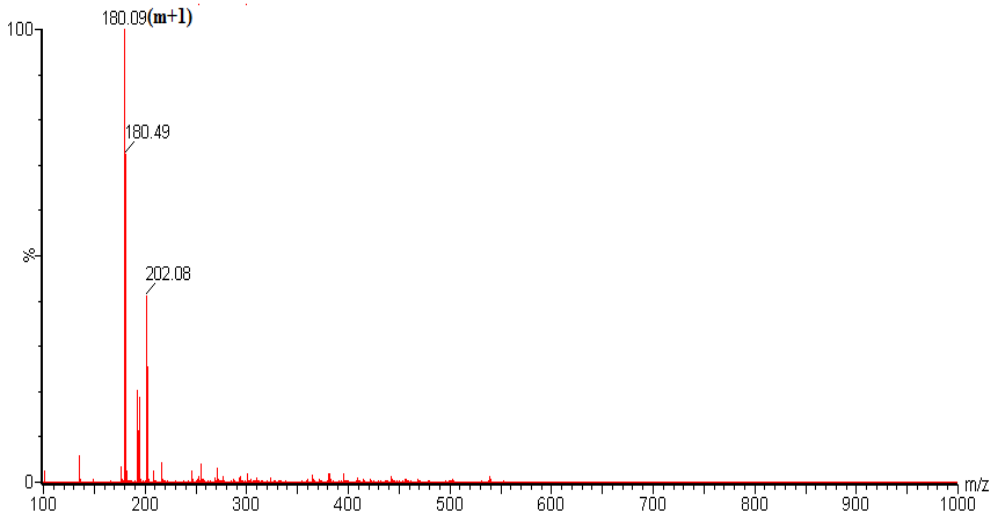

Figure A2.6 Mass spectrum for $\mathbf{L_6}$ in methanol.

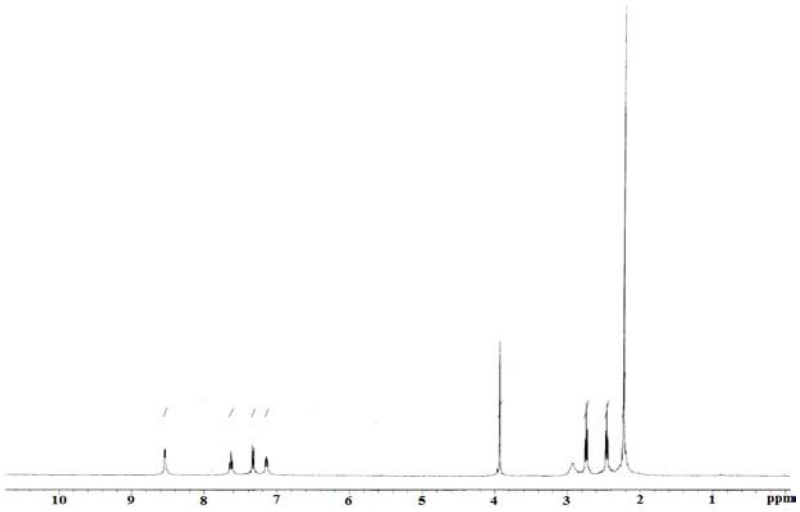

Figure A2.7 ^{1}H-NMR spectrum of **L_6** in $CDCl_3$.

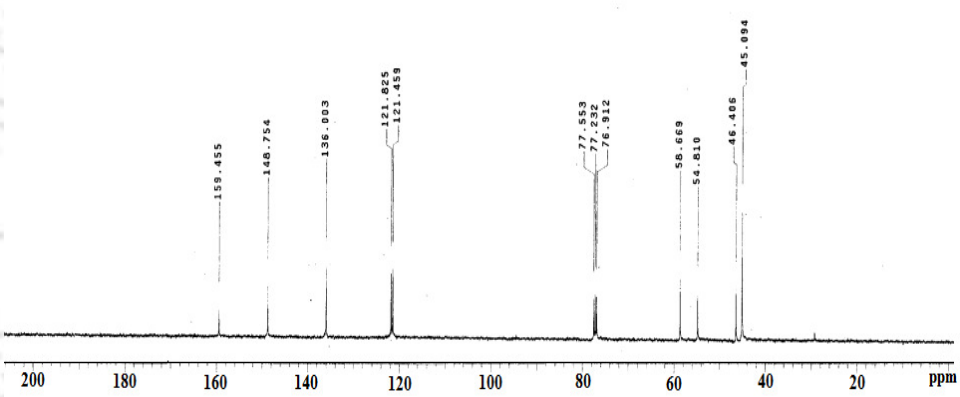

Figure A2.8 ^{13}C-NMR spectrum of **L_6** in $CDCl_3$.

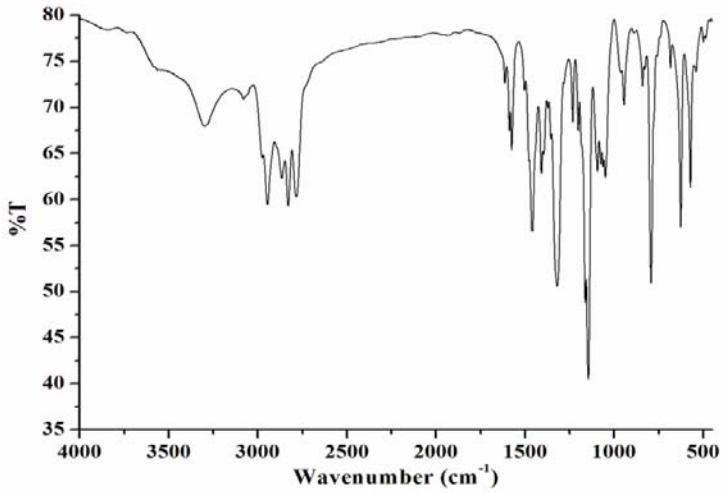

Figure A2.9 FT-IR spectrum of **L_7** in KBr pellet.

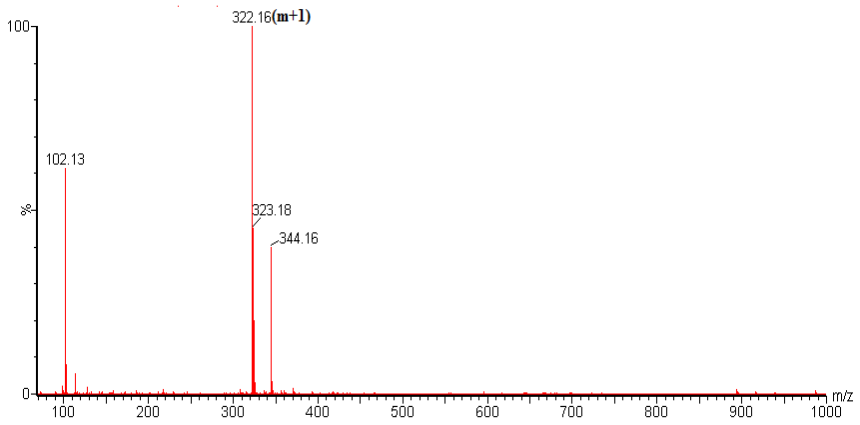

Figure A2.10 Mass spectrum for **L_7** in methanol.

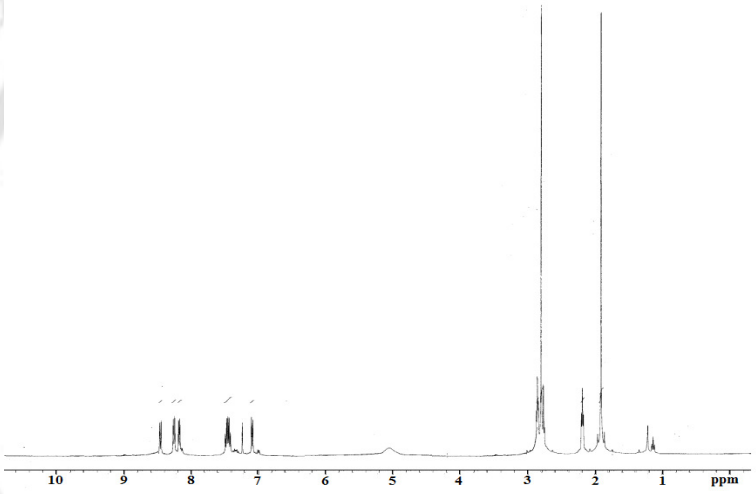

Figure A2.11 ^{1}H-NMR spectrum of **L_7** in $CDCl_3$.

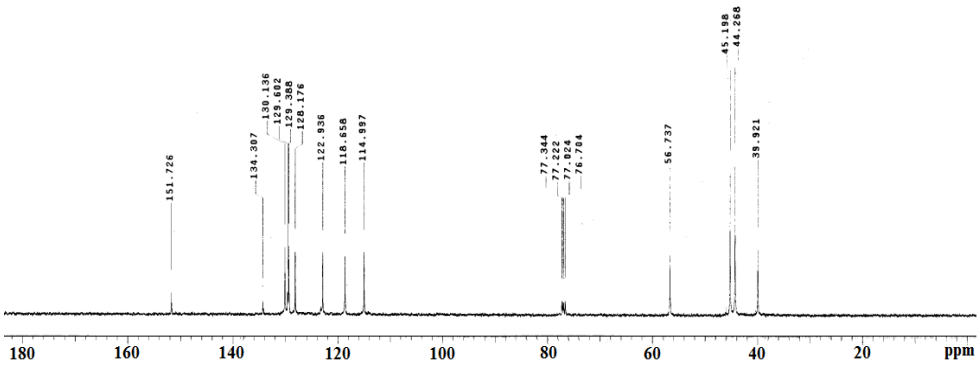

Figure A2.12 ^{13}C-NMR spectrum of **L_7** in $CDCl_3$.

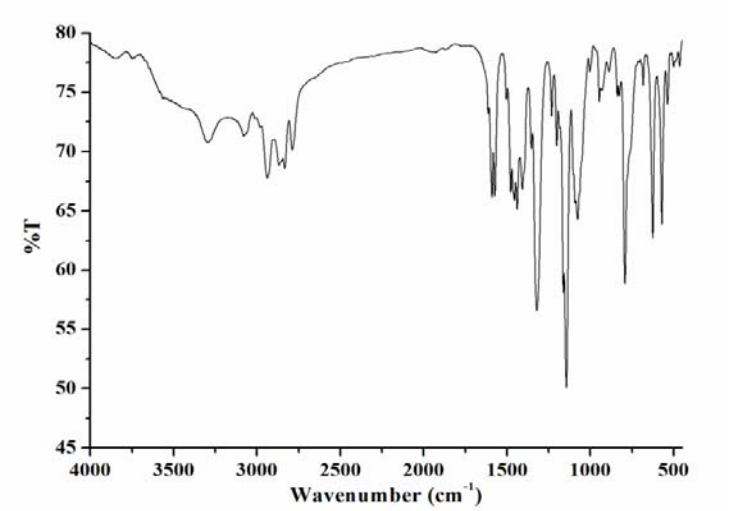

Figure A2.13 FT-IR spectrum of **L_8** in KBr pellet.

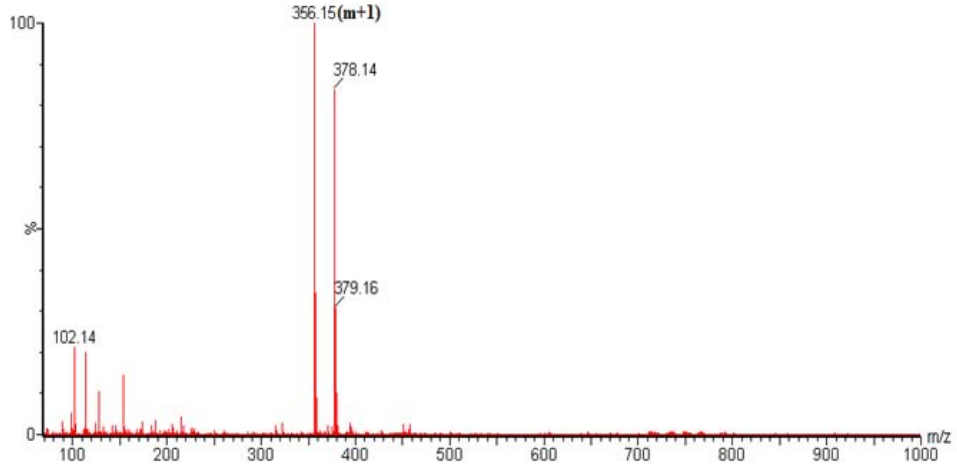

Figure A2.14 Mass spectrum for **L_8** in methanol.

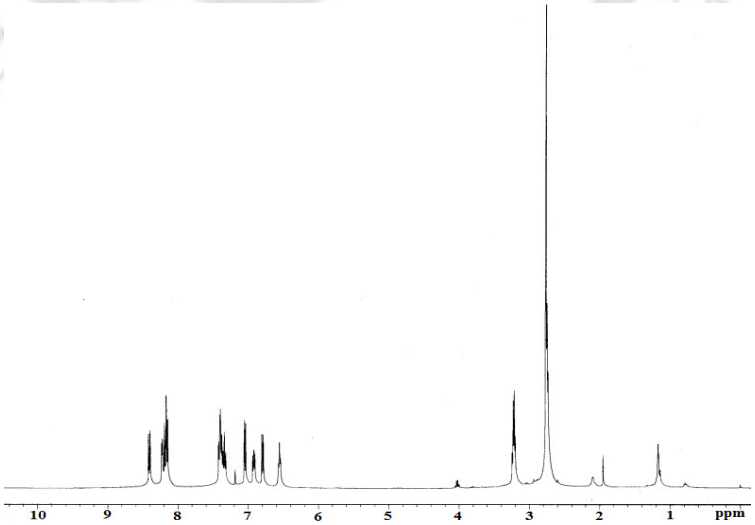

Figure A2.15 ^{1}H-NMR spectrum of **L_8** in $CDCl_3$.

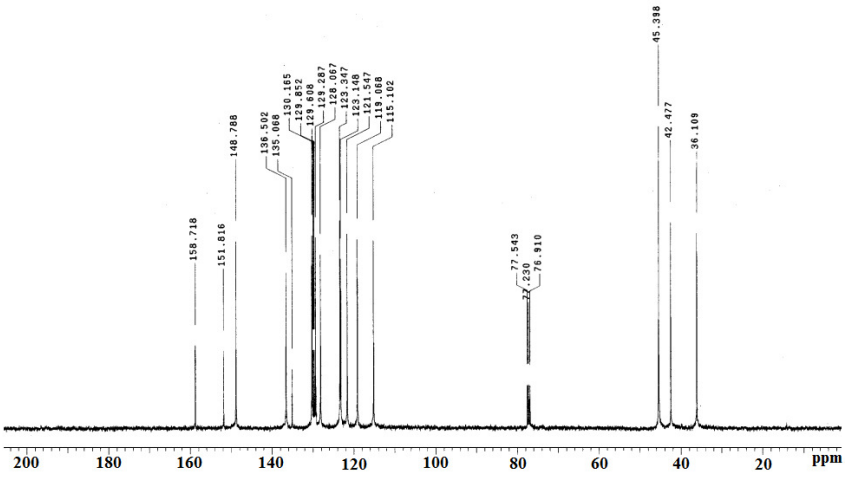

Figure A2.16 ^{13}C-NMR spectrum of **L_8** in $CDCl_3$.

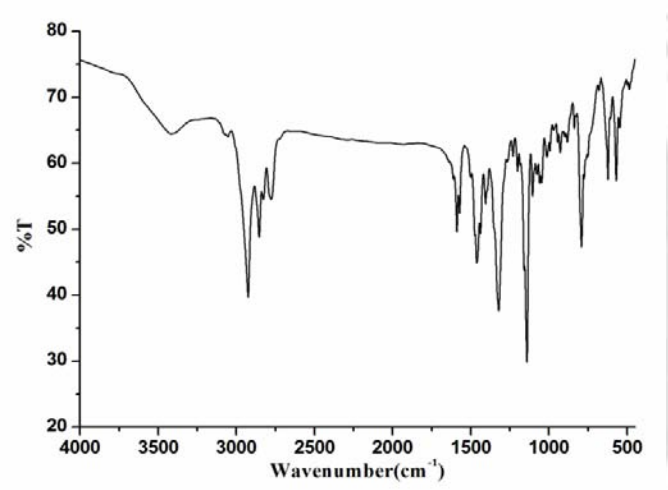

Figure A2.17 FT-IR spectrum of **L_9** in KBr pellet.

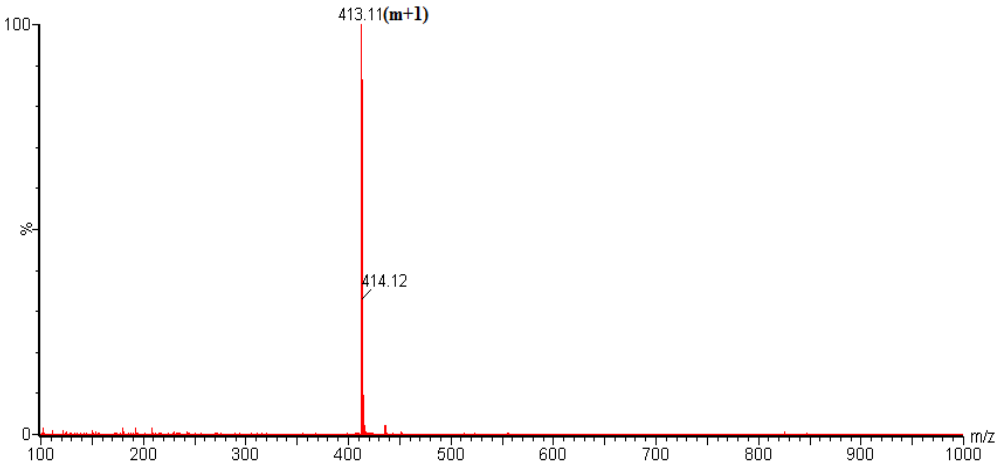

Figure A2.18 Mass spectrum for **L_9** in methanol.

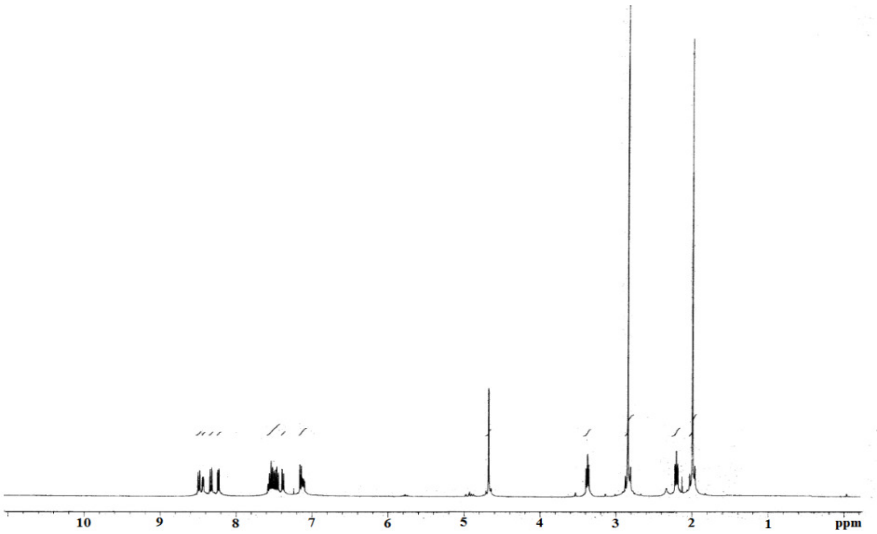

Figure A2.19 ^{1}H-NMR spectrum of **L_9** in $CDCl_3$.

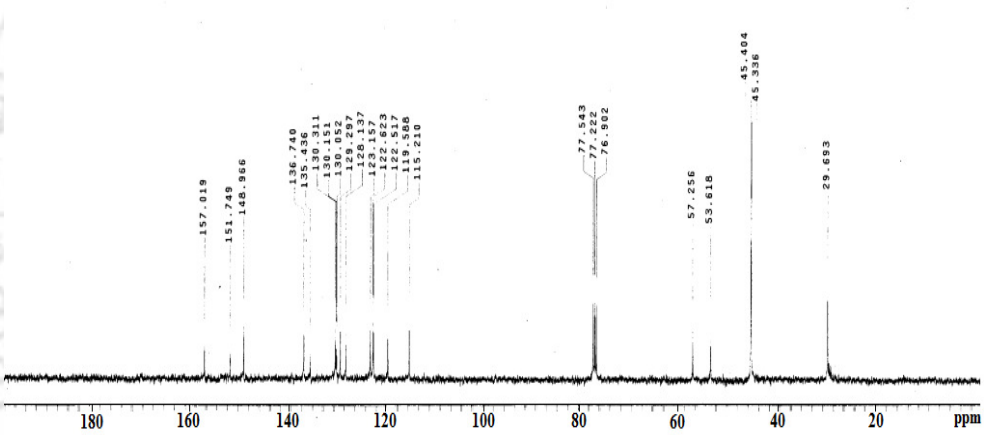

Figure A2.20 ^{13}C-NMR spectrum of **L_9** in $CDCl_3$.

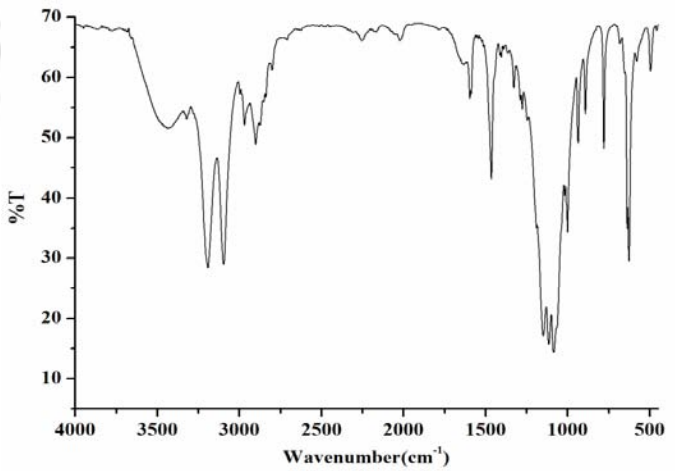

Figure A2.21 FT-IR spectrum of complex **3.1** in KBr pellet.

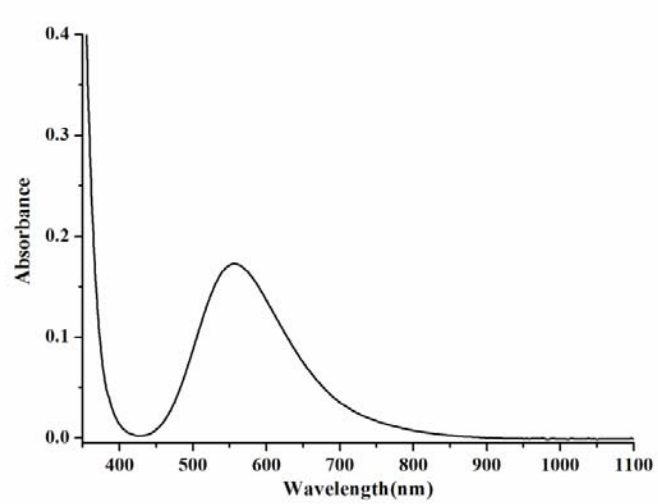

Figure A2.22 UV-visible spectrum of complex **3.1** in methanol.

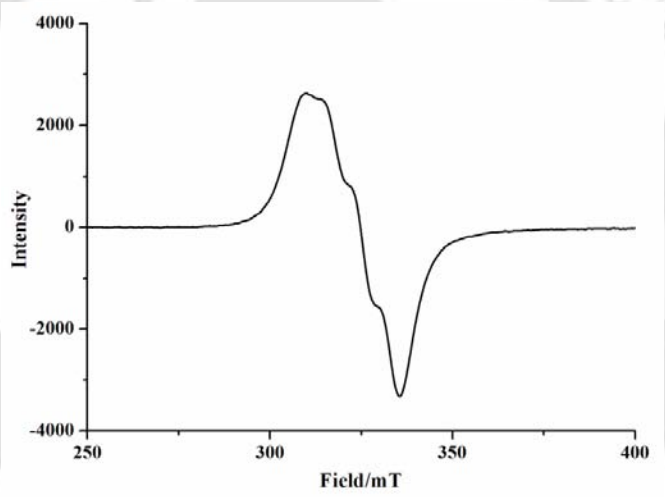

Figure A2.23 X-Band EPR spectrum of complex **3.1** in methanol at 298K.

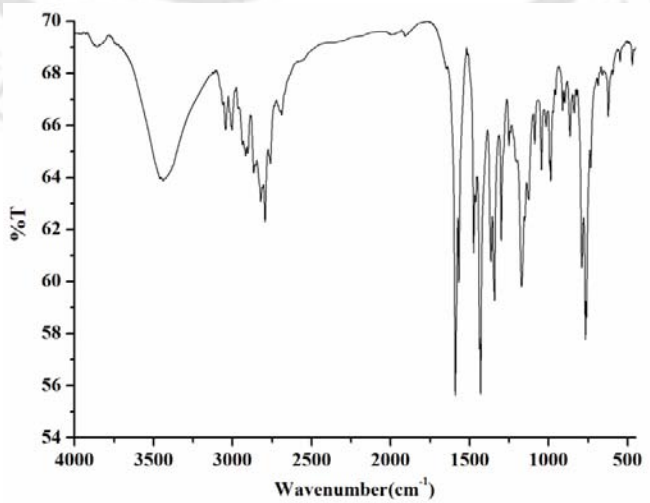

Figure A2.24 FT-IR spectrum of complex **3.2** in KBr pellet.

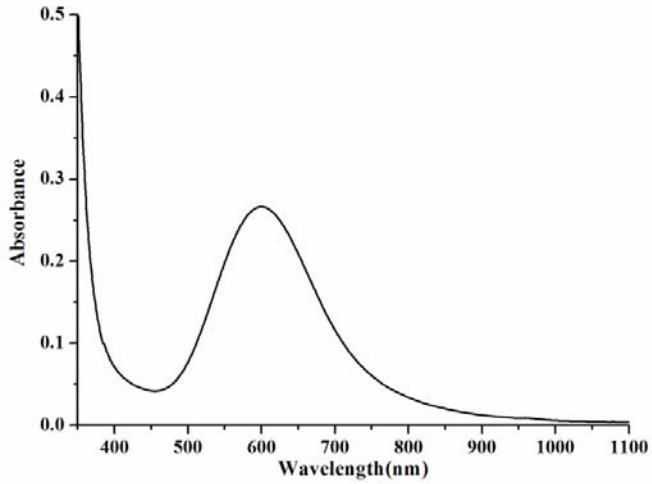

Figure A2.25 UV-visible spectrum of complex **3.2** in methanol.

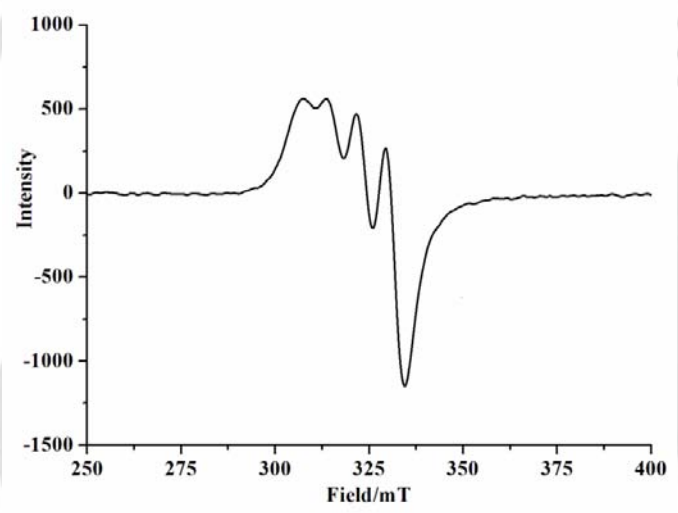

Figure A2.26 X-Band EPR spectrum of complex **3.2** in methanol at 298K.

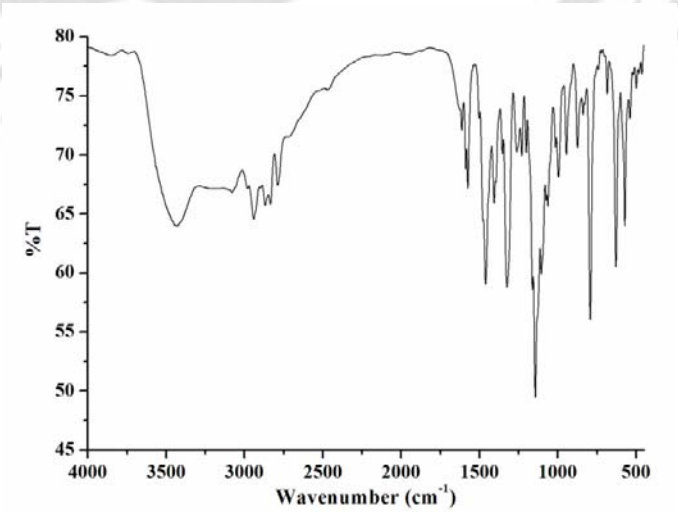

Figure A2.27 FT-IR spectrum of complex **3.3** in KBr pellet.

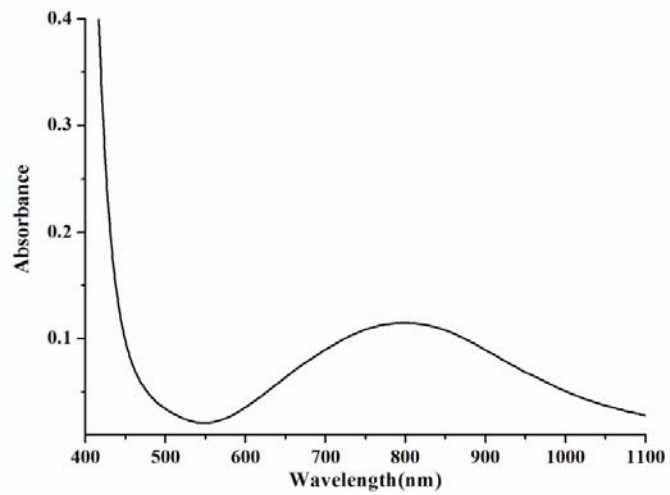

Figure A2.28 UV-visible spectrum of complex **3.3** in methanol.

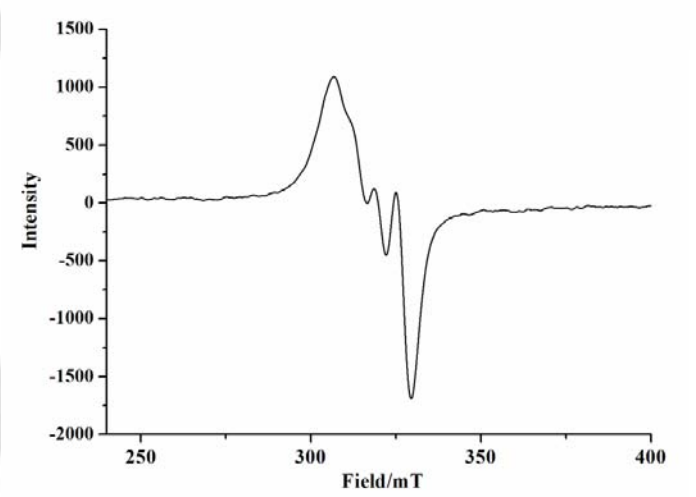

Figure A2.29 X-Band EPR spectrum of complex **3.3** in methanol at 298K.

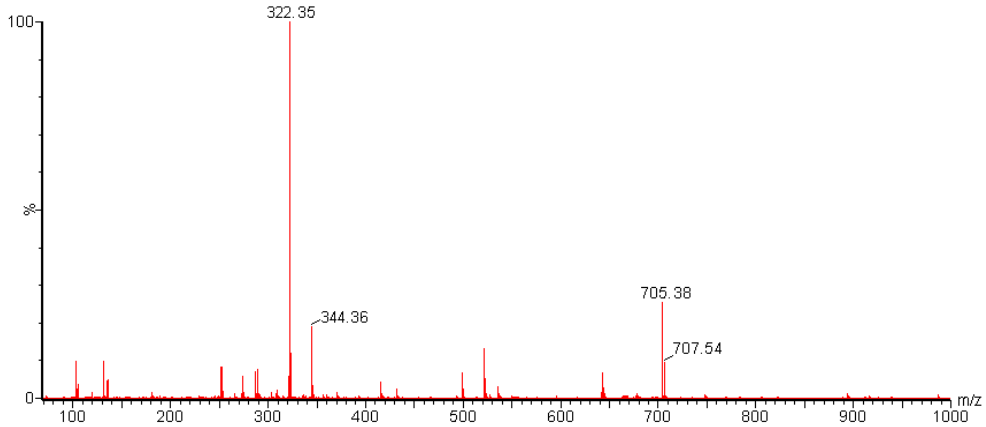

Figure A2.30 Mass spectrum for complex **3.3** in methanol.

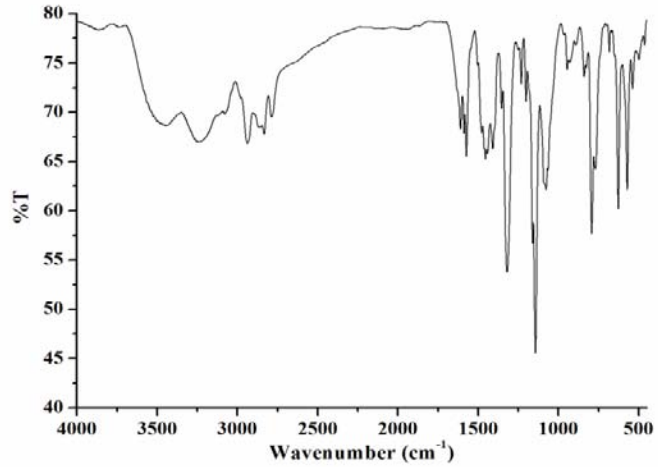

Figure A2.31 FT-IR spectrum of complex **3.4** in KBr pellet.

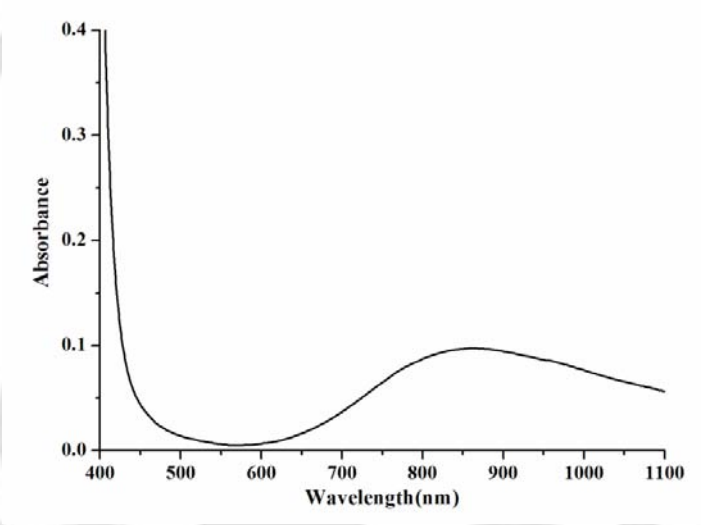

Figure A2.32 UV-visible spectrum of complex **3.4** in methanol.

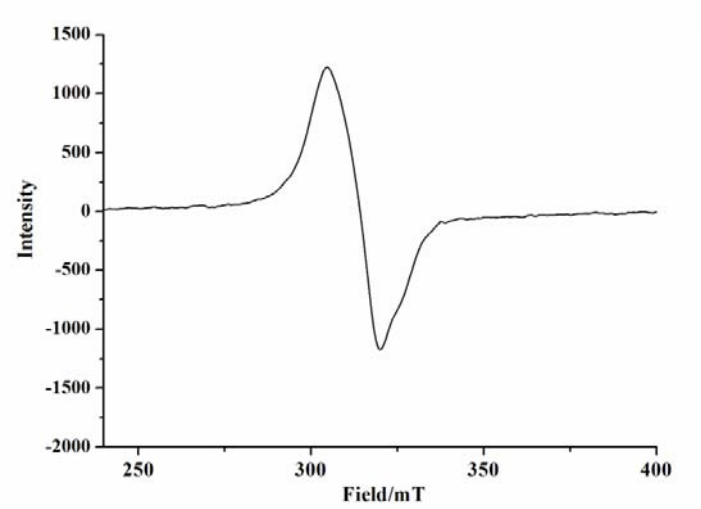

Figure A2.33 X-Band EPR spectrum of complex **3.4** in methanol at 298K.

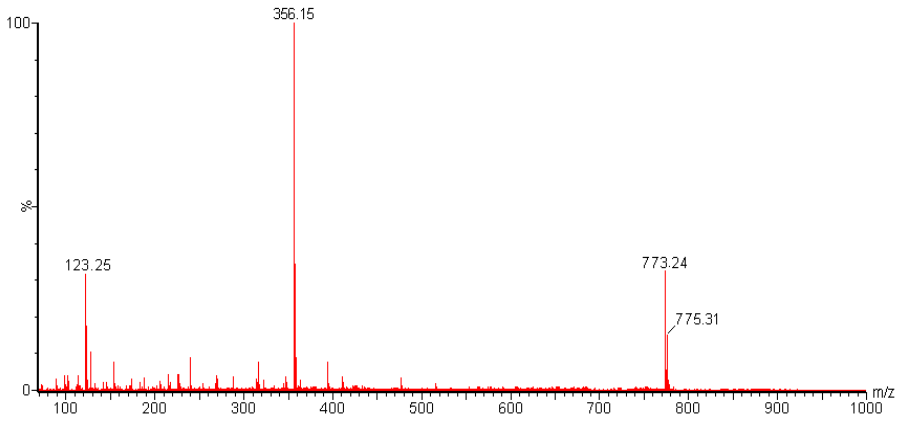

Figure A2.34: Mass spectrum for complex **3.4** in methanol.

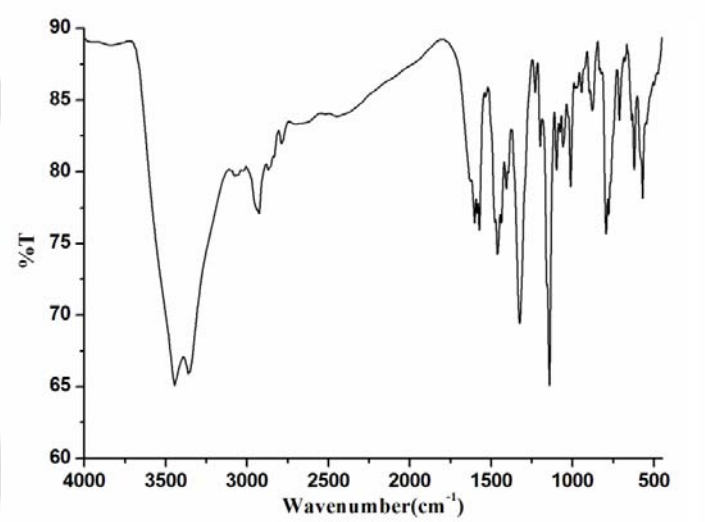

Figure A2.35: FT-IR spectrum of complex **3.5** in KBr pellet

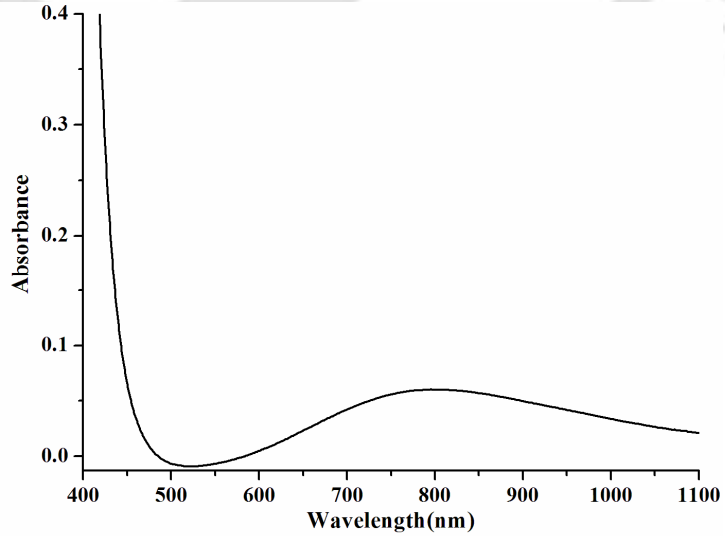

Figure A2.36: UV-visible spectrum of complex **3.5** in methanol.

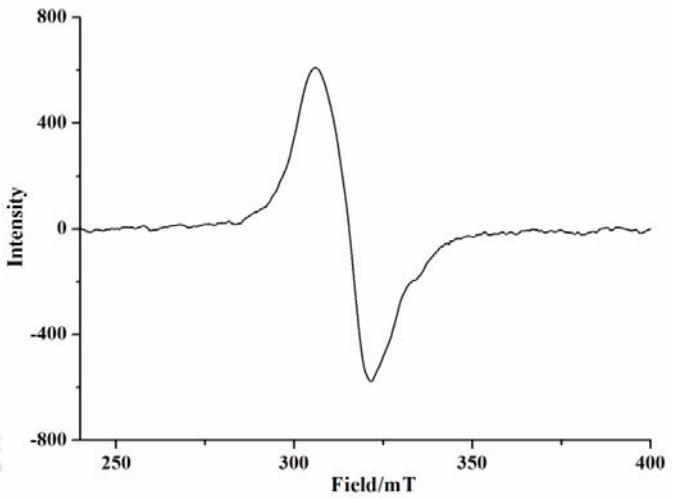

Figure A2.37 X-Band EPR spectrum of complex **3.5** in methanol at 298K.

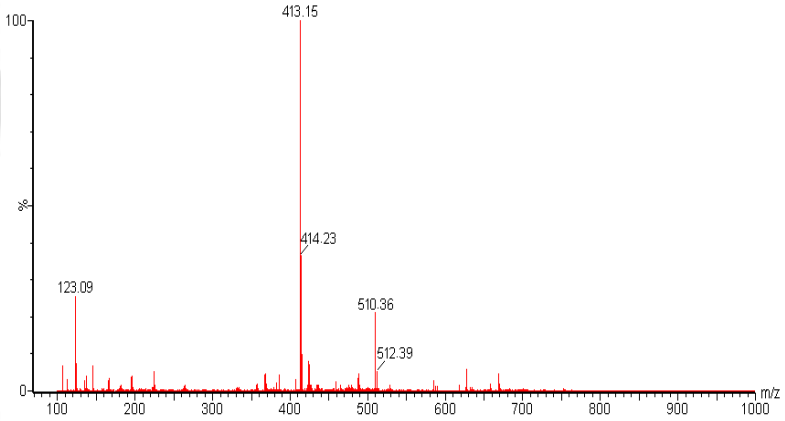

Figure A2.38 Mass spectrum for complex **3.5** in methanol.

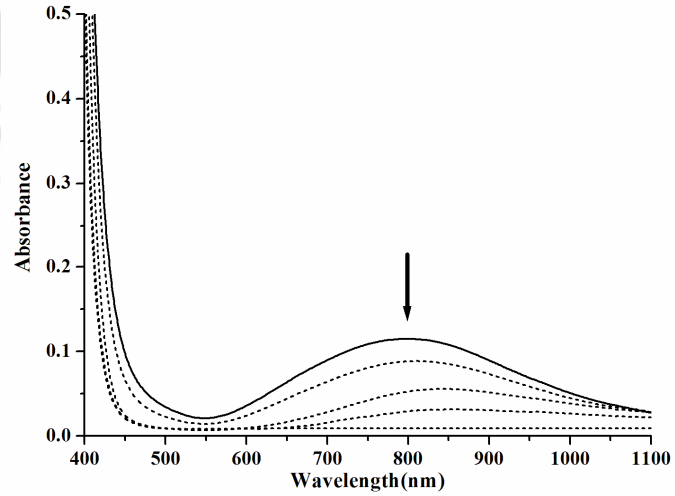

Figure A2.39 UV-visible spectra of complex **3.3** in methanol before (solid line) and after (dashed line) purging nitric oxide.

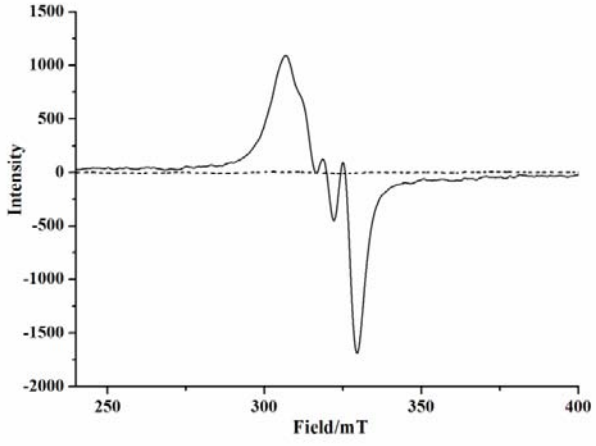

Figure A2.40 X-Band EPR spectra of complex **3.3** in methanol before (solid line) and after (dashed line) purging nitric oxide.

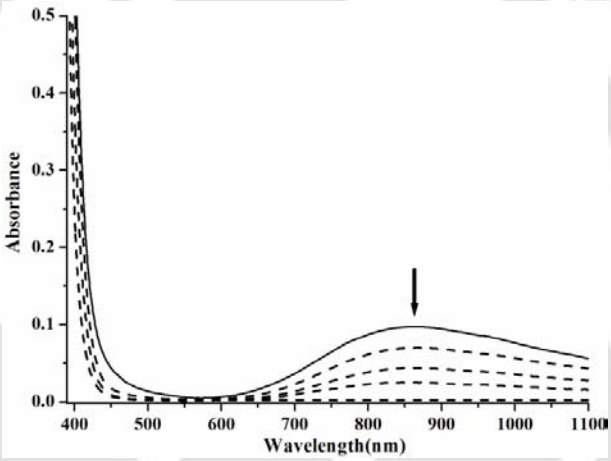

Figure A2.41 UV-visible spectra of complex **3.4** in methanol before (solid line) and after (dashed line) purging nitric oxide.

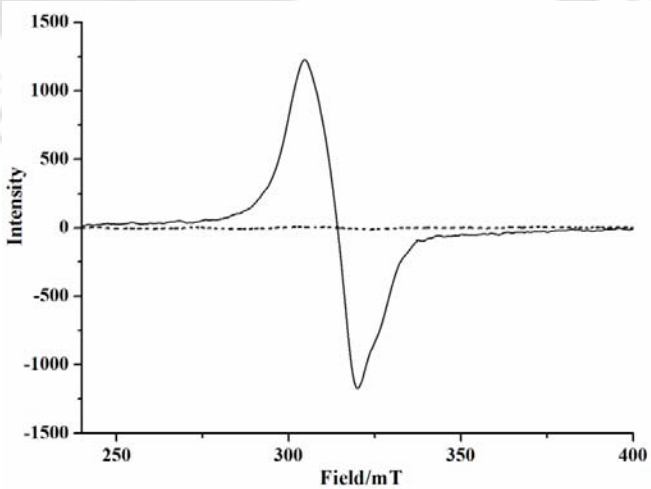

Figure A2.42 X-Band EPR spectra of complex **3.4** in methanol before (solid line) and after (dashed line) purging nitric oxide.

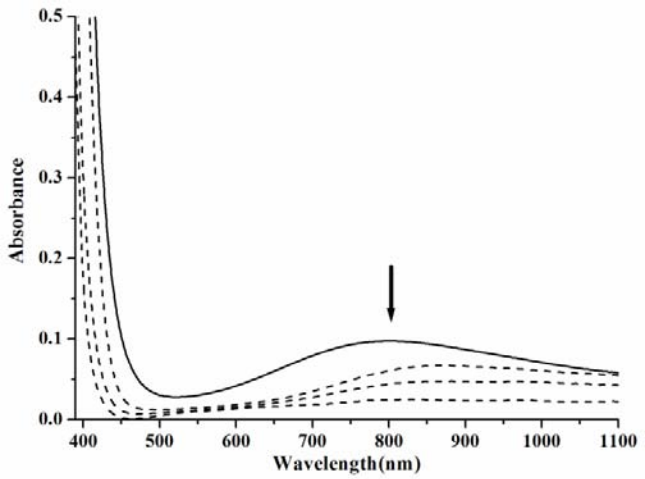

Figure A2.43 UV-visible spectra of complex **3.5** in methanol before (solid line) and after (dashed line) purging nitric oxide.

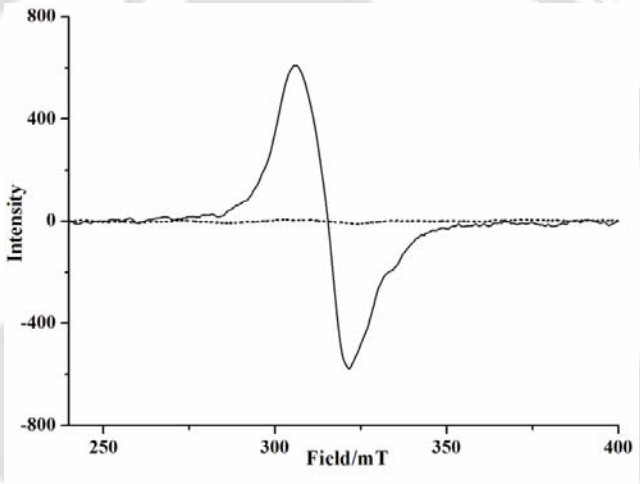

Figure A2.44 X-Band EPR spectra of complex **3.5** in methanol before (solid line) and after (dashed line) purging nitric oxide.

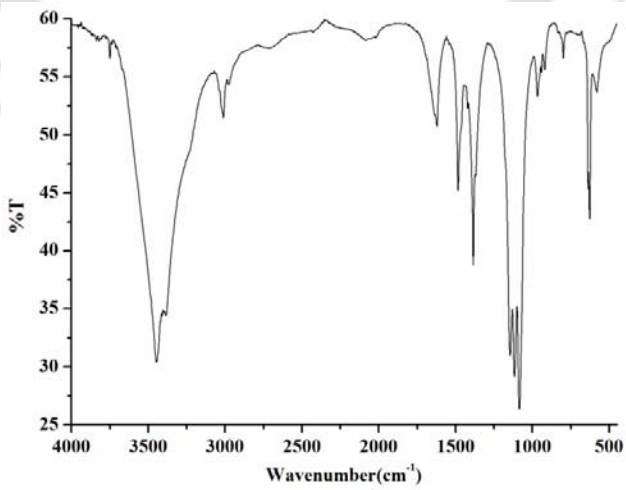

Figure A2.45 FT-IR spectrum of L_5' in KBr pellet.

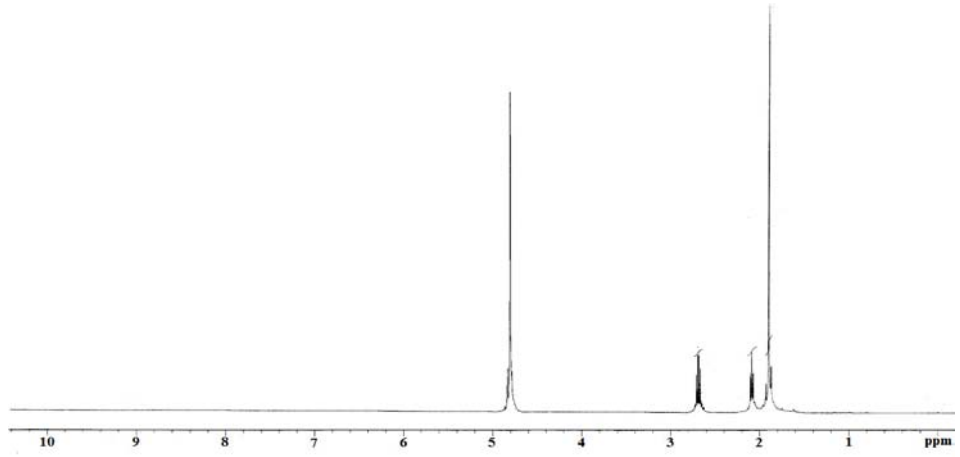

Figure A2.46 ^{1}H-NMR spectrum of $\mathbf{L_5'}$ in D_2O.

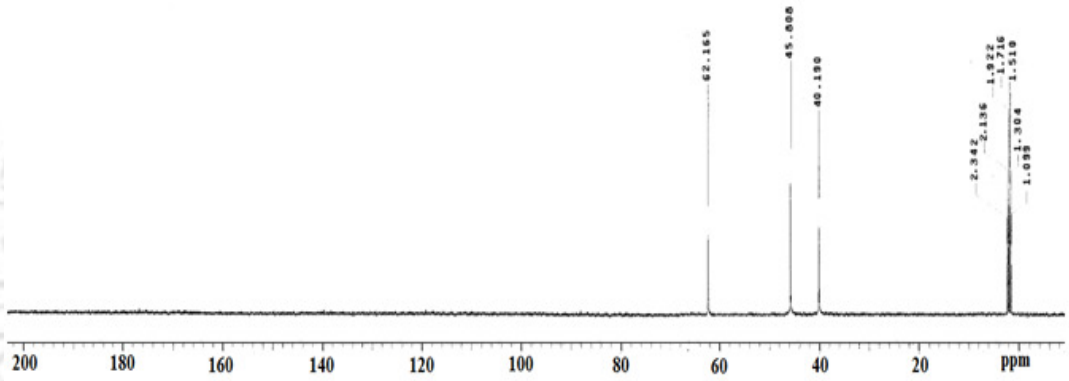

Figure A2.47 ^{13}C-NMR spectrum of $\mathbf{L_5'}$ in D_2O and CD_3CN mixture.

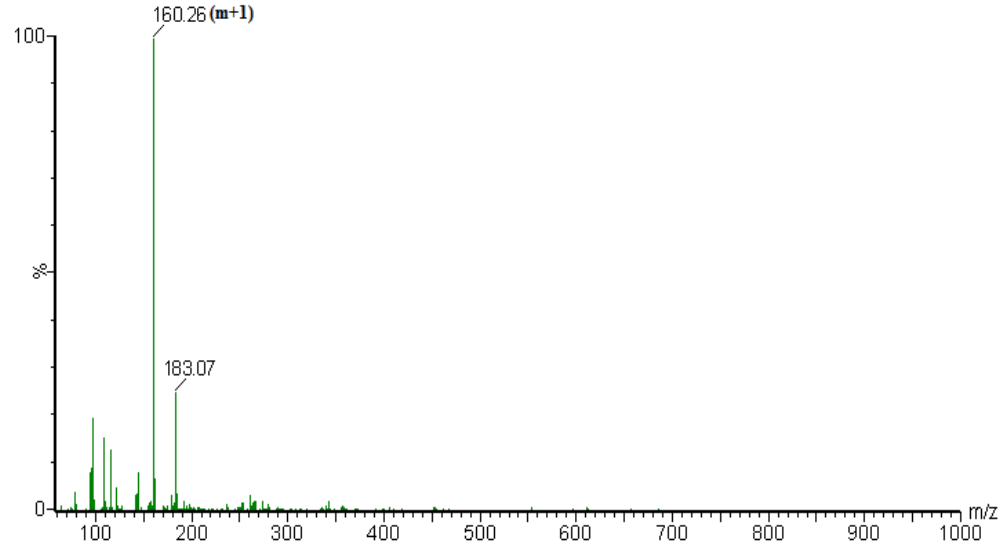

Figure A2.48 ESI-Mass spectrum of $\mathbf{L_5'}$ in methanol.

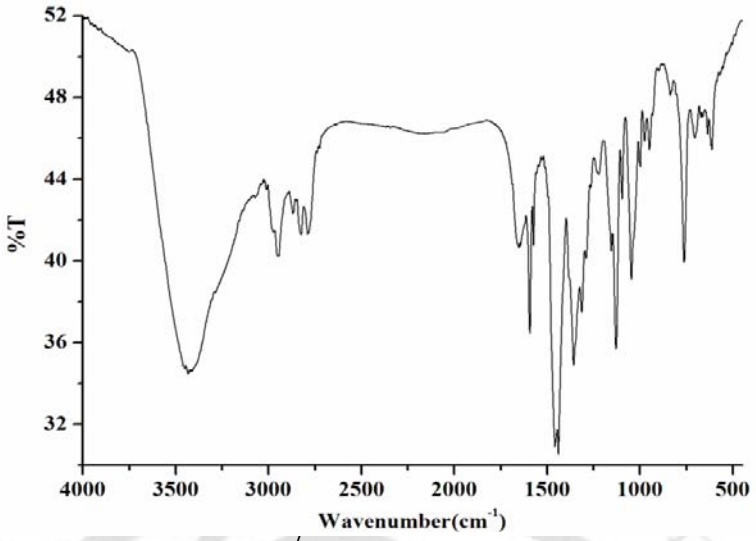

Figure A2.49 FT-IR spectrum of $\mathbf{L_6'}$ in KBr pellet.

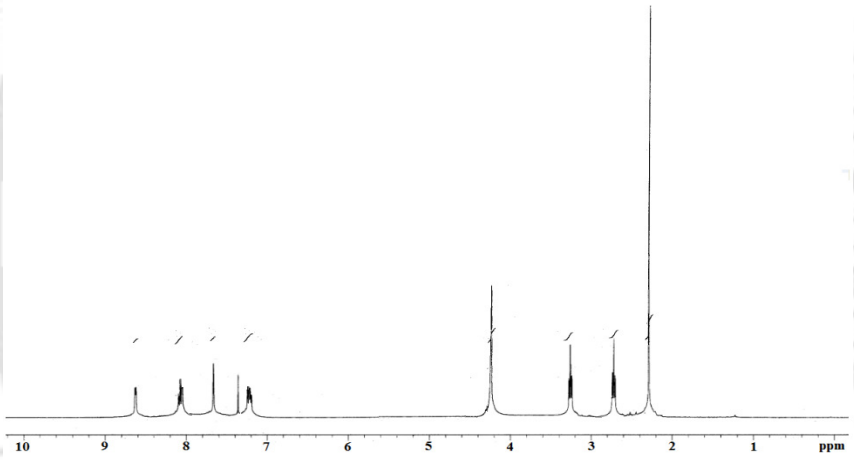

Figure A2.50 ^{1}H-NMR spectrum of $\mathbf{L_6'}$ in $CDCl_3$.

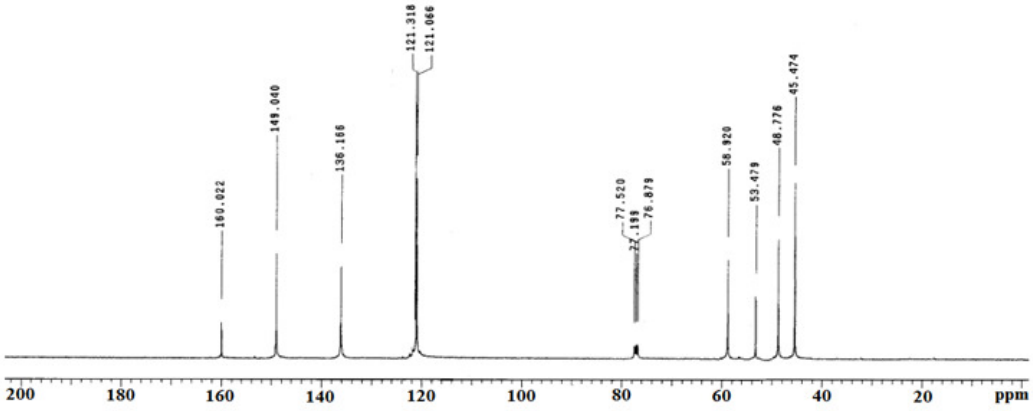

Figure A2.51 ^{13}C-NMR spectrum of $\mathbf{L_6'}$ in $CDCl_3$.

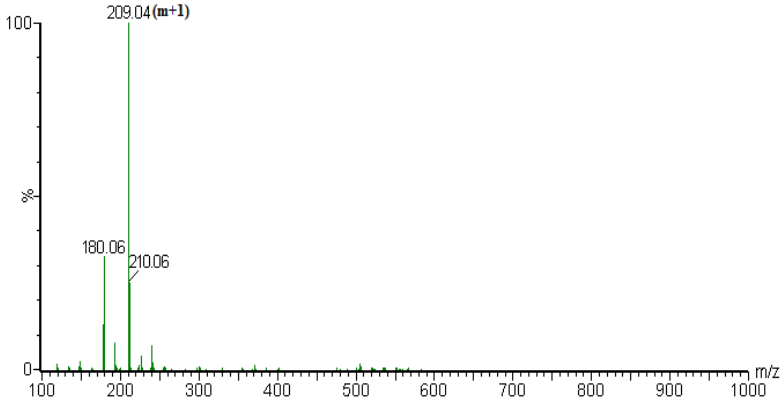

Figure A2.52 ESI-Mass spectrum of $\mathbf{L_6'}$ in methanol.

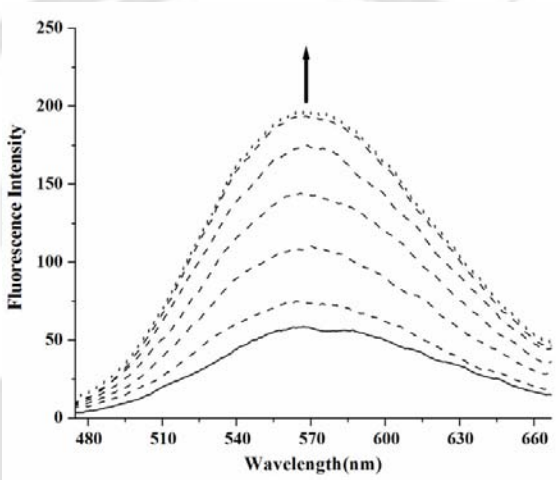

Figure A2.53 Fluorescence responses (λ_{ex}, 342 nm) of deoxygenated tris-buffer solution of complex **3.3** (10μM) before (solid line) and after (dashed lines) purging of 5 equivalent of nitric oxide at 2, 4, 6, 8, 10 and 15 minutes at 298 K (lines I – VI, respectively).

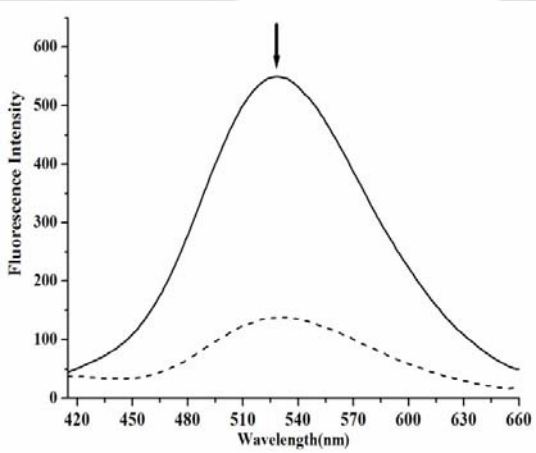

Figure A2.54 Fluorescence responses (λ_{ex}, 342 nm) for 20 μM solution of free ligand, $\mathbf{L_8}$ (dotted line) and after addition of one equivalent of $[Cu(H_2O)_2]Cl_2$(10μM) in methanol (solid line).

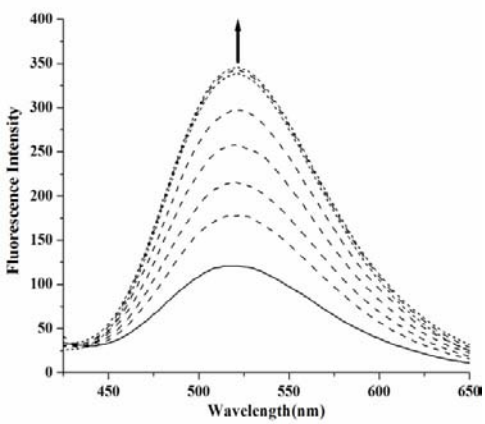

Figure A2.55 Fluorescence responses (λ_{ex}, 342 nm) of deoxygenated methanol solution complex **3.4** (10μM) of before (solid line) and after (dashed lines) purging of 5 equivalent of nitric oxide at 0.5, 1, 2, 3, 4 and 5 minutes at 298 K (lines I – VI, respectively).

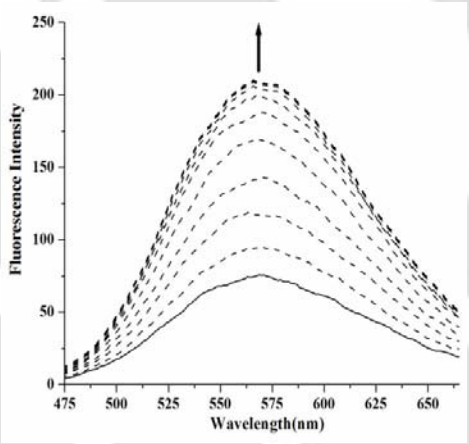

Figure A2.56 Fluorescence responses (λ_{ex}, 342 nm) of deoxygenated tris-buffer solution of complex **3.4** (10μM) before (solid line) and after (dashed lines) purging of 5 equivalent of nitric oxide at 1, 2, 3, 4, 5, 6, 7 and 8 minutes at 298 K (lines I – VII, respectively).

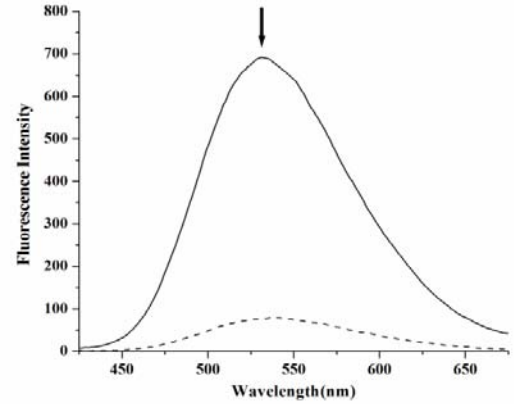

Figure A2.57 Fluorescence responses (λ_{ex}, 342 nm) for 20 μM solution of free ligand, **L_9** (dotted line) and after addition of one equivalent of $[Cu(H_2O)_2]Cl_2$(20μM) in methanol (solid line).

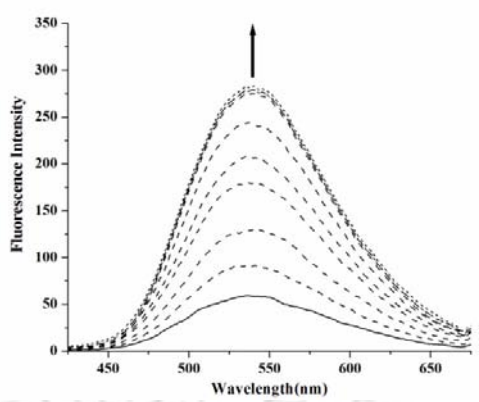

Figure A2.58 Fluorescence responses (λ_{ex}, 342 nm) of deoxygenated methanol solution(20μM) of complex **3.5** before (solid line) and after (dashed lines) purging of 10 equivalent of nitric oxide at 1, 3, 6, 9, 12, 15, 18 and 20 minutes at 298 K (lines I – VI, respectively).

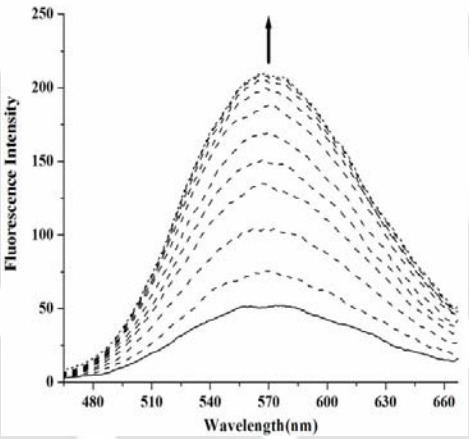

Figure A2.59 Fluorescence responses (λ_{ex}, 342 nm) of deoxygenated tris-buffer solution of complex **3.5** (20μM) before (solid line) and after (dashed lines) purging of 15 equivalent of nitric oxide at 2, 5, 10, 15, 20, 25, 30 and 35 minutes at 298 K (lines I – VIII, respectively).

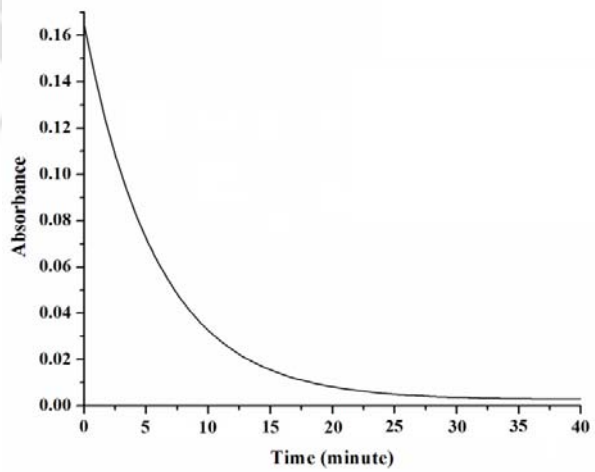

Figure A2.60 Time scan plot of complex **3.1** (λ_{max}= 556 nm) after reaction with nitric oxide in methanol at room temperature.

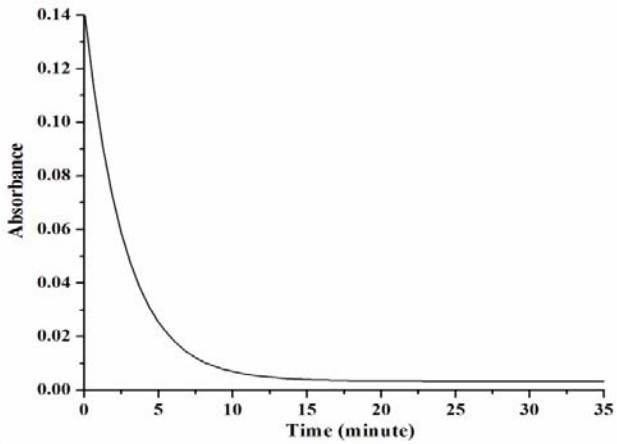

Figure A2.61 Time scan plot of complex **3.2** (λ_{max}= 599 nm) after reaction with nitric oxide in methanol at room temperature.

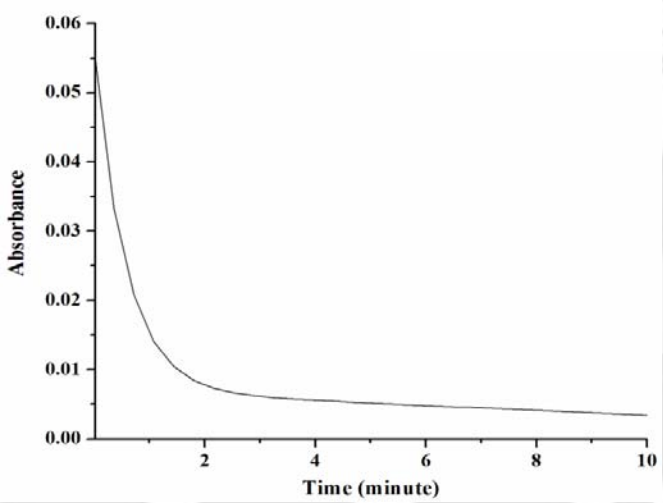

Figure A2.62 Time scan plot of complex **3.3** (λ_{max}= 799 nm) after reaction with nitric oxide in methanol at room temperature.

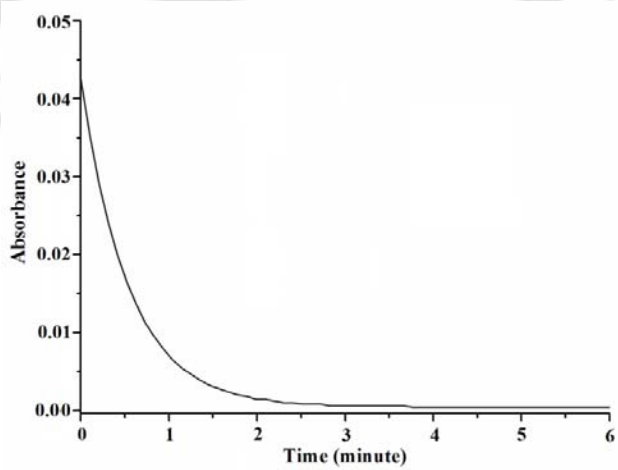

Figure A2.63 Time scan plot of complex **3.4** (λ_{max}= 866 nm) after reaction with nitric oxide in methanol at room temperature.

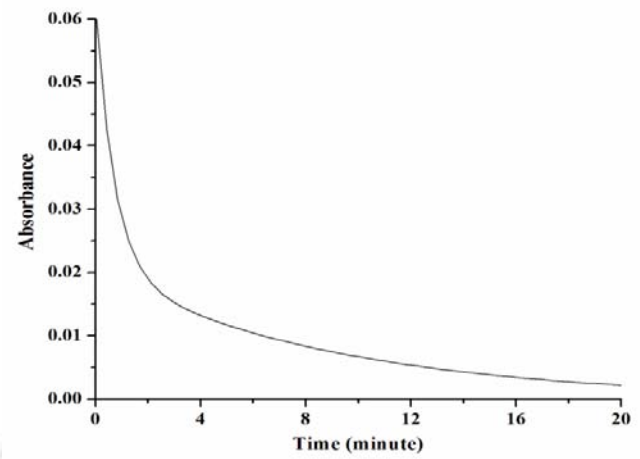

Figure A2.64 Time scan plot of complex **3.5** (λ_{max}= 795 nm) after reaction with nitric oxide in methanol at room temperature.

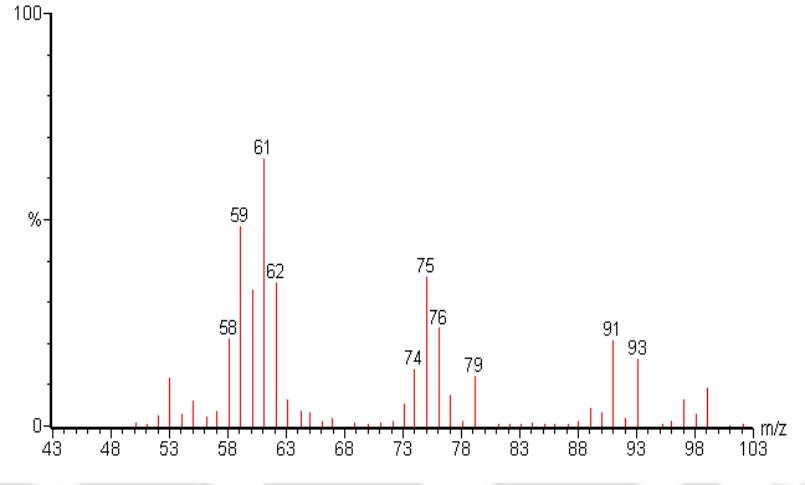

Figure A2.65 Gas chromatographic mass spectrum of complex **3.3** after purging nitric oxide in methanol.

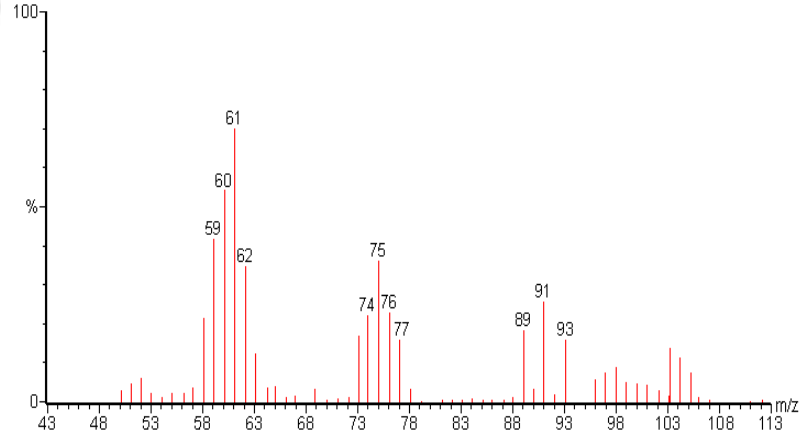

Figure A2.66 Gas chromatographic mass spectrum of complex **3.4** after purging nitric oxide in methanol.

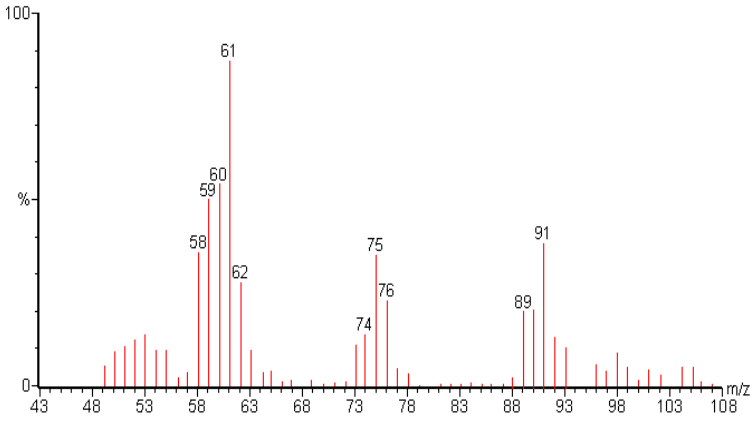

Figure A2.67 Gas chromatographic mass spectrum of complex **3.5** after purging nitric oxide in methanol.

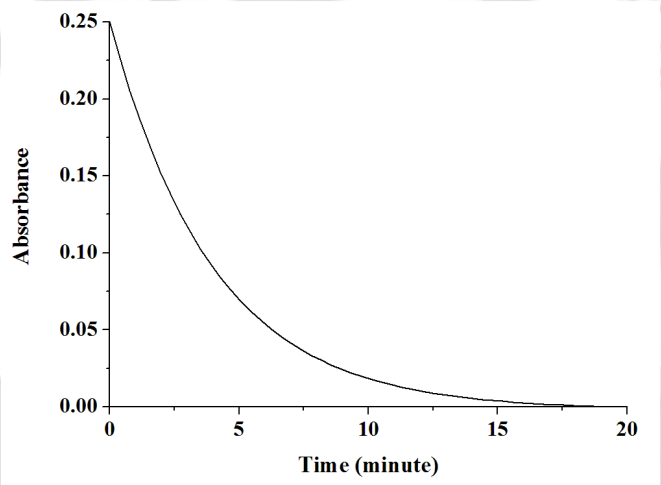

Figure A2.68 Time scan plot of complex **3.1** (λ_{max}= 600 nm) after reaction with nitric oxide in acetonitrile at room temperature.

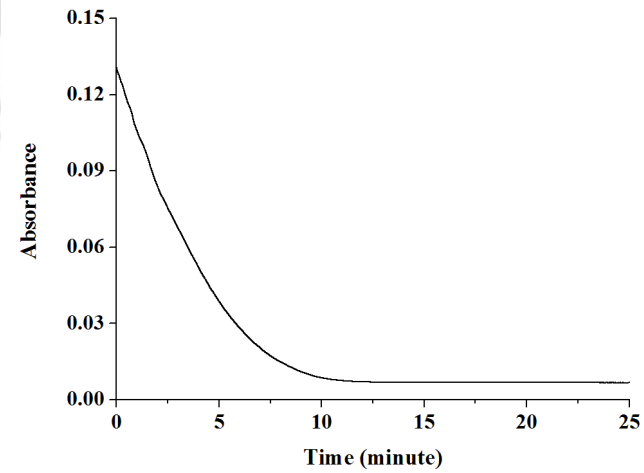

Figure A2.69 Time scan plot of complex **3.2** (λ_{max}= 608 nm) after reaction with nitric oxide in acetonitrile at room temperature.

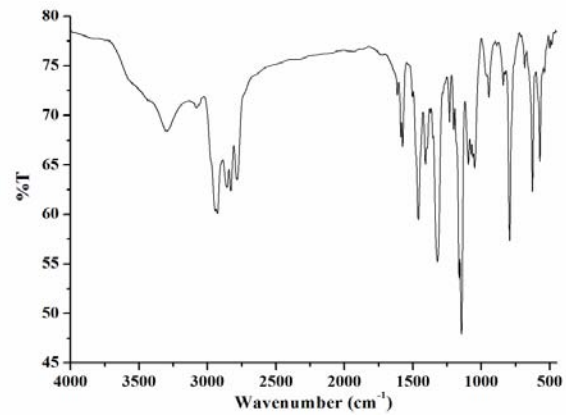

Figure A2.70 FT-IR spectrum of the crude mass obtained after reaction of complex **3.3** with NO in KBr pellet.

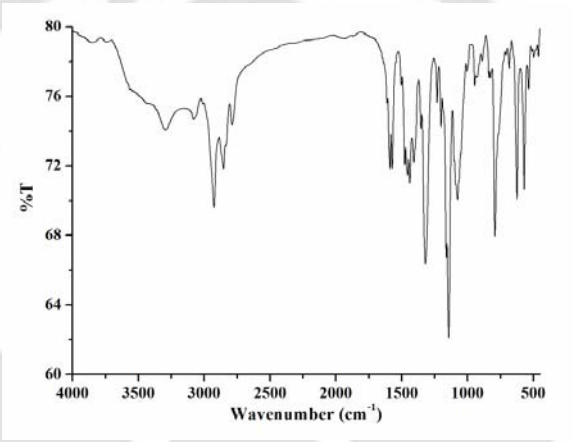

Figure A2.71 FT-IR spectrum of the crude mass obtained after reaction of complex **3.4** with NO in KBr pellet.

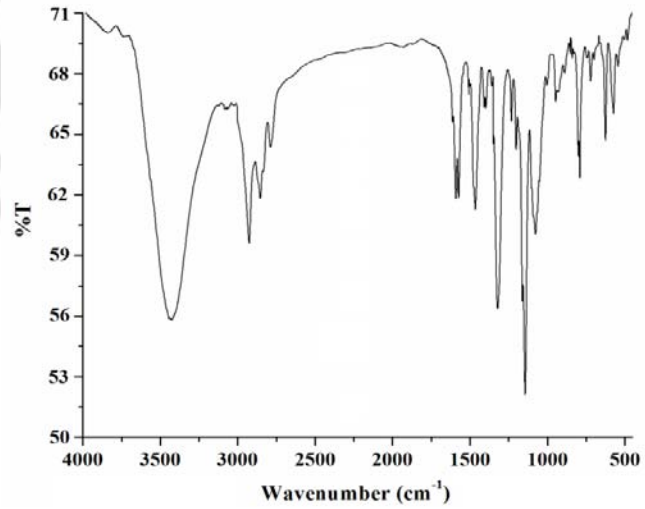

Figure A2.72 FT-IR spectrum of the crude mass obtained after reaction of complex **3.5** with NO in KBr pellet.

Appendix III

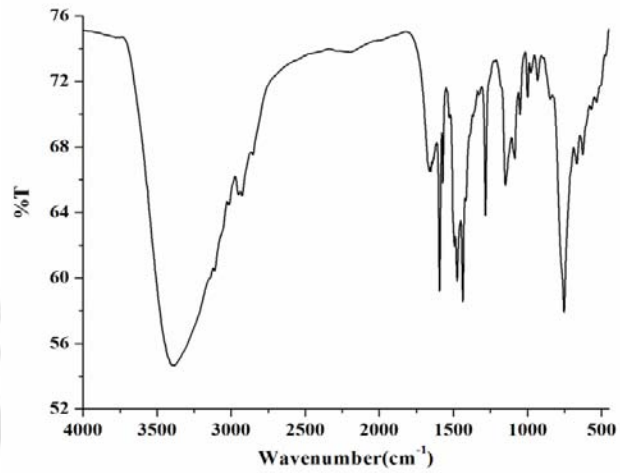

Figure A3.1 FT-IR spectrum of the $\mathbf{L_{10}}$ in KBr pellet.

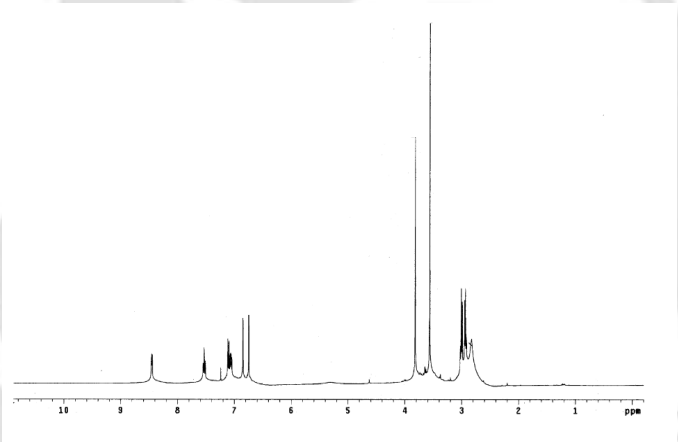

Figure A3.2 ^{1}H-NMR spectrum of $\mathbf{L_{10}}$ in $CDCl_3$.

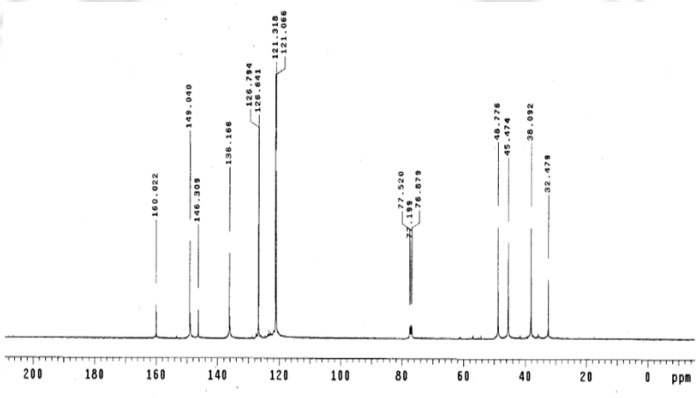

Figure A3. 3 ^{13}C-NMR spectrum of $\mathbf{L_{10}}$ in $CDCl_3$.

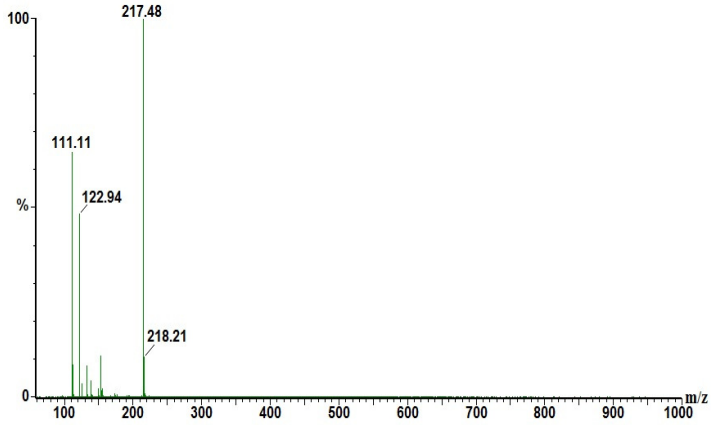

Figure A3. 4 ESI-mass spectrum for $\mathbf{L_{10}}$ in methanol.

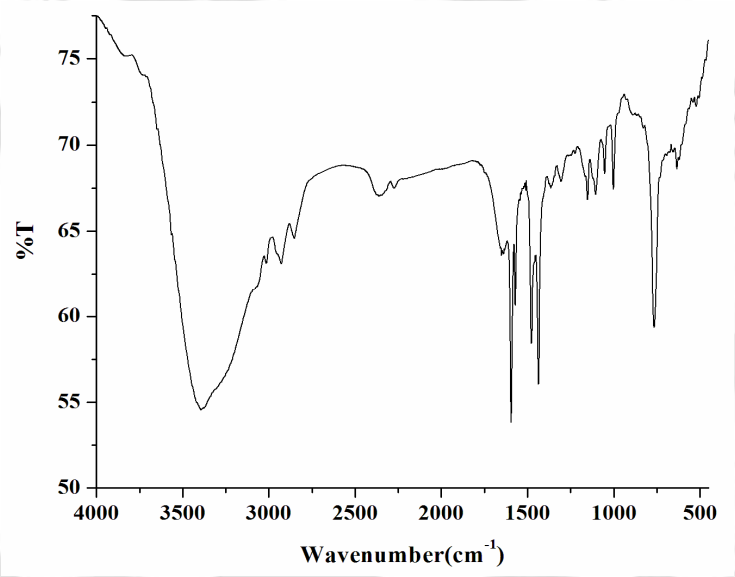

Figure A3. 5 FT-IR spectrum of the $\mathbf{L_{11}}$ in KBr pellet.

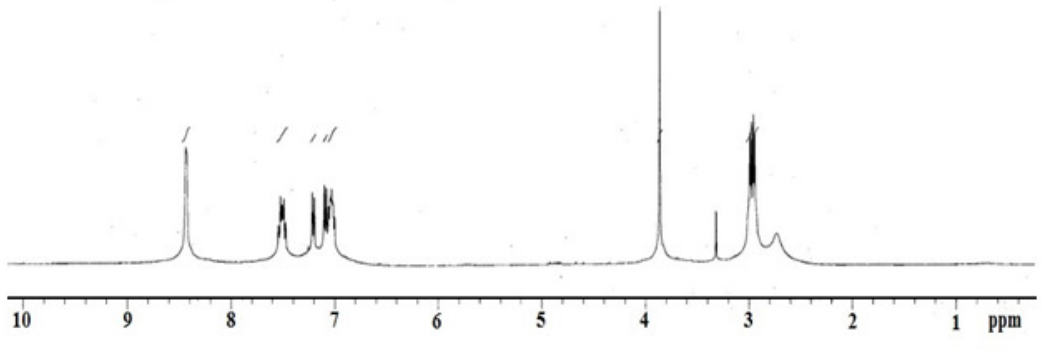

Figure A3. 6 ^{1}H-NMR spectrum of $\mathbf{L_{11}}$ in $CDCl_3$.

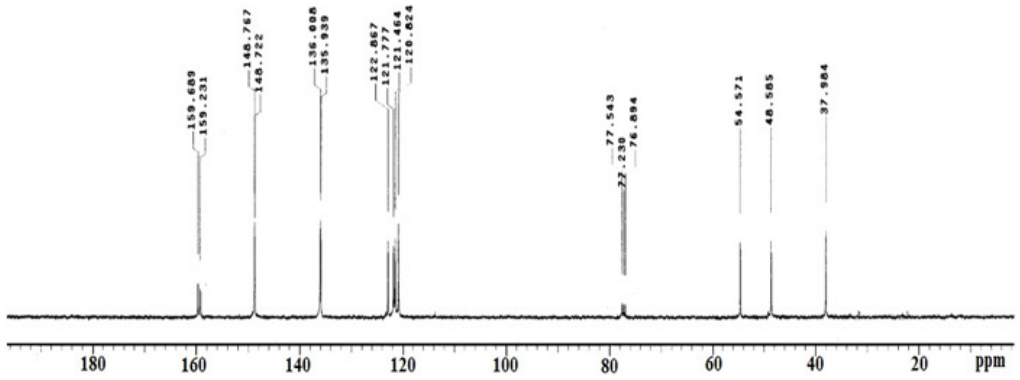

Figure A3. 7 ^{13}C-NMR spectrum of $\mathbf{L_{11}}$ in $CDCl_3$.

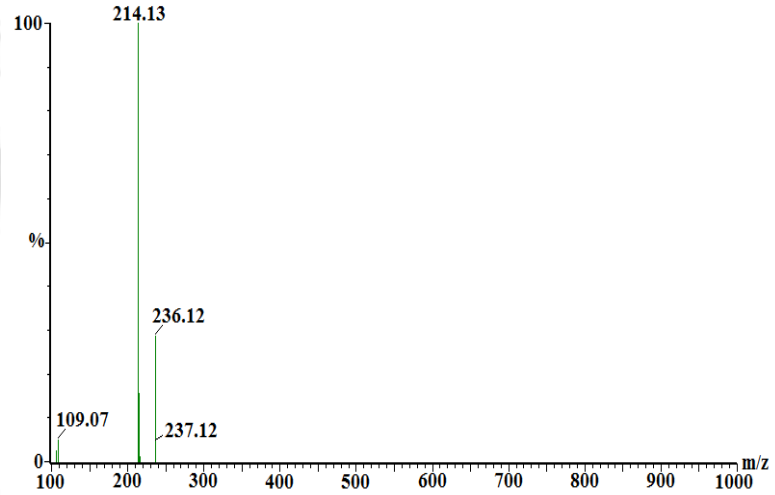

Figure A3. 8 ESI-mass spectrum for $\mathbf{L_{11}}$ in methanol.

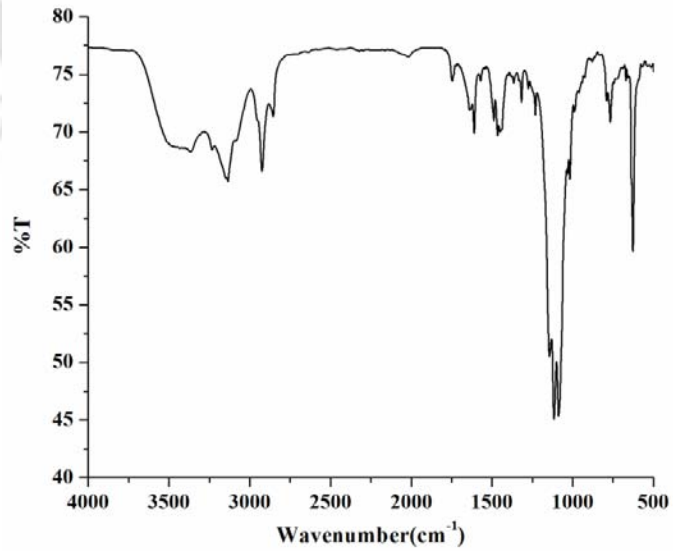

Figure A3. 9 FT-IR spectrum of complex **4.1** in KBr pellet.

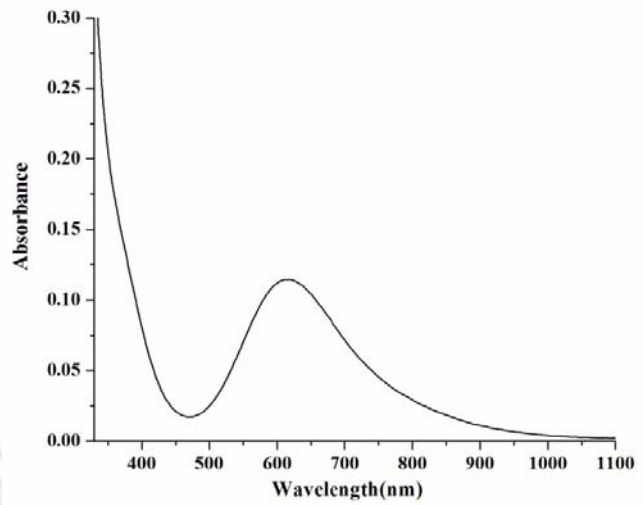

Figure A3. 10 UV-visible spectrum of complex **4.1** in acetonitrile.

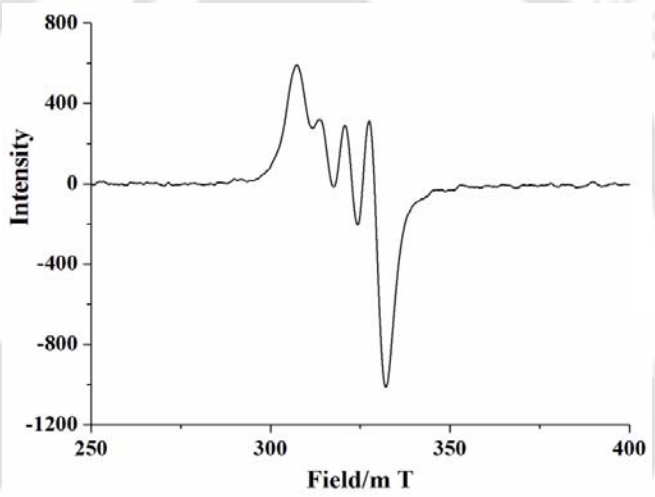

Figure A3. 11 X-Band EPR spectrum of complex **4.1** in acetonitrile at 298K.

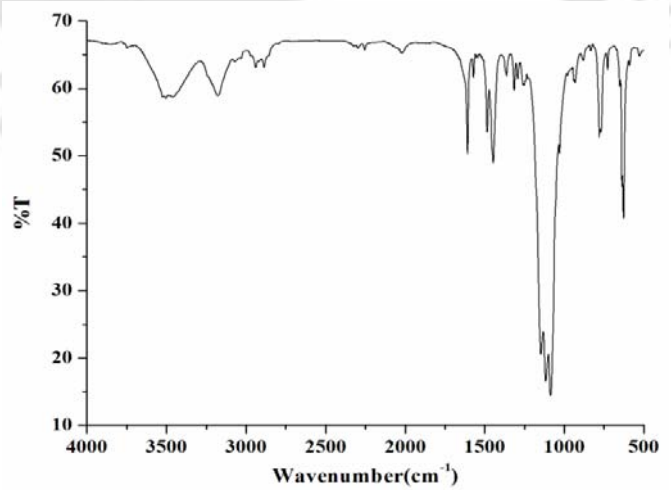

Figure A3. 12 FT-IR spectrum of the complex **4.2** in KBr pallet.

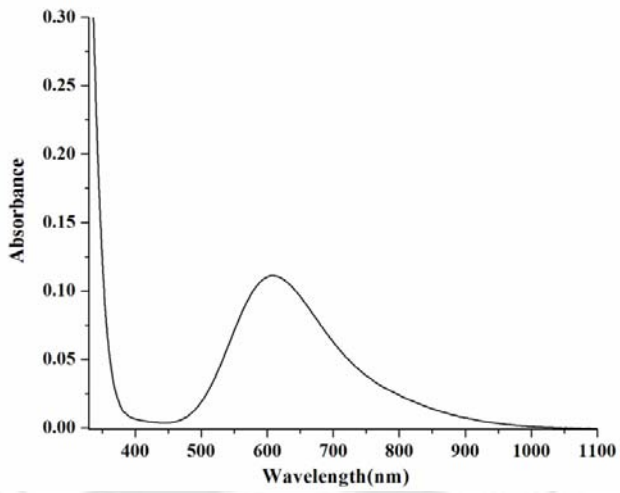

Figure A3. 13 UV-visible spectrum of complex **4.2** in acetonitrile.

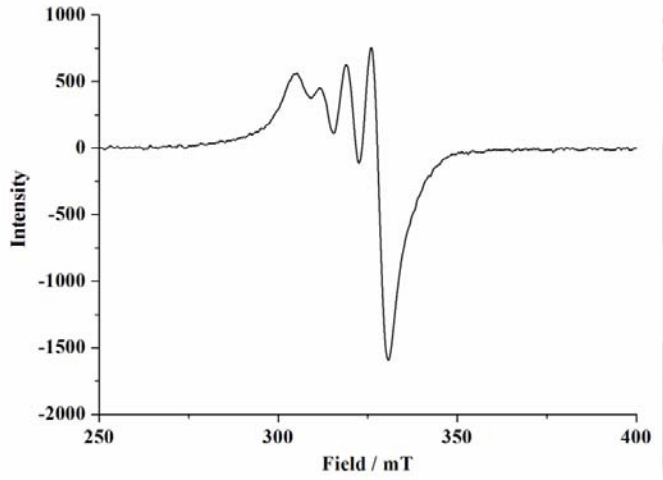

Figure A3. 14 X-Band EPR spectrum of complex **4.2** in acetonitrile at 298K.

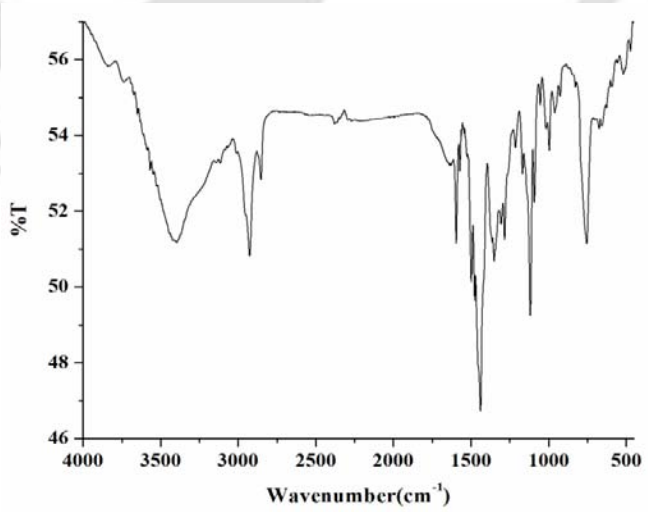

Figure A3. 15 FT-IR spectrum of $\mathbf{L_{10}}''$ in KBr pellet.

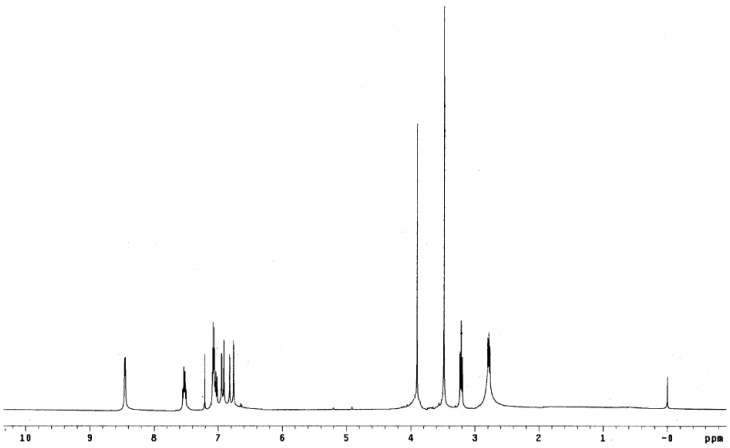

Figure A3. 16 ^{1}H-NMR spectrum of $\mathbf{L_{10}''}$ in $CDCl_3$.

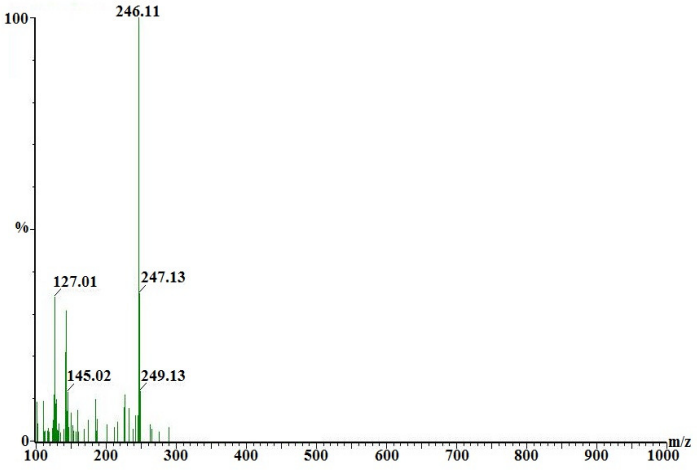

Figure A3. 17 ESI-mass spectrum of $\mathbf{L_{10}''}$ in methanol.

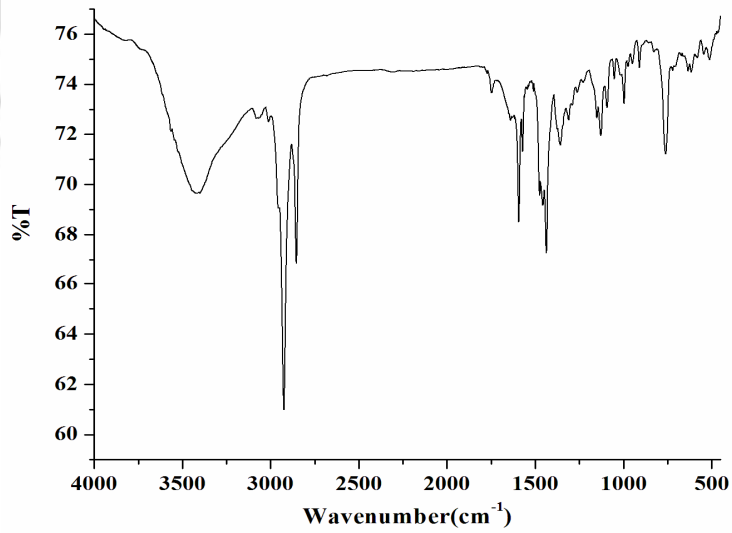

Figure A3. 18 FT-IR spectrum of $\mathbf{L_{11}''}$ in KBr pellet.

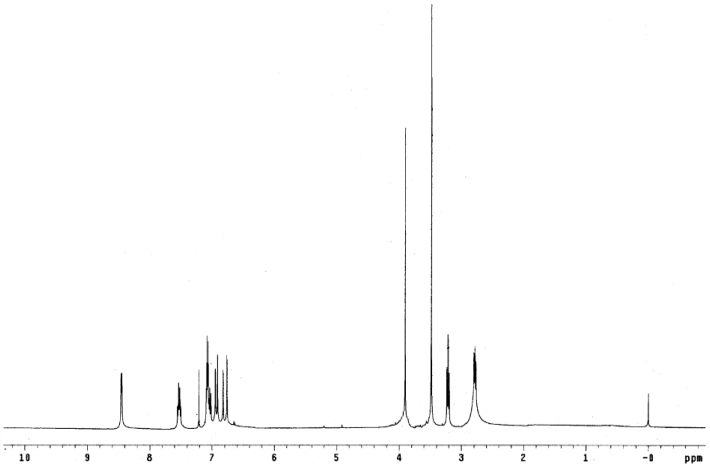

Figure A3. 19 ^{1}H NMR spectrum of $\mathbf{L_{11}''}$ in $CDCl_3$.

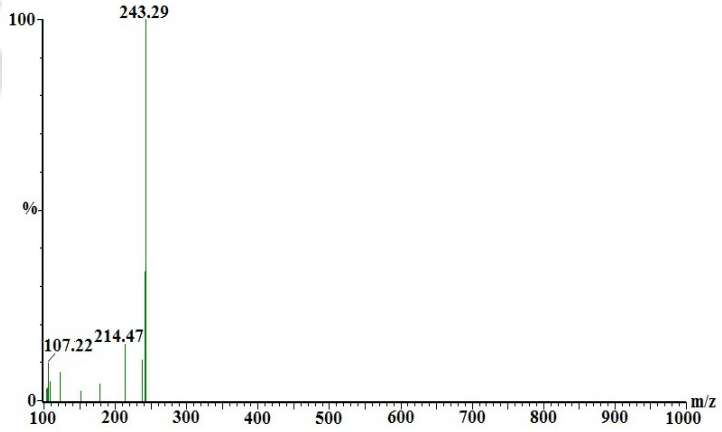

Figure A3. 20 ESI-mass spectrum of $\mathbf{L_{11}''}$ in methanol.

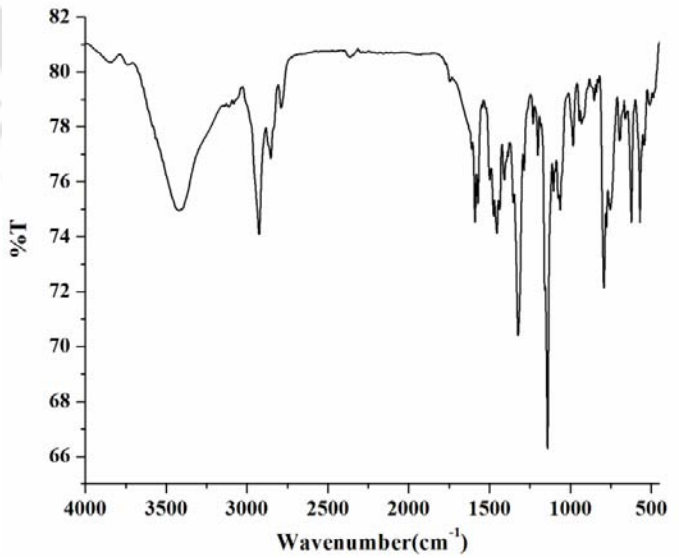

Figure A3. 21 FT-IR spectrum of $\mathbf{L_{12}}$ in KBr pellet.

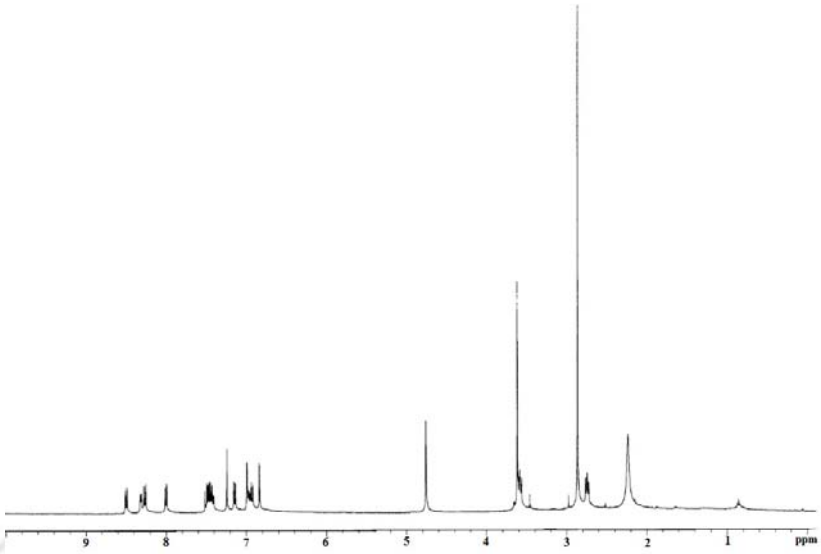

Figure A3. 22 ^{1}H-NMR spectrum of $\mathbf{L_{12}}$ in $CDCl_3$.

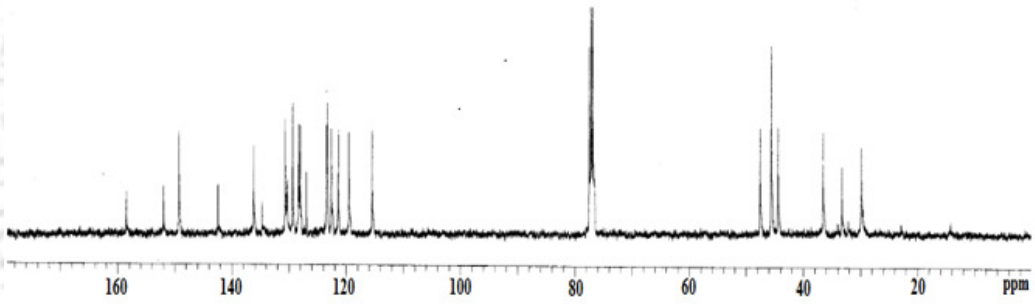

Figure A3. 23 ^{13}C-NMR spectrum of $\mathbf{L_{12}}$ in $CDCl_3$.

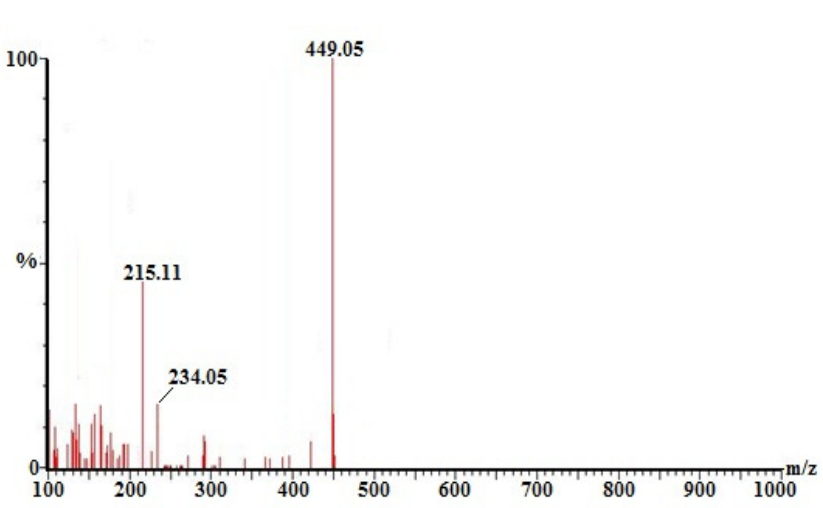

Figure A3. 24 ESI-mass spectrum of $\mathbf{L_{12}}$ in methanol.

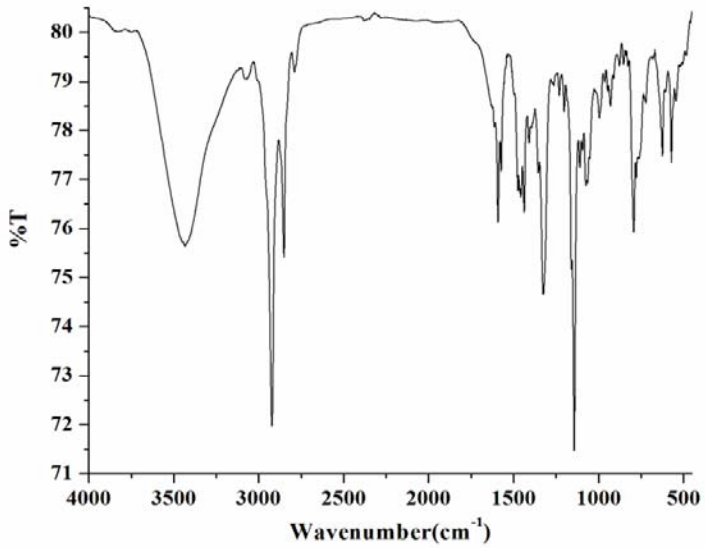

Figure A3. 25 FT-IR spectrum of $\mathbf{L_{13}}$ in KBr pellet.

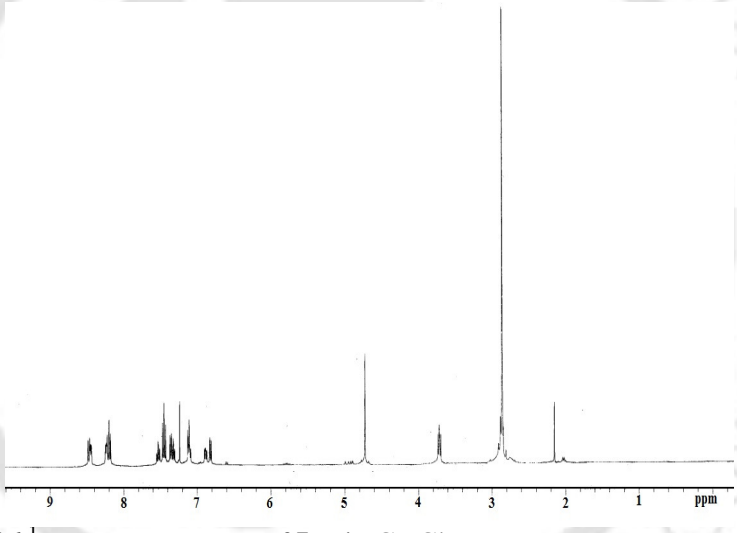

Figure A3. 26 ^{1}H-NMR spectrum of $\mathbf{L_{13}}$ in $CDCl_3$.

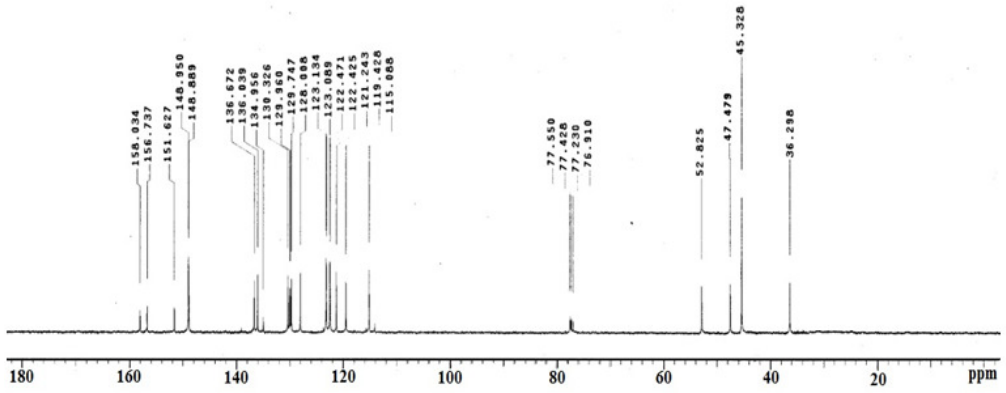

Figure A3. 27 ^{13}C-NMR spectrum of $\mathbf{L_{13}}$ in $CDCl_3$.

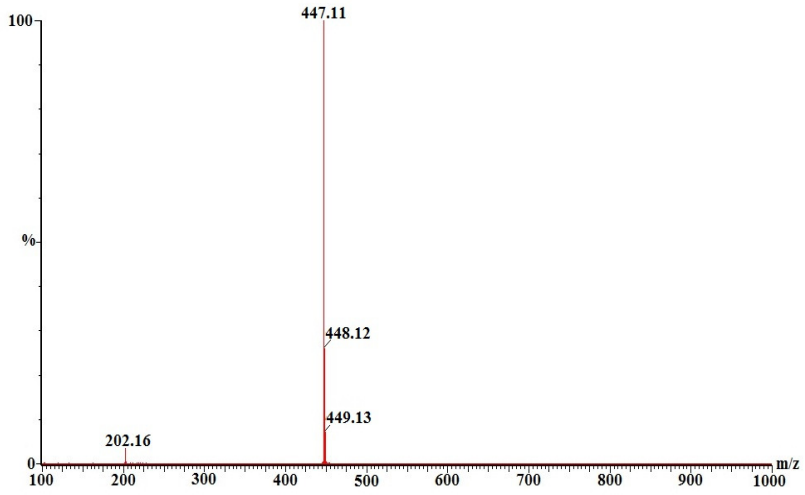

Figure A3. 28 ESI-mass spectrum of $\mathbf{L_{13}}$ in methanol.

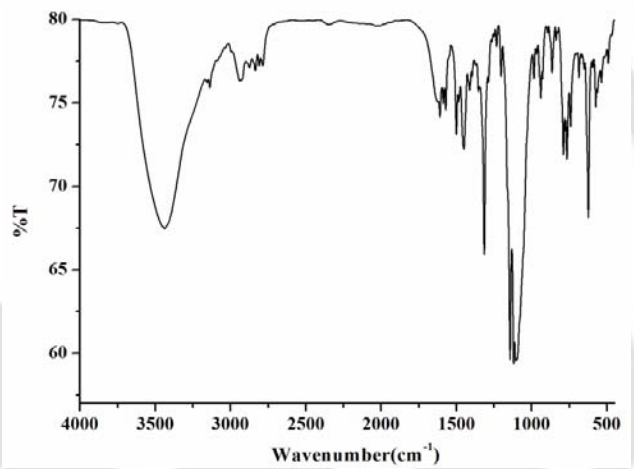

Figure A3. 29 FT-IR spectrum of complex **4.3** in KBr pellet.

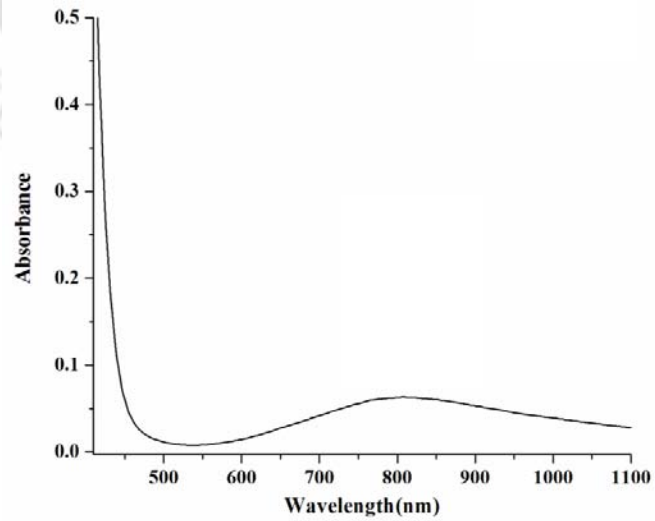

Figure A3. 30 UV-visible spectrum of complex **4.3** in methanol.

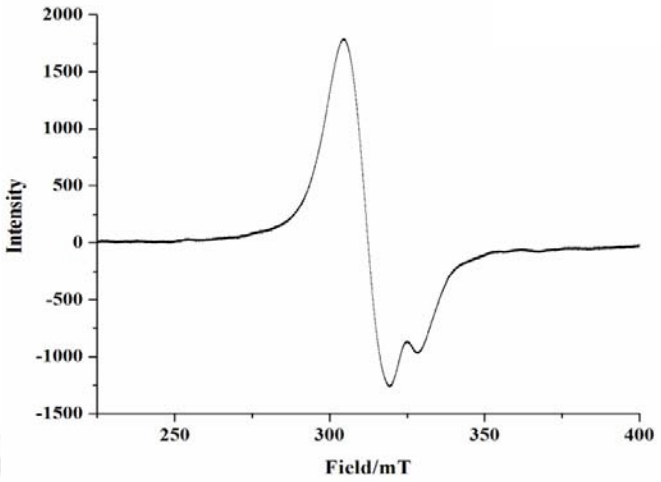

Figure A3. 31 X-Band EPR spectrum of complex **4.3** in methanol at 298K.

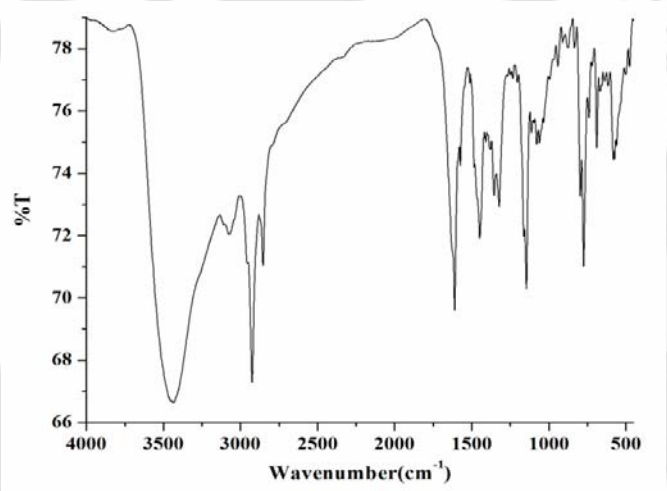

Figure A3. 32 FT-IR spectrum of complex **4.4** in KBr pellet.

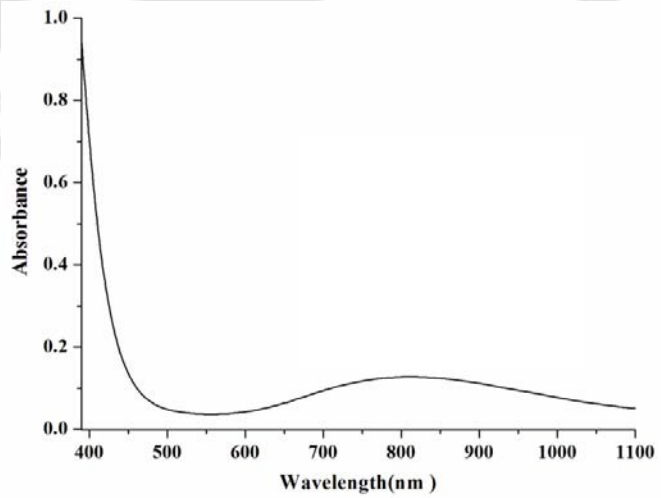

Figure A3. 33 UV-visible spectrum of complex **4.4** in methanol.

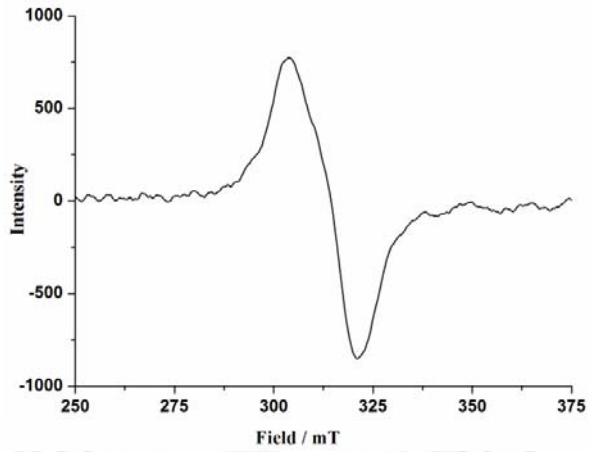

Figure A3. 34 X-Band EPR spectrum of complex **4.4** in methanol at 298K.

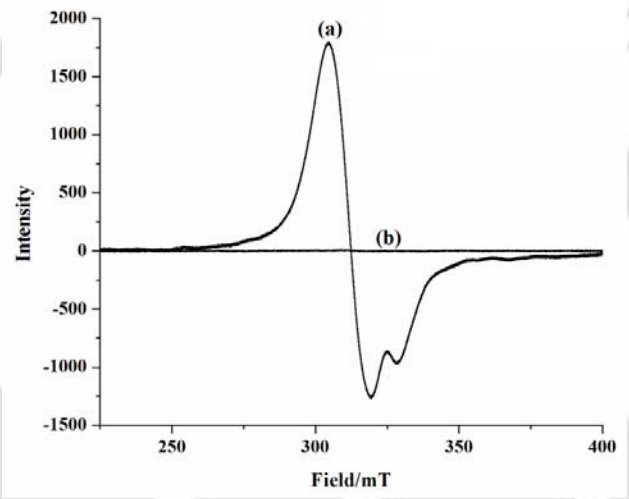

Figure A3. 35 X-Band EPR spectra of complex **4.3** in methanol before (a) and after (b) purging nitric oxide.

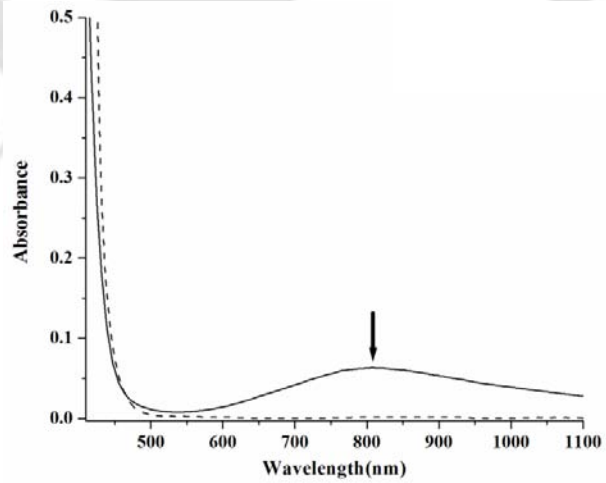

Figure A3. 36 UV-visible spectra of complex **4.3** in methanol before (solid line) and after (dashed line) purging nitric oxide.

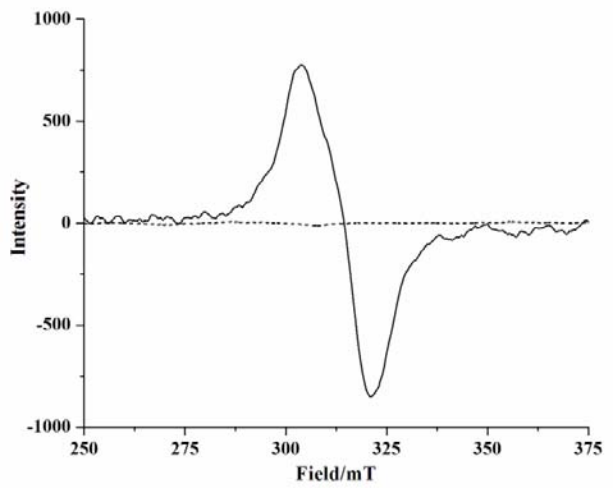

Figure A3. 37 X-Band EPR spectra of complex **4.4** in methanol before (solid line) and after (dashed line) purging nitric Oxide.

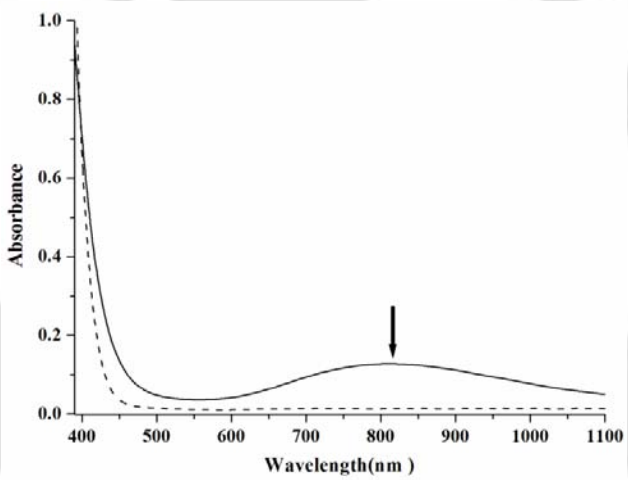

Figure A3. 38 UV-visible spectra of complex **4.4** in methanol before (solid line) and after (dashed line) purging nitric oxide.

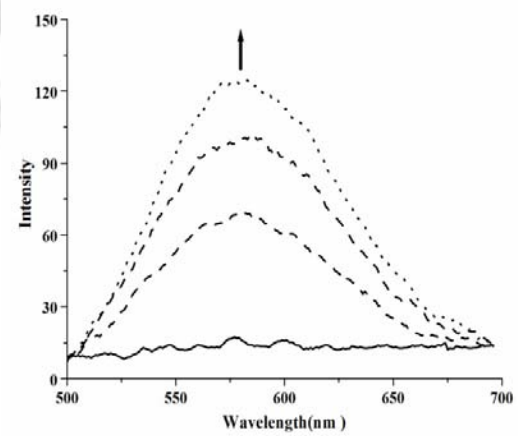

Figure A3.39 Fluorescence emission spectra of the complex **4.3** (25 μM) in water medium upon addition of excess NO.

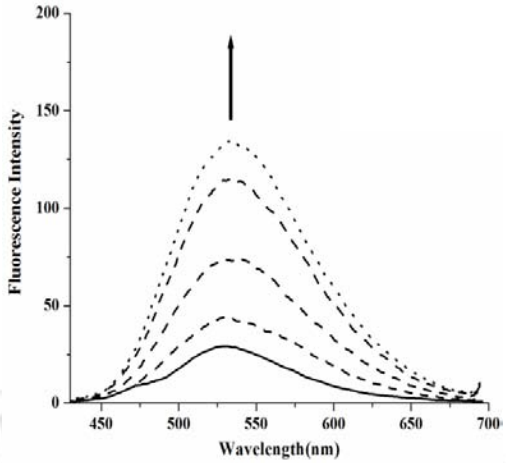

Figure A3. 40 Fluorescence emission spectra of the Complex **4.4** (25 μM) in water medium upon addition of excess NO.

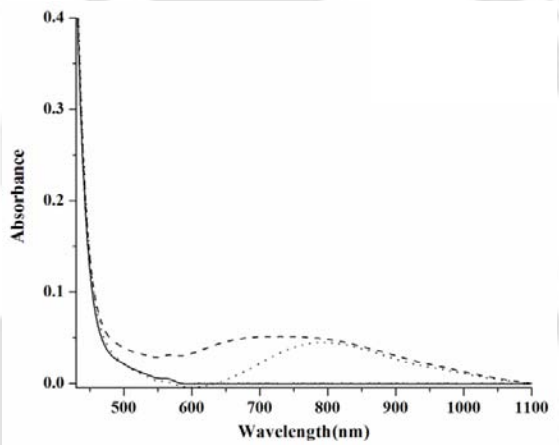

Figure A3. 41 UV-visible spectra of complex **4.3** in methanol before (dashed line) and after (solid line) nitric oxide and upon expose to oxygen (dotted line).

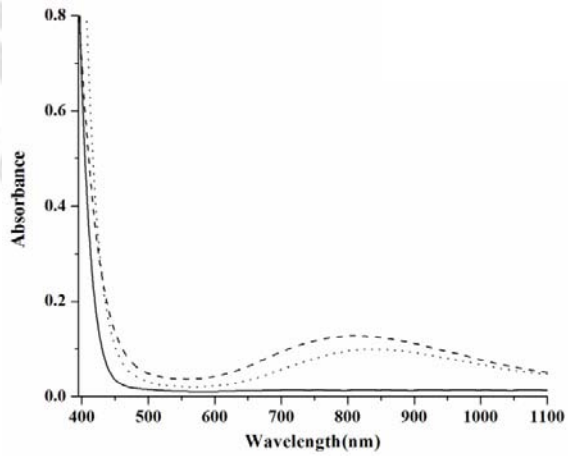

Figure A3. 42 UV-visible spectra of complex **4.4** in methanol before (dashed line) and after (solid line) nitric oxide and upon expose to oxygen (dotted line).

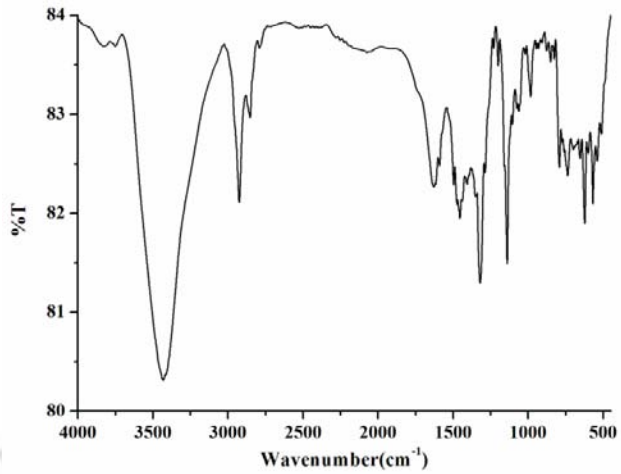

Figure A3. 43 FT-IR spectrum of complex **4.3** after reaction with nitric oxide in KBr pellet.

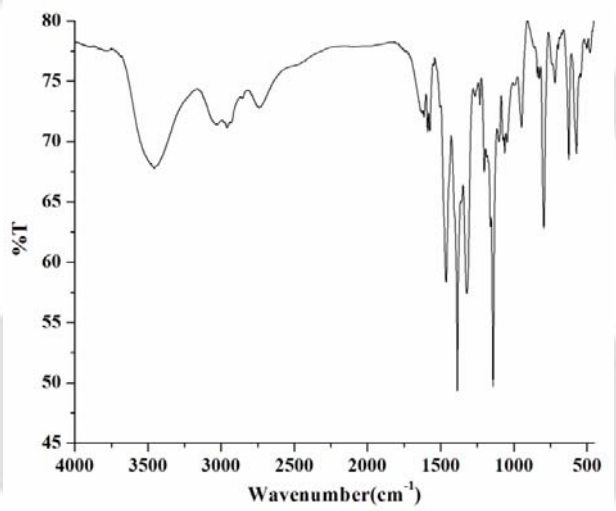

Figure A3. 44 FT-IR spectrum of complex **4.4** after reaction with nitric oxide in KBr pellet.

Appendix IV

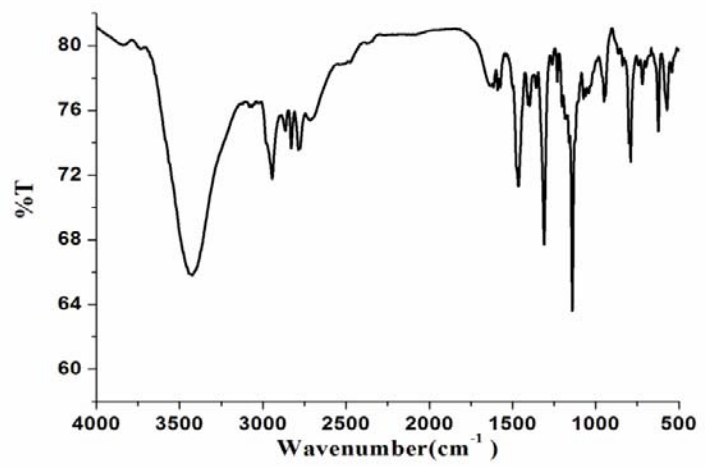

Figure A4.1 FT-IR spectrum of **L_{14}** in KBr pellet.

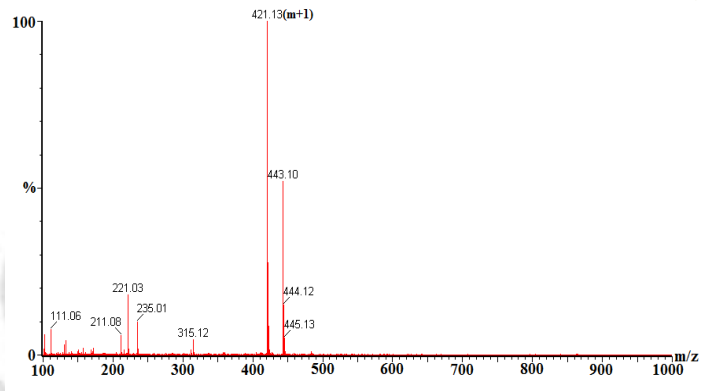

Figure A4.2 ESI-Mass spectrum for **L_{14}** in methanol.

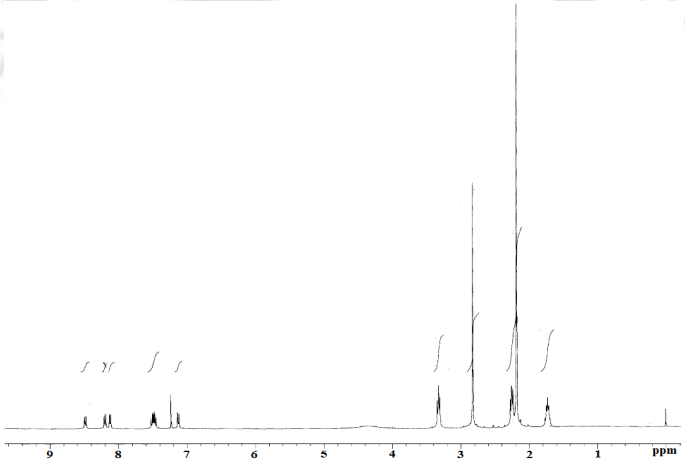

Figure A4.3 ^{1}H-NMR spectrum of **L_{14}** in $CDCl_3$.

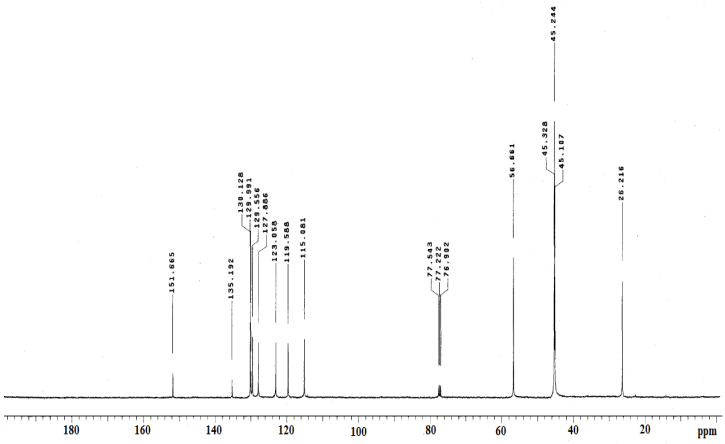

Figure A4.4 ^{13}C-NMR spectrum of **L_{14}** in $CDCl_3$.

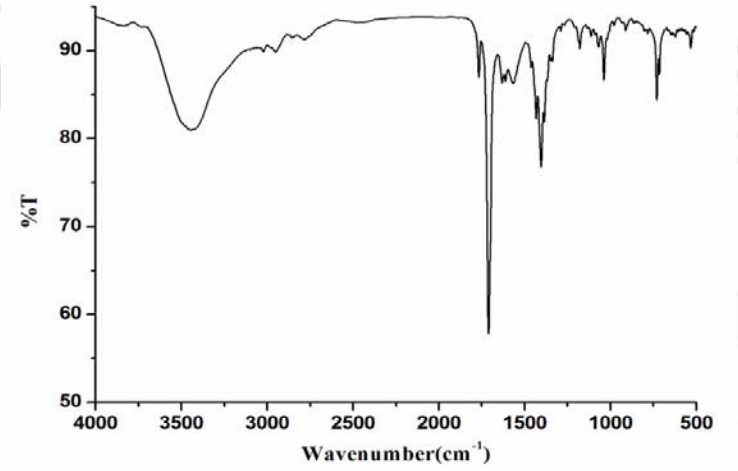

Figure A4.5 FT-IR spectrum of **L_{15}'** in KBr pellet.

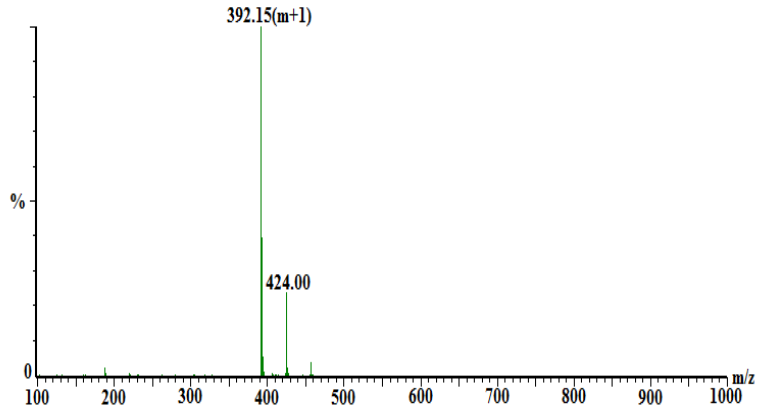

Figure A4.6 Mass spectrum for **L_{15}'** in methanol.

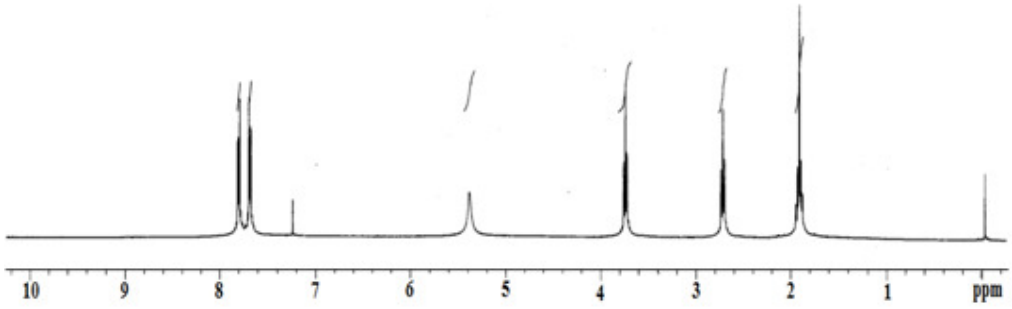

Figure A4.7 ^{1}H-NMR spectrum of $\mathbf{L_{15}}'$ in $CDCl_3$.

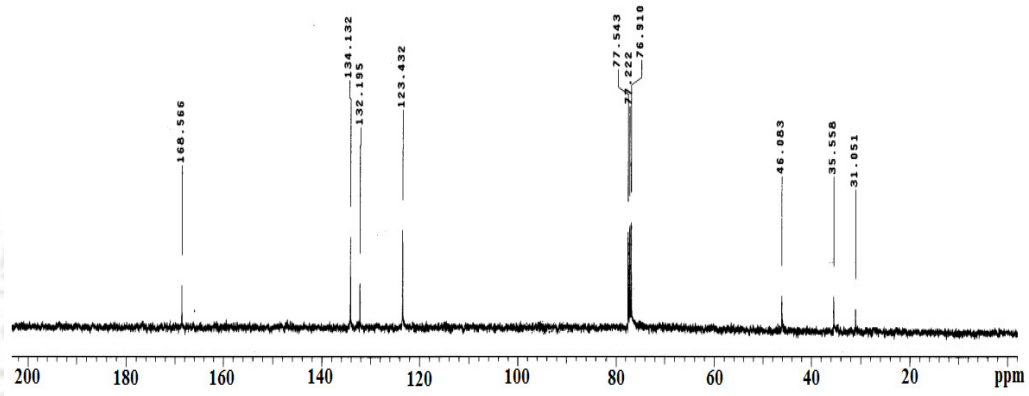

Figure A4.8 ^{13}C-NMR spectrum of $\mathbf{L_{15}}'$ in $CDCl_3$.

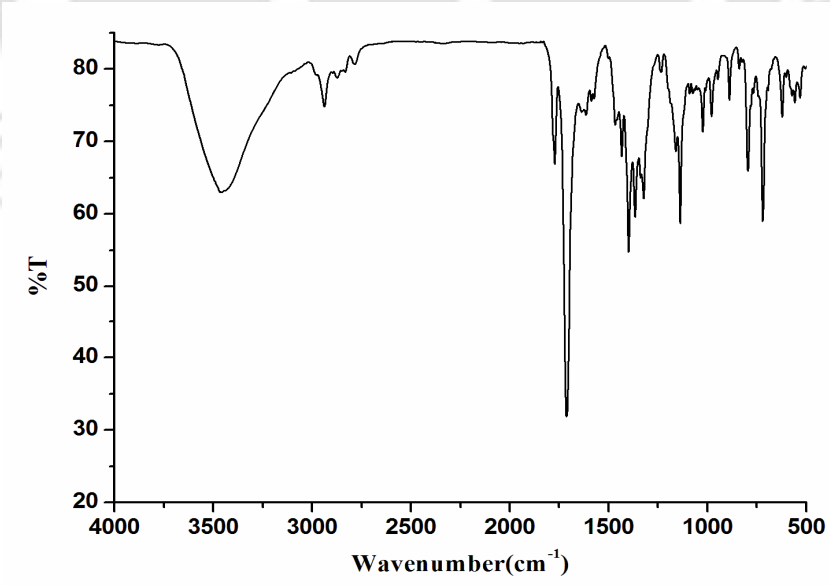

Figure A4.9 FT-IR spectrum of $\mathbf{L_{15}}''$ in KBr pellet.

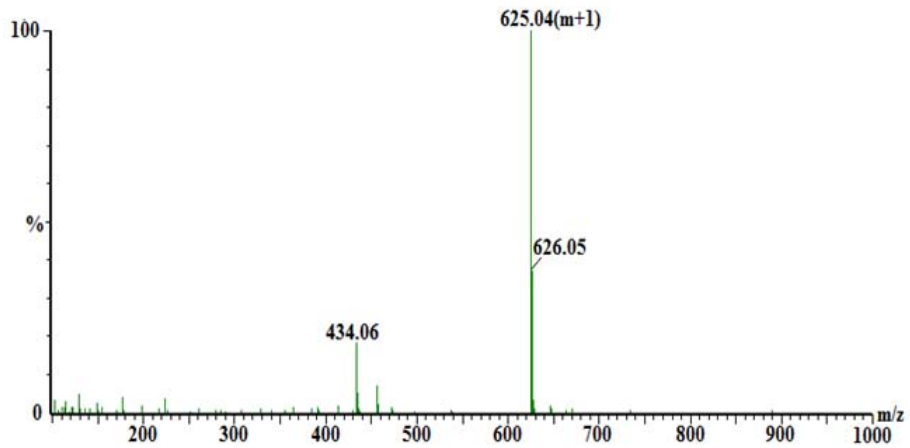

Figure A4.10 Mass spectrum for $\mathbf{L_{15}}''$ in methanol.

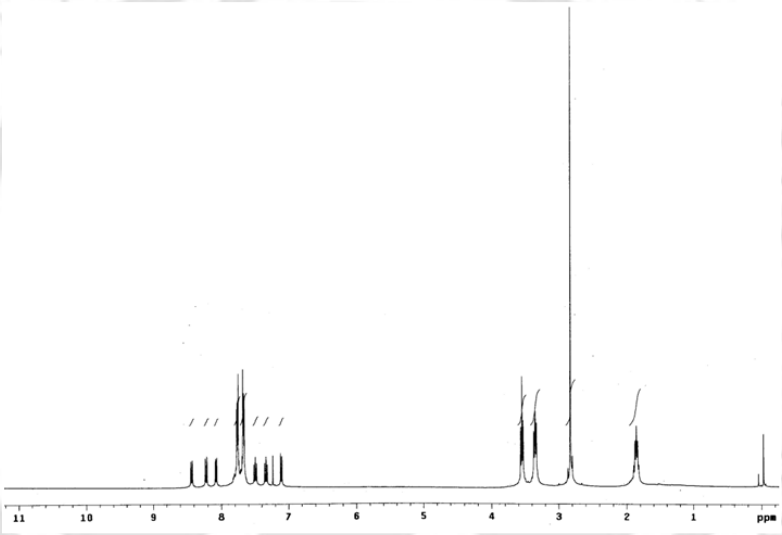

Figure A4.11 ^{1}H-NMR spectrum of $\mathbf{L_{15}}''$ in $CDCl_3$.

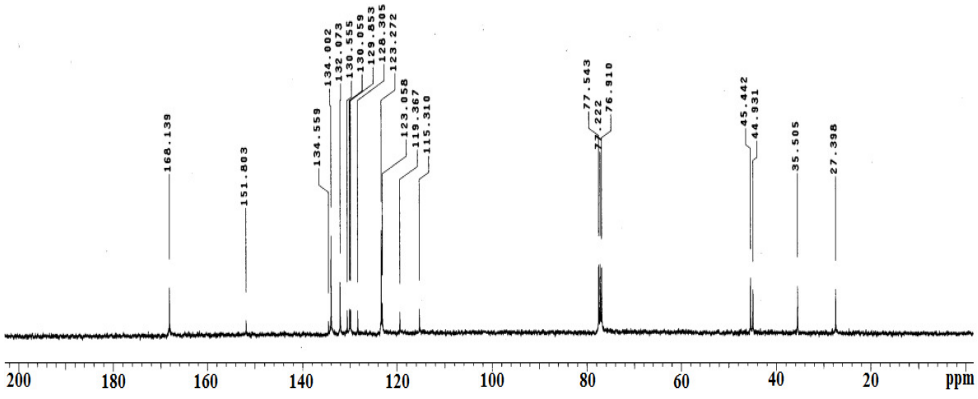

Figure A4.12 ^{13}C-NMR spectrum of $\mathbf{L_{15}}''$ in $CDCl_3$.

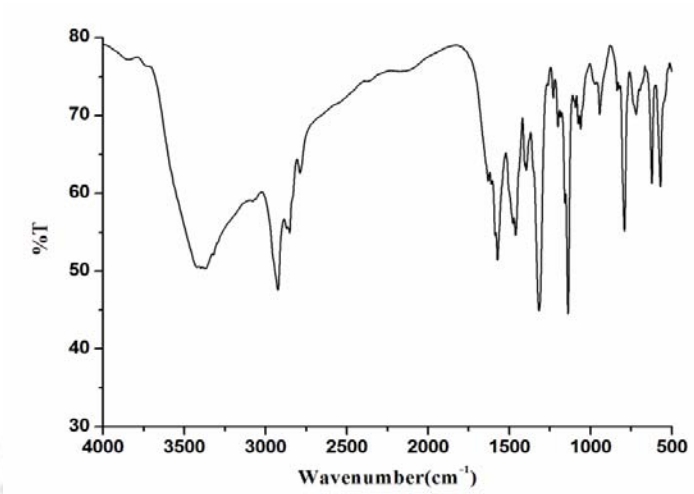

Figure A4.13 FT-IR spectrum of $\mathbf{L_{15}}$ in KBr pellet.

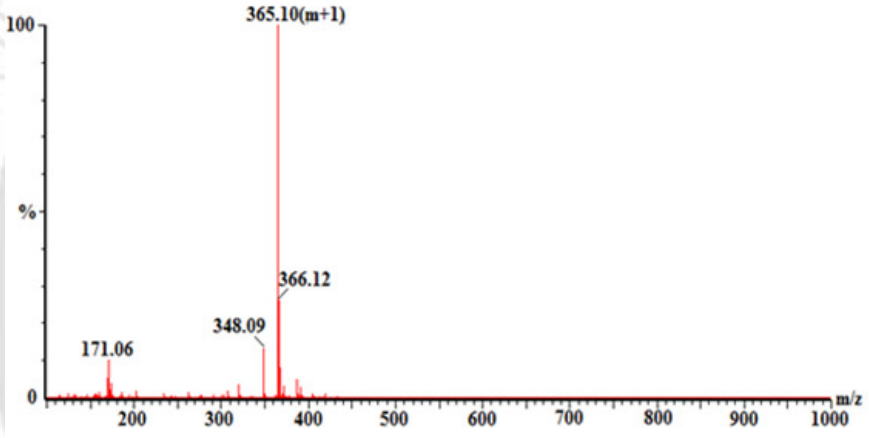

Figure A4.14 Mass spectrum for $\mathbf{L_{15}}$ in methanol.

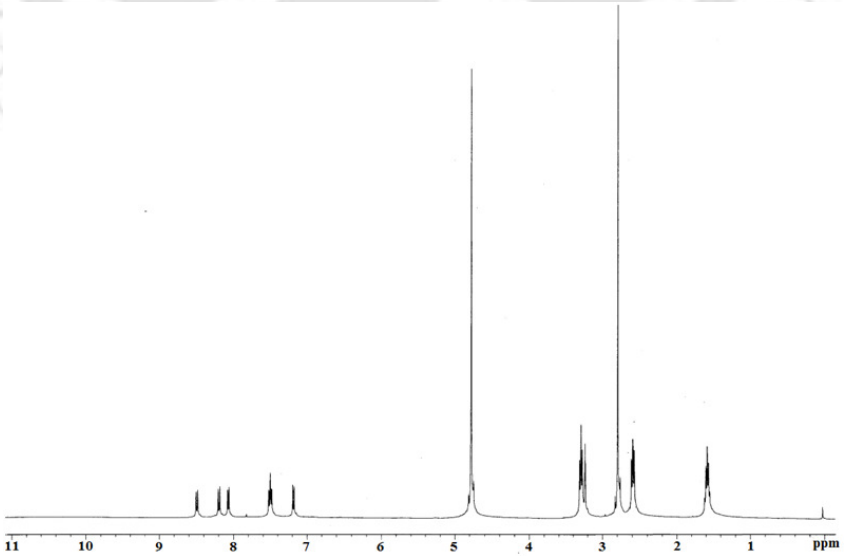

Figure A4.15 ^{1}H-NMR spectrum of $\mathbf{L_{15}}$ in CD_3OD.

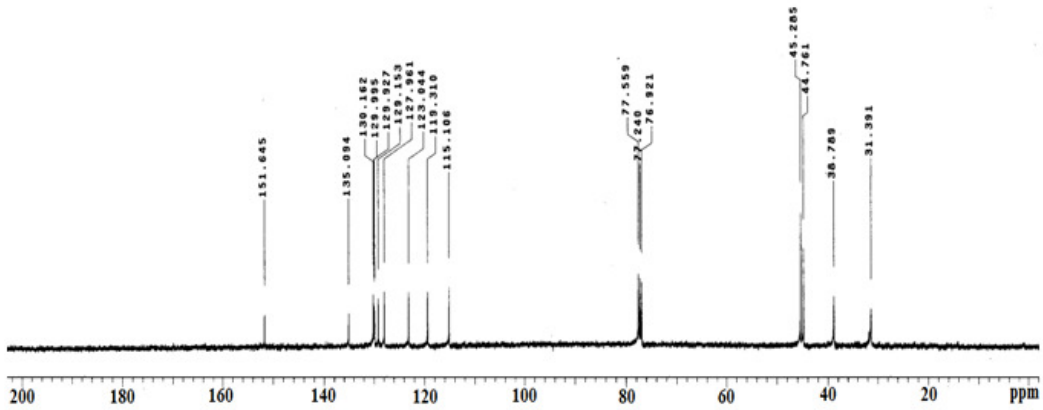

Figure A4.16 ^{13}C-NMR spectrum of $\mathbf{L_{151}}$ in $CDCl_3$.

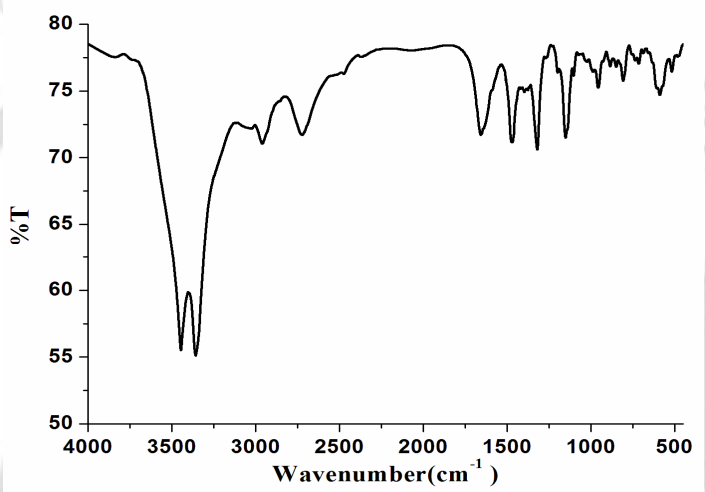

Figure A4.17 FT-IR spectrum of complex **5.1** in KBr pellet.

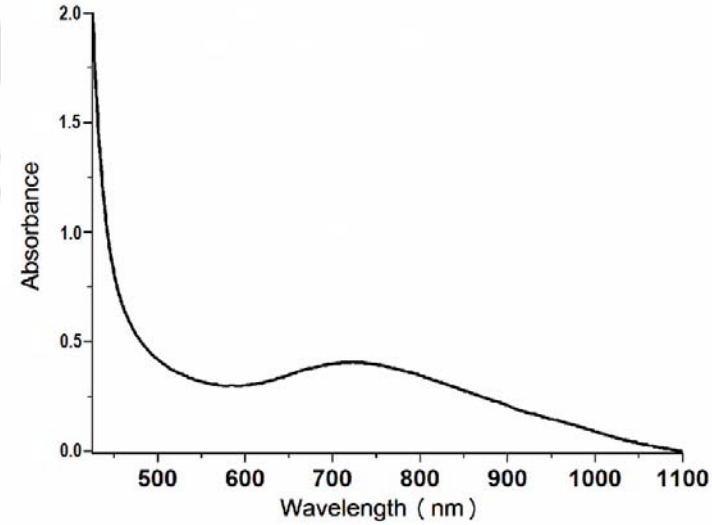

Figure A4.18 UV-visible spectrum of complex **5.1** in methanol.

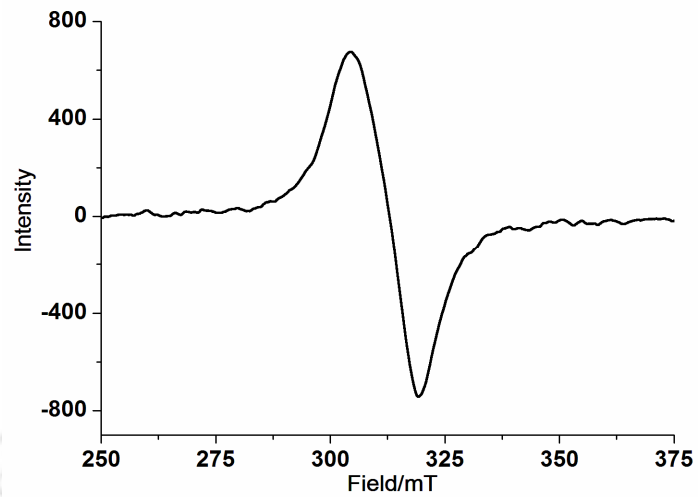

Figure A4.19 X-Band EPR spectrum of complex **5.1** in methanol at 298K.

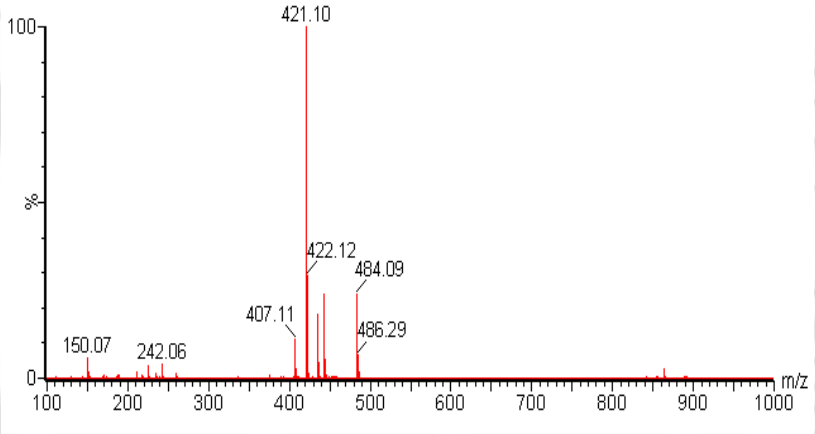

Figure A4.20 Mass spectrum for complex **5.1** in methanol.

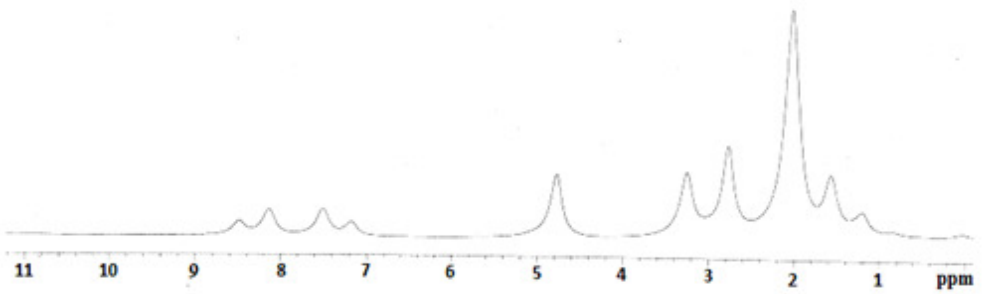

Figure A4.21 ^{1}H-NMR spectrum of complex **5.1** in CD_3OD.

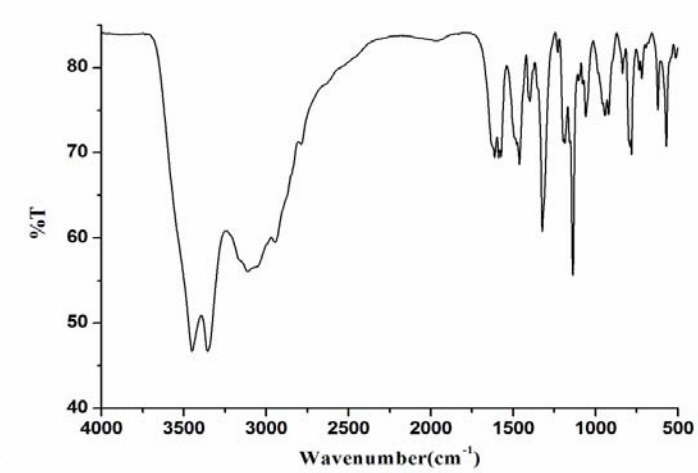

Figure A4.22 FT-IR spectrum of complex **5.2** in KBr pellet.

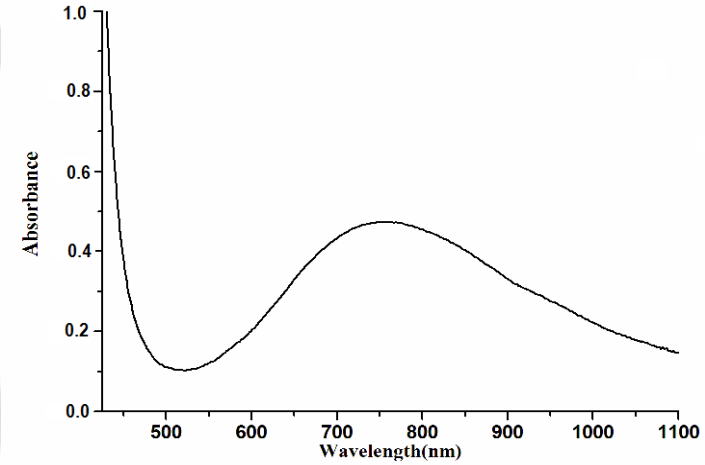

Figure A4.23 UV-visible spectrum of complex **5.2** in methanol.

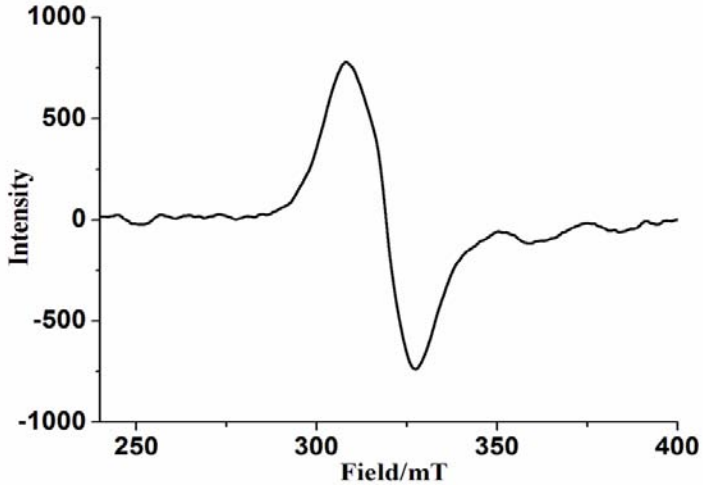

Figure A4.24 X-Band EPR spectrum of complex **5.2** in methanol at 298K.

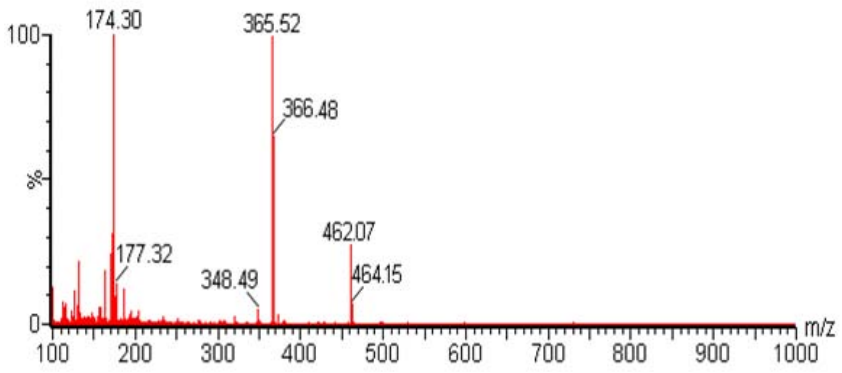

Figure A4.25 Mass spectrum for complex **5.2** in methanol.

\

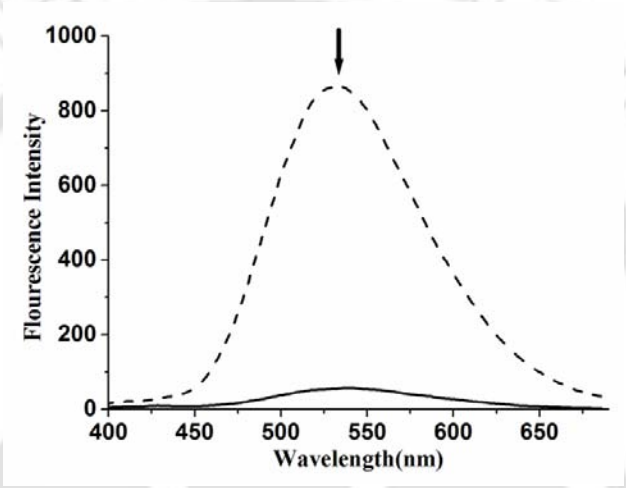

Figure A4.26 Fluorescence responses (λ_{ex}, 340 nm) of 20 μM solution of free ligand, $\mathbf{L_{15}}$ (dashed line) and after addition of one equivalent of $CuCl_2$ in methanol (solid line).

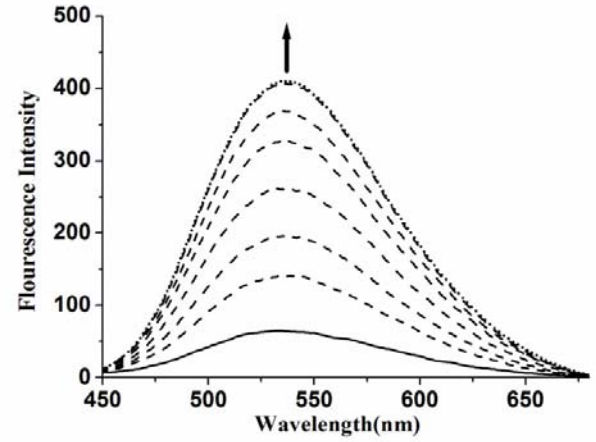

Figure A4.27 Fluorescence responses (λ_{ex}, 340 nm) of 20μM deoxygenated methanol solution of complex **5.2** before (solid line) and after purging of 10 equivalent of nitric oxide (dotted line) at 1, 2, 3, 4, 5, 7 and 10 minutes at 298 K.

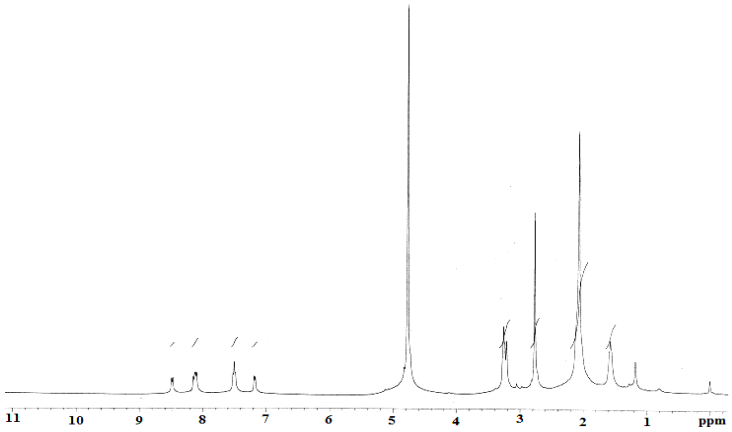

Figure A4.28 ^{1}H-NMR spectrum of complex **5.1** after reaction with nitric oxide in CD_3OD.

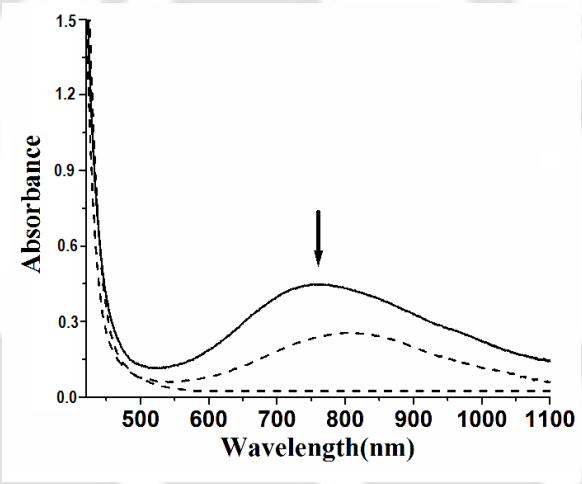

Figure A4.29 UV-visible spectra of complex **5.2** in methanol before (solid line) and after the reaction with nitric oxide (dashed line) in methanol.

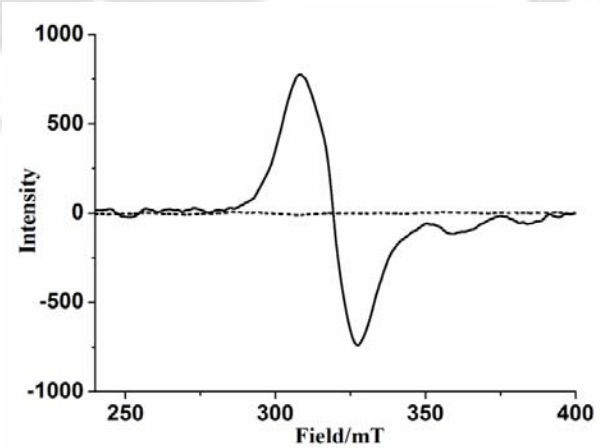

Figure A4.30 X-Band EPR spectra of complex **5.2** before (solid line) and after (dashed line) the reaction with nitric oxide in methanol at 298K.

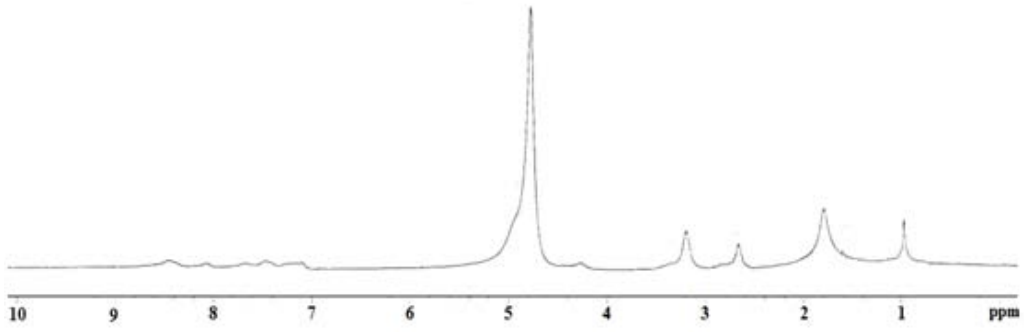

Figure A4.31 ^{1}H-NMR spectrum of complex **5.2** in CD_3OD.

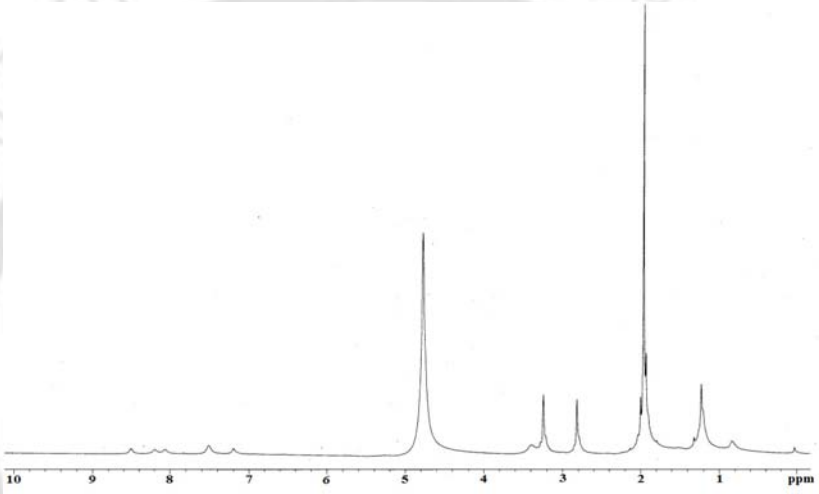

Figure A4.32 ^{1}H-NMR spectrum of complex **5.2** after purging nitric oxide in CD_3OD.

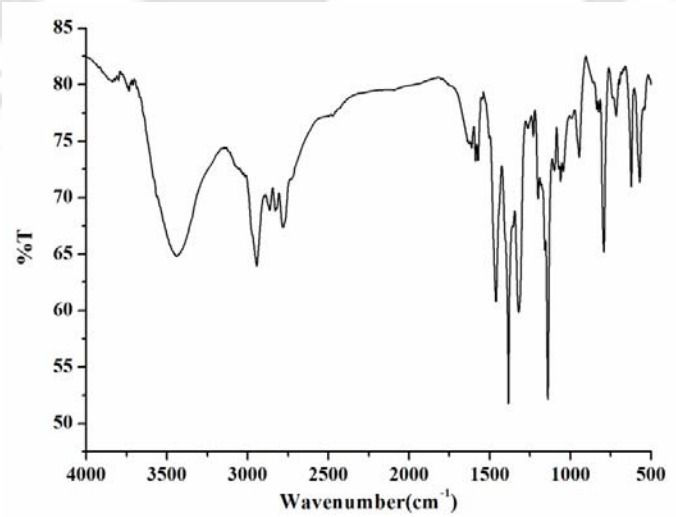

Figure A4.33 FT-IR spectrum of complex **5.1** after NO and then open to air in KBr pellet.

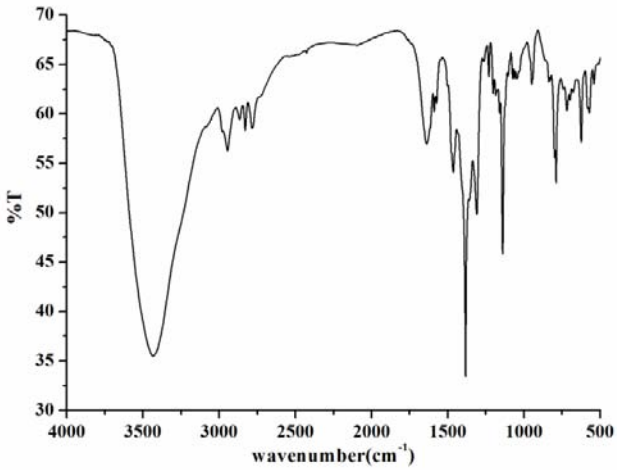

Figure A4.34 FT-IR spectrum of complex **5.2** after NO and then open to air in KBr pellet.

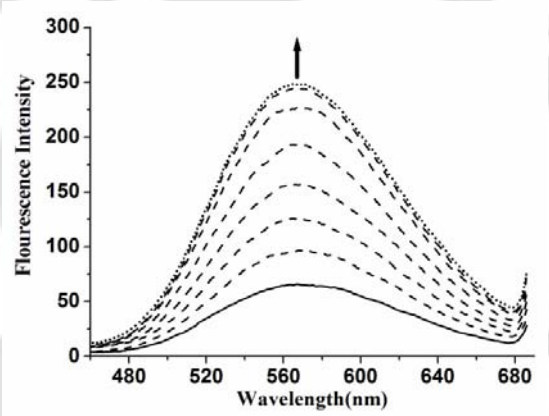

Figure A4.35 Fluorescence responses (λ_{ex}, 340 nm) of 20μM of complex **5.2** in pH 7.2 Tris-buffer before (solid line) and after purging of 10 equivalent of nitric oxide (dotted line) at 1, 2, 3, 5, 7, 10 and 15 minutes at 298 K.

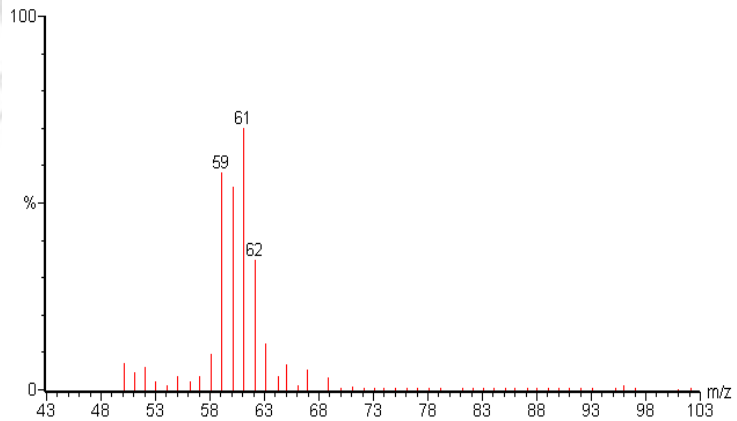

Figure A4.36 Gas chromatographic mass spectrum of complex **5.1** after the reaction with nitric oxide in methanol. The peak at m/z, 61 indicates the formation of CH_3ONO.

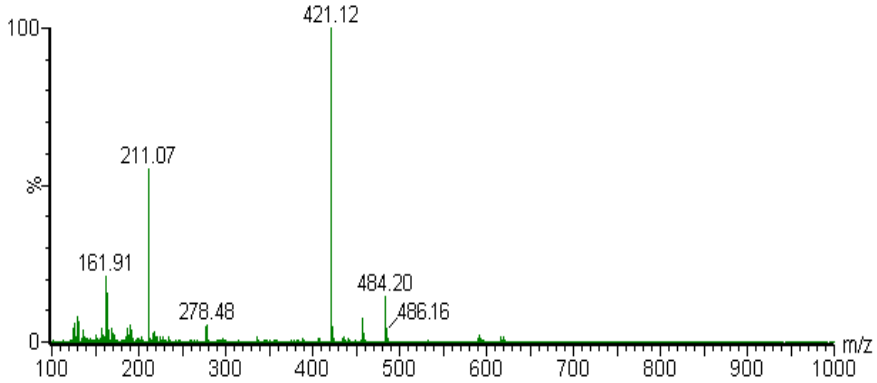

Figure A4.37 Mass spectrum of the reaction mixture after reaction of complex **5.1** with nitric oxide in methanol.

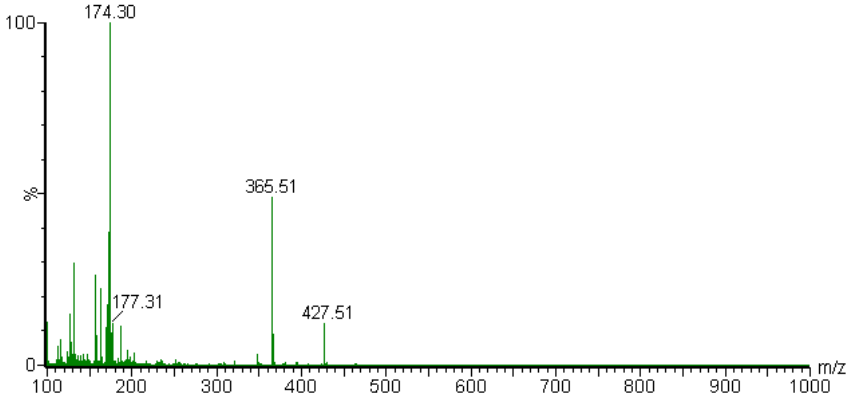

Figure A4.38 Mass spectrum of the reaction mixture after reaction of complex **5.2** with nitric oxide in methanol.

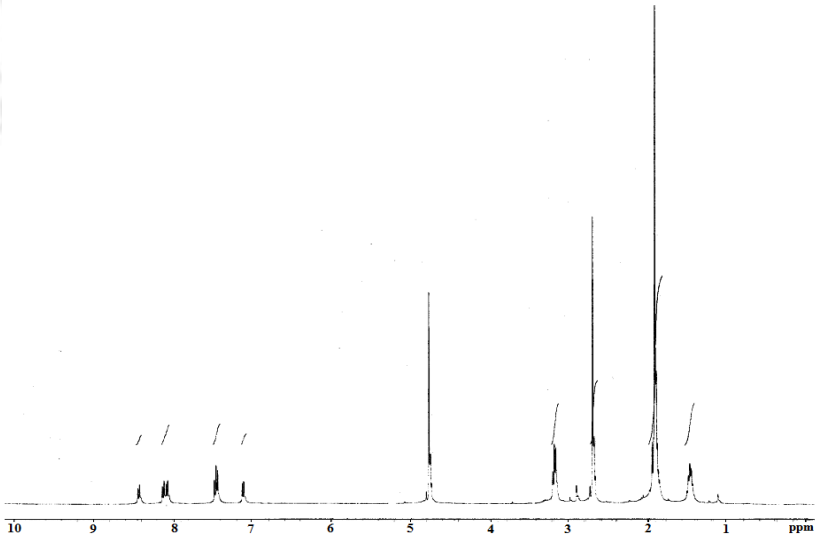

Figure A4.39 ^{1}H-NMR spectrum of $\mathbf{L_{14}}$ in CD_3OD.

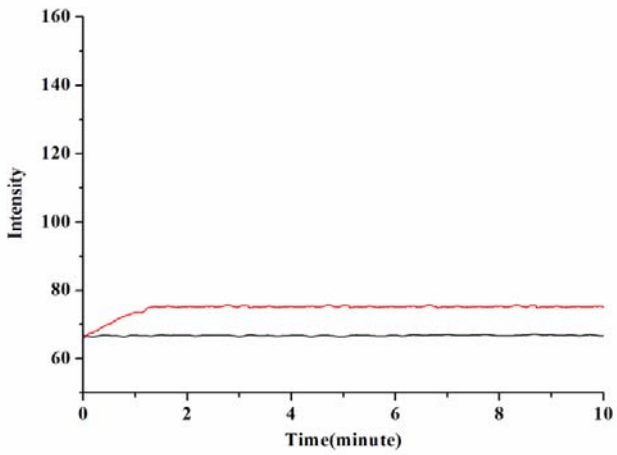

Figure A4.40 Time scan plot (λ_{ex}, 340 nm) of 20μM deoxygenated methanol solution of complex **5.1** (black line) before and (red line) after purging of 1 μM of nitric oxide at 298K.

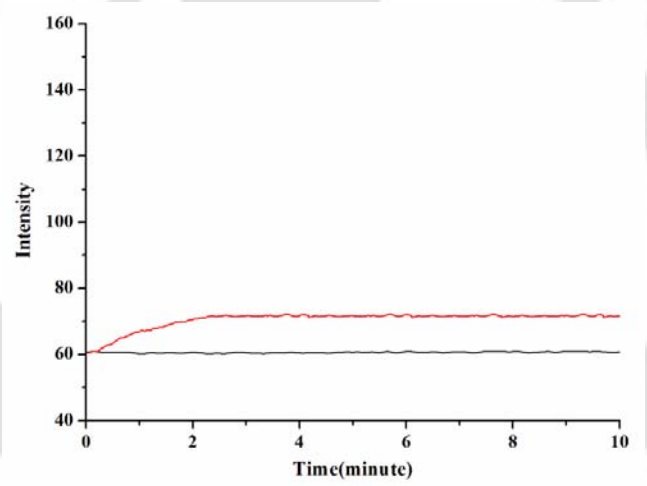

Figure A4.41 Time scan plot (λ_{ex}, 340 nm) of 20μM deoxygenated methanol solution of complex **5.2** (black line) before and (red line) after purging of 1 μM of nitric oxide at 298K.

Chapter 1

Introduction

Nitric oxide (NO) has attracted enormous interest from chemists and biochemists since it has been discovered as a signalling agent in humans.[1–9] It is also known that NO plays diverse roles in biological processes. For instance, when produced in low concentration it regulates vasodialation, defence against pathogens and long-lasting enhancement in signal transmission; however, in micro molar concentration, it stimulates the reactive nitrogen species (RNS) and causes carcinogenesis and neurodegenerative disorders.[1-3, 10-12]

These essentially inspired a wide range of research to identify the precise roles of NO in biology. Since NO is a reactive free radical and easily diffuses through most of the cells and tissues, it is difficult to follow NO immediately after production. Hence, a selective probe to detect the formation and migration of NO with spatiotemporal resolution directly from living cells is highly desirable.

In this aspect, the fluorescence-based detection technique is found to satisfy almost all the requirements, such as biocompatibility, non toxic, specific, fast and direct NO detection. It is also very important that the excitation and emission of the fluorophore of the probe should preferably be in visible or near IR region to avoid harmful effects of ultraviolet light.[13-16] Starting from the early examples of fluorescence-based sensors such as *o*-diaminonaphthalene (DAN) and *o*-diaminofluoresceins (DAFs), a number of fluorescent probes have been reported till date. [13, 17-30] However, they are unable to detect or monitor NO directly as their fluorescent response depends on the formation of a triazole species by oxidized NO products such as N_2O_3. Thus, the NO related bio-events would not be detected in real time. Recently, a highly selective fluorescent imaging agent, NO_{550}, for

NO has been reported which displays a rapid and linear response with a red-shifted turn-on signal.[31]

1.1 Early fluorometric imaging of NO

The first fluorescence-based NO sensors were originally prepared for the measurement of nitrite ion in solution. The sensor molecule, 2,3-diaminonaphthalene (DAN) undergoes diazotization at one of the amines under acidic conditions in the presence of nitrite leading to the formation of 2,3-naphthotriazole (Scheme 1.1).

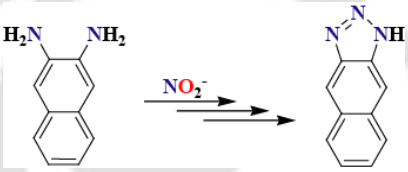

Scheme 1.1

The triazole species, after workup, was detected by fluorometric analysis. The optimal pH for triazole formation was determined to be 1.6 and the maximum fluorescence emission was obtained at a pH of 11.65.[32] Nitrate ion can also be detected by this methodology if it is first reduced to nitrite. It was also observed that formation of 2,3-naphthotriazole is pH dependent, presumably because of the formation of nitrosamine intermediate.[33] Hirobe et al proposed mechanisms for triazole formation with N_2O_3 and N_2O_4, formed by the reaction of NO with O_2 (Scheme 1.2).[34]

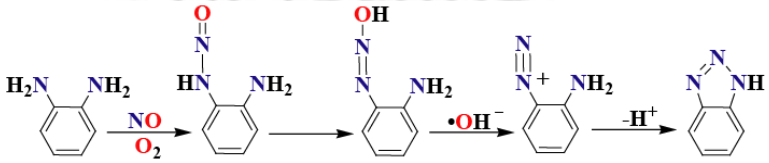

Scheme 1.2

This triazole formation was used for the NO detection in both the systems, *in vitro* and *in vivo*; however, the main problem with DAN is its nonpolar nature which causes in leaking

of DAN out of cells after loading. The first steps towards modification of the diamine-based compounds for intracellular NO detection were undertaken by Nagano and co-workers.[35] To overcome the issue of sensor leakage from the cells after loading, DAN was derivatized to add an ester moiety (Scheme 1.3).

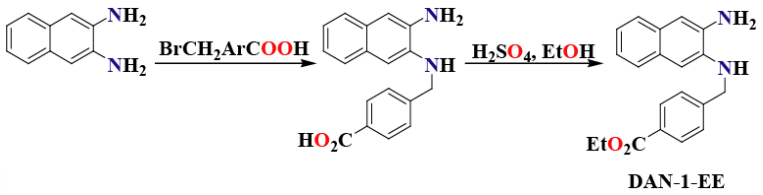

Scheme 1.3

Cell permeable ester of DAN (DAN-1-EE) is hydrolyzed into the non-permeable DAN by intracellular esterases, thus trapping the probe inside the cell. Once hydrolyzed inside the cell, DAN was used to image NO production in activated vascular smooth muscle cells isolated from male Wistar rats. The formation of the corresponding triazole species was monitored by fluorescence microscopy with excitation of the 360 nm absorption band of the triazole which results in emission at 447 nm.

Diaminofluorescein compounds

To improve the fluorescence properties of the *o*-diamine-based compounds for intracellular NO detection, fluorescein was introduced as a scaffold. A series of diaminofluoresceins (Figure 1.1) were prepared and their reactivity with NO in the presence of O_2 was investigated.[17] Fluoresceines generally display low quantum yields (Φ = 0.002 - 0.007) because of photoinduced electron transfer (PET) quenching at excited state by the free amine groups. Conversion of the amines on a diaminofluorescein to a triazole upon reaction with NO was reported to result in enhanced fluorescence emission (Φ = 0.53 - 0.92). For example, DAF-2 has the most desirable fluorescence properties with a quantum efficiency of 0.005 for the diamine and 0.92 for the triazole derivative.[17] The fluorescence

emission from triazole of DAF-sensors are, however depends upon pH and decreased rapidly as pH falls down. [27, 36]

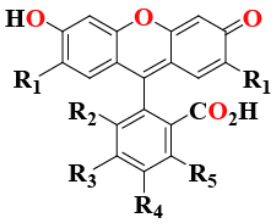

	R_1	R_2	R_3	R_4	R_5
DAF-1	H	H	H	NH_2	NH_2
DAF-2	H	H	NH_2	NH_2	H
DAF-3	H	NH_2	NH_2	H	H
DAF-4	Cl	H	NH_2	NH_2	H
DAF-5	Cl	NH_2	NH_2	H	H

Figure 1.1 A family of diaminonuoiescein derivatives.

Several related *o*-diamine-based sensors have been prepared in recent years.[20, 37] Nagano and coworkers have developed a series of diaminorhodamine (DAR) analogs of the DAF sensors (Figure 1.2). [20, 37] These rhodamine-based sensors do not display pH-dependent fluorescence and have stable emission above pH 4.

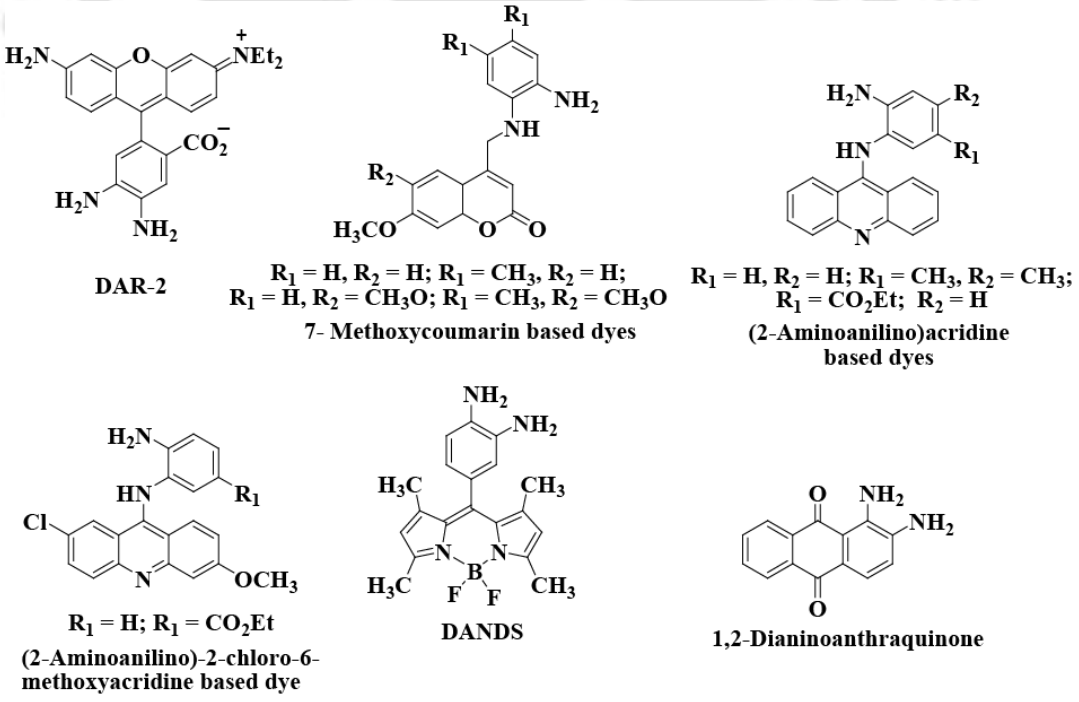

Figure 1.2 Fluorophore systems functionalized with an *o*-diamine moiety to act as NO sensor.

The detection limit of DAR-4M is 7 nM of NO, which is slightly higher than the 3 nM detection limit observed for 4-Amino-5-Methylamino-2',7'-difluorofluorescein.[20, 36] Probes based on the anthracene, coumarin, acridine, and BODIPY fluorophores have also been synthesized (Figure 1.2).[38, 39]

These sensors are synthetically more accessible and their fluorescence emission does not depend substantially on pH variations. Another organic-based compound developed for detecting NO is rhodamine B hydrazide (RBH). The reaction of RBH with NO_2^- under acidic conditions (pH < 5), which favour the formation of NO^+ equivalents, results in ultimate conversion of the non-fluorescent RBH to the fluorescent rhodamine B with the shortest reaction time of 1 h observed in aqueous solution at pH 2 at 60 °C (Scheme 1.4).[40]

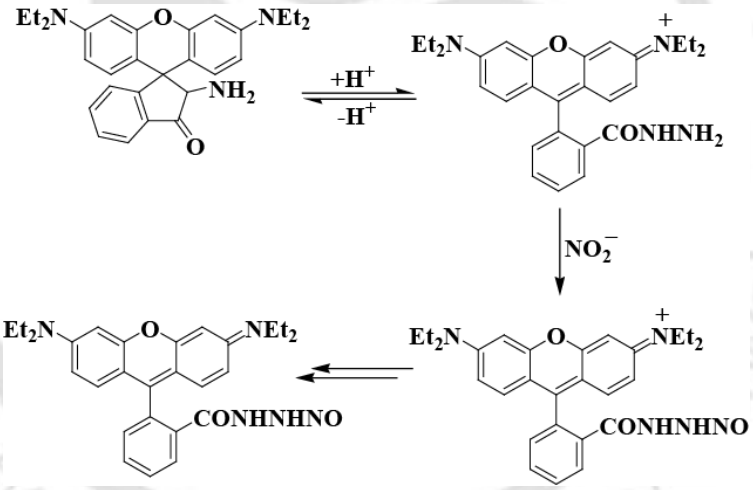

Scheme 1.4 The proposed mechanism for the conversion of RBH into a fluorescent species on reaction with NO.

Exposure of RBH to NO in the presence of O_2 also elicits an increase in fluorescence emission, however, presumably *via* a NO_2 or N_2O_3 reactive intermediate. Because of its indirect reactivity with NO, RBH has shortcomings similar to those observed with the *o*-diamine-based sensors.

To overcome the problems associated with organic fluorescence sensors for NO, the strategies to develop metal based fluorescent NO sensors have been adopted.

1.2 Strategies for metal based fluorescent NO sensors

First example of metal based fluorescence sensor reported was an iron complex showing the diminished fluorescence intensity upon its reaction with NO.[41] Iron-dithiocarbamate complex of acridine-TEMPO ligand also reported to show quenching in fluorescence intensity when allowed to react with NO.[42] In both examples there is a decrease in the fluorescence intensity but in biological systems enhancement in the fluorescence intensity is always preferred over the quenching.

The approaches to develop metal based fluorescent NO sensors, which display turn-on fluorescence, can be categorised into the following classes:

Fluorophore displacement without metal reduction

This approach depends upon the formation of a metal nitrosyl adduct followed by releasing a fluorophore that was initially quenched by coordination to a paramagnetic transition metal centre by electron or energy transfer (Scheme 1.5).[43] Fluorophores can bind the metal centre as axial ligands. Introduction of NO causes their displacement with concomitant increase in the fluorescence intensity. Various metal complexes of iron cyclam,[44] ruthenium porphyrins [45] and dirhodium tetracarboxylate [46] show this type of fluorescence turn-on.

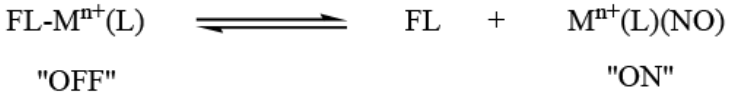

Scheme 1.5

One of the first small molecule fluorescent NO probe to employ a transition metal was designed by analogy to the active site of soluble guanylate cyclase (sGC). In the resting

state of sGC, the heme moiety contains a coordinated histidine. Upon reaction with NO, a heme nitrosyl is formed, which results in dissociation of the coordinated histidine.[41]

The iron(Il) quinoline pendant cyclam complex (Figure 1.3) contains two distinct fragments; an iron(II) cyclam, which can be viewed as a simple model for the heme centre in and a pendant quinoline, which is analogous to the axial histidine in the active site of sGC.

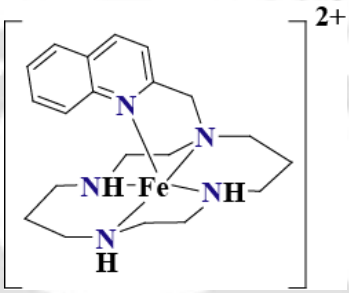

Figure 1.3 A Fe quinoline pendant cyclam sensor, the design of which was based upon the active site of sGC.

When excited at 366 nm, the fluorescence emission from the Fe(II) complex at 460 nm is significantly enhanced in comparison to that of the free ligand as a result of electronic interactions between the lone pair on the quinoline and the Fe(II) centre.[47] Such coordination-induced fluorescence enhancement differs from the more commonly observed quenching properties of transition metals with partially filled *d*-shells. When exposed to NO in pH 7.4 buffer, the 460 nm emission decreases markedly, the lower detection limit being 1 μM NO.[41]

Recently, Soh and co-workers proposed a new type of NO fluorescent probe, which is composed of a iron-dithiocarbamate complex and 2,2,6,6-tetramethylpiperidine-*N*-oxide (TEMPO) labelled with acridine, and confirmed that the probe could detect NO directly in aqueous conditions.[48] Unfortunately, the probe quenches its fluorescence with the capture of NO. An example of NO detection system having dye-labelled cytochrome *c* attached to

an optical fibre along with fluorescent microspheres, was reported for the ratiometric detection of NO.[49]

The design of this fluorescent probe was based on the spin-exchange theory. In guanylyl cyclase, NO binds strongly to the heme iron to make the iron-nitrosyl bond and releases the imidazole moiety coordinated to the central iron where the heme and imidazole moiety in guanylyl cyclase were replaced with an iron complex of a fluorescent methoxycoumarin-pendant cyclam (Mmc-cyclam) and 2,2,5,5-tetramethylpyrrolidine-*N*-oxide labelled with fluorescamine, respectively (Scheme 1.6).[44, 49, 50]

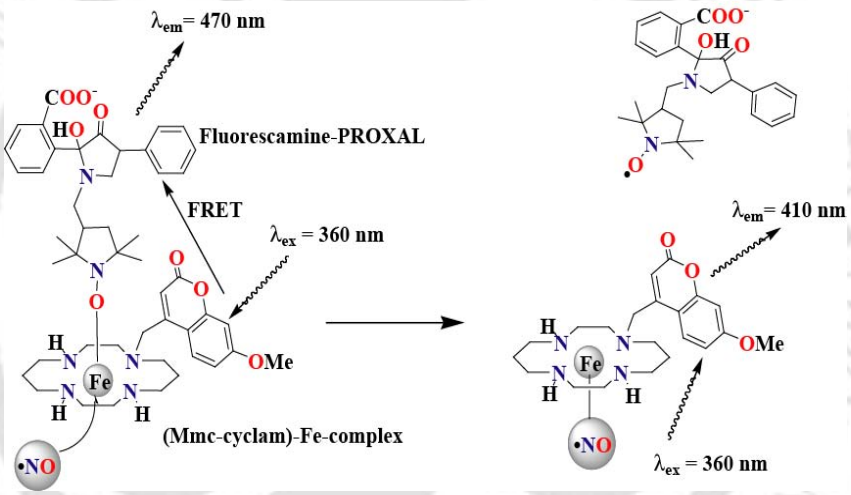

Scheme 1.6 Schematic illustration of detection mechanism of NO using (Mmc-cyclam)-Fe-complex

Rhodium based systems have been used for NO detection, in which reaction of NO with a transition metal complex containing a coordinated fluorophore conjugate results in the removal of the fluorophore from the coordination sphere of the metal with concomitant fluorescence turn-on. The reversible fluorescence-based detection of NO was exemplified with dirhodium tetracarboxylate scaffolds containing bound fluorophore conjugates (Scheme 1.7).[51] Dirhodium tetracarboxylates are air-stable compounds that coordinate a variety of ligands at the axial positions of the tetra bridged dimetallic core. The reaction of

NO with solid $[Rh_2(\mu\text{-}O_2CMe)_4]$ affords a nitrosyl adduct that can be reversed upon heating to 120 °C, although the products were not fully characterized. The only crystallographically defined dirhodium nitrosyl complex is $[Rh_2(\mu\text{-}O_2CMe)_4(NO) - (NO_2)]$, which was prepared by the reaction of $[Rh_2(\mu\text{-}O_2CMe)_4]$ with excess NO in CH_2Cl_2.

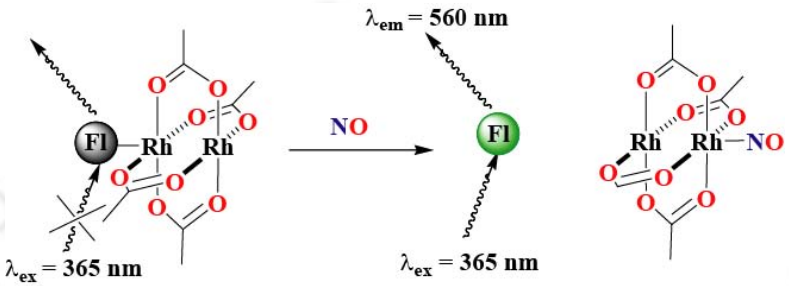

Scheme 1.7

The reactivity of NO with metalloporphyrins has been extensively investigated in this direction.[52, 53] Ruthenium porphyrins form stable nitrosyl adducts upon exposure to NO.[53, 54] Fluorophore coordinated to ruthenium in this manner can be released by NO, resulting in turn-on fluorescence upon excitation (Scheme 1.8).

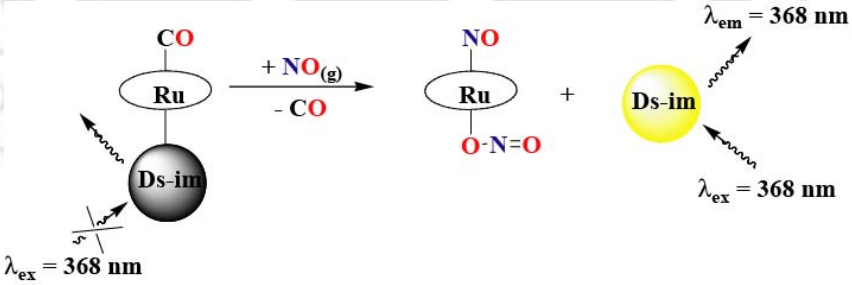

Scheme 1.8

Metal reduction with fluorophore displacement

Many examples of reductive nitrosylation has been reported in the reaction of NO with various metals, including Co and Fe.[55, 56] In this type of reactions, complexes when allowed to react with the NO, metal ion reduces by NO with a concomitant dissociation of

the fluorophore ligands from the coordination environment with an increase in the fluorescence intensity. In the cobalt and the iron system, ligands can be displaced by NO.[48, 53, 55]

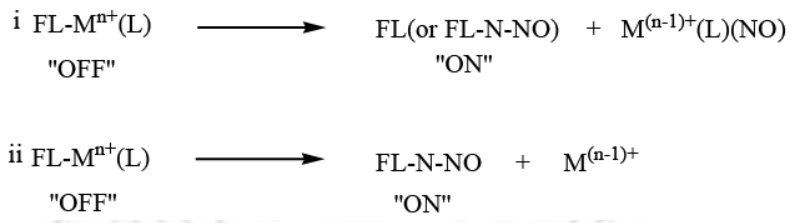

Scheme 1.9

During the reaction of NO with the copper or other metals (M^n), NO^+ formed with simultaneous reduction of the metal centre (M^{n-1}). There are two pathways of NO^+ reactions, first it can react with the amine functionality coordinated to the metal centre to form N-nitrosation *via* intermolecular pathway, followed by removal of fluorophore and concomitant enhancement of fluorescence intensity (Scheme 1.9).[57] Enhancement in fluorescence intensity was observed in case of anthracenyl cyclam Cu(II) complex.[58] Utilizing this strategy Lippard's group synthesized various metal based NO sensor of cobalt(II) tetracarboxylate scaffold and a Cu(II) fluorescien for turn-on fluorescence responces.[22, 59]

For example, a Cu(II) fluorescein-based compound, CuFL, which reacts rapidly with NO to result in the reduction of Cu(II) and ligand nitrosation, has been used to image NO produced in live cells by cNOS and iNOS (Scheme 1.10).[22]

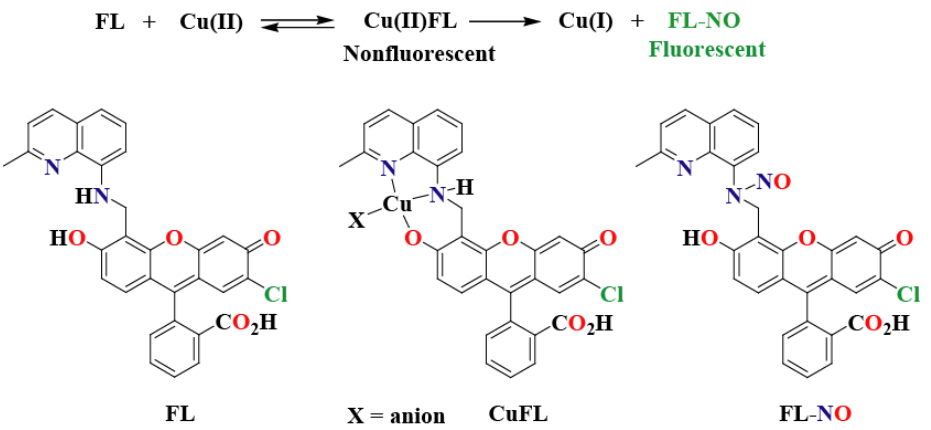

Scheme 1.10

In an another example cobalt complex, (Co- H_2DATI-4), (H_2DATI-4 = Dansyl derivative of two aminotroponiminate ring linked through the other nitrogen by a 4-methylene chain) which showed more than 90% decrease in fluorescence intensity of the free ligand upon reaction with NO results in Co-dinotrosyl species with a tetrahedral coordination around the Co centre having one of the DATI arms dissociate from the metal centre (Scheme 1.11).

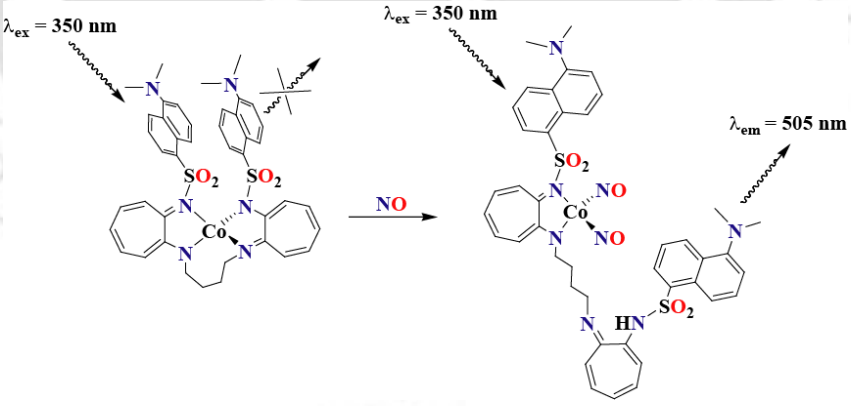

Scheme 1.11

The dissociation of a dansyl-containing ligand fragment restored the fluorescence intensity of the ligand. The NO detection limit of the Co- H_2DATI-4 is estimated to 50-100 μM.

Synthetic non-heme carboxylate bridged diiron and dicobalt complexes were reported as potential systems for use as NO sensors (Figure 1.4).[45]

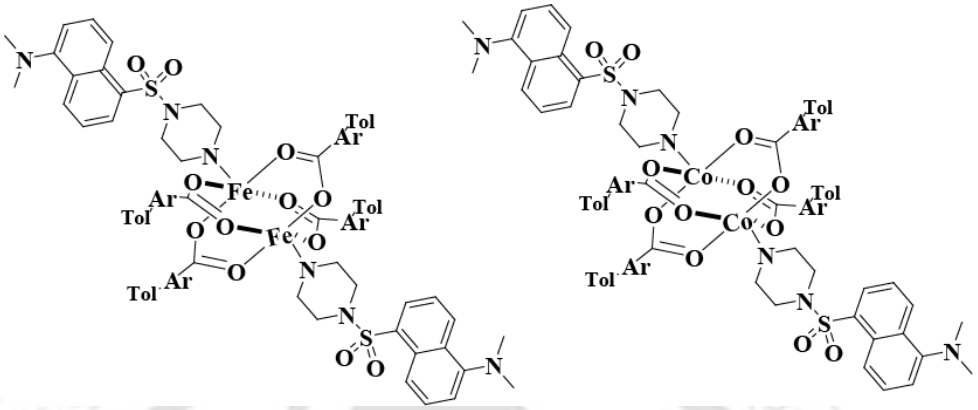

Figure 1.4

Metal reduction without fluorophore displacement

The reduction of Cu(II) centre by NO is well documented in literature. In complexes having fluorophore ligands, paramagnetism of Cu(II) centre quenches the fluorescence intensity of the ligand. The reduction of paramagnetic Cu(II) by NO to diamagnetic Cu(I) is, thus, expected to restore fluorescence intensity without the removal of fluorophore from the coordination environment (Scheme 1.12).

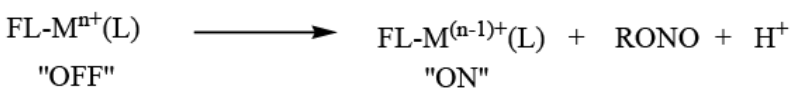

Scheme 1.12

This strategy was used to achieve small molecule-based fluorescent NO sensing with nanomolar sensitivity in organic and, significantly, buffered aqueous solutions (Scheme 1.13). The previously described Cu(II) system that exhibits NO-triggered fluorescence enhancement does so in aqueous methanol by a different mechanism, nitrosylation-induced ligand dissociation from the reduced Cu(I) centre.[58] The Cu(II) complexes $[Cu(Ds\text{-}en)_2]$ [60,

[61] and [Cu(Ds-AMP)$_2$], where Ds-en and Ds-AMP are the conjugate bases of dansyl ethylenediamine (Ds-Hen) and dansyl aminomethylpyridine (Ds-HAMP), respectively. Fluorescence experiments at 25 °C indicated significant copper induced quenching in 20 μM, 4:1 CH_3OH:CH_2Cl_2, solutions of [Cu(Ds-en)$_2$] and [Cu(Ds-AMP)$_2$], with a 31±(2)- and 23±(0.5)-fold reduction in intensity relative to free Ds-Hen and Ds-HAMP (40 μM), respectively. Addition of 100 equivalent of NO to solution immediately restored significant emission intensity under anaerobic conditions; the enhancements in integrated fluorescence being 6.1±(0.2)- and 8.8±(0.1)-fold for [Cu(Ds-en)$_2$] and [Cu(Ds-AMP)$_2$], respectively.

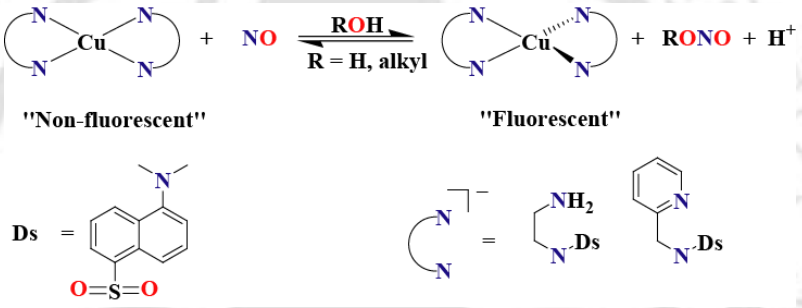

Scheme 1.13

The NO detection limit of these sensors is 10 nM, which is nearly 3 orders of magnitude greater sensitivity than dirhodium complex.[51] Since the complexes [Cu(Ds-en)$_2$] and [Cu(Ds-AMP)$_2$] are water-soluble, their reactivity with NO was further investigated in aqueous buffer (50 mM CHES, pH 9, 100 mM KCl). In this medium, copper remains coordinated by the two bidentate Ds-en ligands in [Cu(Ds-en)$_2$] . A 4.3(0.5)- or 4.5- (0.6)-fold quenching was observed at pH 9 for [Cu(Ds-en)$_2$] and [Cu(Ds-AMP)$_2$] (10 μM), respectively, at 37 °C. Addition of 100 equivalent of NO into these solutions caused a fluorescence increase of 2.3±(0.2)- or 2.0±(0.2)-fold, respectively, within 30 min.

Another report of a turn-on sensor for NO with nM sensitivity employing a π-conjugated polymer (CP) as the fluorescent probe. The successful realization of CPs for fluorescence-

based detection of NO, in the form of a CP-copper complex that exhibits a turn-on response to NO in solution, represents an advantageous new strategy with many possible applications. There is a series of CPs integrating copper-binding units at defined intervals and screened their relative fluorescence intensities in both CP-Cu(I) and CP-Cu(II) forms, anticipating turn-on NO detection by the process depicted in scheme 1.14.

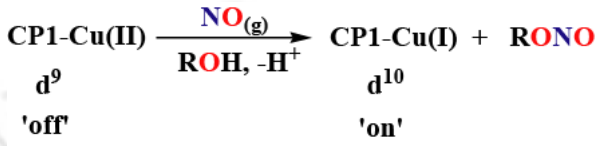

Scheme 1.14

A structurally related CP is reportedly quenched in the presence of Cu(II), whereas only moderate quenching occurs with added Cu(I).[62] CP1 is a bright red-orange solid (λ_{max}, 462 nm) with strong fluorescence emission centred at 542 nm (Φ = 0.30). Upon addition of 1 equivalent of $Cu(OTf)_2$ to a solution of CP1, the integrated fluorescence intensity was quenched 4-fold, whereas addition of 1 equivalent of $[Cu(NCMe)_4][BF_4]$ decreased the fluorescence by ~ 30%. Introduction of 300 equivalent of NO to the CP1-Cu(II) complex rapidly (<1 min) increased the integrated emission by 2.8-fold, producing a fluorescence spectrum similar to that of the CP1-Cu(I) complex; NO did not alter the fluorescence of CP1 in the absence of Cu(II).

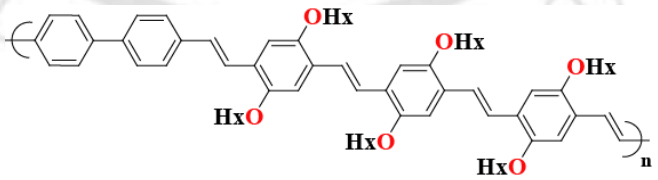

CP1

Figure 1.5 Structure of CP1

For the present study, we have chosen this methodology for fluorescence sensing of NO. As this involves the reduction of Cu(II) centre by NO, the choice of ligand framework

plays a crucial role in the sensor development process. In our laboratory, we have been studying the mechanistic details of NO reduction of copper(II) complexes and as a continuation, the second chapter of this thesis will describe the role of ligand denticity in controlling the mechanistic pathway of reduction of Cu(II) by NO. In the successive chapters, the development of NO sensors using dansyl fluorophore containg ligands will be discussed.

1.3 References

1. Furchgott, R. F. *Angew. Chem. Int. Ed.* **1999**, *38*, 1870.
2. Ignarro, L. J. *Angew. Chem. Int. Ed.* **1999**, *38*, 1882.
3. Murad, F. *Angew. Chem. Int. Ed.* **1999**, *38*, 1856.
4. Bon, C. L. M.; Garthwaite, J. *J. Neurosci.* **2003**, *23*, 1941.
5. Pepicelli, O.; Raiteri, M.; Fedele, E. *Neurochem. Int.* **2004**, *45*, 787.
6. Bonomo, R. P.; Pappalardo, G.; Rizzarelli, E.; Santoro, A. M.; Tabbi, G.; Vagliasindi, L. I. *Dalton Trans.* **2007**, 1400.
7. Bonomo, R. P.; Castronovo B. M. G.; Santoro, A. M. *Dalton Trans.* **2004**, 104.
8. Bonomo, R. P.; Pappalardo, G.; Rizzarelli, E.; Vagliasindi.; L. I. *Dalton Trans.* **2008**, 3805.
9. Bonomo, R. P.; Di Natale, G.; Rizzarelli, E.; Tabbi, G.; Vagliasindi, L. I. *Dalton Trans.* **2009**, 2637.
10. Ricciardolo, E. L. M.; Sterk, P. J.; Gaston, B.; Folkerts, G. *Phsiol. Rev.* **2004**, *84*, 731.
11. Wink, D. A.; Vodovotz, Y.; Laval, J.; Laval, F.; Dewhirst, M. W.; Mitchell, J. B. *Carcinogenesis.* **1998**, *19*, 711.
12. Calabrese, V.; Bates, T. E; Stella, A. M. G. *Neurochem. Res.* **2000**, *25*, 1315.
13. Nagano, T.; Yoshimura, T. *Chem. Rev.* **2002**, *102*, 1235.

14. Hilderbrand, S. A.; Lim, M. H.; Lippard, S. J. *Topics in Fluorescence Spectroscopy*, Geddes, C. D.; Lakowicz, J. R. Eds. Springer: **2005**; pp 163.
15. Maliniski, T.; Mesaros, S.; Tomboulian, P. *Methods Enzymol.* **1998**, *170*, 31.
16. Sasaki, E.; Kojima, H.; Nishimatsu, H.; Urano, Y.; Kikuchi, K.; Hirata, Y.; Nagano, T. *J. Am. Chem. Soc.* **2005**, *127*, 3684.
17. Kojima, H.; Nakatsubo, N.; Kikuchi, K.; Kawahara, S.; Kirino, Y.; Nagoshi, H.; Hirata, Y.; Nagano, T. *Anal. Chem.* **1998**, *70*, 2446.
18. Heiduschka, P.; Thanos, S. *NeuroReport*. **1998**, *9*, 4051.
19. Meineke, P.; Rauen, U.; de Groot, H.; Korth, H.-G.; Sustmann, R. *Chem. Eur. J.* **1999**, *5*, 1738.
20. Kojima, H.; Hirotani, M.; Nakatsubo, N.; Kikuchi, K.; Urano, Y.; Higuchi, T.; Hirata, Y.; Nagano, T. *Anal. Chem.* **2001**, *73,* 1967.
21. Gabe, Y.; Urano, Y.; Kikuchi, K.; Kojima, H. and Nagano, T. *J. Am. Chem. Soc.* **2004**, *126*, 3357.
22. Lim, M. H.; Xu, D.; Lippard, S. J. *Nat. Chem. Biol.* **2006**, *2*, 375.
23. Lim, M. H.; Wong, B. A.; Pitcock, Jr., W. H.; Mokshagundam, D.; Baik, M.-H.; Lippard, S. J. *J. Am. Chem. Soc.* **2006**, *128*, 14363.
24. Zheng, H.; Shang, G.-Q.; Yang, S.-Y.; Gao, X.; Xu, J.-G. *Org. Lett.* **2008**, *10*, 2357.
25. Wang, S.; Han, M.-Y.; Huang, D. *J. Am. Chem. Soc.* **2009**, *131*, 11692.
26. Kim, J.-H.; Heller, D. A.; Barone, P. W.; Song, C.; Zhang, J.; Trudel, L. J.; Wogan, G. N.; Tannenbaum, S. R.; Strano, M. S. *Nat. Chem.* **2009**, *1*, 473.
27. Jourd'heuil, D. *Free Radical Biol. Med.* **2002**, *33*, 676.
28. Wardman, P. *Free Radical Biol. Med.* **2007**, *43*, 995.

29. Zhang, X.; Kim, W. S.; Hatcher, N.; Potgieter, K.; Moroz, L. L.; Gillette R.; Sweedler, J. V. *J. Biol. Chem.* **2002**, *277*, 48472.

30. Ye, X.; Rubakhin, S. S.; Sweedler, J. V. *J. Neurosci. Methods*, **2008**, *168*, 373.

31. Yang, Y.; Seidlits, S. K.; Adams, M. M.; Lynch, V. M.; Schmidt, C. E.; Anslyn, E. V.; Shear, J. B. *J. Am. Chem. Soc.* **2010**, *132*, 13114.

32. Damiani, P.; Burini, G. *Talanta.* **1986**, *33*, 649

33. Miles, A. M.; Chen, Y.; Owens, M. W.; Grisham, M. B. *Methods.* **1995**, *7,* 40.

34. Nagano, T.; Takizawa, H.; Hiiobe, M. *Tet. Lett.* **1995**, *36*, 8239.

35. Kojima, H.; Sakurai, K.; Kikuchi, K.; Kawahara, S.; Kirino, Y.; Nagoshi, H.; Hirata, Y.; Akaike, T.; Maeda, H.; Nagano, T. *Biol. Phann. Bull.* **1997**, *20*, 1229.

36. Kojima, H.; Urano, Y.; Kikuchi, K.; Higuchi, T.; Hirata, Y.; Nagano, T. *Angew. Chem. Int. Ed.* **1999**, *38*, 3209.

37. Kojima, H.; M. Hirotani, Y. Urano, Kikuchi, K.; Higuchi, T.; Nagano, T. *Tet. Lett.* **2000**, *41*, 69.

38. Plater, M. J.; Greig, I.; Helfrich, M. H.; Ralston, S. H. *J. Chem. Soc. Perkin Trans.* **2001**, *1,* 2553.

39. Zhang. X.; Wang, H.; Li, S -C.; Zhang, H.-S. *Anal. Chim. Acta.* **2003**, *481*, 101.

40. (a) Fernandez, B. O.; Lorkovic, I. M.; Ford, P. C. *Inorg. Chem.* **2004**, *43*, 5393. (b) Lehnert, N.; Praneeth, V. K. K.; Paulat, F. *J. Comput. Chem.* **2006**, *27*, 1338.

41. Katayama, Y.; Takahashi, S.; Maeda, M. *Anal. Chim. Acta.* **1998**, *365*, 159.

42. Kim, S.; Deinum, G.; Gardner, M. T.; Marletta, M. A.; Babcock, G. T. *J. Am. Chem. Soc.* **1996**, *118*, 8769.

43. Bergonzi, R.; Fabbrizzi, L.; Licchelli, M.; Mangano, C. *Coord. Chem. Rev.* **1998**, 170.

44. Soh, N.; Imato, T.; Kwamura, K.; Maeda, M.; Katayama, Y. *Chem. Commun.* **2002**, 2650.

45. Lim, M. H.; Lippard, S. *J. Inorg. Chem*. **2004**, *43*, 6366.

46. Rieth, T.; Sasamoto, K. *Anal*. *Commun.* **1998**, *35*, 195.

47. Schneider, J. L.; Carrier, S. M.; Ruggiero, C. E.; Young, V. G. Jr.; Tolman, W. B. *J. Am. Chem. Soc.* **1998**, *120,* 11408.

48. Soh, N.; Katayama Y., Maeda, M. *Analyst*. **2001**, *126*, 564.

49. Katayama, Y.; Soh, N.; Koide, K.; Maeda, M. *Chem. Lett.* **2000**, 1152.

50. Zhao, Y.; Hoganson, C.; Babcock, G. T.; Marletta, M. A. *Biochemistry*. **1998**, *37*, 12458.

51. Hilderbrand, S. A.; Lim, M. H.; Lippard, S. J. *J. Am. Chem. Soc*. **2004**, *126*, 4972.

52. Hoshino, M.; Laverman, L.; Ford, P. C. *Coord. Chem. Re*v. **1999**, *187*, 75.

53. Ford, P. C.; Lorkovic´, I. M. *Chem. Re*v. **2002**, *102*, 993.

54. Kadish, K. M.; Adamian, V. A.; Van Caemelbecke, E.; Tan, Z.; Tagliatesta, P.; Bianco, P.; Boschi, T.; Yi, G.-B.; Khan, M. A.; Richter- Addo, G. B. *Inorg. Chem.* **1996**, *35*, 1343.

55. Ford P. C.; Fernandez B. O.; Lim, M. D. *Chem. Rev*. **2005**, *105*, 2439.

56. Franz, K. J.; Singh, N.; Lippard, S. J. *Angew. Chem. Int. Ed*. **2002**, *39*, 4081.

57. Lee, J.; Chen, L.; West, A. H.; Richter-Addo, G. B. *Chem. Rev*. **2002**, *102*, 1019.

58. Tsuge, K.; DeRosa, F.; Lim, M. D.; Ford, P. C. *J. Am. Chem. Soc.* **2004**, *126*, 6564.

59. Hilderbrand, S. A.; Lippard, S. J. *Inorg. Chem.* **2004**, *43*, 5294.

60. Lim, M. H.; Lippard, S. J. *J. Am. Chem. Soc.* **2005**, *127*, 12171.

61. Prodi, L.; Montalti, M.; Zaccheroni, N.; Dallavalle, F.; Folesani, G.; Lanfranchi, M.; Corradini, R.; Pagliari, S.; Marchelli, R. *Hel*v. *Chim. Acta.* **2001**, *84*, 690.

62. Wang, B.; Wasielewski, M. R. *J. Am. Chem. Soc.* **1997**, *119*, 12

Chapter 2

Role of structures of the Cu(II) complexes in deciding the mechanistic pathway of reduction of Cu(II) by nitric oxide

Abstract

Four Cu(II) complexes, **2.1**, **2.2**, **2.3** and **2.4** were synthesized with ligands, $\mathbf{L_1}$, $\mathbf{L_2}$, $\mathbf{L_3}$ and $\mathbf{L_4}$ [$\mathbf{L_1}$ = N^1,N^2-*bis*{(pyridin-2-yl)methyl}ethane-1,2-diamine, $\mathbf{L_2}$ = N^1,N^3-*bis*{(pyridin-2-yl)methyl}propane-1,3-diamine; $\mathbf{L_3}$ = N^1,N^1,N^2-*tris*{(pyridin-2-yl)methyl}ethane-1,2-diamine; $\mathbf{L_4}$ = N^1-((1-methyl-1H-imidazol-2-yl)methyl)-N^1,N^2-*bis*{(pyridin-2-yl)methyl}ethane-1,2-diamine], respectively, as their perchlorate salts. The complexes were characterized by various spectroscopic techniques as well as single crystal X-ray structure determination. NO reactivity of the complexes was studied in acetonitrile as well as methanol solvent. It has been found that the ligand frameworks have a considerable effect in controlling the mechanism of the reduction of Cu(II) centre by NO. The flexibility of the ligand/s for a Cu(II) complex to attain a trigonal bipyramidal geometry after NO coordination has been found to be most important parameter in dictating the pathway for the reduction. In the present study, all the four compounds, because of structural constrain, were found to follow deprotonation pathway for the reduction of Cu(II) centre by NO rather than [Cu^{II}-NO] intermediate formation. All the ligands were found to yield N-nitrosoamine product along with the reduction of Cu(II) centre by NO.

2.1 Introduction

Activation of NO through its coordination to transition metal ions have been a subject of interest for chemists and biochemists since its discovery to play various roles in mammalian biology.[1-6] In ferriheme proteins, NO is known to coordinate to form iron(III)-nitrosyl intermediate prior to the pH dependent reduction of Fe(III) centre.[4,5] In subsequent steps, the hydroxide ion attacks the activated nitrosonium group (NO^+) to afford nitrite ion.[4] The ferrous protein thus formed, reacts with excess of NO to form stable ferroheme nitrosyl.[6-8] In copper-proteins, for instance, cytochrome *c* oxidase and laccase, the reduction of Cu(II) to Cu(I) by NO is known for a long time.[9-12] Wayland and others suggested a mechanism closer to that of ferriheme reduction involving the initial NO coordination to the Cu(II) centre to form [Cu^{II}-NO ↔ Cu^{I}-NO^+].[13] Recently, a number of examples of the interaction of NO with Cu(II) complexes leading to the reduction of Cu(II) centre have been reported in literature. NO is shown to reduce the Cu(II) centre in $[Cu(dmp)_2(X)]^{2+}$ (dmp = 2,9-dimethyl-1,10-phenanthroline, X = solvent) and analogous complexes through an inner-sphere pathway.[14,15] In different examples, the Cu(II) centre of $[Cu^{II}(DAC)]^{2+}$ and $[Cu(mtad)]^{2+}$ {DAC = 1,8-bis(9-anthracylmethyl) derivative of the macrocyclic tetraamine cyclam (1,4,8,11-tetraazacyclotetradecane) and mtad = 5,5,7,12,12,14-hexamethyl-1,4,8,11-tetraazacyclotetradecane} in methanol are reported to be reduced by NO with concomitant nitrosation of the ligands.[16] Quantitative and theoretical studies suggested that the reaction in these cases proceeds through a pathway analogous to the inner-sphere mechanism for electron transfer between two metal centres through a bridging ligand where NO is the reductant, Cu(II), the oxidant and the coordinated amido anion behaves as the bridging ligand (Scheme 2.1).

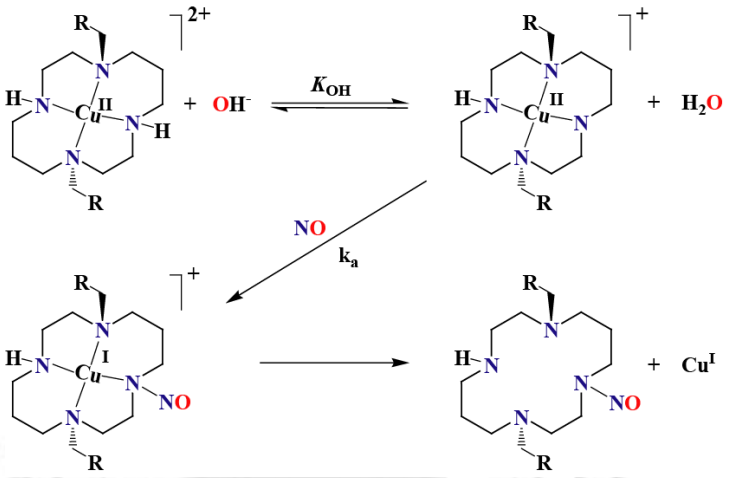

Scheme 2.1

Demetallation of the macrocyclic ring after the reduction of Cu(II) takes place owing to the preference of Cu(I) for tetrahedral coordination and the decreased donor ability of the nitrosated ligand. The formation of Ru(II)-dinitrogen complex, $[Ru(NH_3)_5(N_2)]^{2+}$ from the reaction of $[Ru(NH_3)_6]^{3+}$ with NO in alkaline solution was proposed to follow similar mechanistic pathway.[17] Nitrosation of a coordinated amide ligand with the simultaneous reduction of Ru(III) to Ru(II) results to a nitrosoamine, which on subsequent dehydration affords the dinitrogen complex.

On the other hand, a series of Cu(II) complexes of N- donor ligands were reported to form unstable [Cu^{II}-NO] intermediate on reaction with NO prior to the reduction of Cu(II). For example, in Cu(II) complexes of tripodal tetradentate ligands, $[Cu^{II}(tren)(CH_3CN)]^{2+}$, $[Cu^{II}(taea)(CH_3CN)]^{2+}$, $[Cu^{II}(tiaea)(CH_3CN)]^{2+}$, [tren = *tris*-(2-aminoethyl)amine; taea = *tris*-(2-ethylaminoethyl)amine; tiaea = *tris*-(2-isopropylaminoethyl)amine], the reduction was found to proceed through the formation of a thermally unstable [Cu^{II}-NO] intermediate.[18] In cases of $[Cu(baea)(CH_3CN)]^{2+}$ [baea = *bis*-(2-aminoethyl)amine, a tridentate amine donor ligand], and complexes of various bidentate N-donor ligands, such as pymea, pyeta, dmeta, deaeta [pymea = pyridine-2-methylamine; pyeta = pyridine-2-

ethylamine; dmeta = N,N′-dimethylethylenediamine; deteta = N,N′-diethylethylenediamine] etc, the formation of unstable [Cu^{II}-NO] intermediate was evidenced prior to the reduction of Cu(II) to Cu(I) by NO.[19-20] The stability of the [Cu^{II}-NO] intermediate was found to depend on the denticity, chelate ring size and nature of N-donor atom for these cases. Recently, the example of formation of stable [Cu^{II}-NO] complex from the reaction of Cu(II) complex with NO has been reported.[21] It would be worth mentioning here that Hayton et al recently reported the structurally characterize [Cu^{II}-NO] complex, though prepared in a different pathway.[22] Interestingly, in cases of Cu(II) complexes having ppmea and mimpea [ppmea, 2-(pyridin-2-yl)-N-{(pyridin-2-yl)methyl}ethaneamine; mimpea, N-{(methyl-1H-imidazol-2-yl)methyl}-2-(pyridine-2-yl)ethanamine] ligands, any indication of the formation of a [Cu^{II}–NO] inner-sphere complex was not observed prior to the reduction.[23] This is attributed to the much lower values of the equilibrium constants, K_{NO} (Equation 2.1) as reported earlier in case of $[Cu(dmp)_2(X)]^{2+}$ (X = solvent).[15]

$$[(L)_2Cu^{II}]^{2+} + NO \rightleftharpoons[K_{NO}] [(L)_2Cu^{II}(NO)]^{2+} \quad \text{---------- (2.1)}$$

The difference in ligand environment, perhaps, leads to a different pathway for the reduction of Cu(II) to Cu(I) by NO. This was earlier exemplified by a comparative study of NO reactivity of $[Cu(mtad)]^{2+}$ and $[Cu(tmd)_2]^{2+}$ [mtad = 5,5,7,12,12,14-hexamethyl-1,4,8,11-tetraazacyclotetradecane, tmd = 5,5,7-trimethyl-[1,4]-diazepane].[24] It was observed that in case of $[Cu(mtad)]^{2+}$, though the reduction takes place through a deprotonation pathway; in $[Cu(tmd)_2]^{2+}$, it proceeds through a [Cu^{II}-NO] intermediate formation. In this direction, the NO reactivity of Cu(II) complexes of the following tetra- and pentadentate ligands have been studied to have insight into the factors which control the reduction mechanism (Figure 2.1).

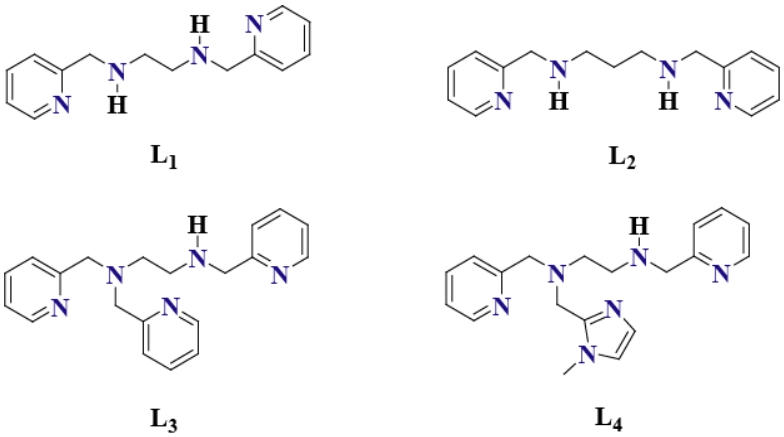

Figure 2.1 Ligands used for the present study.

2.2 Results and discussion

Four Cu(II) complexes, **2.1**, **2.2**, **2.3** and **2.4** were synthesized with ligands, $\mathbf{L_1}$, $\mathbf{L_2}$, $\mathbf{L_3}$ and $\mathbf{L_4}$ [$\mathbf{L_1}$ = *N*^{1},*N*^{2}-*bis*{(pyridin-2-yl)methyl}ethane-1,2-diamine, $\mathbf{L_2}$ = *N*^{1},*N*^{3}-*bis*{(pyridin-2-yl)methyl}propane-1,3-diamine; $\mathbf{L_3}$ = *N*^{1},*N*^{1},*N*^{2}-*tris*{(pyridin-2-yl)methyl}ethane-1,2-diamine; $\mathbf{L_4}$ = *N*^{1}-((1-methyl-1H-imidazol-2-yl)methyl)-*N*^{1},*N*^{2}-*bis*{(pyridin-2-yl)methyl}ethane-1,2-diamine], respectively, as their perchlorate salts. The complexes were characterized by various analytical techniques (experimental section). The single crystal structures of all the complexes were determined. The perspective ORTEP views for the complexes are shown in figure 2.2. The crystallographic data, important bond angles and distances are listed in tables 2.1, 2.2 and 2.3, respectively. In **2.1** and **2.2**, Cu(II) is found to be surrounded by four nitrogen donor atoms from the respective ligands and two oxygen atoms from two perchlorate ions resulting in an overall distorted octahedral coordination geometry around the Cu centre. The Cu-$O_{(perchlorate)}$ distances (2.682/2.592 and 2.697/2.581 Å for **2.1** and **2.2**, respectively) are within the range of reported Cu-$O_{(perchlorate)}$ diatances.[19,20,23,24] The average Cu-N distances in complexes **2.1** and **2.2** are 1.989 Å and 1.994 Å, respectively, which are in the range observed in the reported complexes.[19,20,23,24]

In complexes **2.3** and **2.4**, the Cu centre is found to be surrounded by five N-atoms from the respective ligands and one oxygen atom from a perchlorate anion maintaining an overall distorted octahedral geometry (Figures 2.2c and 2.2d). In complex **2.3**, the four equatorial distances are found to be 1.971, 2.002, 2.026 and 2.041 Å. The axial Cu-N distance (2.102 Å) is observed to be longer compared to the equatorial distances owing to the axial elongation.

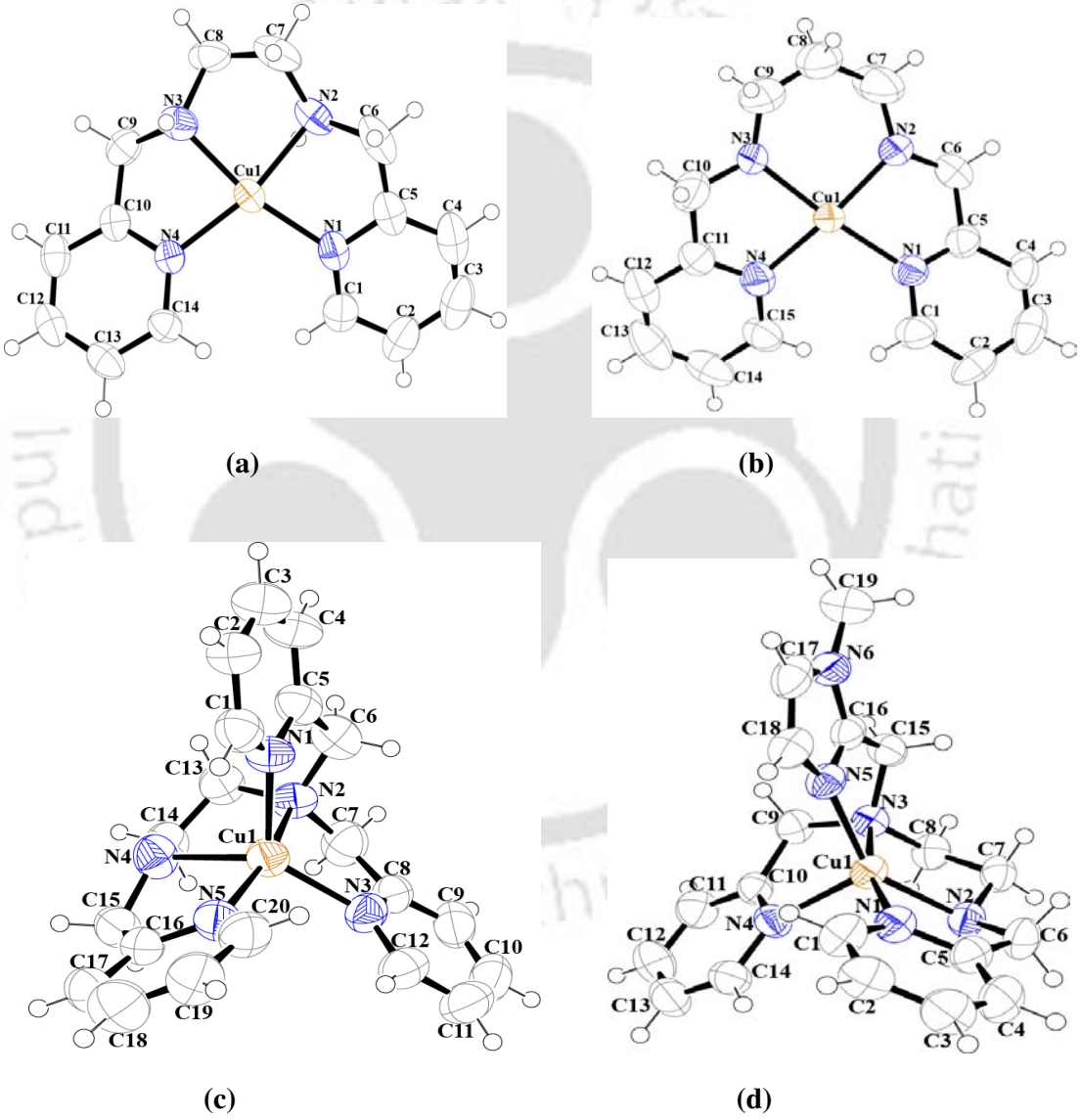

Figure 2.2 ORTEP diagrams for complexes (a) **2.1** (b) **2.2** (c) **2.3** and (d) **2.4** (50% thermal ellipsoid plot; perchlorate and solvent molecules removed for clarity).

In complex **2.4**, the equatorial Cu-N distances are 1.968, 1.987, 2.053 and 2.019 Å and the axial one is 2.137 Å. The Cu-$O_{(perchlorate)}$ distances are 3.967 and 3.900 Å in complexes **2.3** and **2.4**, respectively. These distances are bit longer compared to that observed in complexes **2.1** and **2.2** and other reported analogous examples. This suggests a weak interaction between the Cu(II) and perchlorate anion in these cases.

The complexes **2.1**, **2.2**, **2.3** and **2.4**, in acetonitrile solvent, exhibit broad *d-d* bands at $\lambda_{max}(\varepsilon/ M^{-1}cm^{-1})$ 605 nm (245), and 618 nm (170), 672 nm (208), and 640 nm (173), respectively, along with relatively strong intra-ligand absorptions in the UV region (Appendix I, Figures A1.18, A1.20, A1.22 and A1.24).

The methanol solutions of the complexes displayed characteristic spectra in X-band EPR studies at 77 K (Appendix I, Figures A1.42, A1.43, A1.44 and A1.45).[25] The calculated spectral parameters, $g_{\parallel}$, $g_{\perp}$ and $A_{\parallel}$ are within the observed range (experimental section). All the complexes exhibit one electron praramagnetism at room temperature, as expected.

The cyclic voltammetirc studies of the complexes are carried out in methanol and acetonitrile solvents. The quasi-reversible couple at –0.55 v *versus* Ag/Ag^{+} in the voltammogram of complex **2.1** in methanol is attributed to the Cu^{II}/Cu^{I} process (Figure 2.3). This couple appeared at –0.53, –0.59 and –0.64v *versus* Ag/Ag^{+} electrode in methanol for complexes **2.2**, **2.3** and **2.3**, respectively.

For $[Cu(DAC)]^{2+}$, the couple was reported to appear at –0.61 v *versus* Fe^{+}/Fe in DMF/MeOH (1:1) solution.[16] The difference in potential are attributed to the change in ligand frameworks and denticity. In addition, for complexes **2.3** and **2.4**, the change in axial donor atom from $N_{(Py)}$ to $N_{(im)}$ may also have an effect on the Cu^{II}/Cu^{I} potential. For Cu(II) complexes having bidentate N-donor ligands like N,N-dimethylethylenediamine, N,N-ethylethylenediamine, N,N-diisobutylethylenediamine, tmd (tmd = 5,5,7-trimethyl-[1,4]-diazepane), etc., the Cu^{II}/Cu^{I} couple was also observed to appear in comparable

Table 2.1 Crystallographic data for complexes **2.1**, **2.2**, **2.3** and **2.4**

	2.1	**2.2**	**2.3**	**2.4**
Formulae	C_{28} H_{36} Cl_4 Cu_2 N_8 O_{16}	C_{30} H_{36} Cl_3 Cu_2 N_8 O_{13}	C_{20} H_{22} Cl_2 Cu N_5 O_9	C_{21} H_{27} Cl_2 Cu N_7 O_8
Mol. wt.	1009.55	950.12	610.88	639.95
Crystal system	Orthorhombic	Orthorhombic	Monoclinic	Triclinic
Space group	P n m a	P n m a	P n	P_{-1}
Temperature /K	296(2)	296(2)	296(2)	293(2)
Wavelength /Å	0.71073	0.71073	0.71073	0.71073
a /Å	14.4349(13)	13.6944(4)	8.7895(3)	8.9766(2)
b /Å	26.361(3)	26.3827(8)	12.8229(5)	9.9809(2)
c /Å	10.5333(9)	11.2946(3)	11.1763(5)	16.3225(4)
α/°	90.00	90.00	90.00	91.1700(10)
β/°	90.00	90.00	94.308(2)	94.8440(10)
γ/°	90.00	90.00	90.00	110.2890(10)
V/ $Å^3$	4008.2(6)	4080.7(2)	1256.09(9)	1364.84(5)
Z	4	4	2	2
Density/Mgm^{-3}	1.673	1.546	1.615	1.557
Abs. Coeff. /mm^{-1}	1.406	1.308	1.142	1.054
Abs. correction	None	None	None	None
F(000)	2056	1940.0	624	658
Total no. of reflections	4618	2968	5401	6639
Reflections, $I > 2\sigma(I)$	3024	2197	3406	3939
Max. 2θ/°	27.67	23.18	28.58	28.43
Ranges (h, k, l)	-18 ≥ h ≥ 17 -34 ≥ k ≥ 30 -13 ≥ 1 ≥ 13	-15 ≥ h ≥ 15 -29 ≥ k ≥ 29 -12 ≥ 1 ≥ 12	-11 ≥ h ≥ 11 -17 ≥ k ≥ 14 -15 ≥ 1 ≥ 14	-12 ≥ h ≥ 11 -13 ≥ k ≥ 12 -21 ≥ 1 ≥ 21
Complete to 2θ (%)	96.5	99.7	97.5	96.7
Refinement method	Full-matrix least-squares on F^2	Full-matrix least-squares on F^2	Full-matrix least-squares on F^2	Full-matrix least-squares on F^2
Goof (F^2)	1.186	1.660	0.906	0.992
R indices [$I > 2\sigma(I)$]	0.0613	0.1292	0.0454	0.0549
R indices (all data)	0.0992	0.1450	0.0719	0.0747

Table 2.2 Selected bond angles (°) for complexes **2.1**, **2.2**, **2.3** and **2.4**

	2.1	**2.2**	**2.3**	**2.4**
N(1)-Cu(1)-N(2)	82.5(2)	81.6(4)	83.2(1)	83.1(1)
N(1)-Cu(1)-N(3)	167.5(2)	169.4(4)	124.0(2)	166.8(1)
N(1)-Cu(1)-N(4)	110.5(2)	103.9(3)	100.3(2)	108.4(1)
N(1)-Cu(1)-N(5)	-	-	100.3(2)	102.9(1)
N(2)-Cu(1)-N(3)	85.1(2)	93.8(5)	83.5(2)	85.9(1)
N(3)-Cu(1)-N(4)	81.9(2)	82.5(4)	132.3(2)	81.4(1)
N(4)-Cu(1)-N(5)	-	-	83.1(2)	106.7(1)
C(2)- C(1)-N(1)	122.2(5)	124(1)	122.9(5)	122.7(4)
C(1)-C(2)-C(3)	117.8(6)	116(1)	119.6(6)	118.5(4)
C(1)-N(1)-C(5)	118.3(4)	118.0(9)	118.8(4)	118.7(3)
C(4)-C(5)-C(6)	123.8(5)	122(1)	123.9(5)	122.6(3)

Table 2.3 Selected bond length (Å) for complexes **2.1**, **2.2**, **2.3** and **2.4**

	2.1	**2.2**	**2.3**	**2.4**
Cu(1)-N(1)	1.998(4)	1.987(8)	2.102(4)	1.968(2)
Cu(1)-N(2)	1.996(4)	1.99(1)	2.002(3)	2.019(4)
Cu(1)-N(3)	1.991(4)	2.00(1)	2.026(4)	2.053(2)
Cu(1)-N(4)	1.993(3)	1.978(8)	2.041(4)	2.137(3)
Cu(1)-N(5)	-	-	1.971(4)	1.987(3)
C(1)-C(2)	1.377(8)	1.36(2)	1.371(7)	1.358(5)
C(4)-C(5)	1.348(8)	1.39(1)	1.383(8)	1.384(5)
C(7)-C(8)	1.489(8)	1.45(2)	1.497(9)	1.512(5)
C(10)-C(11)	1.398(6)	1.55(2)	1.39(1)	1.408(6)
C(1)-N(1)	1.338(7)	1.34(1)	1.310(6)	1.349(5)
C(7)-N(2)	1.485(7)	1.34(2)	1.509(7)	1.480(4)
C(8)-N(3)	1.489(7)	-	1.333(8)	1.487(5)

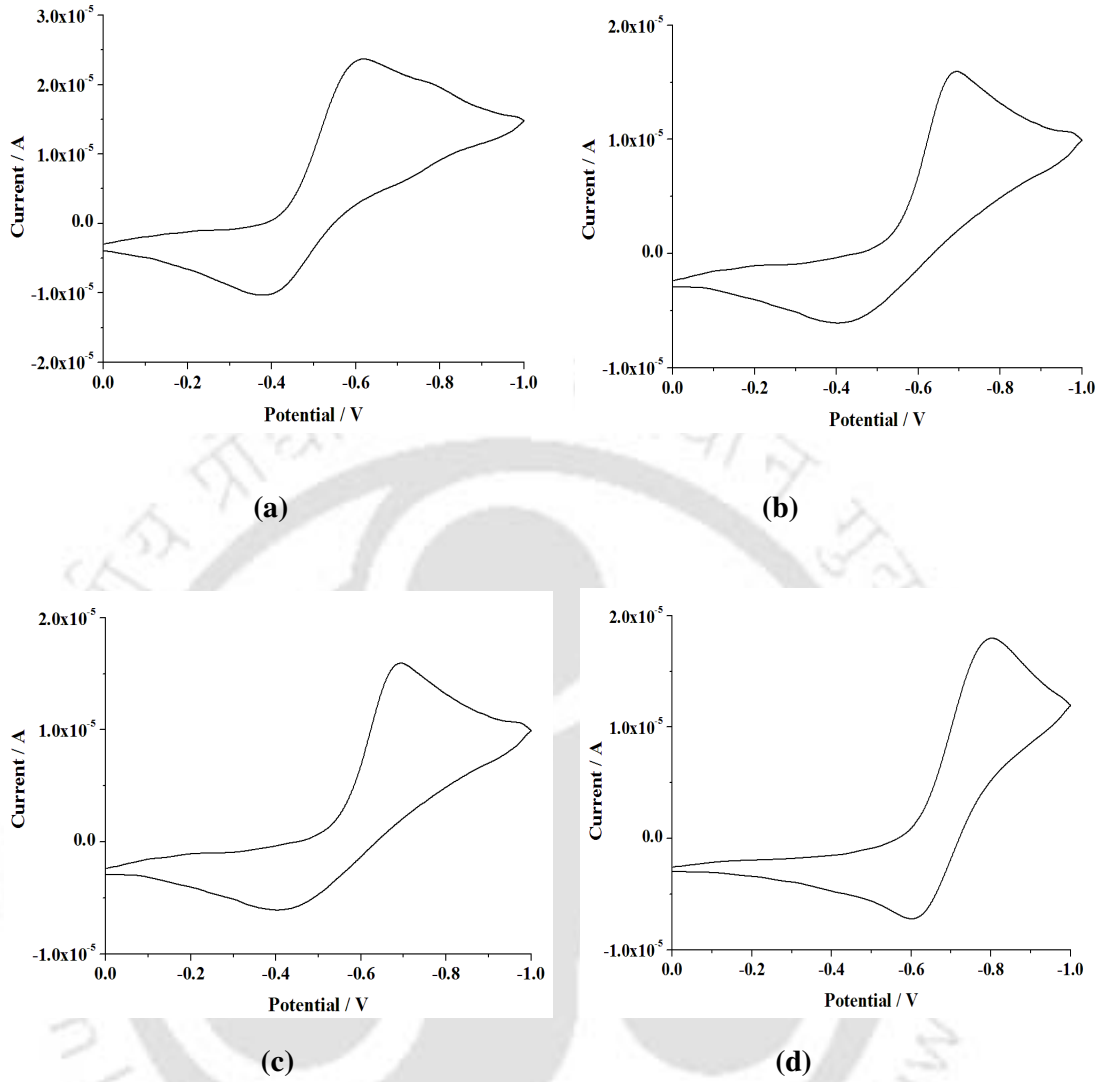

Figure 2.3 Cyclic voltammograms for complexes (a) **2.1** (b) **2.2** (c) **2.3** and (d) **2.4** in acetonitrile solvent. Working electrode, Pt; Reference electrode, Ag/Ag+; TBAP supporting electrolyte; scan rate 50 mv/s.

range.[20,24] Thus, the ligand denticity and the nature of the donor atoms evidently control the potential for the Cu^{II}/Cu^{I} couple. The cyclic voltammograms of the complexes in methanol in presence of one equivalent sodium ethoxide are also recorded and they show the expected change in potential due to the formation of the amido anions of the corresponding ligands (Figure 2.4).

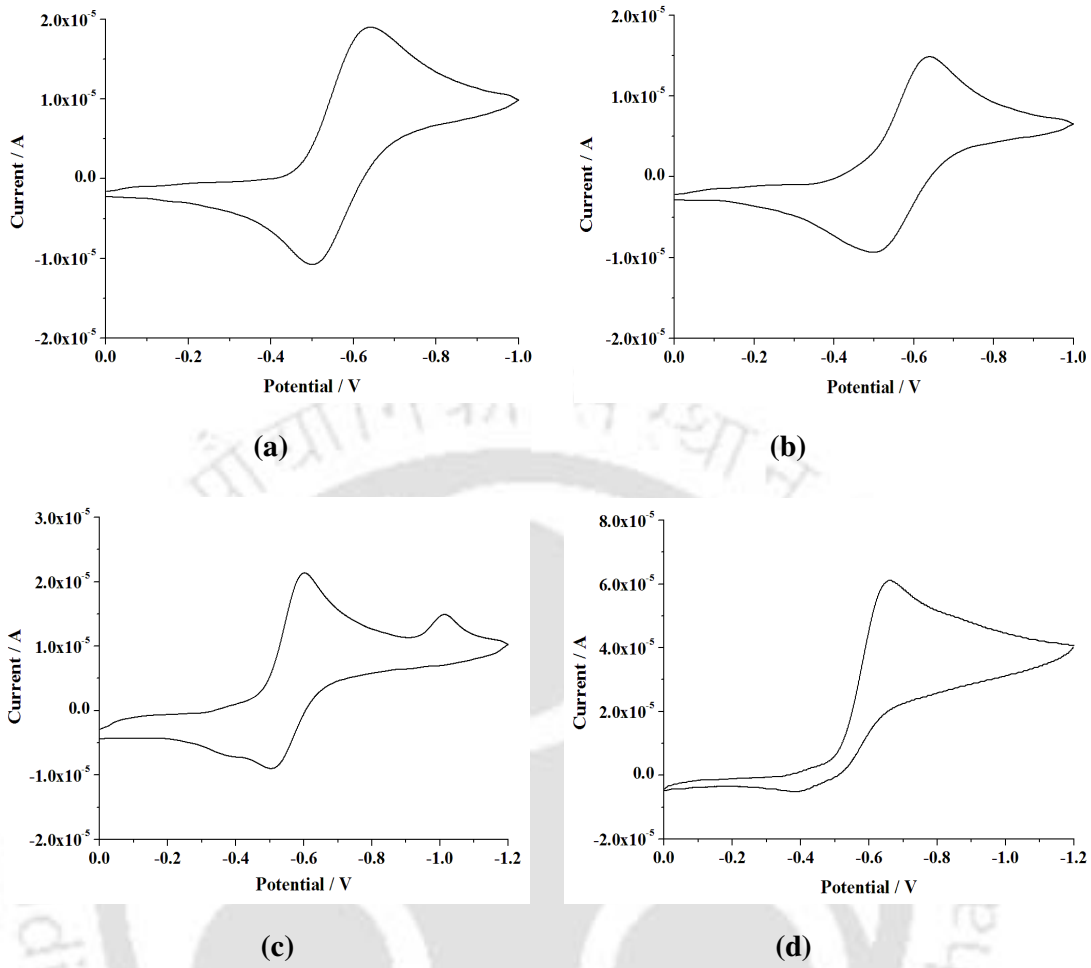

Figure 2.4 Cyclic voltammograms for complexes (a) **2.1** (b) **2.2** (c) **2.3** and (d) **2.4** in presence of one equivalent NaOEt in methanol solvent. Working electrode, Pt; Reference electrode, Ag/Ag+; TBAP supporting electrolyte; scan rate 50 mv/s.

Nitric oxide reactivity

NO reactivity of all the complexes are studied in dry acetonitrile and methanol solution. However, addition of NO gas in acetonitrile solution of the complexes is found to be unreactive. In methanol solution, in presence of one equivalent of sodium ethoxide as base, the complexes are found to react with NO leading to the reduction of Cu(II) centre to Cu(I). This has been monitored by UV-visible, X-band EPR spectroscopy. For complex **2.1**, the *d-d* band appears with λ_{max} at 605 nm in degassed methanol at room temperature. Addition of one equivalent sodium ethoxide shifted the λ_{max} to 642 nm (Figure 2.5). This is

attributed to the formation of corresponding amido anion coordinated complex after deprotonation at the secondary amine position (Scheme 2.1).[16]

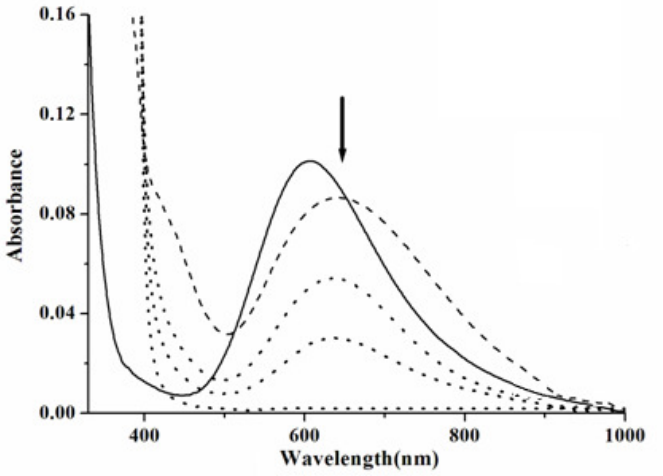

Figure 2.5 UV-visible spectra of complex **2.1** in methanol before (solid line), after (dashed line) addition of one equivalent of NaOEt and after (dotted line) addition of NO.

Addition of NO gas to this solution resulted in immediate decay of the intensity of the absorption band centred at 642 nm and finally disappeared indicating complete reduction of the Cu(II) centre to Cu(I) (Figure 2.5). It should be noted that similar behaviour was reported for the NO reactivity of $[Cu^{II}(DAC)]^{2+}$ and $[Cu^{II}(mtad)]^{2+}$ complexes. The spectral changes for the reduction of Cu(II) by NO in case of $[Cu^{II}(DAC)]^{2+}$ was observed to be condition dependent. In unbufferred MeOH/water mixture, the spectroscopic changes appeared to show an induction period which was no longer apparent in the buffered medium. This was, presumably, because of the shift in effective pH in course of the reaction.[16] In $[Cu^{II}(mtad)],^{2+}$ an induction period was observed in methanol: water (8 : 2, v/v) medium in unbufferred condition. The absorbance of a single wavelength (at 523 nm) was plotted *versus* time, however, there was no indication of the presence of induction period in neutral medium.[24] In the present study, shift in λ_{max} from 605 to 642 nm upon addition of one equivalent of sodium ethoxide suggests the formation of the proposed Cu^{II}-

amido anion complex; which then reacts with NO to afford Cu(I) from Cu(II). This is found to follow a second order rate law which depends on both the (Cu-amido) and NO concentration. A plot of rate constants against [NO] at 298 K shows a linear relationship of the rate constants with [NO] at 298K (Figure 2.6).

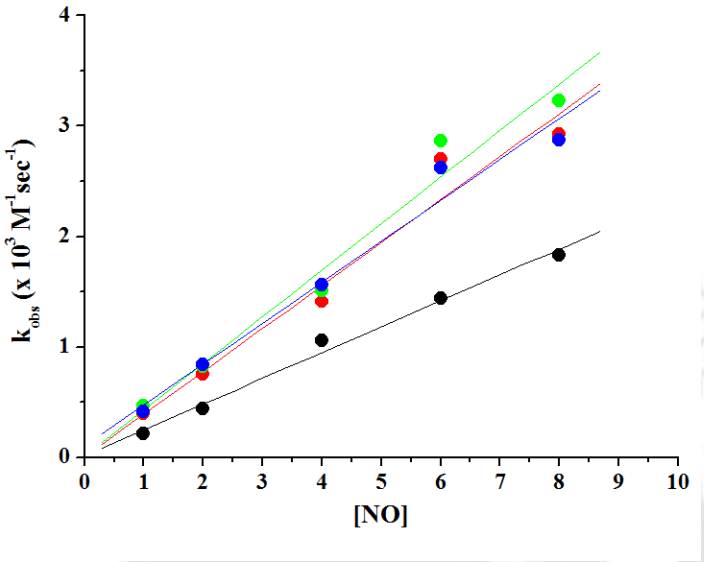

Figure 2.6 Plot of k_{obs} *versus* equivalent of NO added to a methanol solution for complexes **2.1**, **2.2**, **2.3** and **2.4** (black, red, green and blue, respectively) at 298K in prescence of one equivalent NaOEt.

Similar spectral change is observed in case of complex **2.2**, also. The λ_{max} of the *d-d* band in methanol is shifted from 618 to 664 nm upon addition of one equivalent sodium ethoxide suggesting the formation of the corresponding Cu(II)-amido complex (Appendix I, Figure A1.46). Addition of NO gas to this solution is found to diminish the intensity of the *d-d* band indicating the reduction of Cu(II) centre to Cu(I) following a second order rate equation (Figure 2.7).

On the other hand, addition of base to methanol solution of complexes **2.3** and **2.4** did not result in much shifting of λ_{max} like what observed in cases of complexes **2.1** and **2.2**; rather, the appearance of the new absorption bands at ~500 nm, in both the cases is observed owing to the formation of corresponding Cu(II)-amido anion complexes (Figure 2.7,

Scheme 2.2 and Appendix I, Figure A1.47). Upon addition of NO, these bands are found to diminish gradually along with the corresponding *d-d* bands owing to the reduction of Cu(II) to Cu(I). The observed rate constants for complexes **2.3** and **2.4** are also found to be linearly dependent on [NO] (Figure 2.6).

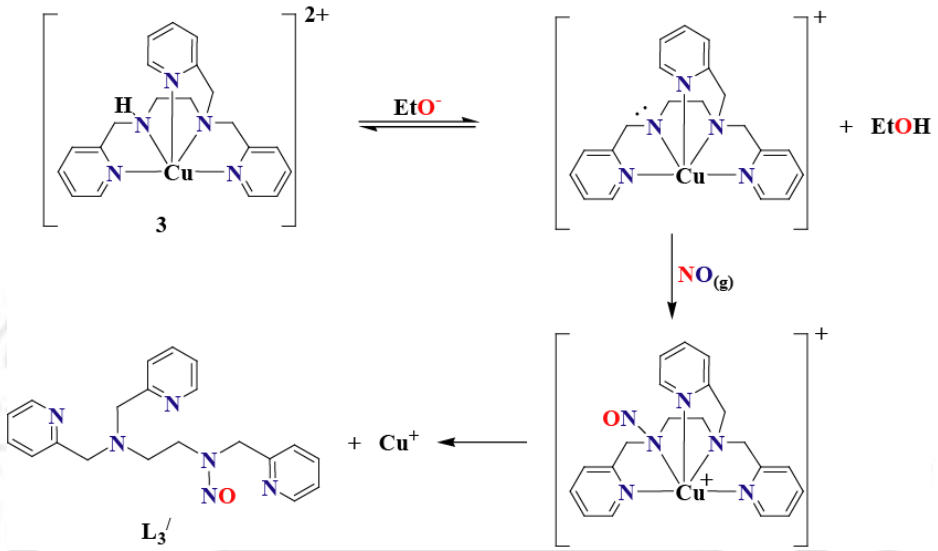

Scheme 2.2

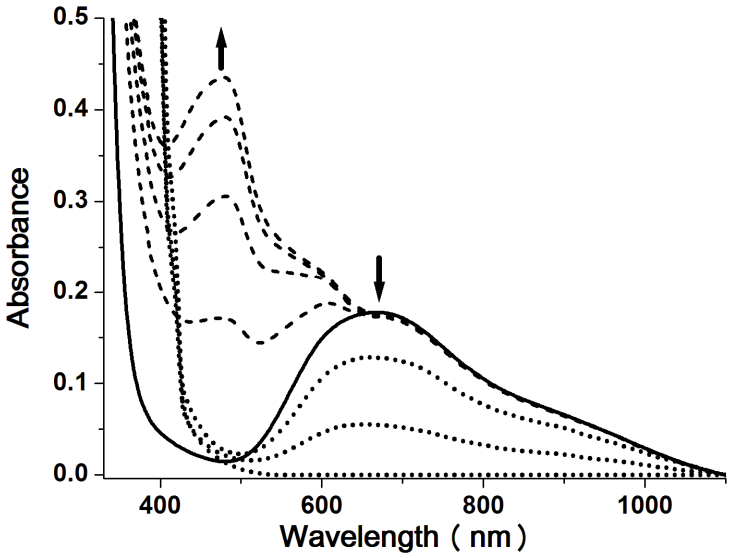

Figure 2.7 UV-visible spectra of complex **2.3** in methanol before (solid line), after (dashed line) addition of one equivalent of NaOEt and after (dotted line) addition of NO.

In the X-band EPR spectroscopy studies, all the complexes display characteristic signals. Addition of one equivalent of sodium ethoxide to the methanol solution of the complexes resulted in a difference in the g values (Figure 2.8 and Appendix I, Figures A1.48, A1.49 and A1.50). NO purging to these solutions, immediately makes them EPR silent. This is because of the formation of diamagnetic Cu(I).

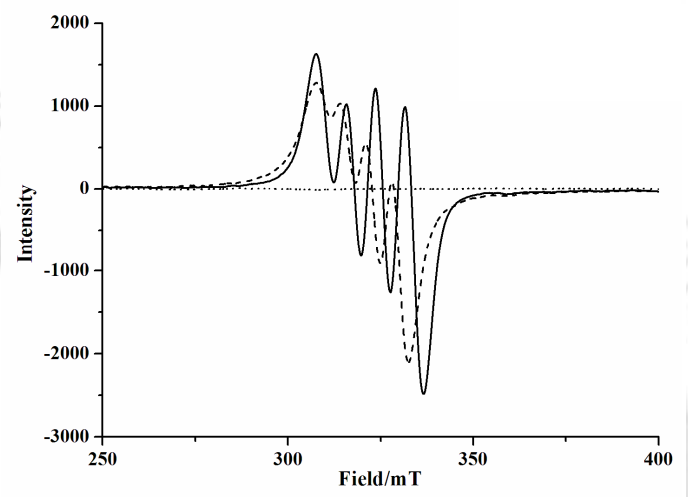

Figure 2.8 X-Band EPR spectra of complex **2.1** in methanol before (solid line), after (dashed line) addition of one equivalent of NaOEt and after (dotted line) addition of NO at room temperature.

Thus, from the present study it is evident that the reduction mechanism of Cu(II) centre by NO is very much dependent upon the coordinated ligands framework and denticity. In earlier reports, it was shown that as the macro-cyclic ligands offer extra inertness to the metal centre in $[Cu(DAC)]^{2+}$ or $[Cu(mtad)]^{2+}$, the reduction of Cu(II) by NO does not proceed through the formation of the corresponding $[Cu^{II}\text{-NO}]$ intermediate; whereas in cases of analogous non-macrocyclic ligands, it follows the $[Cu^{II}\text{-NO}]$ intermediate pathway. In the present study, though the ligands used are non-macrocycles, but they offer an environment to the metal centre which is not susceptible towards the NO binding to form $[Cu^{II}\text{-NO}]$ intermediate. Now the question arises, what factor does play the most important role to dictate whether the $[Cu^{II}\text{-NO}]$ complex will form or not in a particular

case? Is it controlled by the donor ability the ligand (in other words, the electrode potential)? Or, it is a structure dependent phenomenon? On comparative study of the other reported examples, it has been found the electrode potential of Cu^{II}/Cu^{I} couple essentially does not play much role in the formation of [Cu^{II}-NO] intermediate. On the other hand, it has been observed that complexes having structural flexibility to attain trigonal-bipyramidal geometry after coordination to the NO, only form the [Cu^{II}-NO] intermediate. For instance, the tetradentate ligands, such as DAC or mtad, because of structural constrain do not allow the corresponding Cu(II) complex to attain trigonal bipyramidal geometry after NO coordination. On the other hand, mtd ligand, which is analogous to mtad, but bidentate and hence offers the required flexibility to the [Cu^{II}-NO] complex to attain trigonal bipyramidal geometry very easily. Theoretical studies also suggested a trigonal bipyramidal geometry for this intermediate complex.[20b,21,24] In cases of all other reported Cu(II) complexes of bidentate ligands, the formation of the [Cu^{II}-NO] is observed irrespective of the nature of donar atoms. For instance, pyridine-2-ethyl amine or bemim (bemim = *bis*-(2-ethyl-4-methyl-imidazol-5yl)methane), the donor atoms are pyridine and primary amine nitrogen for the earlier and imidazole nitrogen in later; however, the Cu(II) complexes of these two ligands were found to form [Cu^{II}-NO] intermediate upon reaction with NO in acetonitrile solution. The DFT studies again suggested a distorted trigonal bipyramidal geometry for both the cases.[20b,21,24] In the present study, $\mathbf{L_1}$ and $\mathbf{L_2}$, being tetradentate and less flexible, do not allow the corresponding Cu(II) complexes to attain trigonal bipyramidal geometry after NO coordination. On the other hand, $\mathbf{L_3}$ and $\mathbf{L_4}$, by virtue, will allow the metal centre to form only hexa-coordinated [Cu^{II}-NO] complex with a distorted octahedral geometry. Thus, the formation of the [Cu^{II}-NO] intermediate is not observed in the present study. Hence, it is the structural factor which essentially dictates

whether a particular Cu(II) complex will form [Cu^{II}-NO] intermediate upon reaction with NO or not.

The N-nitrosated ligands in all the cases are isolated from the reaction mixture as they are demetallated owing to the weaker donor ability and geometrical preference of Cu(I) and characterized (experimental section). In case of analogous $[Cu(DAC)]^{2+}$, $[Cu(mtad)]^{2+}$ complexes, similar results were exemplified.

2.3 Conclusion

Thus, this chapter demonstrats that the ligand frameworks have a reflective effect in controlling the mechanism of the reduction of Cu(II) centre by NO. The flexibility of the ligand/s for a particular Cu(II) complex to attain a trigonal bipyramidal geometry after NO coordination is found to be most important parameter in dictating the pathway for their interaction. In the present study, all the four compounds, because of structural constrain, are found to follow deprotonation pathway for the reduction of Cu(II) centre by NO rather than [Cu^{II}-NO] intermediate formation.

2.4 Experimental Section

2.4.1 Materials and methods

All reagents and solvents of reagent grade were purchased from commercial sources and used as received except specified. Acetonitrile was distilled from calcium hydride. Deoxygenation of the solvent and solutions was effected by repeated vacuum/purge cycles or bubbling with nitrogen for 30 minutes. NO gas was purified by passing through KOH and P_2O_5 column. UV-visible spectra were recorded on a Perkin Elmer Lambda 25 UV-visible spectrophotometer. FT-IR spectra of the solid samples were taken on a Perkin Elmer spectrophotometer with samples prepared as KBr pellets. Solution electrical conductivity was measured using a Systronic 305 conductivity bridge. ^{1}H-NMR spectra

were recorded in a 400 MHz Varian FT spectrometer. Chemical shifts (ppm) were referenced either with an internal standard (Me_4Si) or to the residual solvent peaks. The X-band Electron Paramagnetic Resonance (EPR) spectra were recorded on a JES-FA200 ESR spectrometer, at room temperature and 77 K with microwave power, 0.998 mW; microwave frequency, 9.14 GHz and modulation amplitude, 2. Elemental analyses were obtained from a Perkin Elmer Series II Analyzer. The magnetic moment of complexes was measured on a Cambridge Magnetic Balance.

Single crystals were grown by slow diffusion followed by slow evaporation technique. The intensity data were collected using a Bruker SMART APEX-II CCD diffractometer, equipped with a fine focus 1.75 kW sealed tube MoK_α radiation (λ, 0.71073 Å) at 273(3) K, with increasing ω (width of 0.3° per frame) at a scan speed of 3 s/frame. The SMART software was used for data acquisition. Data integration and reduction were undertaken with SAINT and XPREP software.[26] Structures were solved by direct methods using SHELXS-97 and refined with full-matrix least squares on F^2 using SHELXL-97.[27] All non-hydrogen atoms were refined anisotropically. Structural illustrations have been drawn with ORTEP-3 for Windows.[28]

2.4.2 Synthesis of ligands

Synthesis of L_1

The ligand **L_1** was reported earlier.[29] To a solution of pyridine-2-carboxaldehyde (2.14 g, 20 mmol) in 20 ml methanol was added ethylenediamine (0.60 g, 10 mmol) into a 50 ml round bottom flask equipped with a stirring bar. The solution was refluxed for 5 h. The resulting reddish-yellow solution was then reduced by $NaBH_4$ (1.52 g, 40 mmol). Removal of solvent under reduced pressure affords a crude mass. It was dissolved in water (50 ml) and extracted with chloroform (50 ml × 4 portion). Organic part was dried under reduced

pressure and the reddish yellow oil thus obtained was subjected to chromatographic purification using silica gel column to yield the pure ligand, **L_1** as yellow oil. Yield: 1.96 g, ~80%. Elemental analyses for $C_{14}H_{18}N_4$: Calcd. (%): C, 69.39; H, 7.49; N, 23.12. Found (%): C, 69.33; H, 7.50; N, 23.01. FT-IR in KBr: 2791, 1591, 1475, 1431, 767 cm^{-1}. ^{1}H-NMR (400 MHz, $CDCl_3$) δ_{ppm}: 2.81 (4H), 3.91 (4H), 7.12-7.15 (2H), 7.30-7.32 (4H) 7.60-7.64 (2H), 8.52-8.53 (2H). ^{13}C-NMR (100 MHz, $CDCl_3$) δ_{ppm}: 46.9, 53.0, 120.7, 121.0, 135.1, 147.6 and 157.6. ESI-Mass (m+1): Calcd. 243.32; Found, 243.04.

Synthesis of L_2

Ligand **L_2** was prepared following the same procedure used for **L_1** from the reaction of pyridine-2-carboxaldehyde and propylenediamine. Yield: 2.18 g, ~85%. Elemental analyses for $C_{15}H_{20}N_4$: Calcd. (%): C, 70.28; H, 7.86; N, 21.86. Found (%): C, 70.23; H, 7.85; N, 21.94. FT-IR in KBr: 2791, 1591, 1475, 1430, 1167, 767 cm^{-1}. ^{1}H-NMR (400 MHz, $CDCl_3$) δ_{ppm}: 1.75-1.79 (2H), 2.70-2.77 (4H), 3.90 (4H), 7.13-7.16 (4H), 7.28-7.30 (2H) 7.60-7.64 (2H), 7.52-7.54 (2H). ^{13}C-NMR (100 MHz, $CDCl_3$) δ_{ppm}: 29.8, 47.5, 54.8, 121.5, 121.9, 136.0, 148.8 and 159.4. ESI-Mass (m+1): Calcd. 257.35; Found, 257.04.

Synthesis of L_3

L_3 was synthesized by following the reported procedure.[30] A solution of 1.21 g (5 mmol) of **L_1** and 0.54 g (5 mmol) of pyridine-2-carboxaldehyde in 20 ml of diethyl ether was stirred at room temperature for 3 h to afford white precipitate. The solid obtained after filtration was washed with diethyl ether. In a 250 ml flask, 1.66 g of the solid (5 mmol) was dissolved in 50 ml methanol and to this 0.315 g (5 mmol) of $NaBH_3CN$ dissolved in 4 ml methanol and 0.77 ml (10 mmol) of CF_3CO_2H were added. The solution was stirred at room temperature for 8 h. To this NaOH solution (15%, 50 ml) was added and then extracted with CH_2Cl_2 (4 × 100 ml portions). Removal of solvent under vacuum affords **L_3**

as yellow oil. Yield: 1.26 g, ~76%. Elemental analyses for $C_{20}H_{23}N_5$: Calcd. (%): C, 72.04; H, 6.95; N, 21.00. Found (%): C, 72.11; H, 6.95; N, 21.10. FT-IR in KBr: 2916, 2786, 1583, 1477, 1432, 765 cm^{-1}. ^{1}H-NMR (400 MHz, $CDCl_3$) δ_{ppm}: 2.16 (1H) 2.78 (4H), 3.82 (6H), 7.12-7.15 (4H), 7.27 (1H), 7.51 (1H), 7.59-7.65 (4H), 7.49 (1H). ^{13}C-NMR (100 MHz, $CDCl_3$) δ_{ppm}: 48.8, 54.0, 54.8, 54.9, 60.5, 121.8, 121.8, 121.9, 122.2, 122.2, 123.1, 136.3, 136.4, 148.8, 149.1, 159.4 and 159.6. ESI-Mass (m+1): Calcd. 334.43; Found, 334.78.

Synthesis of L_4

Ligand $\mathbf{L_4}$ was prepared following the same procedure used for $\mathbf{L_3}$ from the reaction of 1-methylimidazole-2-carboxaldehyde with $\mathbf{L_1}$. Yield: 1.21g, ~72%. Elemental analyses for $C_{19}H_{24}N_6$: Calcd. (%): C, 67.83; H, 7.19; N, 24.98. Found (%): C, 63.77; H, 7.21; N, 24.89. FT-IR in KBr: 2922, 2803, 1593, 1471, 1432, 1141, 767 cm^{-1}. ^{1}H-NMR (400 MHz, $CDCl_3$) δ_{ppm}: 2.71-2.82 (4H) 3.58 (3H), 3.75-3.79 (6H), 6.75 (1H), 6.88 (1H), 7.12-7.16 (2H), 7.25-7.36 (2H), 7.58-7.63 (2H), 8.49-8.53 (2H). ^{13}C-NMR (100 MHz, $CDCl_3$) δ_{ppm}: 32.6, 46.4, 48.8, 53.8, 54.6, 59.9, 121.3, 121.6, 121.8, 121.9, 123.2, 126.7, 136.1, 136.1, 148.7, 148.8, 148.9, 158.8 and 159.5. ESI-Mass (m+1): Calcd. 337.43; Found, 337.22.

2.4.3 Synthesis of complexes

The complexes have been synthesized following a general experimental procedure of the reaction of $[Cu^{II}(H_2O)_6](ClO_4)_2$ with equivalent quantity of the respective ligand. The details are given for complex **2.1**.

Synthesis of complex 2.1

$[Cu^{II}(H_2O)_6](ClO_4)_2$ (1.85 g, 5 mmol) was dissolved in 10 ml distilled acetonitrile. To this solution, $\mathbf{L_1}$ (1.21 g, 5 mmol) was added slowly with constant stirring. The color of the solution turned into greenish-blue. The stirring was continued for 1h at room temperature.

The volume of the solution was then reduced to ~2 ml. To this, benzene (5 ml) was added to layer on it and kept it overnight on freezer. This resulted into dark green crystalline complex **2.1**. Yield: 2.14 g, ~85%. UV-vis. (acetonitrile): λ_{max}, 605 nm (ε, 245 $M^{-1}cm^{-1}$). X-Band EPR (in methanol at 77 K): $g_{\parallel}$, 2.226; $g_{\perp}$, 2.012; $A_{\parallel}$, 160 × 10^{-4} cm^{-1}. FT-IR in KBr: 3140, 2921, 1608, 1467, 1120, 1083, 625 cm^{-1}. Molar conductivity in acetonitrile: Λ_M ($\Omega^{-1}M^{-1}cm^2$), 244. μ_{obs}, 1.56 BM.

Synthesis of complex 2.2

Complex **2.2** was synthesized from $[Cu^{II}(H_2O)_6](ClO_4)_2$ (1.85 g, 5 mmol) and $\mathbf{L_2}$ (1.28 g, 5 mmol). Yield: 2.12 g, ~82%. UV-vis. (acetonitrile): λ_{max}, 618 nm (ε, 166 $M^{-1}cm^{-1}$). X-Band EPR (in methanol at 77 K): $g_{\parallel}$, 2.270; $g_{\perp}$, 2.061; $A_{\parallel}$, 164 × 10^{-4} cm^{-1}. FT-IR in KBr: 3166, 2866, 1608, 1120, 1082, 765, 625cm^{-1}. Molar conductivity in acetonitrile: Λ_M ($\Omega^{-1}M^{-1}cm^2$), 236. μ_{obs}, 1.51 BM.

Synthesis of complex 2.3

Complex **2.3** was synthesized from $[Cu^{II}(H_2O)_6](ClO_4)_2$ (1.85 g, 5 mmol) and $\mathbf{L_3}$ (1.67 g, 5 mmol). Yield: 2.62g, ~88%. UV-vis. (acetonitrile): λ_{max}, 672 nm (ε, 208 $M^{-1}cm^{-1}$). FT-IR in KBr: 3238, 3077, 1610, 1484, 1144, 1108, 1088, 771, 624 cm^{-1}. X-band EPR (in methanol at 77 K): $g_{\parallel}$, 2.207; $g_{\perp}$, 2.013; $A_{\parallel}$, 158 × 10^{-4} cm^{-1}. Molar conductivity in acetonitrile: Λ_M ($\Omega^{-1}M^{-1}cm^2$), 205. μ_{obs}, 1.56 BM.

Synthesis of complex 2.4

Complex **2.4** was synthesized from $[Cu^{II}(H_2O)_6](ClO_4)_2$ (1.85 g, 5 mmol) and $\mathbf{L_4}$ (1.68 g, 5 mmol). Yield: 2.54 g, ~85%. UV-vis. (acetonitrile): λ_{max}, 640 nm (ε, 173 $M^{-1}cm^{-1}$). The X-Band EPR (in methanol at 77 K): $g_{\parallel}$, 2.230; $g_{\perp}$, 2.035; $A_{\parallel}$, 138 × 10^{-4} cm^{-1}. FT-IR in KBr:

3255, 1611, 1447, 1144, 1108, 1089, 767, 626 cm^{-1}. Molar conductivity in acetonitrile: Λ_M ($\Omega^{-1}M^{-1}cm^2$), 236. μ_{obs}, 1.54 BM.

2.4.4 Isolation of L_1'

Complex **2.1** (0.252 g, 0.5 mmol) was dissolved in 10 ml of distilled and degassed methanol. To this solution one equivalent of the sodium ethoxide was added and then excess of NO gas was purged. The resulting colorless solution was stirred for 1 h at room temperature. After removing the excess NO by several cycles of vacuum/purge, 10 ml of degassed benzene was added to this under dinitrogen atmosphere. The reaction mixture was kept in freezer for overnight. The **L_1'**-perchlorate was found to be precipitated out. Yield: 0.133g, ~70%. Elemental analyses for $C_{14}H_{22}N_5ClO_7$: Calcd. (%): C, 41.23; H, 5.43; N, 17.17. Found (%): C, 41.15; H, 5.44; N, 17.26. FT-IR in KBr: 3282, 1589, 1437, 1358, 1117, 755, 623 cm^{-1}. ^{1}H-NMR (400 MHz, D_2O) δ_{ppm}: 4.08-4.13 (2H), 4.27-4.34 (2H), 4.90 (2H), 5.45 (2H), 7.22-7.32 (4H), 7.69-7.76 (2H), 7.57-8.59 (2H). ^{13}C-NMR (100 MHz, D_2O + CD_3CN) δ_{ppm}: 43.4, 50.2, 51.8, 58.6, 123.8, 123.9, 123.9, 124.0, 138.4, 138.5, 150.6, 150.9, 155.3 and 156.2. ESI-Mass (m+1): Calcd. 272.32; Found, 272.12.

2.4.5 Isolation of L_2'

L_2' was isolated as its perchlorate salt from the reaction of complex **2.2** (0.260 g, 0.5 mmol) with NO following the procedure used for the isolation of the **L_1'**-perchlorate. Yield: 0.132 g, ~70%. Elemental analyses for $C_{15}H_{22}N_5ClO_6$: Calcd. (%): C, 44.62; H, 5.49; N, 17.84. Found (%): C, 42.65; H, 5.49; N, 17.91. FT-IR in KBr: 3067, 2927, 1451, 1437, 1358, 1083, 1123, 755, 629 cm^{-1}. ^{1}H-NMR (400 MHz, D_2O) δ_{ppm}: 2.36-2.39 (2H), 3.60-3.64 (2H), 4.32-4.35 (2H), 4.87 (2H), 5.43 (2H), 7.25-7.29 (4H), 7.70-7.73 (2H), 7.58-8.59 (2H). ^{13}C-NMR (100 MHz, D_2O + CD_3CN) δ_{ppm}: 30.2, 42.8, 50.5, 51.9, 58.4, 123.6, 123.8,

123.9, 124.5, 138.1, 138.5, 150.7, 150.9, 155.6 and 155.7. ESI-Mass (m+1): Calcd. 286.34; Found, 286.12.

2.4.6 Isolation of L_3'

L_3' was isolated as L_3'-perchlorate from the reaction of complex **2.3** (0.305 g, 0.5 mmol) and NO following the protocol used for L_1'. Yield: 0.148 g, ~65%. Elemental analyses for $C_{20}H_{22}N_6ClO_5$: Calcd. (%): C, 52.01; H, 4.80; N, 18.19. Found (%): C, 52.08; H, 4.81; N, 18.12. FT-IR in KBr: 2936, 1594, 1438, 1118, 1087, 630 cm^{-1}. ^{1}H-NMR (400 MHz, D_2O) δ_{ppm}: 3.81 (2H), 4.46 (2H), 4.93 (4H), 5.27 (2H), 7.14-7.19 (3H), 7.36-7.37 (2H), 7.53-7.62 (3H) 7.86 (2H), 8.48 (2H). ^{13}C-NMR (100 MHz, D_2O + CD_3CN) δ_{ppm}: 42.8, 49.9, 50.9, 52.7, 61.0, 123.5, 123.8, 123.9, 124.1, 124.3, 124.5, 137.8, 138.1, 135.2, 150.2, 150.6, 150.9, 155.7, 156.7 and 160.5. ESI-Mass (m+1): calcd. 363.43; Found, 363.45.

2.4.7 Isolation of L_4'

L_4' was isolated from the reaction of complex **2.4** (0.308 g, 0.5 mmol) with NO following the procedure used for the isolation of L_3'. Yield: 0.155 g, ~67%. Elemental analyses for $C_{19}H_{23}N_7ClO_5$: Calcd. (%): C, 48.67; H, 4.94; N, 20.91. Found (%): C, 48.73; H, 4.94; N, 20.83. FT-IR in KBr: 1598, 1448, 1123, 756, 630 cm^{-1}. ^{1}H-NMR (400 MHz, D_2O) δ_{ppm}: 2.20 (2H), 3.78 (2H), 4.26 (3H), 4.62 (4H), 5.02 (2H), 6.61 (1H), 6.80 (1H), 7.14 (2H) 7.65 (2H), 7.83 (2H), 8.46 (2H). ^{13}C-NMR (100 MHz, D_2O + CD_3CN) δ_{ppm}: 33.6, 49.0, 51.3, 51.5, 51.9, 61.0, 123.5, 123.8, 123.9, 124.4, 127.5, 137.8, 136.1, 135.4, 150.1, 150.6, 150.9, 155.6 and 160.0. ESI-Mass (m+1): Calcd. 366.43; Found, 366.37.

2.5 References

1. (a) *Nitric Oxide: Biology and Pathobiology*, Ignarro, L. J. Ed. Academic Press; San Diego, **2000**. (b) Moncada, S.; Palmer, R. M. J.; Higgs, E. A. *Pharmacol. Rev*. **1991**, *43*, 109. (c) Butler, A. R.; Williams, D. L. *Chem. Soc. Rev*. **1993**, *22*, 233. (d) *Methods in Nitric Oxide Research*; Feelisch, M.; Stamler, J. S. Eds. John Wiley and Sons; Chichester, England, **1996**.
2. (a) Jia, L.; Bonaventura, C.; Bonaventura, J.; Stamler, J. S. *Nature*, **1996**, *380*, 221. (b) Galdwin, M. T.; Lancaster, J. R. Jr.; Freeman, B. A.; Schechter, A. N. *Nat. Med.* **2003**, *9*, 496. (c) Ye, R. W.; Toro-Suarez, I.; Tiedje, J. M.; Averill, B. A. *J. Biol. Chem.* **1991**, *266*, 12848. (d) Hulse, C. L.; Averill, B. A.; Tiedje, J. M. *J. Am. Chem. Soc.* **1989**, *111*, 2322. (e) Jackson, M. A.; Tiedje, J. M.; Averill, B. A. *FEBS Lett.* **1991**, *291*, 41.
3. (a) Godden, J. W.; Turley, S.; Teller, D. C.; Adman, E. T.; Liu, M. Y.; Payne, W. J.; LeGall, J. *Science*, **1991**, *153*, 438. (b) Adman, E. T.; Turley, S. in *Bioinorganic Chemistry of Copper;* Karlin, K. D.; Tyekllr, Z. Eds. Chapman & Hall, Inc.; New York, 1993; pp 397. (c) Ferguson, S. J. *Curr. Opin. Chem. Biol.* **1998**, *2*, 182.
4. (a) Richardson, D. J.; Watmough, N. J. *Curr. Opin. Chem. Biol.* **1999**, *3*, 207. (b) Moura, I.; Moura, J. J. G. *Curr. Opin. Chem. Biol.* **2001**, *5*, 168. (c) Tocheva, E. I.; Rosell, F. I.; Mauk, A. G.; Murphy, M. E. P. *Biochem.* **2007**, *46*, 12366. (d) Zhou, X.; Espey, M. G.; Chen, J. X.; Hofseth, L. J.; Miranda, K. M.; Hussain, S. P.; Winks, D. A.; Harris, C. C. *J. Biol. Chem.* **2000**, *275*, 21241.
5. (a) Chien, J. C. W. *J. Am. Chem. Soc.* **1969**, *91*, 2166. (b) Trofimova, N. S.; Safronov, A. Y.; Ikeda, O. *Inorg. Chem.* **2003**, *42*, 1945.

6. (a) Walker, F. A. *J. Inorg. Biochem.* **2005**, *99*, 216. (b) Rousseau, D. L.; Li, D.; Couture, M.; Yeh, S. R. *J. Inorg. Biochem.* **2005**, *99*, 306. (c) George, S. J.; Allen, J. W. A.; Ferguson, S. J.; Thorneley, R. N. F. *J. Biol. Chem.* **2000**, *275*, 33231.

7. (a) Pinakoulaki, E.; Gemeinhardt, S.; Saraste, M.; Varotsis, C. *J. Biol. Chem.* **2002**, *277*, 23407. (b) Praneeth, V. K. K.; Paulat, F.; Berto, T. C.; DeBeer George, S.; Nather, C.; Sulok, C.; Lehnert, N. *J. Am. Chem. Soc.* **2008**, *130*, 15288. (c) Soldatova, A. V.; Ibrahim, M.; Olson, J. S.; Czernuszewicz, R. S.; Spiro, T. G. *J. Am. Chem. Soc.* **2010**, *132*, 4614. (d) Wasser, I. M.; de Vries, S.; Moe¨nne-Loccoz, P.; Schro¨der, I.; Karlin, K. D. *Chem. Rev.* **2002**, *102*, 1201.

8. (a) Hoshino, M.; Maeda, M.; Konishi, R.; Seki, H.; Ford, P. C. *J. Am. Chem. Soc.* **1996**, *118*, 5702. (b) Fernandez, B. O.; Lorkovic, I. M.; Ford, P. C. *Inorg. Chem.* **2004**, *43*, 5393. (c) Lehnert, N.; Praneeth, V. K. K.; Paulat, F. *J. Comput. Chem.* **2006**, *27*, 1338. (d) Ellison, M. K.; Scheidt, W. R. *J. Am. Chem. Soc.* **1999**, *121*, 5210. (e) Linder, D. P.; Rodgers, K. R.; Banister, J.; Wyllie, G. R. A.; Ellison, M. K.; Scheidt, W. R. *J. Am. Chem. Soc.* **2004**, *126*, 14136. (f) Lim, M. D.; Lorkovic, I. M.; Ford, P. C. *J. Inorg. Biochem.* **2005**, *99*, 151. (g) Shamir, D.; Zilbermann, I.; Maimon, E.; Gellerman, G.; Cohen, H.; Meyerstein, D. *Eur. J. Inorg. Chem.* **2007**, 5029.

9. (a) Torres, J.; Svistunenko, D.; Karlsson, B.; Cooper, C. E.; Wilson, M. T. *J. Am. Chem. Soc*. **2002**, *124*, 963. (b) Torres, J.; Cooper, C. E.; Wilson, M. T. *J. Biol. Chem.* **1998**, *273*, 8756. (c) Martin, C. T.; Morse, R. H.; Kanne, R. M.; Gray, H. B.; Malmstrom, B. G.; Chan, S. I. *Biochemistry*, **1981**, *20*, 5147.

10. Gorren, A. C. F.; de Boer, E.; Wever, R. *Biochem. Biophys. Acta* **1987**, *916*, 38.

11. Tran, D.; Ford, P. C. *Inorg. Chem.* **1996**, *35,* 2411.

12. (a) Brown, G. C. *Biochim. Biophys. Acta* **2001**, *1504*, 46. (b) Torres, J.; Sharpe, M. A.; Rosquist, A.; Cooper, C. E.; Wilson, M. T. *FEBS Lett.* **2000**, *475*, 263. (c) Wijma, H. J.; Canters, G. W.; de Vries, S.; Verbeet, M. P. *Biochem.* **2004**, *43*, 10467.

13. Wayland, B. B.; Olson, L. W. *J. Am. Chem. Soc.* **1974**, *96*, 6037.

14. Tran, D.; Skelton, B. W.; White, A. H.; Laverman, L. E.; Ford, P. C. *Inorg. Chem.* **1998**, *37*, 2505.

15. Lim, M. D.; Capps, K. B.; Karpishin, T. B.; Ford, P. C. *Nitric Oxide, Biol. Chem.* **2005**, *12*, 244.

16. (a) Tsuge, K.; DeRosa, F.; Lim, M. D.; Ford, P. C. *J. Am. Chem. Soc*. **2004**, *126*, 6564. (b) Khin, C.; Lim, M. D.; Tsuge, K.; Iretskii, A.; Wu, G.; Ford, P. C. *Inorg. Chem.* **2007**, *46*, 9323.

17. Pell, S. D.; Armor, J. N. *J. Am. Chem. Soc.* **1973**, *95*, 7625.

18. (a) Sarma, M.; Singh, A.; Gupta, S. G.; Das, G.; Mondal, B. *Inorg. Chim. Acta*, **2010**, *363*, 63. (b) Sarma, M.; Kalita, A.; Kumar, P.; Singh, A.; Mondal, B. *J. Am. Chem. Soc.* **2010**, *132*, 7846.

19. Sarma, M.; Mondal, B. *Inorg. Chem.* **2011**, *50*, 3206.

20. (a) Sarma, M.; Mondal, B. *Dalton Trans.* **2012**, *41*, 2927. (b) Sarma, M.; Kumar, V.; Kalita, A.; Deka, R. C.; Mondal, B. *Dalton Trans*., **2012**, *41*, 9543.

21. Kalita, A.; Kumar, P.; Deka, R. C.; Mondal, B. *Chem. Commun*. **2011**, *48*, 1551.

22. Wright, A. M.; Wu, G.; Hayton, T. W. *J. Am. Chem. Soc*. **2010**, *132*, 14336.

23. Kumar, P.; Kalita, Mondal, B. *Dalton Trans.* **2011**, *40*, 8656.

24. Kalita, A.; Kumar, P.; Deka, R. C.; Mondal, B. *Inorg. Chem.* **2011**, *50*, 11868.

25. (a) Hathaway, B. J.; Tomlinson, A. A. G. *Coord. Chem. Rev.* **1970**, *5*, 1. (b) Hathway, B. J.; Billing, D. E.; Nicols, P.; Procter, I. M. *J. Chem. Soc. A*, **1969**, 312. (c) Hathway, B. J. in *Comprehensive Coordination Chemistry*, Wilkinson, G.; Gillard, R. D.;

McCleverty, J. A. Eds. Pergamon, Oxford, **1987**, Vol 5, pp 533. (d) Patra, A. K.; Ray, M.; Mukherjee, R. *Dalton Trans.* **1999**, 2461.

26. SMART, SAINT and XPREP, Siemens Analytical X-ray Instruments Inc., Madison, Wisconsin, USA, 1995.

27. Sheldrick, G. M. SHELXS-97, University of Gottingen, Germany, 1997.

28. Farrugia, L. J. *J. Appl. Crystallogr.* **1997**, *30*, 565.

29. Michelsen, K. *Acta Chem. Scand.* **1977**, *A31*, 429

30. Mialane, P.; Nivorojkine, A; Pratviel, G.; Aze éma, L.; Slany, M.; Godde, F.; Simaan, A.; Banse, F.; Kargar-Grisel, T.; Bouchoux, Guy.; Sainton, J.; Horner, O.; Cuilhem, J.; Tchertanova, L.; Meunier, B.; Girerd, J. *Inorg. Chem* **1999**, *38*, 1085.

Chapter 3

Nitric oxide reactivity of copper(II) complexes of N-donor ligand and NO detection

Abstract

Two Cu(II) complexes, **3.1** and **3.2**, were synthesized with N-donor ligands $\mathbf{L_5}$ and $\mathbf{L_6}$ [$\mathbf{L_5}$ = N^1,N^1-dimethylethane-1,2-diamine, $\mathbf{L_6}$ = N^1,N^1-dimethyl-N^2-{(pyridin-2-yl)methyl}ethane-1,2-diamine], respectively and were characterized. Complexes **3.1** and **3.2** upon reaction with NO, found to show reduction of Cu(II) to Cu(I) in various solvents. Ligands $\mathbf{L_7}$, $\mathbf{L_8}$ and $\mathbf{L_9}$ are the dansyl derivatives of $\mathbf{L_5}$, 2-(pyridin-2-yl)ethanamine and $\mathbf{L_6}$, respectively. Three Cu(II) complexes, **3.3**, **3.4** and **3.5** were synthesized with ligands $\mathbf{L_7}$, $\mathbf{L_8}$ and $\mathbf{L_9}$ respectively. The fluorescence intensity of these ligands were found to be quenched significantly on complexation due to the paramagnetism of the Cu(II) centre. However, when exposed to NO in methanol / aqueous medium, the fluorescence intensity of the fluorophores has been found to be restored because of reduction of paramagnetic Cu(II) to diamagnetic Cu(I).

3.1 Introduction

Since the discovery of nitric oxide (NO) as a signalling molecule in humans, it has attracted enormous interest from chemists and biochemists.[1–9] It is also known that NO plays diverse roles in biological processes. For instance, it regulates vasodialation, defence against pathogens and long-lasting enhancement in signal transmission when produced in low concentration; however, in micro molar concentration, it stimulates the reactive nitrogen species (RNS) and causes carcinogenesis and neurodegenerative disorders.[1-3, 10-12] These essentially inspired a wide range of research to identify the precise roles of NO in biology and to understand the various biological reaction pathways of NO *in vivo*. Since NO is a reactive free radical and easily diffuses through most of the cells and tissues, it is difficult to follow NO immediately after production. Hence, a selective probe to detect the formation and migration of NO with spatiotemporal resolution directly from living cells is highly desirable compare to other methods such as spectroscopy[13], chemoluminscence[14], EPR and amperometry.[15]

In this aspect, the fluorescence-based detection technique is found to satisfy almost all the requirements, such as biocompatibility, non toxic, specific, fast and direct NO detection. It is also very important that the excitation and emission of the fluorophore of the probe should preferably be in visible or near IR region to avoid harmful effects of ultraviolet light.[13-16] Starting from the early examples of fluorescence-based sensors such as *o*-diaminonaphthalene (DAN) and *o*-diaminofluoresceins (DAFs), a number of fluorescent probes have been exemplified in literature. [13, 17-30] However, some of them are unable to detect or monitor NO itself, as their fluorescent response depends on the formation of a triazole species by oxidized NO products such as N_2O_3 and thus the NO related bio-events would not be detected in real time. Recently, a highly selective fluorescent imaging agent,

for NO has been reported which displays a rapid and linear response with a red-shifted turn-on signal.[31]

On the other hand, fluorophore-displacement strategy has been used for transition-metal complexes based NO sensors; however, the low sensitivity and water insolubility of these complexes precluded their application.[13] A number of iron complexes were reported to sense NO in aqueous medium; but exhibit diminished fluorescence, which is not desirable for biological applications.[32] In addition, iron complexes which show fluorescence enhancement, are air sensitive and exhibit only modest turn-on emission with NO.[33] These difficulties essentially prevent the applications of iron complexes as NO sensor.

In recent times, a number of metal complexes have been exemplified as direct fluorescent sensors for NO. This exhibit fluorescence enhancement due to the fluorophore displacement by NO from the metal centre.[34-38] However, this strategy for the direct detection of NO is mostly found to be compatible only with organic solvents. In aqueous environments, fluorescence turn-on/enhancement may arise from the replacement of the fluorophore ligand from the metal centre by water itself. Thus, the strategy of reduction of a metal centre by NO with a concomitant fluorescence enhancement has been adopted. The fluorescence intensity of fluorescent ligand is known to be quenched on coordination to Cu(II) centre. The reduction of Cu(II) by NO to diamagnetic Cu(I) is expected to restore the quenched fluorescence of a ligand fluorophore.[39] The reduction of Cu(II) centre to Cu(I) by NO has been reported earlier in Cu(II)- dithiocarbamate, Cu(II)-phen or dmp (phen = 1,10-phenanthroline; dmp = 2,9-dimethyl-1,10-phenanthroline) complexes.[40] Recently, Cu(II) centre in complexes of various amine ligands have also been reported to undergo reduction by NO.[41]

This strategy has been adopted by Ford et al in their report of Cu(II) complexes of *bis*{2-(3,5-dimethyl-1-pyrazolyl)ethyl)-ammine} (pza) with appended Ru(II) and Re(I)

luminophores as possible luminescent sensor for NO; though these were found to be too labile to be a practical sensor.[42] On the other hand, this strategy indeed found to work in the reaction of NO with $[Cu^{II}(DAC)]^{2+}$ [DAC is the N-derivatized cyclam-1,8-*bis*(anthracen-9-ylmethyl)-1,4,8,11-tetraazacyclotetradecane].[43] However, the reaction was found to be too slow under near neutral condition to use for sensor. In addition, in this case, the reduction of Cu(II) centre by NO was found to result in the simultaneous formation of N-nitrosamine due to the nitrosation of the coordinated amine.

Lippard's group used the same strategy to develop copper complex based NO sensors. They reported the examples of Cu(II) complexes of anthracenyl and dansyl fluorophore ligands.[34, 37] The quenched fluorescence intensity of the ligand fluorophore was observed to restore in presence of NO in methanol/dichloromethane solutions of the complexes. In addition, $[Cu(Ds\text{-}en)_2]$ and $[Cu(Ds\text{-}AMP)_2]$, where Ds-en and Ds-AMP are the conjugate bases of dansylethylenediamine (Ds-Hen) and dansyl aminomethylpyridine (Ds-HAMP), respectively, have found to detect NO in aqueous solution, also.[37b, 44] However, these compounds were unable to sense NO at a physiologically more relevant pH. [37b] Xiang et al also reported an example utilizing this approach.[45] In all these cases except $[Cu(Ds\text{-}en)_2]$ and $[Cu(Ds\text{-}AMP)_2]$, it has been observed that demetallation of the fluorophore ligands takes place after the reduction.[44]

An important report from the Lippard's group described the direct imaging of NO in cell using Cu(II) complexes of fluoresceine-based ligands.[22] In the reaction of NO with the Cu(II) complex to generate NO^+ which immediately reacts with the fluoresceine-based ligands to result in the nitrosated ligand which then released from the Cu(I) centre with a substantial turn-on fluorescence. Another example of similar mechanism based NO imaging also reported from the Lippard's group.[38c]

From our laboratory, recently we have reported the two examples of Cu(II) complex-based

fluorescent NO sensor for methanol and water medium buffered at pH ~7.2.[46] It is important to note that in these cases no ligand nitrosation was observed. However, these have not been found to behave as turn on/off sensors; perhaps, because of the demetallation of the ligand after reduction followed by undefined product formation during air oxidation of the reduced Cu(I).[47]

In this direction we have studied the NO reactivity of two Cu(II) complexes of ligands **L_5** and **L_6**, respectively. Successively, three fluorophore ligands with pendant dansyl group have been synthesized and studied as fluorescence sensors for NO (Figure 3.1).

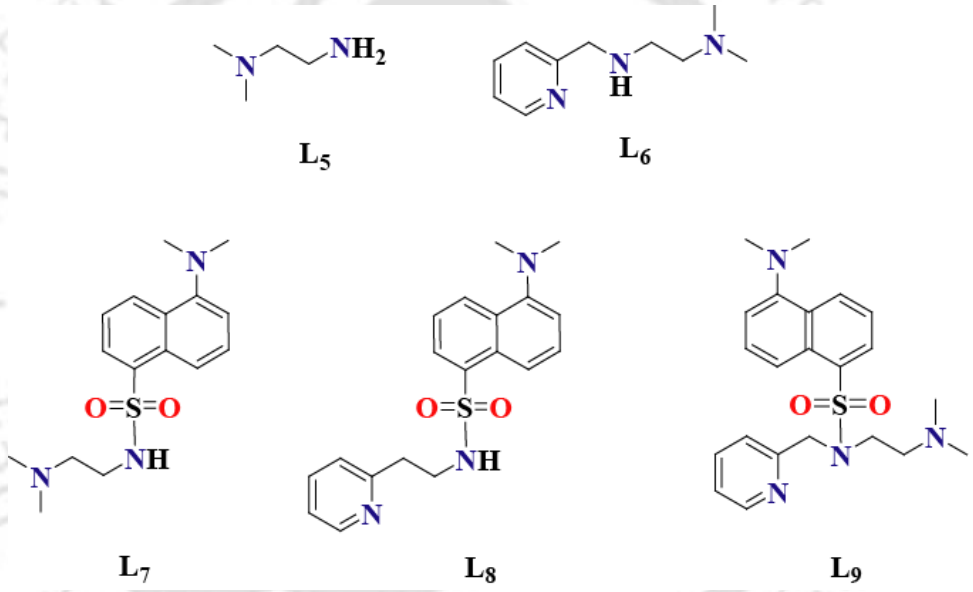

Figure 3.1 Ligands used for the present study.

3.2 Results and discussion

Ligand **L_5** was purchased from Sigma Aldrich. **L_6** was prepared from the reaction of pyridine 2-carboxaldehyde with N,N-dimethylethylenediamine followed by the reduction of the imine with sodium borohydride (experimental section). It was characterized by elemental analysis and other spectroscopic studies (experimental section). The ligands **L_7**, **L_8** and **L_9** were synthesized by incorporating the dansyl group into the amine site of **L_5**, 2-

aminoethylpyridine and $\mathbf{L_6}$, respectively, following reported procedure (experimental section).[48] $\mathbf{L_7}$ – $\mathbf{L_9}$ were found to display satisfactory elemental analyses and were characterized further by various spectroscopy (experimental section). All the complexes were prepared using a general method where a Cu(II) salt was made to react with equivalent quantity of the respective ligands (experimental section). All the complexes showed satisfactory elemental analyses. Formation of complex **3.1** and **3.2** has been further confirmed by their single crystal X-ray structures.

Crystal structure

Single crystal structures of complexes **3.1** and **3.2** have been determined. The perspective views of the ORTEP diagrams are shown in figure 3.2. In complex **3.1**, Cu(II) is found to be coordinated with two units of $\mathbf{L_5}$ and a solvent water molecule in an axial position to form a distorted square pyramidal geometry.

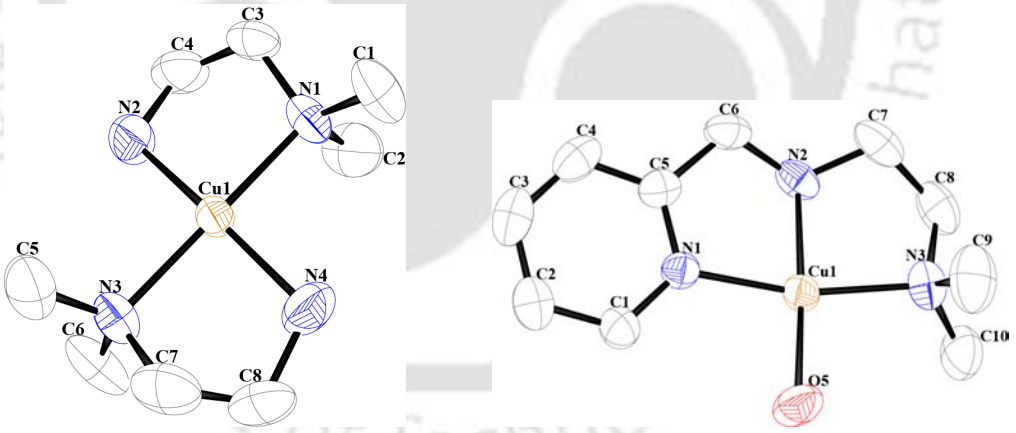

(a) **(b)**

Figure 3.2 ORTEP diagrams of complexes (a) **3.1** and (b) **3.2** (50% thermal ellipsoid plot). (Hydrogen atoms, perchlorate anions and solvent of crystallization were removed for clarity).

In complex **3.2**, however, Cu(II) is coordinated to one tridentate ligand $\mathbf{L_6}$, a solvent water molecule in a square plane and a weakly bonded perchlorate ion from the axial position. The distance between the perchlorate oxygen atoms and Cu(II) ion suggests a weak interaction. The crystallographic data, important bond angles and distances were listed in tables 3.1, 3.2 and 3.3, respectively.

Table 3.1 Crystallographic data for complexes **3.1** and **3.2**

	3.1	**3.2**
Formulae	C_8 H_{24} Cl_2 Cu N_4 O_9	C_{10} H_{19} Cl_2 Cu N_3 O_{10}
Mol. wt.	454.76	475.73
Crystal system	orthorhombic	monoclinic
Space group	P 21	P 21/c
Temperature /K	296(2)	296(2)
Wavelength /Å	0.71073	0.71073
a /Å	8.6454(5)	9.1118(2)
b /Å	14.3954(8)	9.2782(2)
c /Å	14.9911(8)	22.1845(6)
α/°	90.00	90.00
β/°	90.00	100.0410(10)
γ/°	90.00	90.00
V/ $Å^3$	1865.70(18)	1846.78(8)
Z	4	4
Density/Mgm^{-3}	1.619	1.711
Abs. Coeff. /mm^{-1}	1.504	1.526
Abs. correction	none	none
F(000)	940.0	972.0
Total no. of reflections	4038	4593
Reflections, $I > 2\sigma(I)$	4033	3479
Max. 2θ/°	27.99	28.33
Ranges (h, k, l)	-11≤ h ≤ 11 -18≤ k ≤ 18 -19≤ 1≤ 19	-12≤ h ≤ 12 -12≤ k ≤ 11 -29≤ 1 ≤ 29
Complete to 2θ (%)	93.1	99.8
Refinement method	Full-matrix least-squares on F^2	Full-matrix least-squares on F^2
Goof (F^2)	1.020	
R indices [$I > 2\sigma(I)$]	0.0951	0.0526
R indices (all data)	0.0735	0.0402

Table 3.2 Selected bond angles (°) for complexes **3.1** and **3.2**

	3.1	**3.2**
N(1)-Cu(1)-N(2)	85.1(3)	82.86(9)
N(1)-Cu(1)-N(3)	179.6(2)	164.03(9)
N(1)-Cu(1)-N(4)	94.5(3)	-
N(1)-Cu(1)-O(1)	90.6(3)	96.58(7)
N(2)-Cu(1)-N(3)	94.6(3)	86.8(1)
N(3)-Cu(1)-N(4)	85.9(3)	-
O(1)-Cu(1)-O(5)	-	99.16(9)
O(1)-Cu(1)-N(3)	-	95.09(8)
O(1)-Cu(1)-N(2)	-	87.43(9)
N(4)-Cu(1)-N(1)	5.5(3)	-
N(4)-Cu(1)-N(2)	170.1(3)	-
C(2)- C(1)-N(1)	-	122.1(2)
C(1)-C(2)-C(3)	-	118.4(3)
C(1)-N(1)-C(2)	110.0(7)	122.1(2)
C(1)-N(1)-C(3)	109.0(6)	
C(7)-N(3)-C(5)	106.6(7)	-

Table 3.3 Selected bond length (Å) for complexes **3.1** and **3.2**

	3.1	**3.2**
Cu(1)-N(1)	2.007(4)	1.985(2)
Cu(1)-N(2)	1.996(4)	1.985(2)
Cu(1)-N(3)	2.091(4)	2.037(3)
Cu(1)-N(4)	2.002(3)	-
Cu(1)-O(1)	2.455(8)	2.419(2)
Cu(1)-O(5)	-	1.947(2)
N(1)-C(1)	1.45(1)	1.338(3)
N(1)-C(5)	1.50(1)	1.341(3)
N(2)-C(6)	1.54(1)	1.470(4)
N(2)-C(7)	1.46(1)	1.466(4)
N(3)-C(9)	-	1.474(4)
C(3)-C(2)	1.49(1)	1.362(5)
C(5)-C(6)	1.46(2)	1.484(4)
C(7)-C(8)	-	1.493(5)

Nitric oxide reactivity of complexes 3.1 and 3.2

Addition of NO to a degassed acetonitrile solution of complex **3.1** results in the shift of the λ_{max} of *d-d* band from 556 to 600 nm which is attributed to the formation of corresponding [Cu^{II}-NO] intermediate (Figure 3.3a). This intermediate is found to be unstable and

decomposed gradually leading to the reduction of Cu(II) to Cu(I). In cases of analogous complexes, $[Cu(dmen)_2]^{2+}$, $[Cu(deen)_2]^{2+}$, and $[Cu(diben)_2]^{2+}$ [dmen = N,N-dimethylethylenediamine; deen = N,N-diethylethylenediamine; diben = N,N-diisobutylethylenediamine], the *d-d* band of the corresponding [Cu^{II}-NO] intermediate was found to appear at 605, 582 and 652 nm, respectively, upon addition of NO in acetonitrile solution. $[Cu(tiaea)(CH_3CN)]^{2+}$ and $[Cu(teaea)(CH_3CN)]^{2+}$ [tiaea = *tris*(2-isopropylaminoethyl)amine and teaea = *tris*(2-ethylaminoethyl)amine], on reaction with NO afforded [Cu^{II}-NO] intermediate having λ_{max} at 640 nm and 605 nm, respectively.[41b] The *d-d* transitions for the intermediate was found to appear at 660 nm and 595 nm in cases of $[Cu(amepy)_2]^{2+}$ and $[Cu(aeta)_2]^{2+}$ [amepy = 2-aminomethyl pyridine; aeta = *bis*-(2-aminoethyl)amine], respectively.[41c]

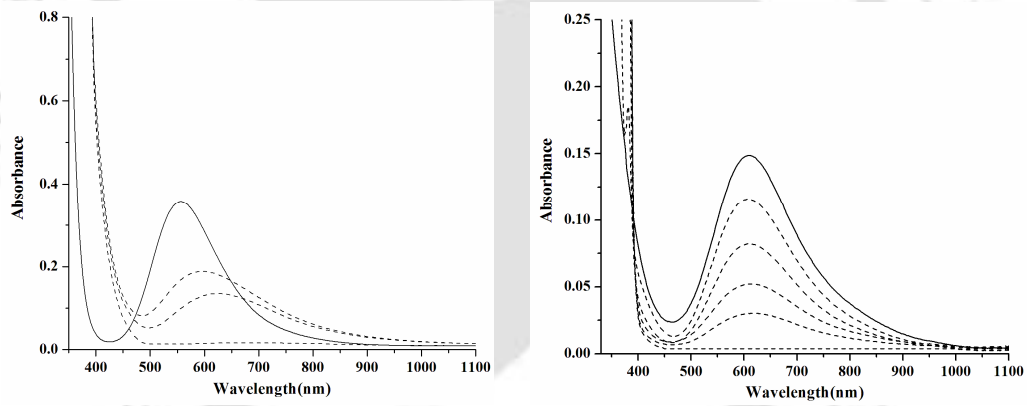

(a) **(b)**

Figure 3.3 UV-visible spectra of complexes (a) **3.1** and (b) **3.2** before (solid line) and after (dashed lines) reaction with NO in acetonitrile solution.

On the other hand, in acetonitrile solution of complex **3.2**, purging of NO does not show the formation of [Cu^{II}-NO] intermediate prior to the reduction of Cu(II) to Cu(I). This is presumably because of the low value of K_{NO} for the formation of [Cu^{II}-NO] intermediate from the reaction of complex **3.2** with NO. Upon addition of excess NO to the degassed methanol solution of complexes **3.1** and **3.2**, the Cu(II) centre is found to undergo rapid re-

duction to Cu(I). UV-visible spectroscopy was used to monitor the reduction and the observed spectral changes are shown in figures 3.4a and 3.4b, respectively.

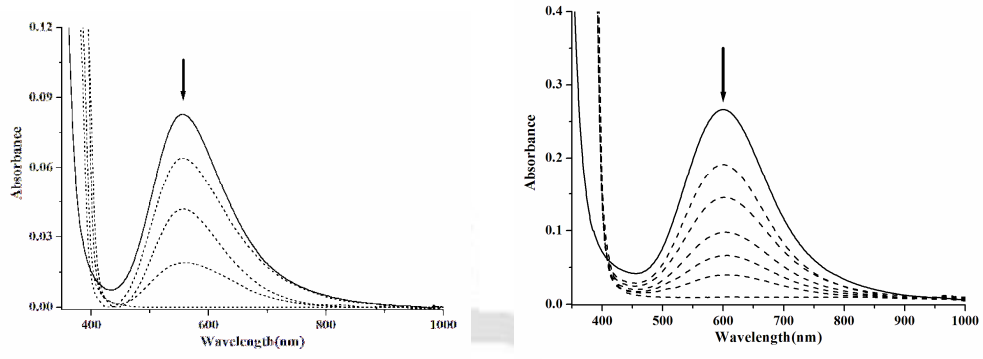

(a) **(b)**

Figure 3.4 UV-visible spectral changes of complexes (a) **3.1** and (b) **3.2** upon their reaction with NO in methanol.

The reduction of Cu(II) in presence of NO is noticed in water and methanol/water mixture, as well. In methanol, the reduction was found to be yield $\mathbf{L_5'}$ and $\mathbf{L_6'}$ in cases of complexes **3.1** and **3.2**, respectively, along with the formation of minor amount of methyl nitrite. However, in water, exclusive formation of nitrite ion was observed in both the cases and confirmed qualitatively by the Griess test.[49]

$$[Cu(L)(CH_3CN)]^{2+} + NO_{(g)} \xrightarrow{CH_3CN} [Cu(CH_3CN)_4]^{+} + L' + H^{+} \quad \text{---------- (3.1)}$$

From equation 3.1, it is expected that the reduction of Cu(II) by NO would result in the formation of H^+ ion. This has been evidenced by the decrease in pH of the un-buffered aqueous solution with the progress of the reactions. The reduction is found to follow a first order kinetics in water, methanol and acetonitrile media. $[Cu(dmp)_2(H_2O)]^{2+}$ and $[Cu(phen)_2(H_2O)]^{2+}$ (dmp = 2,9-dimethyl-1,10-phenanthroline; phen = 1,10-phenanthroline) were reported to show similar reaction with NO in presence of protic solvent, but not in pure acetonitrile or dichloromethane. [40a-b] However, Cu(II) centres in $[Cu(tren)(CH_3CN)]^{2+}$, $[Cu(tiaea)(CH_3CN)]^{2+}$ and $[Cu(teaea)(CH_3CN)]^{2+}$ [tren: *tris*(2-

aminoethyl)amine; tiaea = *tris*(2-isopropylaminoethyl)amine and teaea = *tris*(2-ethylaminoethyl)amine] are known to undergo reduction in presence of NO in pure acetonitrile and the reduction was reported to be accompanied with either the N-nitrosation or the diazotization of the primary amine centre of the ligand.[41a-b] The Cu(II) centre in $[Cu(DAC)]^{2+}$, DAC = 1,8-*bis*(9-anthracylmethyl)-derivative of the macrocyclic tetraamine cyclam, in methanol solution is found to be reduced by NO along with simultaneous N-nitrosation of the ligand.[43b, 50]

The rate is found to be independent of the initial concentration of the complexes having rate constants 2.86×10^{-3} and 4.63×10^{-3} s^{-1} at 298 K for complexes **3.1** and **3.2**, respectively, in methanol solution. The pseudo first order rate constants for $[Cu(pymea)_2]^{2+}$ and $[Cu(baea)(CH_3CN)]^{2+}$ [pymea = pyridine-2-methylamine and baea = *bis*(2-aminoethyl)amine] are also reported to be 3.10×10^{-3} and 2.20×10^{-3} s^{-1}, respectively, at 298 K.[41c] In addition, Cu(II) complexes of tiaea and teaea ligands are also reported to undergo reduction by NO following a pseudo first order kinetics with rate constants 5.64×10^{-2} and 6.45×10^{-3} s^{-1}. Notably, the rate of reductive nitrosylation of ferriheme proteins in aqueous medium are strongly dependent on the hydroxide ion concentration in the pH range 6 - 9 because of the rate limiting attack of hydroxide ion on the Fe^{III} coordinated NO.[50]

The NO reduction of Cu(II) centres can be rationalized by an inner-sphere mechanism involving three steps: (i) reversible displacement of the solvent by NO from the coordination sphere of Cu(II) leading to the formation of a inner-sphere $[Cu^{II}\text{-}NO]$ intermediate; (ii) nucleophilic attack of H_2O or CH_3OH (in case of water and methanol media) or the generation of highly electrophilic NO^+ owing to $[Cu^{II}\text{-}NO \leftrightarrow Cu^{I}\text{-}NO^+]$ charge distribution followed by the (iii) release of NO_2^- (or CH_3ONO) or N-nitrosated ligand. The geometrical prefence of Cu(I) for tetrahedral coordination also facilitates the third step.

In complexes **3.1** and **3.2**, upon addition of NO, any indication of formation of [Cu^{II}-NO] inner-sphere complex is not observed in methanol or water solution. Earlier, with $[Cu(dmp)_2(H_2O)]^{2+}$ and $[Cu(phen)_2(H_2O)]^{2+}$, even at the early stage of mixing no spectral change for the inner-sphere complex formation was reported.[40a-b] This can be rationalized in two ways: (i) either the spectral pattern of the complexes **3.1** and **3.2** are very similar to their respective [Cu^{II}-NO] intermediates or (ii) the values of the equilibrium constant, K_{NO} are very less. Since, no ν_{NO} frequency corresponding to the formation of [Cu^{II}-NO] was observed in the FT-IR spectroscopy, the second option seems more probable.

The complete reduction of Cu(II) centres in complexes **3.1** and **3.2** by NO was further confirmed by X-band EPR studies. The complexes displayed characteristic signals in X-band EPR spectroscopy; but, the colorless solutions are found to be silent (Figures 3.5a and 3.5b) owing to the reduction of paramagnetic Cu(II) to diamagnetic Cu(I). The N-nitrosated ligands in both the cases were isolated and characterized completely using various spectroscopic techniques.

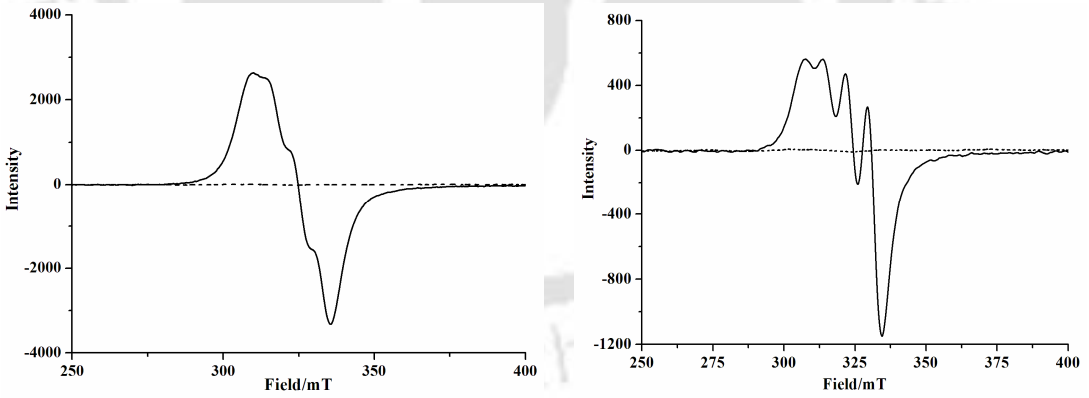

(a) **(b)**

Figure 3.5 X-band EPR spectra of complexes **3.1** (a) and **3.2** (b) in acetonitrile solvent at room temperature (solid traces correspond to the respective complexes and dashed traces represent the spectra of the colorless solutions obtained after reaction of the respective complexes with NO).

NO reactivity of complexes 3.3 - 3.5

As the Cu(II) centres in complexes **3.1**, **3.2** and $[Cu(pyeam)(CH_3CN)]^{2+}$ undergo rapid reduction by NO in methanol and water, these in combination with a pendant fluorophore group can be used to detect NO. Ligands $\mathbf{L_7}$ – $\mathbf{L_9}$ were prepared by incorporating the pendant dansyl group into $\mathbf{L_5}$, pyeam and $\mathbf{L_6}$, respectively. It should be noted that the parent complex of pyeam ligand on reaction with NO results in the formation of $[Cu^{II}\text{-NO}]$ intermediate in acetonitrile. However, in water, the formation of $[Cu^{II}\text{-NO}]$ intermediate was not evidenced prior to the reduction of Cu(II) to Cu(I). The fluorophore ligands display moderate fluorescence at room temperature in methanol and water. The fluorescence quantum yields were calculated to be 0.179, 0.186 and 0.192 for $\mathbf{L_7}$, $\mathbf{L_8}$ and $\mathbf{L_9}$, respectively, in methanol at room temperature. Addition of Cu(II) ion to the solution of these ligands is found to quench their fluorescence intensities (Figure 3.6a, Appendix II, figures A2.54 and A2.57).

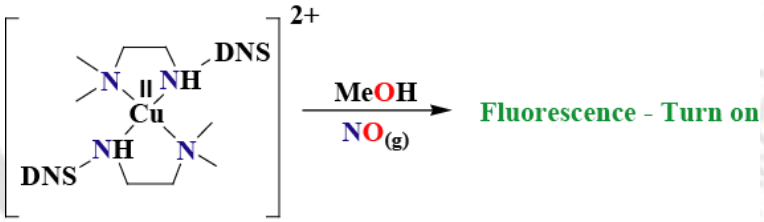

3.3

Fluorescence - Turn off

Scheme 3.1

The quenched fluorescence intensity of these ligand fluorophores in complexes **3.3 - 3.5** is expected to be restored on reduction of Cu(II) centre by NO (Scheme 3.1).[23] Presence of equivalent amount of Cu(II) ion in the aqueous medium buffered at pH 7.2 was also result in a significant (< 90%) quenching. To a degassed methanol solution of complex **3.3**, addition of 2-5 equivalent of NO immediately restored the emission intensity significantly (Figure 3.6b).

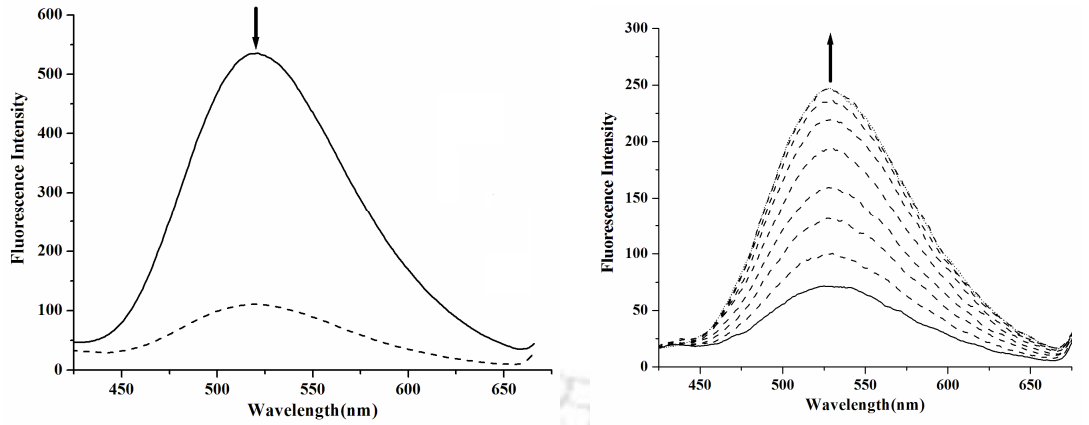

(a) **(b)**

Figure 3.6 Fluorescence responses (λ_{ex}, 342 nm) for (a) 20 μM solution of free ligand, $\mathbf{L_7}$ (solid line) and after addition of one equivalent of $[Cu(H_2O)_6]^{2+}$ in methanol (dashed line); (b) Fluorescence responses (λ_{ex}, 342 nm) of deoxygenated methanol solution (10 μM) of complex **3.3** before (solid line) and after (dashed lines) purging of 5 equivalent of NO at 1, 2, 3, 4, 5, 6 and 7 minutes at 298 K (lines I – VII, respectively).

The extent of the restored emission intensity is found to be less in aqueous medium buffered at pH 7.2, compare to that in methanol solution (Appendix II, Figures A2.53, A2.56 and A2.59). In the present cases, the restored emission intensities are found to be 3.43(±0.2) and 3.32(±0.2)-fold in methanol and aqueous (at pH 7.2) medium, respectively. The NO detection limit of the present complex is observed to be ~10 nM.[46a]

Addition of equivalent amount of Cu(II) in the methanol solution of $\mathbf{L_8}$ and $\mathbf{L_9}$, also resulted in a significant (> 75%) quenching of their fluorescence at 298 K (Appendix II, Figures A2.54 and A2.57). This has been observed in aqueous medium buffered at pH 7.2 using TRIS-HCl buffer, too. Again, addition of 2-5 equivalent of NO into a degassed methanol solution of complexes **3.4** and **3.5** immediately restored the emission intensity. In case of $[Cu(Ds\text{-}en)_2]$ and $[Cu(Ds\text{-}AMP)_2]$, the ligand fluorescence intensity was found to quench to 31(± 2)- and 23(± 0.5)-fold relative to free Ds-Hen and Ds-HAMP (40 μM), respectively, upon addition of Cu(II).[37b, 38a] In buffered aqueous or methanol solution of the

complexes [Cu(Ds-en)$_2$] and [Cu(Ds-AMP)$_2$], under anaerobic condition, the emission intensity was found to be restored significantly upon addition of 100 equivalent of NO and the enhancements in integrated fluorescence were reported to be 6.1(±0.2)- and 8.8(±0.1)-fold, respectively. [37b, 38a]

Except a few, all earlier examples of Cu(II) complexes as fluorescent sensor in aqueous methanol or in an aqueous pH 7.0 buffer and in cells, were found to detect NO by a different mechanism; and that involves the reduction of Cu(II) by NO followed by dissociation of the N-nitrosated ligand.[41a, 22] [Cu(Ds-en)$_2$] and [Cu(Ds-AMP)$_2$], where Ds-en and Ds-AMP are the conjugate bases of dansylethylenediamine (Ds-Hen) and dansylaminomethylpyridine (Ds-HAMP), respectively, were reported recently as the probe for fluorescence-based NO detection in aqueous solution. [37b, 38a] However, these Cu(II) dansyl compounds were unable to sense NO at a physiologically more relevant pH. The fluorescence enhancement in case of Ds-HAMP ligand is attributed to both the sulphonamide functionality following protonation by H^+ formed in the reaction. [37b] The dissociation was confirmed by the presence of sulphonamide group ($\nu_{N\text{-}H} \approx 3083$ cm^{-1} in KBr) in the FT-IR spectrum of the reaction product which indicates that ligand protonation also occurs. The protonated sulfonamide group is anticipated to contribute to the fluorescence intensity.[37b] In contrary, in cases of complexes **3.3** - **3.5** no indication of dissociation of sulphonamide group was observed in the FT-IR spectra of the reaction products (Appendix II, Figures A2.70, A2.71 and A2.72). Hence, the restored emission intensity, in these cases, is attributed to the reduction of Cu(II) centre to the diamagnetic Cu(I) by NO. In the present case, no N-nitrosoamine formation was observed because of the reaction of NO^+, formed during the reaction of Cu(II) with NO, with methanol solvent to form CH_3ONO and H^+.[37b, 40b] The formation of the NO_2^- in aqueous medium has been established by the Griess's test.[49]

3.3 Conclusion

In this chapter, two Cu(II) complexes **3.1** and **3.2** have been prepared with N-donor ligands and their NO reactivity were studied in acetonitrile and methanol media. The Cu(II) centres in complexes **3.1** and **3.2** were found to undergo reduction in presence of NO in acetonitrile, methanol and water solvents. Three Cu(II) complexes, **3.3, 3.4** and **3.5** having a pendant dansyl fluorophore showed substantial increase in fluorescence intensity upon addition of NO. Thus the complexes can act as fluorescence-based NO sensor in methanol and aqueous (pH 7.2) medium.

3.4 Experimental Section

3.4.1 Materials and methods

All reagents and solvents were purchased from commercial sources and were of reagent grade. Acetonitrile was distilled from calcium hydride. Deoxygenation of the solvent and solutions were effected by repeated vacuum/purge cycles or bubbling with nitrogen for 30 minutes. NO gas was purified by passing through KOH and P_2O_5 column. UV-visible spectra were recorded on a Perkin Elmer Lambda 25 spectrophotometer. FT-IR spectra of the solid samples were taken on a Perkin Elmer spectrophotometer with samples prepared as KBr pellets. The fluorescence spectra were recorded in solution in Varian Cary Eclipse Fluorescence Spectrophotometer at room temperature. Quinine sulfate in acidic medium was used as the reference compound for the determination of fluorescence quantum yield. Solution electrical conductivity was checked using a Systronic 305 conductivity bridge. ^{1}H-NMR spectra were obtained with a 400 MHz Varian FT spectrometer. Chemical shifts (ppm) were referenced either with an internal standard (Me_4Si) or to the residual solvent peaks. The X-band Electron Paramagnetic Resonance (EPR) spectra were recorded on a JES-FA200 ESR spectrometer, at room temperature. Elemental analyses were obtained

from a Perkin Elmer Series II Analyzer. The magnetic moment of complexes is measured on a Cambridge Magnetic Balance.

Single crystals were grown by slow diffusion followed by slow evaporation technique. The intensity data were collected using a Bruker SMART APEX-II CCD diffractometer, equipped with a fine focus 1.75 kW sealed tube MoK_α radiation (λ = 0.71073 Å) at 276(3) K, with increasing ω (width of 0.3° per frame) at a scan speed of 3 s/frame. The SMART software was used for data acquisition. Data integration and reduction were undertaken with SAINT and XPREP software.[51] Multi-scan empirical absorption corrections were applied to the data using the program SADABS.[52] Structures were solved by direct methods using SHELXS-97 and refined with full-matrix least squares on F^2 using SHELXL-97.[33] All non-hydrogen atoms were refined anisotropically. Structural illustrations have been drawn with ORTEP-3 for Windows.[54]

3.4.2 Synthesis of ligands

Synthesis of L_6

Pyridine-2-carbaldehyde (1.07 g, 10 mmol) and N,N-dimethylethylenediamine (0.880 g, 10 mmol) of in 20 ml methanol was refluxed at 60 °C for 5 hours (Scheme 3.2). The resulting reddish brown solution was dried under reduced pressure and the dark oil thus obtained was subjected to chromatographic purification using silica gel column to yield the pure Schiff base, as reddish oil. The Schiff base was then reduced to the corresponding ligand, **L_6**, using 2.5 equivalent $NaBH_4$ in methanol solution.

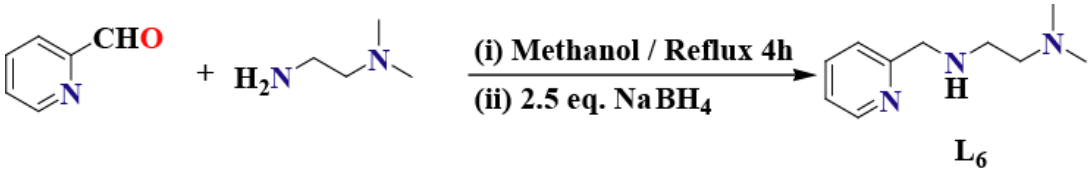

Scheme 3.2

The pure **L_6** was obtained after chromatographic purification using silica gel column and characterized using various spectroscopic techniques. Yield: 1.21 g, ~69%. FT-IR in KBr: 2793, 1590, 1429, 1341, 1170, 766 cm^{-1}. ^{1}H-NMR (400 MHz, $CDCl_3$) δ_{ppm}: 2.21(6H), 2.44-2.47(2H), 2.72-2.75(2H), 3.93(2H), 7.13-7.16(1H), 7.32-7.34(1H), 7.61-7.65(1H), 8.54-8.55(1H). ^{13}C-NMR (100 MHz, $CDCl_3$) δ_{ppm}: 45.1, 46.4, 54.8, 58.7, 121.4, 121.8, 136.0, 148.7, and 159.4. ESI-Mass (m+1): Calcd. 180.14; Found, 180.09.

Synthesis of L_7

The fluorescent ligand **L_7** has been prepared by the introducing of the dansyl group in the ligand N,N-dimethylethane-1,2-diamine, **L_5**. This has been done by stirring an equimolar mixture of N,N-dimethylethane-1,2-diamine (0.176 g, 2 mmol) and dansyl chloride (538 g, 2 mmol) in presence of triethylamine in distilled chloroform for 5 h at room temperatures (Scheme 3.3). The volume of the resulting solution was dried under reduced pressure and the greenish yellow fluorescent mass was subjected to column chromatographic purification to result the pure greenish yellow fluorescent ligand **L_7**.

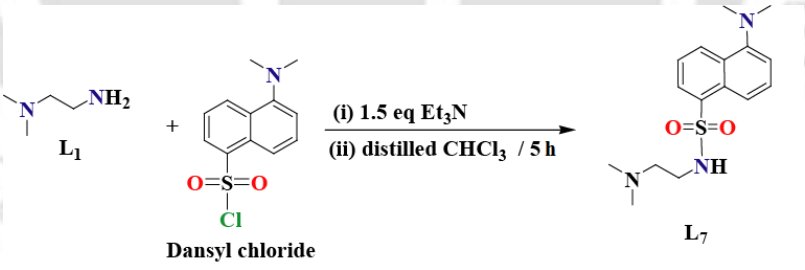

Scheme 3.3

Yield: 0.526 g, ~82%. FT-IR in KBr: 2944, 2863, 1457, 1320, 1144, 791, 625 cm^{-1}. ^{1}H-NMR (400 MHz, $CDCl_3$) δ_{ppm}: 1.90 (6H), 2.16-1.19 (2H), 2.76-2.86 (8H), 7.08-7.10 (1H), 7.43-7.47 (2H), 8.16-8.19 (1H), 8.24-8.26 (1H) 8.44-8.47 (1H). ^{13}C-NMR (100 MHz, $CDCl_3$) δ_{ppm}: 39.9, 44.3, 45.2, 56.7, 114.9, 118.6, 122.9, 128.2, 129.4, 129.6, 130.1, 134.3 and 151.7. ESI-Mass (m+1): Calcd. 322.15; Found, 322.16.

Synthesis of L_8

Ligand **L_8** was prepared from the reaction of pyridine-2-aethylamine and dansyl chloride by following the same procedure as used for the ligand **L_7**. Yield: 0.568 g, ~80%. FT-IR in KBr: 2938, 1572, 1321, 1143, 791, 624 cm^{-1}. ^{1}H-NMR (400 MHz, $CDCl_3$) δ_{ppm}: 2.73-2.76 (8H), 3.19-3.24 (2H), 6.54-6.56 (1H), 6.78-6.80 (1H), 6.90-6.93 (1H), 7.03-7.05 (1H), 7.31-7.42 (3H) 8.39-8.41 (1H), 8.14-8.23 (2H). ^{13}C-NMR: (100 MHz, $CDCl_3$) δ_{ppm}: 36.1, 42.5, 45.4, 115.1, 119.1, 121.5, 123.1, 123.3, 128.0, 129.3, 129.6, 129.8, 130.2, 135.1, 136.5, 148.8, 151.8 and 158.7. ESI-Mass (m+1): Calcd. 356.14; Found, 356.15.

Synthesis of L_9

Ligand **L_9** was prepared from the reaction of **L_6** and dansyl chloride by following the same procedure as used for ligand **L_7**. Yield: 0.618 g, ~75%. FT-IR in KBr: 2793, 1587, 1427, 1170, 768 cm^{-1}. ^{1}H-NMR (400 MHz, $CDCl_3$) δ_{ppm}: 1.99(6H), 2.18-2.22(2H), 2.84(6H), 3.35-3.39(2H), 4.67(2H), 7.09-7.15(2H), 7.37-7.39(1H0, 7.44-7.56(3H), 8.22-8.24(1H), 8.31-8.34(1H), 8.42-8.50(2H). 13C-NMR: (100 MHz, $CDCl_3$) δ_{ppm}: 29.7, 45.3, 45.4, 53.6, 57.2, 115.2, 119.6, 122.5, 122.6, 123.1, 128.1, 129.3, 130.0, 130.1, 130.3, 135.4, 136.7, 148.9, 151.7 and 157.0. ESI-Mass (m+1): Calcd. 413.19; Found, 413.31.

3.4.3 Synthesis of Complexes

Complexes **3.1** and **3.2** were synthesized following the same procedure. The details are given for complex **3.1**.

Synthesis of complex 3.1

Copper(II)perchlorate hexahydrate, $[Cu^{II}(H_2O)_6](ClO_4)_2$, (1.85 g, 5.0 mmol) was dissolved in 10 ml distilled acetonitrile (Scheme 3.4). To this solution, **L_5** (0.881 g, 10.0 mmol) was added slowly with constant stirring. The color of the solution turned into deep blue. The stirring was continued for 1 h at room temperature. The volume of the solution was then

reduced to ~5 ml. To this, benzene (10 ml) was added to layer on it and kept it overnight on freezer at -20 ºC. This resulted into deep blue color microcrystals of complex **3.1**.

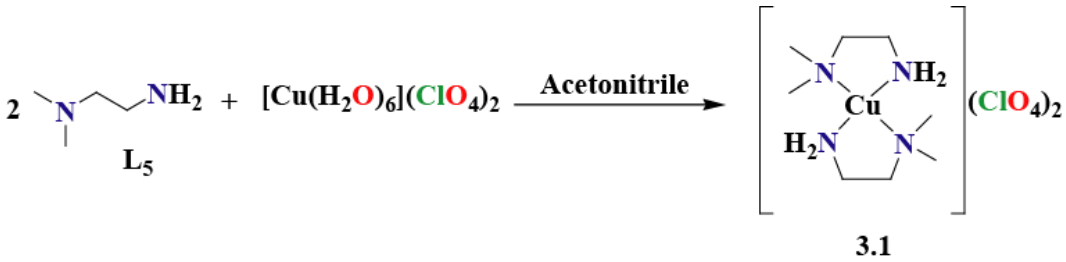

Scheme 3.4

Yield: 1.88 g, ~86%. UV-vis. (methanol): λ_{max}, 556 nm (ε, 172 M^{-1} cm^{-1}). FT-IR in KBr: 3191, 3095, 1464, 1148, 1114, 1058, 625 cm^{-1}. X-band EPR: g_{av}, 2.16. Molar conductivity in acetonitrile: Λ_M ($\Omega^{-1}M^{-1}cm^2$), 222. μ_{obs}, 1.52 BM.

Synthesis of complex 3.2

Complex **3.2** was synthesized from $[Cu^{II}(H_2O)_6](ClO_4)_2$ and $\mathbf{L_6}$. Yield: 1.87 g, ~85%. UV-vis. (methanol): λ_{max}, 599 nm (ε, 216 M^{-1} cm^{-1}). FT-IR in KBr: 3144, 1612, 1457, 1119, 1082, 624 cm^{-1}. X-band EPR: g_{av}, 2.10. Molar conductivity in methanol: Λ_M ($\Omega^{-1}M^{-1}cm^2$), 222. μ_{obs}, 1.52 BM.

Synthesis of complexes 3.3, 3.4 and 3.5

Complexes **3.3**, **3.4** and **3.5** were synthesized following the same procedure. Details are given for complex **3.3**.

Synthesis of complex 3.3

Copper(II)chloride dihydrate, $[Cu(H_2O)_2]Cl_2$ (0.170 g, 1.0 mmol) was dissolved in freshly distilled methanol (10 ml) and to this, $\mathbf{L_7}$ (0.642 g, 2.0 mmol) was added(Scheme 3.5). The color of the solution changed to green. The resulting solution was stirred at room temperature for 2 h. Then the volume of the solution was reduced to ~5 ml and diethyl

ether (~15 ml) was added. Storage in a freezer at -20 ºC for overnight afforded a light green precipitate of complex **3.3**. Yield: 0.635 g, ~82%. Elemental Analyses: Calcd.(%) for $C_{32}H_{46}Cl_2CuN_6O_4S_2$: C, 49.44; H, 5.96; N, 10.81. Found (%): C, 49.11; H, 5.88; N, 10.80. UV-vis. (methanol): λ_{max}, 799 nm (ε, 114 M^{-1} cm^{-1}). FT-IR in KBr: 2940, 1574, 1459, 1324, 1143, 791, 628 cm^{-1}. X-band EPR: g_{av}, 2.14. Molar conductivity in methanol: Λ_M ($\Omega^{-1}M^{-1}cm^2$), 228. μ_{obs}, 1.53 BM.

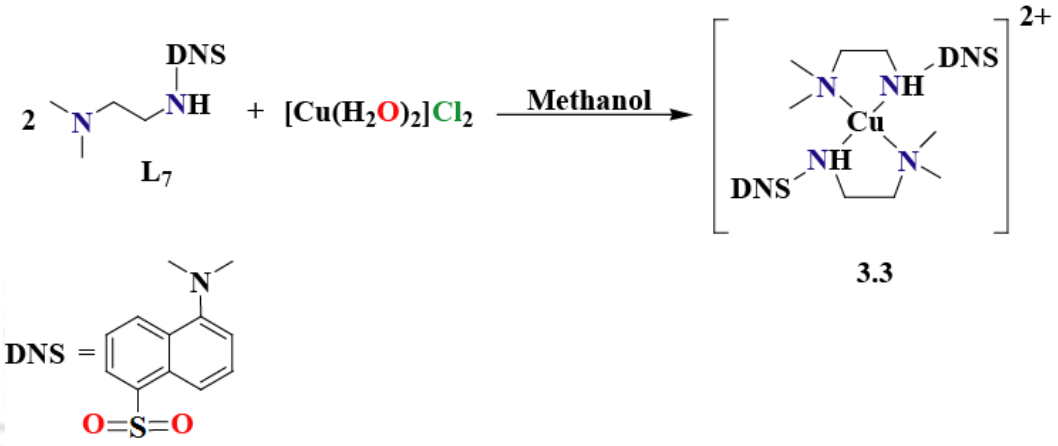

Scheme 3.5

Synthesis of complex 3.4

Complex **3.4** was synthesized from $[Cu(H_2O)_2]Cl_2$ and $\mathbf{L_8}$. Yield: 0.70 g, ~83%. Elemental Analyses: Calcd.(%) for $C_{38}H_{42}Cl_2CuN_6O_4S_2$: C, 53.99; H, 5.01; N, 9.94. Found (%): C, 53.86; H, 5.03; N, 9.92. UV-vis. (methanol): λ_{max}, 866 nm (ε, 97 M^{-1} cm^{-1}). FT-IR in KBr pellet: 3243, 2938, 1573, 1319, 1142, 791, 626 cm^{-1}. X-band EPR: g_{av}, 2.11. Molar conductivity in methanol: Λ_M ($\Omega^{-1}M^{-1}cm^2$), 218. μ_{obs}, 1.51 BM.

Synthesis of complex 3.5

Complex **3.5** was synthesized from $[Cu(H_2O)_2]Cl_2$ and $\mathbf{L_9}$. Yield: ~0.83 g, 76%. Elemental Analyses: Calcd.(%) for $C_{23}H_{32}Cl_2CuN_4O_3S$: C, 47.71; H, 5.57; N, 9.68 Found (%): C, 47.33; H, 5.55; N, 9.63. UV-vis. (methanol): λ_{max}, 795 nm (ε, 60 M^{-1} cm^{-1}). FT-IR in KBr

pellet: 2925, 1580, 1461, 1323, 1142, 795 cm^{-1}. X-band EPR: $g_{av,}$ 2.12. Molar conductivity: Λ_M ($\Omega^{-1}M^{-1}cm^2$), 165. μ_{obs}, 1.54 BM.

3.4.4 Isolation of L_5'

Complex **3.1** (0.438 g, 1.0 mmol) was dissolved in 10 ml of distilled and degassed acetonitrile (Scheme 3.6). To this solution an excess of NO gas was purged for 1 minute and the resulting colorless solution was stirred for 1 h at room temperature. After removing the excess NO by several cycles of vacuum/purge, 10 ml of degassed benzene was added to this under dinitrogen atmosphere. The reaction mixture was kept in freezer for overnight. The L_5'-perchlorate was found to be precipitated out.

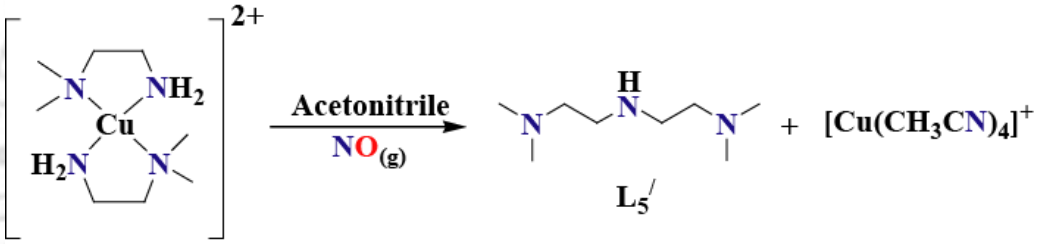

3.1

Scheme 3.6

Yield: 0.130 g, ~70%. FT-IR in KBr pellet: 3011, 1620, 1438, 1384, 1144, 1116, 1084, 626 cm^{-1}. ^{1}H-NMR (400 MHz, D_2O) δ_{ppm}: 1.90 (6H), 2.09-2.12 (4H), 2.68-2.71 (4H). ^{13}C-NMR: (100 MHz, D_2O and CD_3CN) δ_{ppm}: 40.2, 45.8 and 62.2. ESI-Mass (m+1): Calcd. 160.16; Found, 160.28.

3.4.5 Isolation of L_6'

Complex **3.2** (0.459 g, 1.0 mmol) was dissolved in 10 ml of distilled and degassed acetonitrile (Scheme 3.7). To this solution an excess of NO gas was purged for 1 minute and the resulting colorless solution was stirred for 1 h at room temperature. The solvent was then dried under reduced pressure using a rotavapor. Water (5 ml) was added to the

dried mass followed by the addition of 5 ml of saturated Na_2S solution. The black precipitate of CuS was filtered out. The crude organic part was then extracted from the aqueous layer using $CHCl_3$ (25 ml × 4 portions). The crude product, obtained after removal of solvent, was then purified by column chromatography using a neutral alumina column and a hexane/ethyl acetate solvent mixture to get the pure $\mathbf{L_6'}$.

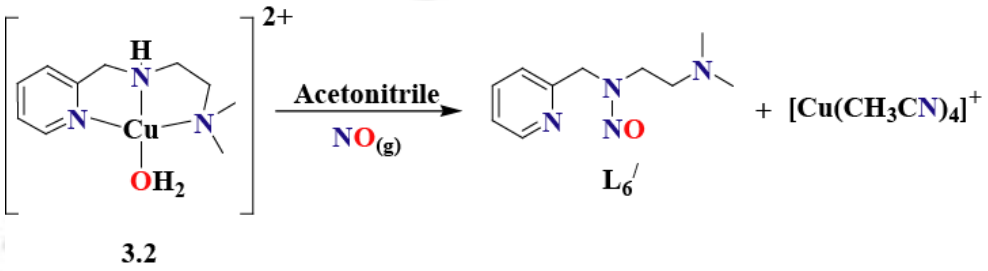

3.2 $\mathbf{L_6'}$

Scheme 3.7

Yield: 0.162 g, ~78%. FT-IR in KBr: 2945, 1592, 1451, 1438, 1356, 1129, 761 cm^{-1}. ^{1}H-NMR (400 MHz, CD_3Cl) δ_{ppm}: 2.28 (6H), 2.72-2.75 (2H), 3.34-3.36 (2H), 4.24 (2H), 7.20-7.24(1H), 7.65(1H), 8.06-8.08(1H), 8.63-8.64(1H). ^{13}C-NMR: (100 MHz, CD_3Cl) δ_{ppm}: 45.5, 48.8, 59.5, 58.9, 121.1, 121.3, 136.2, 149.0 and 160.0. ESI-Mass (m+1): Calcd. 209.13; Found, 209.04.

3.5 References

1. Furchgott, R. F. *Angew. Chem. Int. Ed.* **1999**, *38*, 1870.
2. Ignarro, L. J. *Angew. Chem. Int. Ed.* **1999**, *38*, 1882.
3. Murad, F. *Angew. Chem. Int. Ed.* **1999**, *38*, 1856.
4. Bon, C. L. M.; Garthwaite, J. *J. Neurosci.* **2003**, *23*, 1941.
5. Pepicelli, O.; Raiteri, M.; Fedele, E. *Neurochem. Int.* **2004**, *45*, 787.
6. Bonomo, R. P.; Pappalardo, G.; Rizzarelli, E.; Santoro, A. M.; Tabbi, G.; Vagliasindi, L. I. *Dalton Trans.* **2007**, 1400.
7. Bonomo, R. P.; Castronovo B. M. G.; Santoro, A. M. *Dalton Trans.* **2004**, 104.

8. Bonomo, R. P.; Pappalardo, G.; Rizzarelli, E.; Vagliasindi.; L. I. *Dalton Trans.* **2008**, 3805.

9. Bonomo, R. P.; Di Natale, G.; Rizzarelli, E.; Tabbi, G.; Vagliasindi, L. I. *Dalton Trans.* **2009**, 2637.

10. Ricciardolo, E. L. M.; Sterk, P. J.; Gaston, B.; Folkerts, G. *Phsiol. Rev.* **2004**, *84*, 731.

11. Wink, D. A.; Vodovotz, Y.; Laval, J.; Laval, F.; Dewhirst, M. W.; Mitchell, J. B. *Carcinogenesis.* **1998**, *19*, 711.

12. Calabrese, V.; Bates, T. E; Stella, A. M. G. *Neurochem. Res.* **2000**, *25*, 1315.

13. Nagano, T.; Yoshimura, T. *Chem. Rev.* **2002**, *102*, 1235.

14. Hilderbrand, S. A.; Lim, M. H.; Lippard, S. J. *In Topics in Fluorescence Spectroscopy*, Geddes, C. D.; Lakowicz, J. R. Eds. Springer: **2005**; pp 163.

15. Maliniski, T.; Mesaros, S.; Tomboulian, P. *Methods Enzymol.* **1998**, *170*, 31.

16. Sasaki, E.; Kojima, H.; Nishimatsu, H.; Urano, Y.; Kikuchi, K.; Hirata, Y.; Nagano, T. *J. Am. Chem. Soc.* **2005**, *127*, 3684.

17. Kojima, H.; Nakatsubo, N.; Kikuchi, K.; Kawahara, S.; Kirino, Y.; Nagoshi, H.; Hirata, Y.; Nagano, T. *Anal. Chem.* **1998**, *70*, 2446.

18. Heiduschka, P.; Thanos, S. *NeuroReport*. **1998**, *9*, 4051.

19. Meineke, P.; Rauen, U.; de Groot, H.; Korth, H.-G.; Sustmann, R. *Chem. Eur. J.* **1999**, *5*, 1738.

20. Kojima, H.; Hirotani, M.; Nakatsubo, N.; Kikuchi, K.; Urano, Y.; Higuchi, T.; Hirata, Y.; Nagano, T. *Anal. Chem.* **2001**, *73,* 1967.

21. Gabe, Y.; Urano, Y.; Kikuchi, K.; Kojima, H. and Nagano, T. *J. Am. Chem. Soc.* **2004**, *126*, 3357.

22. Lim, M. H.; Xu, D.; Lippard, S. J. *Nat. Chem. Biol.* **2006**, *2*, 375.

23. Lim, M. H.; Wong, B. A.; Pitcock, Jr., W. H.; Mokshagundam, D.; Baik, M.-H.; Lippard, S. J. *J. Am. Chem. Soc.* **2006**, *128*, 14363.

24. Zheng, H.; Shang, G.-Q.; Yang, S.-Y.; Gao, X.; Xu, J.-G. *Org. Lett.* **2008**, *10*, 2357.

25. Wang, S.; Han, M.-Y.; Huang, D. *J. Am. Chem. Soc.* **2009**, *131*, 11692.

26. Kim, J.-H.; Heller, D. A.; Barone, P. W.; Song, C.; Zhang, J.; Trudel, L. J.; Wogan, G. N.; Tannenbaum, S. R.; Strano, M. S. *Nat. Chem.* **2009**, *1*, 473.

27. Jourd'heuil, D. *Free Radical Biol. Med.* **2002**, *33*, 676.

28. Wardman, P. *Free Radical Biol. Med.* **2007**, *43*, 995.

29. Zhang, X.; Kim, W. S.; Hatcher, N.; Potgieter, K.; Moroz, L. L.; Gillette R.; Sweedler, J. V. *J. Biol. Chem.* **2002**, *277*, 48472.

30. Ye, X.; Rubakhin, S. S.; Sweedler, J. V. *J. Neurosci. Methods*, **2008**, *168*, 373.

31. Yang, Y.; Seidlits, S. K.; Adams, M. M.; Lynch, V. M.; Schmidt, C. E.; Anslyn, E. V.; Shear, J. B. *J. Am. Chem. Soc.* **2010**, *132*, 13114.

32. a) Katayama, Y.; Takahashi, S.; Maeda, M. *Anal. Chim. Acta.* **1998**, *365*, 159. b) Katayama, Y.; Soh, N.; Koide, K.; Maeda, M. *Chem. Lett.* **2000**, 1152.

33. Soh, N.; Imato, T.; Kawamura, K.; Maeda, M.; Katayama, Y. *Chem. Commun.* **2002**, 2650.

34. a) Franz, K. J.; Singh, N.; Lippard, S. J. *Angew. Chem. Int. Ed.* **2000**, *39*, 2120. b) Franz, K. J.; Singh, N.; Spingler, B.; Lippard, S. J. *Inorg. Chem.* **2000**, *39*, 4081.

35. a) Hilderbrand, S. A.; Lippard, S. J. *Inorg. Chem.* **2004**, *43*, 4674. b) Lim, M. H.; Lippard, S. J. *Inorg. Chem.* **2004**, *43*, 6366.

36. a) Hilderbrand, S. A.; Lim, M. H.; Lippard, S. J. *J. Am. Chem. Soc.* **2004**, *126*, 4972. b) Hilderbrand, S. A.; Lippard, S. J. *Inorg. Chem.* **2004**, *43,* 5294.

37. a) Lim, M. H.; Kuang, C.; Lippard, S. J. *Chem. Bio. Chem.* **2006**, *7*, 1571. b) Lim, M. H.; Lippard, S. J. *J. Am. Chem. Soc.* **2005**, *127*, 12170.

38. a) Smith, R. C.; Tennyson, A. G.; Lim, M. H.; Lippard, S. J. *Org. Lett.* **2005**, *7*, 3573. b) McQuade, L. E.; Ma, J.; Lowe, G.; Ghatpande, A.; Gelperin, A.; Lippard, S. J. *Proc. Natl. Acad. Sci. USA*, **2010**, *107*, 8525.

39. Lim, M. H.; Wong, B. A.; Pitcock, Jr., W. H.; Mokshagundam, D.; Baik, M.; Lippard, S. J. *J. Am. Chem. Soc*. **2006**, *128*, 14364.

40. a) Dıaz, A.; Ortiz, M.; Sanchez, I.; Cao, R.; Mederos, A.; Sanchiz, J.; Brito, F. *J. Inorg*. *Biochem.* **2003**, *95*, 283. b) Tran, D.; Skelton, B. W.; White, A. H.; Laverman, L. E.; Ford, P. C. *Inorg. Chem.* **1998**, *37*, 2505.

41. a) Sarma, M.; Singh, A.; Gupta, S. G.; Das G.; Mondal, B. *Inorg. Chim. Acta*, **2010**, *363*, 63. b) Sarma, M.; Kalita, A.; Kumar, P.; Singh, A.; Mondal, B. *J. Am. Chem. Soc*. **2010**, *132*, 7846. c) Sarma, M.; Mondal, B. *Inorg. Chem*. **2011**, *50*, 3206. d) Kalita, A.; Kumar, P.; Deka, R. C.; Mondal, B. *Inorg. Chem.*, **2011**, *50*, 11868. e) Sarma, M.; Mondal, B. *Dalton Trans*. **2012**, *41*, 2927.

42. Riklin, M.; Tran, D.; Bu, X.; Laverman, L. E.; Ford, P. C. *Dalton Trans*. **2001**, 1813.

43. a) Tsuge, K.; DeRosa, F.; Lim, M. D.; Ford, P. C. *J. Am. Chem. Soc*. **2004**, *126*, 6564. b) Khin, C.; Lim, M. D.; Tsuge, K.; Iretskii, A.; Wu, G.; Ford, P. C. *Inorg. Chem*. **2007**, *46*, 9323.

44. Lim, M. H.; Lippard, S. J. *Inorg. Chem*. **2006**, *45*, 8980.

45. Xing, C.; Wang, M.; Yu, S.; Shi, Z.; Li, Y.; Zhu, D. *Macromol. Rapid Commun.* **2007**, *28*, 241.

46. a) Mondal, B., Kumar, P.; Ghosh, P.; Kalita, A. *Chem. Commun*. **2011**, *47*, 2964. b) Kumar, P.; Kalita, A.; Mondal, B. *Dalton Trans.* **2011**, *40*, 8656.

47. a) Halfen, J. A.; Mahapatra, S.; Wilkinson, E. C.; Kaderli, S.; Young, Jr., V. G.; Que, Jr., L.; A. Zuberbhler, D.; Tolman, W. B. *Science.* **1996**, *271*, 1397. b) Holland, P. L.; Tolman, W. B. *Coord. Chem. Rev*. **1999**, *190-192*, 855. c) Mahadevan, V.; Henson, M. J.; Solomon, E. I.; Stack, T. D. P. *J. Am. Chem. Soc.* **2000**, *122*, 10249. d) Mahadevan, V.; Hou, Z.; Cole, A. P.; Root, D. E.; Lal, T. K.; Solomon, E. I.; Stack, T. D. P. *J. Am. Chem. Soc.* **1997**, *119*, 11996.

48. Reed, C.; Roper, W. J. *Dalton Trans.* **1972**, 1243.

49. Nims, R. W.; Darbyshire, J. F.; Saavedra, J. E.; Christodoulou, D.; Hanbauer, I.; Cox, G. W.; Grisham, M. B.; Laval, F.; Cook, J. A.; Krishna, M. C.; Wink, D. A. *In Methods: A Companion to Methods in Enzymology*; Academic Press: San Diego, CA, **1995**; Vol. 7, pp 48.

50. Rhodes, M. R.; Barley, M. H.; Meyer, T. J. *Inorg. Chem*. **1991**, *30*, 629.

51. SMART, SAINT and XPREP, Siemens Analytical X-ray Instruments Inc., Madison, Wisconsin, USA, **1995**.

52. Sheldrick, G. M. SADABS: software for Empirical Absorption Correction, University of Gottingen, Institut fur Anorganische Chemieder Universitat, Tammanstrasse 4, D-3400 Gottingen, Germany, **1999–2003**.

53. Sheldrick, G. M. SHELXS-97, University of Gottingen, Germany, **1997**.

54. Farrugia, L. J. *J. Appl. Crystallogr.* **1997**, *30*, 565.

Chapter 4

Reduction of copper (II) complexes of tridentate ligands by nitric oxide and fluorescent detection of NO in methanol and water media

Abstract

Two copper complexes, **4.1** and **4.2** with tridentate N-donor ligands, $\mathbf{L_{10}}$ and $\mathbf{L_{11}}$ [$\mathbf{L_{10}}$ = (1-Methyl-1H-imidazol-2-ylmethyl)-(2-pyridin-2-yl-ethyl)amine, $\mathbf{L_{11}}$ = (2-Pyridin-2-yl-ethyl)-pyridin-2 yl-methylamine], respectively, were synthesized and characterized. On exposure to nitric oxide, the Cu(II) centres in complexes **4.1** and **4.2** were found to undergo reduction in various solvents. In acetonitrile solvent the reduction was accompanied with a simultaneous N-nitrosation on the secondary amine centre on the ligand frameworks. Complexes **4.3** and **4.4** were prepared with ligands $\mathbf{L_{12}}$ and $\mathbf{L_{13}}$, respectively. $\mathbf{L_{12}}$ and $\mathbf{L_{13}}$ [$\mathbf{L_{12}}$ = 5-dimethylamino-naphthalene-1-sulfonic acid (1-methyl-1H-imidazol-2-ylmethyl)-(2-pyridin-2-yl-ethyl)-amide; $\mathbf{L_{13}}$ = 5-dimethylamino-naphthalene-1-sulfonicacid (2-pyridin-2-yl-ethyl)-pyridin-2-methyl-amide] are the dansyl derivatives of $\mathbf{L_{10}}$ and $\mathbf{L_{11}}$, respectively. Complexes **4.3** and **4.4**, due to paramagnetic quenching, do not display significant fluorescence; however, on addition of NO to a methanol or water solution of the complexes **4.3** and **4.4**, the fluorescence intensity of the fluorophore was found to be restored. This is attributed to the reduction of Cu(II) centre by NO to diamagnetic Cu(I).

4.1 Introduction

NO has attracted an enormous interest of chemists and biochemists since it has been discovered as the signalling agent in human.[1-13] It is also known to play roles in various physiological processes like vascular regulation, neurotransmission and cytotoxicity.[14-18] These essentially inspired a wide range of research to identify the precise roles of NO in biology. To study the NO induced reactions in cellular systems, most challenging aim is to detect the location of NO formation. Thus, a selective probe to detect the formation and migration of NO with spatiotemporal resolution directly from living cells is highly desirable. In this aspect, the fluorescence-based detection technique has been found to satisfy almost all the requirements.[19, 20]

Starting from the early examples of fluorescence-based sensors like *o*-diaminonaphthalene (DAN) and *o*-diaminofluoresceins (DAFs), a number of fluorescent probes have been reported to date.[21-36] However, they are unable to detect or monitor NO itself as their fluorescent response depends on the formation of a triazole species by oxidized NO products such as N_2O_3. Thus, the NO-related bio-events would not be detected in real time. Recently, a highly selective fluorescent imaging agent, NO_{550}, for NO has been reported which displays rapid and linear response with a red-shifted turn-on signal.[37] A number of metal complex-based fluorescence sensors for NO are reported recently based on fluorophore displacement strategy.[38-43] However, the low sensitivity and water insolubility of most of the cobalt, ruthenium and di-rhodium complexes, precluded their further application in biological systems.[21-36] Though, a number of iron complexes are reported to sense NO in aqueous medium, some of them either display diminished fluorescence or are air sensitive and exhibit only modest turn-on emission with NO, which again precluded their biological applications.[44-46] On the hand, it has been observed that the fluorophore displacement technique to sense NO works mostly in organic solvents.[38-43] In aqueous

medium, since the replacement of the fluorophore ligand from the metal can also be achieved by water, the turn-on fluorescence may also be possible in absence of NO. Hence, the reduction of metal centre by NO has been found to be a more effective strategy. The fluorescence intensity of a ligand comprising a fluorophore is expected to be quenched on its complexation with paramagnetic Cu(II) centre and the reduction of Cu(II) centre to diamagnetic Cu(I) by NO will restore the quenched fluorescence intensity of the fluorescent ligand.[47-53]

In continuation to our study of the reduction of Cu(II) complexes by NO and ligand nitrosation,[54-57] in this chapter, the NO reactivity of Cu(II) complexes of two tridentate ligands; and the use of the Cu(II) complexes of those ligands with dansyl fluorophore to sense NO in aqueous and methanol media (Figure 4.1) has been described.

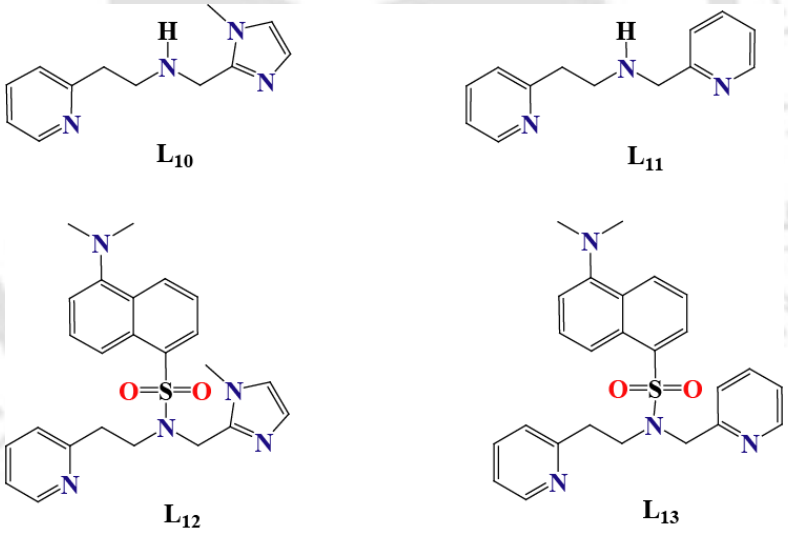

Figure 4.1 Ligands used for the present study.

4.2 Results and discussion

Ligands $\mathbf{L_{10}}$ and $\mathbf{L_{11}}$ were prepared from the reaction of pyridine 2-ethylamine with the appropriate aldehyde followed by reduction of the imine (experimental section). The formation of the ligands was authenticated by elemental analysis and other spectroscopic studies (experimental section). The ligands $\mathbf{L_{12}}$ and $\mathbf{L_{13}}$ were synthesized by incorporating

the dansyl group into the secondary amine site of $\mathbf{L_{10}}$ and $\mathbf{L_{11}}$, respectively following reported procedure (experimental section).[62-67] $\mathbf{L_{12}}$ and $\mathbf{L_{13}}$ were found to display satisfactory elemental analyses and were characterized further by various spectral analysis (experimental section). All the complexes were prepared using a general method where Cu(II) perchlorate hexahydrate or Cu(II) chloride dihydrate was made to react with equivalent quantity of the respective ligands (experimental section). All the complexes showed satisfactory elemental analyses (experimental section).

Crystal structure

Single crystal structures of complexes **4.1** and **4.2** have been determined. The perspective views of the ORTEP diagrams are shown in figure 4.2. In both the complexes, Cu(II) is found to be coordinated with the tridentate ligand and a solvent molecule in a distorted square planar geometry. Weak interactions between the perchlorate oxygen atoms and Cu(II) ion have been found in both the complexes. In complex **4.1**, the coordinated solvent is water and in complex **4.2**, it is acetonitrile. The crystallographic data, important bond angles and distances were listed in tables in tables 4.1, 4.2 and 4.3, respectively. From the spectral analysis, presumably, the complexes attain the distorted square planar geometry in solution, also.

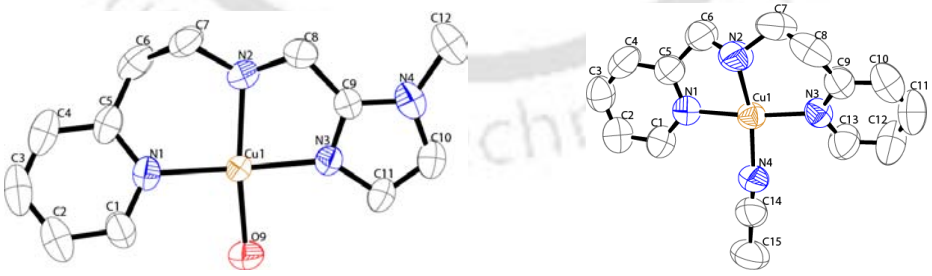

(a) **(b)**

Figure 4.2 ORTEP diagrams of complexes (a) **4.1** and (b) **4.2** (50% thermal ellipsoid plot). (Hydrogen atoms, perchlorate anions and solvent of crystallization were removed for clarity).

Table 4.1 Crystallographic data for complexes **4.1** and **4.2**

	4.1	**4.2**
Formulae	C_{12} H_{15} Cl_2 Cu N_4 O_{10}	C_{15} H_{17} Cl_2 Cu N_4 O_8
Mol. wt.	509.73	515.78
Crystal system	Triclinic	Monoclinic
Space group	P -1	P 21/c
Temperature /K	293(2)	296(2)
Wavelength /Å	0.71073	0.71073
a /Å	8.3087(2)	8.4963(9)
b /Å	10.3152(3)	9.0426(10)
c /Å	11.6673(3)	26.440(3)
α/°	85.8490(10)	90.00
β/°	83.5950(10)	90.769(7)
γ/°	85.1690(10)	90.00
V/ Å^3	988.18(5)	2031.1(4)
Z	2	4
Density/Mgm^{-3}	1.713	1.687
Abs. Coeff. /mm^{-1}	1.434	1.383
Abs. correction	None	None
F(000)	516.0	1048.0
Total no. of reflections	4211	2355
Reflections, $I > 2\sigma(I)$	3287	1670
Max. 2θ/°	27.50	21.70
Ranges (h, k, l)	-10<= h <=10 -9<= k <=13 -15<= l <= 15	-8<= h <=8 -9<= k <=9 -26<= l <= 27
Complete to 2θ (%)	92.8	98.3
Refinement method	Full-matrix least-squares on F^2	Full-matrix least-squares on F^2
Goof (F^2)	1.277	1.056
R indices [$I > 2\sigma(I)$]	0.0486	0.0847
R indices (all data)	0.0623	0.1045

Table 4.2 Selected bond angles (°) for complexes **4.1** and **4.2**

	4.1	**4.2**
N(1)-Cu(1)-N(2)	95.3(1)	79.7(4)
N(2)-Cu(1)-N(3)	81.8(1)	96.9(4)
N(1)-Cu(1)-N(3)	170.1(1)	170.9(3)
C(1)-N(1)-C(5)	117.7(3)	117.7(8)
C(6)-C(5)-N(1)	118.3(3)	114.6(9)
C(4)-C(5)-C(6)	121.3(4)	126(1)
C(7)-N(2)-C(8)	114.8(3)	-
C(6)- N(2)-C(7)	-	114(1)
C(7)-C(6)-C(5)	115.0(3)	-
C(7)-C(8)-C(9)	-	111(1)

N(4)-C(14)-C(15)	-	178(1)
N(4)-C(10)-C(11)	106.9(4)	-
C(9)-N(3)-C(11)	106.3(3)	-
C(9)-N(3)-C(13)	-	117(1)
Cu(1)-N(1)-C(1)	117.4(3)	127.9(7)
Cu(1)-N(1)-C(5)	124.9(2)	114.4(6)
Cu(1)-N(2)-C(7)	116.7(3)	114.6(8)
Cu(1)-N(2)-C(8)	111.9(3)	-
Cu(1)-N(2)-C(6)	-	109.8(7)
Cu(1)-N(3)-C(9)	114.1(2)	124.0(7)
Cu(1)-N(3)-C(11)	139.5(2)	-
Cu(1)-N(3)-C(13)	-	119.0(7)
C(1)-C(2)-C(3)	119.4(5)	118(1)

Table 4.3 Selected bond length (Å) for complexes **4.1** and **4.2**

	4.1	**4.2**
Cu(1)-N(1)	2.000(3)	2.008(8)
Cu(1)-N(2)	2.024(4)	2.00(1)
Cu(1)-N(3)	1.955(3)	2.007(8)
Cu(1)-N(4)	-	1.97(1)
Cu(1)-O(1)	2.002(3)	-
C(2)-C(1)	1.369(6)	1.38(2)
C(2)-C(3)	1.362(8)	1.36(2)
C(1)-N(1)	1.354(6)	1.34(1)
C(5)-N(1)	1.356(4)	1.33(1)
C(10)-C(11)	1.334(6)	1.33(2)
N(2)-C(7)	1.485(5)	1.50(2)
C(7)-C(8)	-	1.48(2)
N(2)-C(8)	1.439(5)	-
C(9)-C(10)	-	1.40(2)
C(4)-C(5)	1.395(6)	1.43(2)
C(5)-C(6)	1.494(6)	1.49(2)
C(8)-C(9)	1.492(5)	1.54(2)
C(9)-N(3)	1.315(5)	1.32(1)

Nitric oxide reactivity of complexes 4.1 and 4.2

Purging of excess NO to the degassed acetonitrile solution of complexes **4.1** and **4.2**, resulted in the rapid reduction of Cu(II) centre to Cu(I). The reduction was monitored by UV-visible spectroscopy, figures 4.3(a) and (b) represent the observed spectral changes during the reaction.

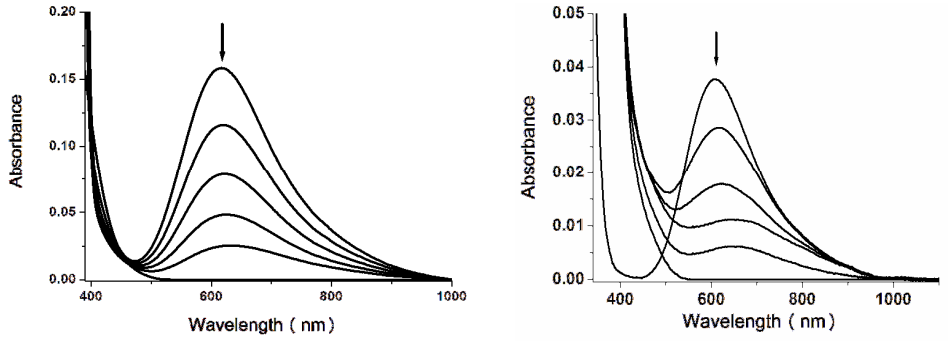

(a) **(b)**

Figure 4.3 UV-visible spectral changes of complexes (a) **4.1** and (b) **4.2** upon their reaction with NO in acetonitrile.

The reduction of Cu(II) in presence of NO was noticed in water, methanol, methanol/water mixture, also. In methanol and water medium, the reduction led to the formation of methyl nitrite and nitrite ion, respectively. The formation of methyl nitrite was confirmed quantitatively by GC-Mass spectral studies and nitrite ion in aqueous solution was authenticated by the Griess test.[58]

$$[Cu(L)(CH_3CN)]^{2+} + NO_{(g)} \xrightarrow{CH_3CN} [Cu(CH_3CN)_4]^{+} + L^{/} + H^{+} \quad \text{---------- (4.1)}$$

Generation of H^+ (eq. 4.1) was confirmed qualitatively in unbuffered aqueous solution by monitoring the decrease in pH as the reactions proceeded. Similar reduction was reported with $[Cu(dmp)_2(H_2O)]^{2+}$ and $[Cu(phen)_2(H_2O)]^{2+}$ (dmp = 2,9-dimethyl-1,10-phenanthroline; phen = 1,10-phenanthroline).[50,51] The striking difference between the these two cases and the present ones is, in case of $[Cu(dmp)_2(H_2O)]^{2+}$ and $[Cu(phen)_2(H_2O)]^{2+}$, the reduction was observed only in presence of a protic solvent, but not in pure acetonitrile and dichloromethane.[50,51] On the other hand, the Cu(II) centres in $[Cu(tren)(CH_3CN)]^{2+}$, $[Cu(tiaea)(CH_3CN)]^{2+}$ and $[Cu(teaea)(CH_3CN)]^{2+}$ [tren: *tris*-(2-aminoethyl)amine; tiaea = *tris*-(2-isopropylaminoethyl)amine and teaea = *tris*-(2-ethylaminoethyl)amine] were found to undergo reduction in presence of NO in pure acetonitrile, also.[54,55] In these cases, the

reduction was accompanied with either the N-nitrosation or the diazotization of the primary amine centre of the ligand followed by ligand transformation.[54,55] In the present cases, the reduction in acetonitrile medium, led to the N-nitrosation of the ligand (Scheme 4.1). The N-nitrosation was reported in case of $[Cu(DAC)]^{2+}$, DAC = 1,8-bis(9-anthracylmethyl)-derivative of the macrocyclic tetraamine cyclam, also.[59, 60]

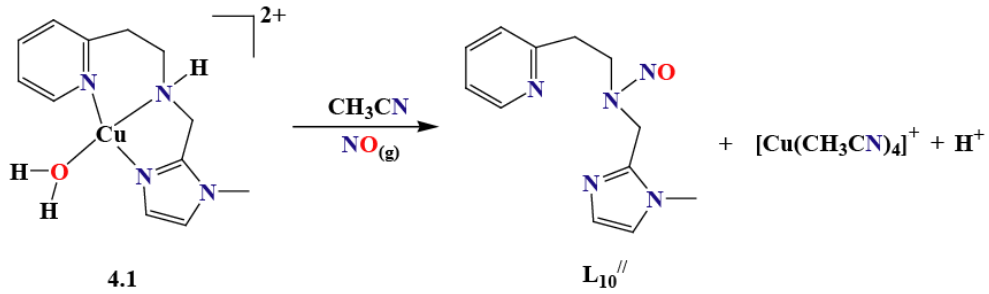

4.1 **L_{10}**

Scheme 4.1

The *d-d* band at 616 and 606 nm in case of complexes **4.1** and **4.2**, respectively, were studied during the reduction of Cu(II) centres in presence of NO (Figure 4.3). In presence of excess NO, the reduction of Cu(II) to Cu(I) was found to follow a simple first-order kinetics in water, methanol and acetonitrile media and the rate was observed to be independent of the initial concentration of the complexes. The observed rate constants at 298 K for complexes **4.1** and **4.2** are 15.55×10^{-5} s^{-1} and 7.35×10^{-5} s^{-1}, respectively. For $[Cu(tiaea)(CH_3CN)]^{2+}$ and $[Cu(teaea)(CH_3CN)]^{2+}$, the observed rates at 298 K were 5.64×10^{-2} and 6.55×10^{-3} s^{-1}, respectively.[55] The pseudo first order rate constants for $[Cu(pymea)_2]^{2+}$ and $[Cu(baea)(CH_3CN)]^{2+}$ [pymea = pyridine-2-methylamine and baea = *bis*-(2-aminoethyl)amine] are also reported to be 3.10×10^{-3} and 2.20×10^{-3} s^{-1}, respectively, at 298 K.[57] Thus, the rate of reduction of Cu(II) centre to Cu(I) for the present set of complexes are much slower than the earlier reported ones. This is, presumably, because of the difference in ligand denticity and the nature of N-donor atoms. From eq. 4.1 and Scheme 4.1, generation of H^+ is obvious during the reduction; it is expected to be catalyzed

by the presence of base. However, no effect pH of was observed on the rates of the reactions indicating that the conjugate base has very little role in the reaction. It would be worth mentioning here, that the rate of reductive nitrosylation of ferriheme proteins in aqueous medium are demonstrated to be strongly dependent on the hydroxide ion concentration in the pH range 6-9.[61] This was presumably because of the rate limiting attack of hydroxide ion on the Fe^{III} coordinated NO.

The NO reduction of Cu(II) centres in complexes **4.1** and **4.2** can be rationalized by an inner-sphere mechanism involving three steps (Scheme 4.1). (i) reversible displacement of the solvent by NO from the coordination sphere of Cu(II) leading to the formation of a inner-sphere [Cu^{II}-NO] intermediate; (ii) nucleophilic attack of H_2O or CH_3OH (in case of water and methanol media) or the generation of highly electrophilic NO^+ owing to [Cu^{II}-NO $\leftrightarrow$ Cu^{I}-NO^+] charge distribution followed by the (iii) release of NO_2^- (or CH_3ONO) or N-nitrosated ligand. Step three, perhaps, became more facile owing to the geometrical preference of Cu(I) complexes for tetrahedral coordination. In our earlier studies with $[Cu(tren)(CH_3CN)]^{2+}$, $[Cu(tiaea)(CH_3CN)]^{2+}$ and $[Cu(teaea)(CH_3CN)]^{2+}$ the formation of the transient [Cu^{II}-NO] intermediate complex was observed.[54,55] Similar instances of nucleophilic attack at the coordinated NO were reported in the reaction of hydroxide ion in [Ru^{II}-NO] to result in the corresponding nitro complexes and also in the reaction of alcohols with Ir(III)-NO to yield alkyl nitrite complexes.[62, 63]

In the present cases, we have not observed any indication of formation of [Cu^{II}-NO] inner-sphere complex (Figure 4.3). With $[Cu(dmp)_2(H_2O)]^{2+}$ and $[Cu(phen)_2(H_2O)]^{2+}$, even at the early stage of mixing no spectral change for the inner-sphere complex formation was reported.[50,51] This can be rationalized in two ways: (i) either the spectral pattern of the complexes **4.1** and **4.2** are very similar to their respective [Cu^{II}-NO] intermediates or (ii) the values of the equilibrium constant, K_{NO} are very less. Since, in FT-IR studies also, no

υ_{NO} frequency corresponding to the formation of [Cu^{II}-NO] was observed, the second option is more logical.

The complete reduction of Cu(II) centres in complexes **4.1** and **4.2** by NO was further confirmed by X-band EPR studies. Though both the complexes in acetonitrile solvent displayed characteristic EPR spectra, the colorless solutions are found to be silent (Figure 4.4). This can be attributed to the reduction of paramagnetic Cu(II) to diamagnetic Cu(I). The N-nitrosated ligands in both the cases were isolated and characterized completely using various spectroscopic techniques.

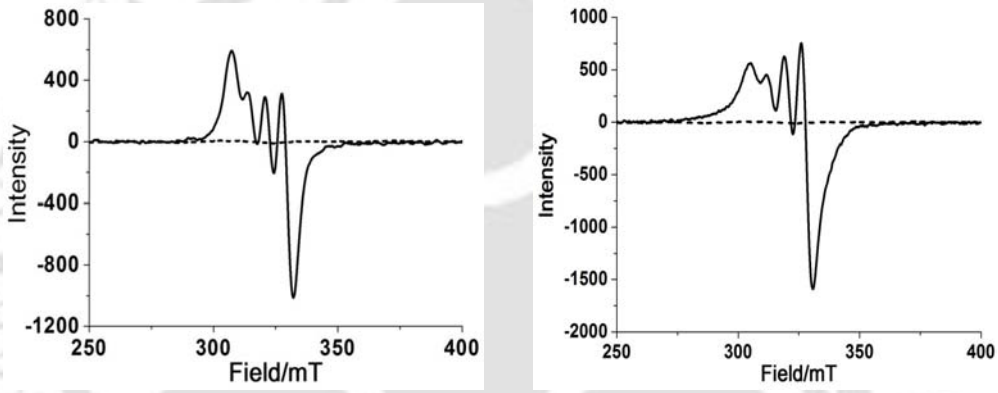

(a) **(b)**

Figure 4.4 X-band EPR spectra of the reaction of complexes **4.1** (a) and **4.2** (b) with NO in acetonitrile solvent at room temperature. (solid traces correspond to the respective complexes and dashed traces represent the spectra of the colorless solutions obtained after reaction of the respective complexes with NO).

NO reactivity of complexes 4.3 and 4.4

Since the Cu(II) centres in complexes **4.1** and **4.2** exhibit reduction in presence of NO, these in combination with a pendant fluorophore might be good sensors for NO. Ligands $\mathbf{L_{12}}$ and $\mathbf{L_{13}}$ were prepared by incorporating the pendant dansyl group into $\mathbf{L_{10}}$ and $\mathbf{L_{11}}$, respectively. $\mathbf{L_{12}}$ and $\mathbf{L_{13}}$ displayed moderate fluorescence at room temperature in methanol, water and methanol/water solvent systems. The fluorescence quantum yields were calculated to be 0.198 and 0.177 for $\mathbf{L_{12}}$ and $\mathbf{L_{13}}$, respectively, in methanol at room

temperature. Metallation with paramagnetic Cu(II), resulted into the quenching of the fluorescence intensity of free $\mathbf{L_{12}}$ and $\mathbf{L_{13}}$ (Figures 4.5a and 4.6a). The quenched fluorescence intensity of the ligand fluorophore is expected to restore on reduction of Cu(II) centre by NO (Scheme 4.2).[29] Fluorescence studies at 298 K displayed significant (> 90%) quenching of the ligand fluorescence in presence of equivalent amount of Cu(II) in aqueous medium buffered at pH 7.2 using TRIS-HCl buffer. The similar quenching was observed in methanol solution, also (Figure 4.5a). To a degassed methanol solution of complex **4.3**, addition of 2-5 equivalent of NO immediately restored the emission intensity significantly (Figure 4.5b).

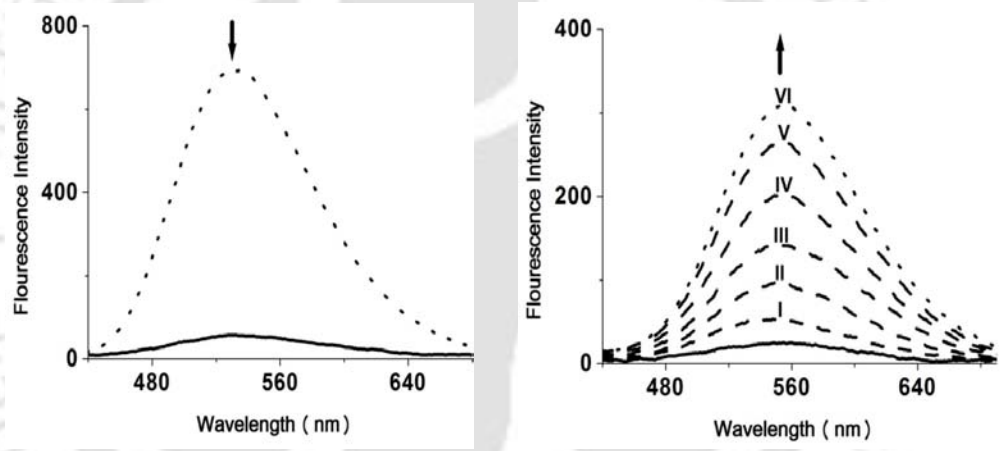

Figure 4.5 Fluorescence responses (λ_{ex}, 350 nm) for (a) 25 μM solution of free ligand, $\mathbf{L_{12}}$ (dotted line) and after addition of one equivalent of $[Cu(H_2O)_6]^{2+}$ in methanol (solid line); (b) deoxygenated methanol solution of complex **4.3** before (solid line) and after (dashed lines) purging of 5 equivalent of NO at 10, 20, 30, 40, 50 and 60 minutes at 298 K (lines I – VI, respectively).

The enhancement of the restored emission is found to be less in aqueous medium buffered at pH 7.2, compare to that in methanol solution (Appendix III, Figure A3.39). In the present case the restored emission intensities are found to be 12.5 (±0.2)- and 8.3(±0.2)-fold in methanol and aqueous (at pH 7.2) medium, respectively. The NO detection limit of the present complex is observed to be ~10 nM.[56]

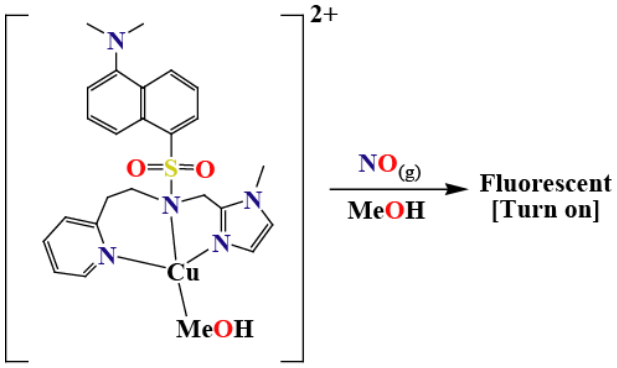

4.3
Non-fluorescent

Scheme 4.2

Addition of equivalent amount of Cu(II) in the methanol solution of $\mathbf{L_{13}}$, displayed a significant (> 85%) quenching of the ligand fluorescence at 298 K (Figure 4.6a). This has been observed in aqueous medium buffered at pH 7.2 using TRIS-HCl buffer, also. It has been found that addition of 2-5 equivalent of NO into a degassed methanol solution of complex **4.4**, immediately restored the emission intensity significantly (Figure 4.6b). However, the restored emission was observed to be less in aqueous medium buffered at pH 7.2, compare to that in methanol (Appendix III, Figure A3.40,). Similar behaviour was observed in case of complex **4.3**, also. In case of $[Cu(Ds\text{-}en)_2]$ and $[Cu(Ds\text{-}AMP)_2]$, the ligand fluorescence intensity was found to quench to 31(± 2)- and 23(± 0.5)-fold relative to free Ds-Hen and Ds-HAMP (40 μM), respectively, upon addition of Cu(II).[48,49] In buffered aqueous or methanol solution of the complexes $[Cu(Ds\text{-}en)_2]$ and $[Cu(Ds\text{-}AMP)_2]$, under anaerobic condition, the emission intensity was found to be restored significantly upon addition of 100 equivalent of NO and the enhancements in integrated fluorescence were reported to be 6.1(±0.2)- and 8.8(±0.1)-fold, respectively.[48,49] In case of complex **4.3**, the restored emission intensities are found to be 12.5 (±0.2)- and 8.3(±0.2)-fold in methanol and aqueous (at pH 7.2) medium, respectively.[56]

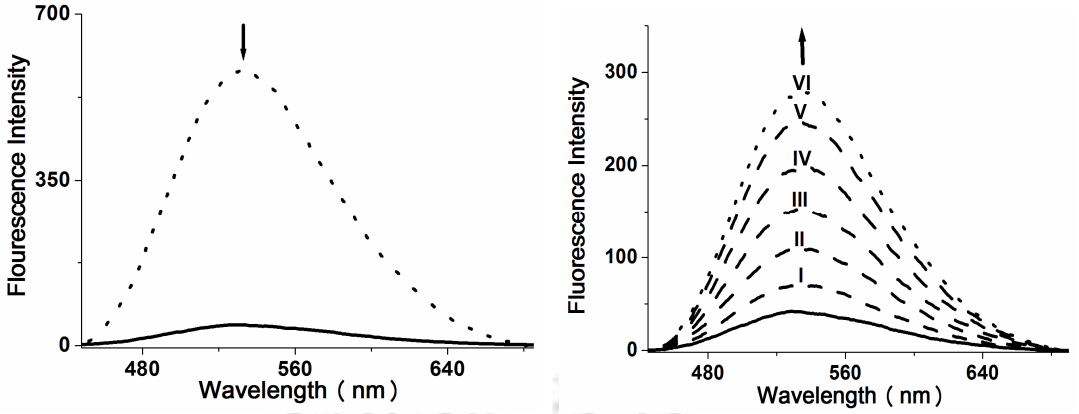

Figure 4.6 Fluorescence responses (λ_{ex}, 350 nm) for (a) 25 μM solution of free ligand, $\mathbf{L_{13}}$ (dotted line) and after addition of one equivalent of $CuCl_2.(H_2O)_2$ in methanol (solid line); (b) deoxygenated methanol solution of complex **4.4** before (solid line) and after (dashed lines) purging of 5 equivalent of NO at 10, 20, 30, 40, 50 and 60 minutes at 298 K (lines I – VI, respectively).

Addition of 5 equivalent of NO to a degassed aqueous (buffered at pH 7.2) or methanol solution of complex **4.4** restored the emission intensity to 6.7 (±0.2)- and 4.6(±0.2)-fold, respectively. Except a few, all earlier examples of Cu(II) complexes as fluorescent sensor in aqueous methanol or in an aqueous pH 7.0 buffer and in cells, were found to detect NO by a different mechanism; and that involves the reduction of Cu(II) by NO followed by dissociation of the N-nitrosated ligand.[56,63] $[Cu(Ds\text{-}en)_2]$ and $[Cu(Ds\text{-}AMP)_2]$, where Ds-en and Ds-AMP are the conjugate bases of dansylethylenediamine (Ds-Hen) and dansyl aminomethylpyridine (Ds-HAMP), respectively, were reported recently as the probe for fluorescence-based NO detection in aqueous solution.[48,49] However, these Cu(II) dansyl compounds were unable to sense NO at a physiologically more relevant pH.[63] The fluorescence enhancement in case Ds-HAMP ligand is attributed to both the sulphonamide functionality following protonation by H^+ formed in the reaction.[48] The dissociation was confirmed by the presence of sulphonamide group ($\nu_{N\text{-}H} \approx 3083$ cm^{-1} in KBr) in the FT-IR spectrum of the reaction product which indicates that ligand protonation also occurs. The

protonated sulfonamide group is anticipated to contribute to the fluorescence intensity.[48] In contrary, in cases of complexes **4.3** and **4.4**, no indication of dissociation of sulphonamide group was observed in the FT-IR spectra of the reaction products (Appendix III, Figures A3.43 and A3.44). Hence, the restored emission intensity, in these cases, is attributed to the reduction of Cu(II) centre to the diamagnetic Cu(I) by NO. In the present case, no N-nitrosoamine formation was observed because of the reaction of NO^+, formed during the reaction of Cu(II) with NO, with methanol solvent to form CH_3ONO and H^+.[48,51] The formation of the NO_2^- in aqueous medium has been established by the Griess's test.[58]

4.3 Conclusion

In conclusion, two Cu(II) complexes have been prepared with two tridentate N-donor ligands and their NO reactivity were studied. The Cu(II) centres in complexes **4.1** and **4.2** were found to undergo reduction in presence of NO in acetonitrile, methanol and water medium. No [Cu^{II}-NO] intermediate was observed in the present cases presumably because of very low value of K_{NO}. The reduction in acetonitrile solvent was found to accompany with N-nitrosation of the ligands. However, in water and methanol solvent, the formation of NO_2^- and CH_3ONO were observed. Addition of NO to methanol or aqueous (at pH 7.2) solutions of the complex **4.3** and **4.4** resulted into the reduction of Cu(II) centre to Cu(I) with a substantial increase in fluorescence intensity. Thus the complexes **4.3** and **4.4** can function as fluorescence-based NO sensor. It has been found that the present complexes can be used to sense nanomolar quantities of NO in both methanol and pH 7.2 buffered-aqueous medium. The fluorescence enhancement is attributed mostly to the formation of diamagnetic Cu(I) species after reduction of paramagnetic Cu(II) centre by NO.

4.4 Experimental Section

4.4.1 Materials and methods

All reagents and solvents were purchased from commercial sources and were of reagent grade. Acetonitrile was distilled from calcium hydride. Deoxygenation of the solvent and solutions were effected by repeated vacuum/purge cycles or bubbling with nitrogen for 30 minutes. NO gas was purified by passing through KOH and P_2O_5 column. UV-visible spectra were recorded on a Perkin Elmer Lambda 25 UV-visible spectrophotometer. FT-IR spectra of the solid samples were taken on a Perkin Elmer spectrophotometer with samples prepared as KBr pellets. The fluorescence spectra were recorded in solution in Varian Cary Eclipse Fluorescence Spectrophotometer at room temperature. Quinine sulfate in acidic medium was used as the reference compound for the determination of fluorescence quantum yield. Solution electrical conductivity was checked using a Systronic 305 conductivity bridge. ^{1}H-NMR spectra were obtained with a 400 MHz Varian FT spectrometer. Chemical shifts (ppm) were referenced either with an internal standard (Me_4Si) or to the residual solvent peaks. The X-band Electron Paramagnetic Resonance (EPR) spectra were recorded on a JES-FA200 ESR spectrometer, at room temperature. Elemental analyses were obtained from a Perkin Elmer Series II Analyzer. The magnetic moment of complexes is measured on a Cambridge Magnetic Balance.

Single crystals were grown by slow diffusion followed by slow evaporation technique. The intensity data were collected using a Bruker SMART APEX-II CCD diffractometer, equipped with a fine focus 1.75 kW sealed tube MoK_α radiation (λ = 0.71073 Å) at 273(3) K, with increasing ω (width of 0.3° per frame) at a scan speed of 3 s/frame. The SMART software was used for data acquisition. Data integration and reduction were undertaken with SAINT and XPREP software.[64] Multi-scan empirical absorption corrections were applied to the data using the program SADABS.[65] Structures were solved by direct

methods using SHELXS-97 and refined with full-matrix least squares on F^2 using SHELXL-97.[66] All non-hydrogen atoms were refined anisotropically. Structural illustrations have been drawn with ORTEP-3 for Windows.[67]

4.4.2 Synthesis of ligands

Synthesis of L_{10}

The ligands **L_{10}** and **L_{11}** were reported earlier [68-73] and have been prepared by the reaction of pyridine-2-ethylamine with the appropriate aldehyde followed by reduction of the imine with sodium borohydride (Scheme 4.3). Yield: 0.834 g, ~60%. Elemental analyses for $C_{12}H_{16}N_4$: Calcd. (%): C, 66.21; H, 7.22; N, 25.11. Found (%): C, 66.26; H, 7.23; N, 25.04. FT-IR in KBr: 3504, 2923, 1596, 1437, 749 cm^{-1}. ^{1}H-NMR (400 MHz, $CDCl_3$) δ_{ppm}: 2.86 (1H), 2.95 (2H), 3.01 (2H), 3.58 (3H), 3.83 (2H), 6.76 (1H), 6.86 (1H) 7.0-7.1 (2H), 7.52 (1H), 8.47 (1H). ^{13}C-NMR (100 MHz, $CDCl_3$) δ_{ppm}: 32.4, 38.0, 45.4, 48.7, 121.0, 121.3, 126.6, 126.7, 136.6, 146.3, 149.0, and 160.0. ESI-Mass (m+1): Calcd. 217.13; Found, 217.48.

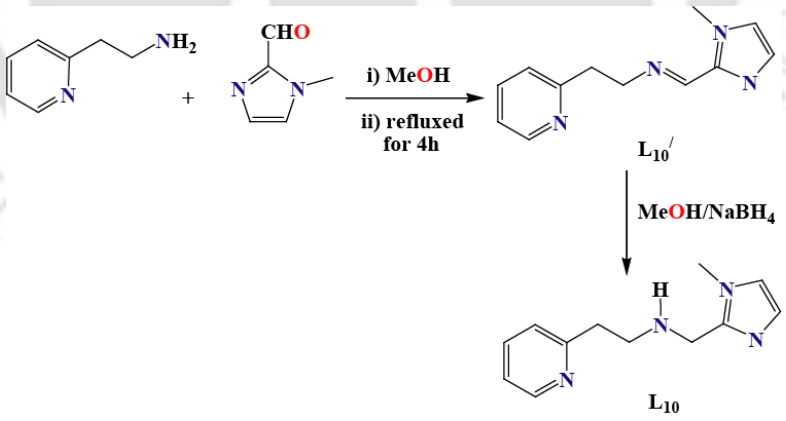

Scheme 4.3

Synthesis of L_{11}

Ligand **L_{11}** was prepared following the same procedure like **L_{10}** from pyridine-2-ethylamine (1.22 g, 10 mmol) and pyridine-2-carbaldehyde (1.07 g, 10 mmol). Yield: 1.11

g, ~70%. Elemental Analyses for $C_{13}H_{14}N_3$: Calcd. (%): C, 73.55 ; H, 7.13; N, 19.82. Found (%): C, 73.49; H, 7.13; N, 19.74. FT-IR in KBr: 2928, 2852, 1594, 1476, 1435, 765 cm^{-1}. ^{1}H-NMR (400 MHz, $CDCl_3$) δ_{ppm}: 2.64-2.99 (4H), 3.86 (2H), 7.00-7.05 (2H), 7.08-7.10 (1H), 7.19-7.21 (1H), 7.47-7.54 (2H). ^{13}C-NMR (100 MHz, $CDCl_3$) δ_{ppm}: 37.9, 48.5, 54.5, 120.8, 121.4, 121.7, 122.8, 135.9, 136.0, 148.7, 148.7, 159.2, and 159.6. ESI-Mass (m+1): Calcd. 214.12; Found, 214.13.

Synthesis of L_{12}

The fluorescent ligand **L_{12}** has been prepared by the incorporation of the dansyl group into the ligand **L_{10}** (Scheme 4.4). This has been done by stirring an equimolar mixture of the yellow oil, **L_{10}** and dansyl chloride in presence of triethylamine in distilled chloroform for 5 h at room temperature. The volume of the resulting solution was then reduced in rotavapour and the greenish yellow fluorescent mass was subjected to column chromatographic purification to result into the pure greenish yellow fluorescent ligand **L_{12}**.

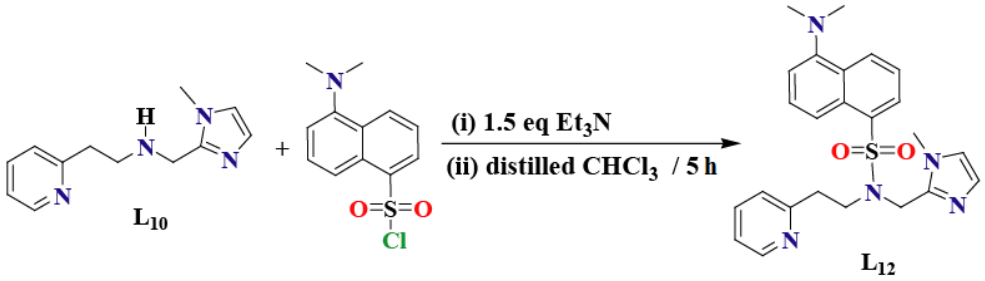

Scheme 4.4

Yield: 1.57 g, ~70%. Elemental Analyses for $C_{24}H_{27}N_5O_2S$: Calcd. (%): C, 64.12; H, 6.05; N, 15.58. Found (%): C, 64.09; H, 6.06; N, 15.61. FT-IR in KBr: 2927, 2851, 2788, 1322, 1140 cm^{-1}. ^{1}H-NMR (400 MHz, $CDCl_3$) δ_{ppm}: 2.74 (2H), 2.86 (6H), 3.58 (2H), 3.61 (3H), 4.756 (2H), 6.8-7.00 (4H), 7.12 (1H), 7.34-7.52 (3H), 8.02 (1H), 8.28 (2H) 8.48 (1H). ^{13}C-NMR (100 MHz, $CDCl_3$) δ_{ppm}: 29.8, 33.2, 36.5, 44.4, 45.6, 47.5, 76.9, 77.2, 77.5, 115.4,

119.5., 121.4, 122.5, 123.3, 123.4, 127.7, 128.0, 128.3, 129.4, 130.3, 130.6, 134.6, 136.2, 142.45, 149.2, 151.9, 158.5. ESI-Mass (m+1): Calcd. 449.05; Found, 449.18.

Synthesis of L_{13}

L_{13} has been prepared following the same procedure used for **L_{12}** (Scheme 4.4). Yield: 0.625 g, ~70%. Elemental Analyses: Calcd.(%) for $C_{25}H_{26}N_4O_2S$: C, 67.24; H, 5.87; N, 12.55. Found (%): C, 67.52; H, 5.79; N, 12.34. FT-IR in KBr: 2921, 2850, 1590, 1436, 1323, 1142 and 791cm^{-1}. ^{1}H-NMR (400 MHz, $CDCl_3$) δ_{ppm}: 2.82-2.89 (8H), 3.70 (2H), 4.71 (2H), 6.81 (1H), 7.88 (1H), 7.12(2H), 7.30-7.37 (2H), 7.43-7.47 (2H), 7.53 (1H) 8.19 (3H), 8.45 (2H). ^{13}C-NMR (100 MHz, $CDCl_3$) $\delta_{ppm:}$ 36.29, 45.32, 47.47, 52.8, 115.0, 119.4, 121.2, 122.4, 122.4, 123.0, 123.1, 128.0, 129.7, 129.9, 130.3, 134.9, 136.0, 136.6, 148.8, 148.9, 151.6, 156.7, 158.0. ESI-Mass (m+1): Calcd. 447.17; Found, 447.11.

4.4.3 Synthesis of complexes

Complexes **4.1** and **4.2** were synthesized following the same procedure. The details are given for complex **4.1**.

Synthesis of complex 4.1

$[Cu^{II}(H_2O)_6](ClO_4)_2$ (0.370 g, 1.0 mmol) was dissolved in 10 ml distilled acetonitrile. To this solution, **L_{10}** (0.216 g, 1.0 mmol) was added slowly with constant stirring. The color of the solution turned into deep blue. The stirring was continued for 1h at room temperature. The volume of the solution was then reduced to ~2 ml. To this, benzene (5 ml) was added to layer on it and kept it overnight on freezer. This resulted into blue color microcrystals of complex **4.1**. Yield: 0.423 g, ~83%. Elemental Analyses: Calcd.(%) for $CuC_{12}H_{19}N_4O_{10}Cl_2$: C, 28.05; H, 3.70; N, 10.91. Found (%): C, 28.11; H, 3.69; N, 10.86. UV-vis. (acetonitrile): λ_{max}, 616 nm (ε, 114 M^{-1}cm^{-1}). X-Band EPR: g_{av}, 2.060. FT-IR in

KBr: 2927, 1083, 1119, 626 cm^{-1}. Molar conductivity in acetonitrile: Λ_M ($\Omega^{-1}M^{-1}cm^2$), 244. μ_{obs}, 1.56 BM.

Synthesis of complex 4.2

Complex **4.2** was synthesized from $[Cu^{II}(H_2O)_6](ClO_4)_2$ (0.370 g, 1.0 mmol) and $\mathbf{L_{11}}$ (0.213 g, 1.0 mmol). Yield: 0.405 g, ~78%. Elemental Analyses: Calcd.(%) for $CuC_{15}H_{17}N_4O_8Cl_2$: C, 34.90; H, 3.29; N, 10.86. Found (%): C, 34.95; H, 3.27; N, 10.81.UV-vis. (acetonitrile): λ_{max}, 606 nm (ε, 111 $M^{-1}cm^{-1}$). X-Band EPR: g_{av}, 2.042. FT-IR in KBr: 2938, 1086, 1116, 1145, 626 cm^{-1}. Molar conductivity in acetonitrile: Λ_M ($\Omega^{-1}M^{-1}cm^2$), 236. μ_{obs}, 1.51 BM.

Synthesis of complex 4.3

Copper(II)perchlorate hexahydrate, $[Cu(H_2O)_6](ClO_4)_2$ (0.370 g, 1.0 mmol) was dissolved in 20 ml of freshly distilled methanol and to this light blue solution, the ligand $\mathbf{L_{12}}$, (0.449 g, 1.0 mmol), was added drop wise. The color of the solution was changed to light green. The resulting mixture was stirred for 1 h. Then the solution was dried under reduced pressure and the solid mass thus obtained was washed with diethyl ether to afford complex **4.3** as light green solid. Yield: 0.640 g, ~85%. Elemental Analyses: Calcd.(%) for $CuC_{25}H_{30}Cl_2N_5O_{11}S$: C, 40.42; H, 4.03; N, 9.42. Found (%): C, 40.45; H, 4.03; N, 9.38. UV-vis. (methanol): λ_{max}, 805 nm (ε, 63 $M^{-1}cm^{-1}$). FT-IR in KBr: 1081, 625. X-band EPR: g_{av}, 2.07. Molar conductivity in acetonitrile: Λ_M ($\Omega^{-1}M^{-1}cm^2$), 217. μ_{obs}, 1.77 BM.

Synthesis of complex 4.4

Copper(II)chloride dihydrate, $[Cu(H_2O)_2]Cl_2$ (0.170 g, 1.0 mmol) was dissolved in freshly distilled methanol (20 ml) and to this, $\mathbf{L_{13}}$ (0.449 g, 1.0 mmol) was added. The color of the solution changed to light green. The resulting solution was stirred at room temperature for

3 h. Then the volume of the solution was reduced to 5 ml and diethyl ether (15 ml) was added. Storage on freezer for overnight afforded light green precipitate of complex **4.4**. Yield: 0.522g, ~85%. Elemental Analyses: Calcd.(%) for $CuC_{25}H_{26}Cl_2N_4O_2S$: C, 51.68; H, 4.51; N, 9.64. Found (%): C, 51.61; H, 4.48; N, 9.65. UV-vis. (methanol): λ_{max}, 744 nm (ε, 70 $M^{-1}cm^{-1}$). FT-IR in KBr: 2925, 1143, 794 cm^{-1}. X-band EPR: g_{av}, 2.03. Molar conductivity in methanol: Λ_M ($\Omega^{-1}M^{-1}cm^2$), 205. μ_{obs}, 1.52 BM.

Isolation of $L_{10}^{//}$

Complex **4.1** (0.510 g, 1.0 mmol) was dissolved in 10 ml of distilled and degassed acetonitrile (Scheme 4.1). To this solution excess of NO gas was purged for 1 min. and the resulting colorless solution was stirred for 1 h at room temperature. The solvent was then removed under reduced pressure using rotavapor. Water (5 ml) was added to the dried mass followed by the addition of 5 ml of saturated Na_2S solution. The black precipitate of CuS was filtered out. The crude organic part was then extracted from the aqueous layer using $CHCl_3$ (25 ml × 4 portions). The crude product, obtained after removal of solvent, was then purified by column chromatography using neutral alumina column and hexane/ethyl acetate solvent mixture to get the pure $\mathbf{L_{10}^{//}}$. Yield: 0.137 g, 64%. Elemental Analyses: Calcd.(%) for $C_{12}H_{15}N_5O$: C, 58.76; H, 6.16; N, 28.55. Found (%): C, 58.56; H, 6.11; N, 28.23. FT-IR in KBr: 3399, 2926, 1437, 1116, 752 cm^{-1}. ^{1}H-NMR (400 MHz, $CDCl_3$) δ_{ppm}: 2.8 (2H), 3.22 (2H), 3.50 (3H), 3.95 (2H), 6.8-7.15 (4H), 7.55 (1H), 8.22 (1H). ESI-Mass (m+1): Calcd. 246.12; Found, 246.11.

Isolation of $L_{11}^{//}$

$\mathbf{L_{11}^{//}}$ was isolated after the reaction of complex **4.2** (0.513 g, 1.0 mmol) with NO in degassed acetonitrile following the same procedure used for $\mathbf{L_{10}^{//}}$. Yield: 0.134 g, 62%. Elemental Analyses: Calcd.(%) for $C_{13}H_{14}N_4O$: C, 64.45; H, 5.82; N, 23.13. Found (%): C,

64.28; H, 5.77; N, 23.25. FT-IR in KBr: 2924, 2853, 1593, 1436, 1454, 1436, 1128, 760 cm^{-1}. ^{1}H-NMR (400 MHz, $CDCl_3$) δ_{ppm} : 2.94 (2H, t), 3.32 (2H, t), 4.89 (2H, s), 6.91-7.03 (3H, m), 7.13 (1H, t), 7.42 (2H, s), 8.36 (2H, m). ESI-Mass (m+1): Calcd. 243.27; Found, 243.29.

4.5 References

1. Furchgott, R. F. *Angew. Chem. Int. Ed.* **1999**, *38*, 1870.
2. Ignarro, L. J. *Angew. Chem. Int. Ed.* **1999**, *38*, 1882.
3. Murad, F. *Angew. Chem. Int. Ed.* **1999**, *38*, 1856.
4. Bon, C. L. M.; Garthwaite, J. *J. Neurosci.* **2003**, *23*, 1941.
5. Pepicelli, O.; Raiteri, M.; Fedele, E. *Neurochem. Int.* **2004**, *45*, 787.
6. Ignarro, L. J.; Buga, G. M.; Wood, K. S.; Byrns, R. E.; Chaudhuri, G. *Proc. Natl. Acad. Sci. U. S. A.* **1987**, *84*, 9265.
7. Palmer, R. M. J.; Ferrige, A. G.; Moncada, S. *Nature*. **1987**, *327*, 524.
8. Bonomo, R. P.; Pappalardo, G.; Rizzarelli, E.; Santoro, A. M.; Tabbi, G.; Vagliasindi, L. I. *Dalton Trans.* **2007**, 1400.
9. Bonomo, R. P.; Castronovo, B. M. G.; Santoro, A. M. *Dalton Trans.* **2004**, 104.
10. Bonomo, R. P.; Pappalardo, G.; Rizzarelli, E.; Tabb`ı, G.; Vagliasindi, L. I. *Dalton Trans.* **2008**, 3805.
11. Bonomo, R. P.; Di Natale, G.; Rizzarelli, E.; Tabb`ı, G.; Vagliasindi, L. I. *Dalton Trans.* **2009**, 2637.
12. Ostrowski, A. D.; Ford, P. C. *Dalton Trans.* **2009**, 10660.
13. Sortino, S. *Chem. Soc. Rev*. **2010**, *39*, 2903.
14. *Nitric Oxide: Biology and Pathobiology*, ed. Ignarro, L. J. Academic Press, San Diego, **2000**.
15. Butler, A. R.; Williams, D. L. *Chem. Soc. Rev*. **1993**, *22*, 233.

16. *Methods in Nitric Oxide Research*, ed. Feelisch, M.; Stamler, J. S., John Wiley and Sons, Chichester, England, **1996**.

17. Jia, L.; Bonaventura, C.; Bonaventura, J.; Stamler, J. S.; *Nature*. **1996**, *380*, 221.

18. Galdwin, M. T.; Lancaster Jr., J. R.; Freeman, B. A.; Schechter, A. N. *Nat. Med.* **2003**, *9*, 496.

19. Hilderbrand, S. A.; Lim, M. H.; Lippard, S. J. in *Topics in Fluorescence Spectroscopy*, ed. Geddes, C. D.; Lakowicz, J. R. Springer, Berlin, **2005**, p. 163.

20. Sasaki, E.; Kojima, H.; Nishimatsu, H.; Urano, Y.; Kikuchi, K.; Hirata, Y.; Nagano, T. *J. Am. Chem. Soc.* **2005**, *127*, 3684.

21. Nagano, T.; Yoshimura, T. *Chem. Rev.* **2002**, *102*, 1235.

22. Hampl, V.; Walters, C. L.; Archer, S. L. In *Methods in Nitric Oxide Research*; ed. Feelisch, M.; Stamler, J. S. John Wiley & Sons: New York, **1996**; pp 309.

23. Kojima, H.; Nakatsubo, N.; Kikuchi, K.; Kawahara, S.; Kirino, Y.; Nagoshi, H.; Hirata, Y.; Nagano, T. *Anal. Chem.* **1998**, *70*, 2446.

24. Heiduschka, P.; Thanos, S. *Neuro Report.* **1998**, *9*, 4051.

25. Meineke, P.; Rauen, U.; de Groot, H.; Korth, H.-G.; Sustmann, R. *Chem. Eur. J.* **1999**, *5*, 1738.

26. Kojima, H.; Hirotani, M.; Nakatsubo, N.; Kikuchi, K.; Urano, Y.; Higuchi, T.; Hirata, Y.; Nagano, T. *Anal. Chem.* **2001**, *73*, 1967.

27. Gabe, Y.; Urano, Y.; Kikuchi, K.; Kojima, H.; Nagano, T. *J. Am. Chem. Soc.* **2004**, *126*, 3357.

28. Lim, M. H.; Xu, D.; Lippard, S. J. *Nat. Chem. Biol.* **2006**, *2*, 375.

29. Lim, M. H.; Wong, B. A.; Pitcock, Jr., W. H.; Mokshagundam, D.; Baik, M.-H. Lippard, S. J. *J. Am. Chem. Soc.* **2006**, *128*, 14363.

30. Zheng, H.; Shang, G.-Q.; Yang, S.-Y.; X.; Gao, Xu, J.-G.; *Org. Lett.* **2008**, *10*, 2357.

31. Wang, S.; Han, M.-Y.; Huang, D. *J. Am. Chem. Soc.* **2009**, *131*, 11692.

32. Kim, J.-H.; Heller, D. A.; Barone, P. W.; Song, C.; Zhang, J.; Trudel, L. J.; Wogan, G. N.; Tannenbaum, S. R.; Strano, M. S. *Nat. Chem.* **2009**, *1*, 473.

33. Jourdheuil, D. *Free Radical Biol. Med.* **2002**, *33*, 676.

34. Wardman, P. *Free Radical Biol. Med.* **2007**, *43*, 995.

35. Zhang, X.; Kim, W. Hatcher, N.; Potgieter, K.; Moroz, L. L.; Gillette, R.; Sweedler, J. V. *J. Biol. Chem.* **2002**, *277*, 48472.

36. Ye, X.; Rubakhin, S. S.; Sweedler, J. V. *J. Neuroscince. Methods.* **2008**, *168*, 373.

37. Yang, Y.; Seidlits, S. K.; Adams, M. M.; Lynch, V. M.; Schmidt, C. E.; Anslyn, E. V.; Shear, J. B. *J. Am. Chem. Soc.* **2010**, *132*, 13114.

38. Franz, K. J.; Singh, N.; Lippard, S. J. *Angew. Chem. Int. Ed.* **2000**, *39*, 2120.

39. Franz, K. J.; Singh, N.; Spingler, B.; Lippard, S. J. *Inorg. Chem.* **2000**, *39*, 4081.

40. Hilderbrand, S. A.; Lim, M. H.; Lippard, S. J. *J. Am. Chem. Soc.* **2004**, *126*, 4972.

41. Lim, M. H.; Lippard, S. J. *Inorg. Chem.* **2004**, *43*, 6366.

42. Lim, M. H.; Kuang, C.; Lippard, S. J. *ChemBioChem* **2006**, *7*, 1571.

43. Hilderbrand, S. A.; Lippard, S. J. *Inorg. Chem.* **2004**, *43*, 5294.

44. Katayama, Y.; Takahashi, S.; Maeda, M. M. *Anal. Chim. Acta*, **1998**, *365*, 159.

45. Katayama, Y.; Soh, N.; Koide, K.; Maeda, M. *Chem. Lett.* **2000**, *40*, 1152.

46. Soh, N.; Imato, T.; Kawamura, K.; Maeda, M.; Katayama, Y. *Chem. Commun.* **2002**, 2650.

47. Lim, M. H.; Lippard, S. J. *Inorg. Chem.* **2006**, *45*, 8980.

48. Lim, M. H.; Lippard, S. J. *J. Am. Chem. Soc.* **2005**, *127*, 12170.

49. Smith, R. C.; Tennyson, A. G.; Lim, M. H.; Lippard, S. J. *Org. Lett.* **2005**, *7*, 3573.

50. Dı´az, A.; Ortiz, M.; Sa´nchez, I.; Cao, R.; Mederos, A.; Sanchiz, J.; Brito, F. *J. Inorg. Biochem.* **2003**, *95*, 283.

51. Tran, D.; Skelton, B. W.; White, A. H.; Laverman, L. E.; Ford, P. C. *Inorg. Chem.* **1998**, *37*, 2505.

52. Tsuge, K.; DeRosa, F.; Lim, M. D.; Ford, P. C. *J. Am. Chem. Soc.* **2004**, *126*, 6564.

53. Lim, M. H.; Xu, D.; Lippard, S. J. *Nat. Chem. Biol.* **2006**, *2*, 375.

54. Sarma, M.; Singh, A.; Gupta, S. G.; Das, G.; Mondal, B. *Inorg. Chim. Acta.* **2010**, *363*, 63.

55. Sarma, M.; Kalita, A.; Kumar, P.; Singh, A.; Mondal, B. *J. Am. Chem. Soc.* **2010**, *132*, 7846.

56. Mondal, B.; Kumar, P.; Ghosh, P.; Kalita, A. *Chem. Commun*. **2011**, *47*, 2964.

57. Sarma, M.; Mondal, B. *Inorg. Chem*. **2011**, *50*, 3206.

58. Nims, R. W.; Darbyshire, J. F.; Saavedra, J. E.; Christodoulou, D.; Hanbauer, I.; Cox, G. W.; Grisham, M. B.; Laval, F.; Cook, J. A.; Krishna, M. C.; Wink, D. A. *In Methods: A Companion to Methods in Enzymology*; Academic Press: San Diego, CA, **1995**; Vol. 7, pp 48.

59. Khin, C.; Lim, M. D.; Tsuge, K.; Iretskii, A.; Wu, G.; Ford, P. C. *Inorg. Chem.* **2007**, *46*, 9323.

60. Hosino, M.; Maeda, M.; Konishi, R.; Seki, H.; Ford, P. C. *J. Am. Chem. Soc.* **1996**, *118*, 5702.

61. Rhodes, M. R.; Barley, M. H.; Meyer, T. J. *Inorg. Chem*. **1991**, *30*, 629.

62. Reed, C.; Roper, W. J. *Dalton Trans.* **1972**, 1243.

63. Lim, M. H.; Xu, D.; Lippard, S. J. *Nat. Chem. Biol.* **2006**, *2*, 375.

64. SMART, SAINT and XPREP, Siemens Analytical X-ray Instruments Inc., Madison, Wisconsin, USA, **1995**.

65. Sheldrick, G. M. SADABS: software for Empirical Absorption Correction, University of Gottingen, Institut fur Anorganische Chemieder Universitat, Tammanstrasse 4, D-3400 Gottingen, Germany, **1999–2003**.

66. Sheldrick, G. M. SHELXS-97, University of Gottingen, Germany, **1997**.

67. Farrugia, L. J. *J. Appl. Crystallogr.* **1997**, *30*, 565.

68. Tamboura, F. B.; Gaye, M.; Sall, A. S.; Barry, A. H.; Jouini, *Inorg.*T. *Chem. Commun.* **2002**, *5*, 235.

69. Greatti, A.; Scarpellini, M.; Peralta, R. A.; Casellato, A.; Bortoluzzi, A. J.; Xavier, F. R.; Jovito, R.; de Aires, B. M.; Szpoganicz, B.; Tomkowicz, Z.; Rams, M.; Haase, W.; Neves, A. *Inorg. Chem.* **2008**, *47*, 1107.

70. Rojas, D.; Garcı´a, A. M.; Vega, A.; Moreno, Y.; Venegas-Yazigi, D.; Garland, M. T.; Manzur, J. *Inorg. Chem*. **2004**, *43*, 6324.

71. Manzur, J.; Mora, H.; Vega, A.; Venegas-Yazigi, D.; Novak, M. A.; Sabino, J. R.; Paredes-Garcia, V.; Spodine, E. *Inorg. Chem.* **2009**, *48*, 88455.

72. Arora, H.; Lloret, F.; Mukherjee, R. *Inorg. Chem.*, **2009**, *48*, 1158.

73. Canon-Mancisidor, W.; Spodine, E.; Venegas-Yazigi, D.; Rojas, D.; Manzur, J.; Alvarez, S. *Inorg. Chem*. **2008**, *47*, 3687.

Chapter 5

Copper (II) complexes as turn on fluorescent sensors for nitric oxide

Abstract

Two Cu(II) complexes, **5.1** and **5.2**, of two tridentate N-donor ligands, $\mathbf{L_{14}}$ and $\mathbf{L_{15}}$ [$\mathbf{L_{14}}$ = dansyl derivative of *bis*-[3-(dimethylamino)-propyl]amine; $\mathbf{L_{15}}$ = dansyl derivative of dipropylenetriamine] were synthesized and characterized. The quenched fluorescence intensity of complexes **5.1** and **5.2**, in degassed methanol and aqueous (buffered at pH 7.2) solution, was found to reappear on exposure to nitric oxide (NO). This is attributed to the reduction of paramagnetic Cu(II) center by NO to diamagnetic Cu(I).

5.1 Introduction

The detection of NO directly from the living cell has attracted an enormous attention of chemists since it has been identified to play the key roles in a number of physiological processes.[1-3] Fluorescence-based detection techniques are found to be the one satisfying almost all the requirements.[4,5] Fluorescence sensors for NO based on organic molecules did not find extensive application in biological systems as their fluorescence response depends on their oxidation products.[4,5] On the other hand, fluorophore-displacement strategy has been used for transition-metal complexes based NO sensors; however, the low sensitivity and water insolubility of these complexes precluded their application.[4] A number of iron complexes were reported to sense NO in aqueous medium; but some of them exhibit diminished fluorescence, which is not desirable for biological applications.[6] In addition, iron complexes which show fluorescence enhancement, are air sensitive and exhibit only modest turn-on emission with NO.[7] These difficulties essentially prevent the applications of iron complexes as NO sensor. On the other hand, the reduction of Cu(II) to Cu(I) by NO can offer a methodology for its detection.

In recent times, a number of metal complexes have been exemplified as direct fluorescent NO sensors. These exhibited fluorescence enhancement due to the fluorophore displacement by NO from the metal center.[8-12] However, this strategy for the direct detection of NO is mostly found to be compatible only with organic solvents. In aqueous environment, fluorescence turn-on/enhancement may arise from the replacement of the fluorophore ligand from the metal centre by water itself. Thus, the strategy of reduction of a metal centre by NO with a concomitant fluorescence enhancement has been adopted. The fluorescence intensity of fluorescent ligand is known to be quenched on coordination to Cu(II) centre. The reduction of Cu(II) by NO to diamagnetic Cu(I) is expected to restore the quenched fluorescence of a ligand

fluorophore.[13] The reduction of Cu(II) center to Cu(I) by NO has been reported earlier in Cu(II) dithiocarbamate, Cu(II)-phen or dmp (phen = 1,10-phenanthroline; dmp = 2,9-dimethyl-1,10-phenanthroline) complexes.[14] Recently, Cu(II) complexes of various amine ligands have also been reported to undergo reduction by NO.[15c]

This strategy has been adopted by Ford et al in their report of Cu(II) complexes of *bis*(2-(3,5-dimethyl-1-pyrazolyl)ethyl)-ammine) (pza) with appended Ru(II) and Re(I) luminophores as possible luminescent sensor for NO; though these were found to be too labile to be a practical sensor.[16] On the other hand, this strategy indeed found to work in the reaction of NO with $[Cu^{II}(DAC)]^{2+}$ [DAC is the N-derivatizedcyclam-1,8-*bis*(anthracen-9-ylmethyl)-1,4,8,11-tetraazacyclotetradecane].[17] However, the reaction was found to be too slow under near neutral condition to use for sensor. In addition, in this case, the reduction of Cu(II) centre by NO was found to result in the simultaneous formation of N-nitrosamine due to the nitrosation of the coordinated amine.

Lippard's group used the same strategy to develop copper complex based NO sensors. They reported the examples of Cu(II) complexes of anthracenyl and dansyl fluorophore ligands.[11,18] The quenched fluorescence intensity of the ligand fluorophore was observed to restore in presence NO in methanol/dichloromethane solutions of the complexes. In addition, $[Cu(Ds\text{-}en)_2]$ and $[Cu(Ds\text{-}AMP)_2]$, where Ds-en and Ds-AMP are the conjugate bases of dansylethylenediamine (Ds-Hen) and dansyl aminomethylpyridine (Ds-HAMP), respectively, have found to detect NO in aqueous solution, also.[11b] However, these compounds were unable to sense NO at a physiologically more relevant pH.[11b] Xiang et al also reported an example utilizing this approach.[19] In all these cases except $[Cu(Ds\text{-}en)_2]$ and $[Cu(Ds\text{-}AMP)_2]$, it has been observed that demetallation of the fluorophore ligands takes place after the reduction.[18]

An important report from the Lippard's group described the direct imaging of NO in

cell using Cu(II) complexes of fluoresceine-based ligands.[12b] In the reaction of NO with the Cu(II) complex to generate NO(I) which immediately reacts with the fluoresceine-based ligands to result in the nitrosated ligand which then released from the Cu(I) center with a substantial turn-on fluorescence. Another example of similar mechanism based NO imaging also reported from the Lippard's group.[12c]

In chapter 4, two examples of Cu(II) complex-based fluorescent NO sensor for methanol and water medium buffered at pH ~7.2 have been reported.[20] It is important to note here that in these cases no ligand nitrosation was observed. However, these have not been found to behave as turn on/off sensors; perhaps, because of the demetallation of the ligand after reduction followed by undefined product formation during air oxidation of the reduced Cu(I).[21]

In this direction we have studied the NO reactivity of two Cu(II) complexes of ligands **L_{14}** and **L_{15}** having pendant dansyl fluorophore, respectively have been studied.

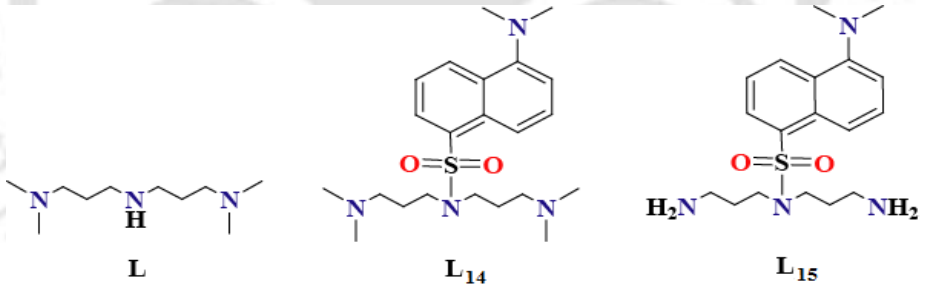

Figure 5.1

Karlin's group reported earlier that the parent tridentate triamine ligand, **L** forms Cu(I) complex with a distorted trigonal planar geometry.[22] Thus, it is assumed that after the reduction of Cu(II) by NO, demetallation of the ligands will not occur.

5.2 Results and discussion

The ligands, **L_{14}** and **L_{15}** were prepared by incorporating the dansyl fluorophore on the secondary amine position of *bis*-[3-(dimethylamino)-propyl]amine and

dipropylenetriamine, respectively (Schemes 5.1 and 5.2, respectively; experimental section).

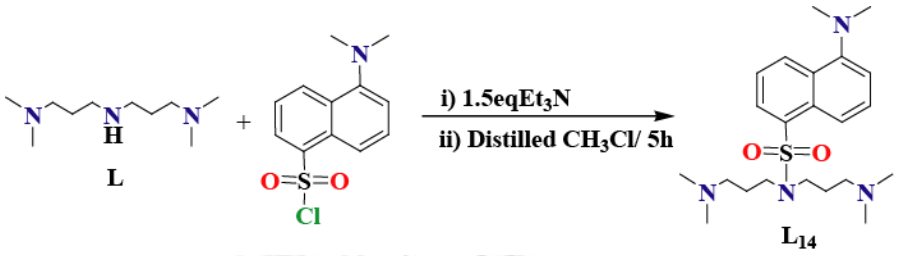

Scheme 5.1

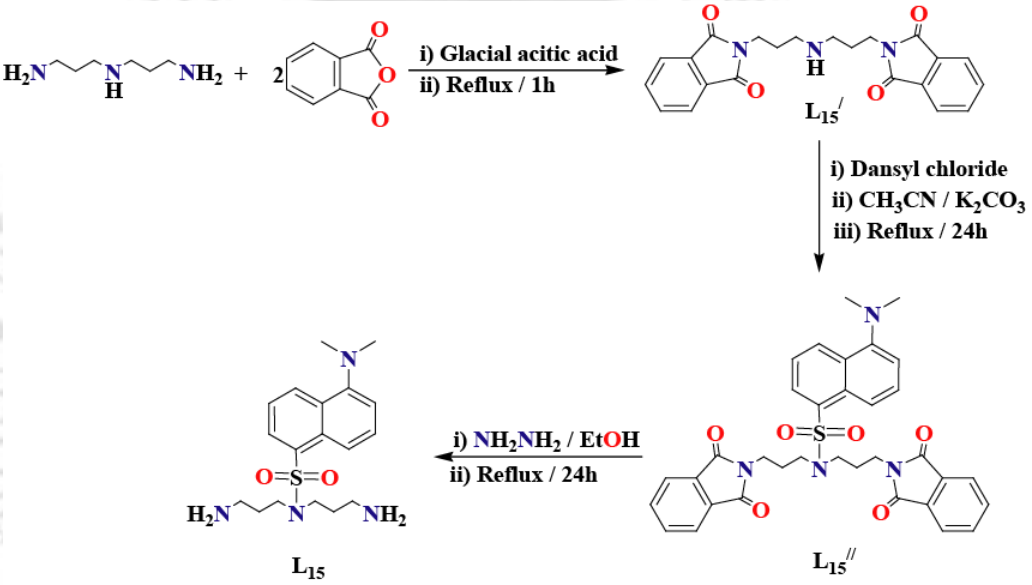

Scheme 5.2

They were characterized by elemental analyses as well as various spectroscopic methods (experimental section). The complexes were prepared by stoichiometric reaction of Cu(II) chloride dihydrate with the respective ligands in methanol and characterized by UV-visible, FT-IR, Mass, EPR spectroscopic analyses. The microanalysis are also in well agreement with the calculated values (experimental section). Even after several attempts to grow X-ray quality crystals of the complexes, we have failed.

Nitric oxide reactivity

Ligand $\mathbf{L_{14}}$ was found to display modest fluorescence emission upon excitation at 340 nm in methanol solution at room temperature. The quantum yield was calculated to be 0.1845 with respect to quinine sulphate in methanol at room temperature. Addition of equivalent amount of Cu(II) ion into the methanol solution of $\mathbf{L_{14}}$ has been found to display significant (> 80%) quenching in fluorescence spectroscopic studies at 298 K (Figure 5.2a). On the other hand, addition of 10 equivalent of NO to the degassed methanol solution of complex **5.1** was found to restore the emission intensity significantly (Figure 5.2b). The quenching of fluorescence intensity of ligand $\mathbf{L_{15}}$ in methanol was observed upon addition of Cu(II) ion (Appendix IV, Figure A4.26). Addition of NO to the methanol solution of complex **5.2** restored the quenched intensity of $\mathbf{L_{15}}$ in fluorescence spectroscopy at room temperature (Appendix IV, Figure A4.27). The restored intensity in the complexes **5.1** and **5.2** starts appearing within 20 seconds of NO addition and become 5.61(± 0.2) and 6.30(± 0.3) fold, respectively, within 10 minutes of addition of NO.

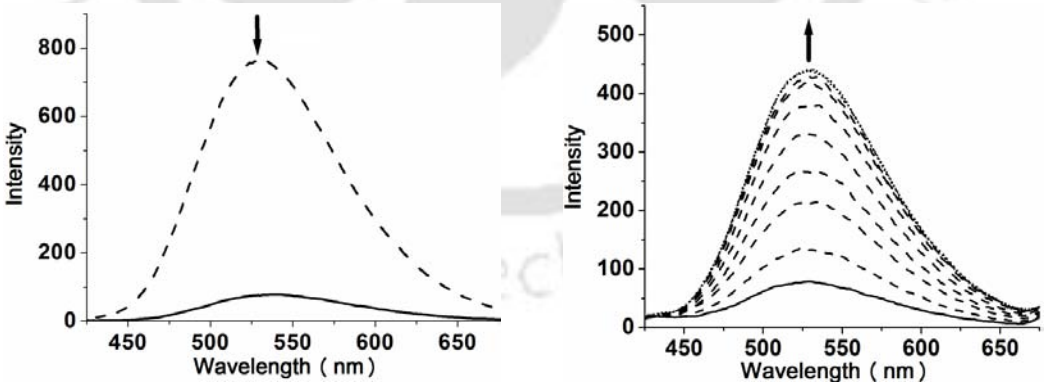

(a) (b)

Figure 5.2 Fluorescence responses (λ_{ex}, 340 nm) of 20 μM deoxygenated methanol solution of (a) free ligand, $\mathbf{L_{14}}$ (dashed line) and after addition of one equivalent of $CuCl_2$ (solid line); (b) complex **5.1** (solid) before and after purging of 10 equivalent of NO (dashed lines) at 1, 2, 3, 4, 5, 7 and 8 minutes at 298 K.

In cases of complexes [Cu(Ds-en)$_2$] and [Cu(Ds-AMP)$_2$], addition of 100 equivalent of NO to the degassed buffered aqueous or methanol solution of the complexes was reported to restore the emission intensity and the respective enhancements in integrated fluorescence were 6.1(±0.2)- and 8.8(±0.1)-fold, respectively.[11b] In our earlier reports with [Cu(Ds-mpea)(X)]$^{2+}$ and [Cu(Ds-pepm)(X)]$^{2+}$ [Ds-mpea = 5-dimethylamino-naphthalene-1-sulfonic acid (1-methyl-1H-imidazol-2-ylmethyl)-(2-pyridin-2-yl-ethyl)-amide; Ds-pepm = 5-dimethylamino-naphthalene-1-sulfonicacid(2-pyridin-2-yl-ethyl)-pyridin-2-yl-methyl-amide; X = solvent] the restored emission intensities were found to be 12.5 (±0.2)- and 6.7(±0.2)-fold in methanol solutions, respectively.[20] In the present study, the complexes were found to display fluorescence enhancement for as low as 1μM of NO.

The fluorescence enhancement in the present cases are mostly attributed to the formation of Cu(I) species after reduction of Cu(II) center by NO (Scheme 5.3). This has been confirmed by the UV-visible, X-band EPR and ^{1}H-NMR spectroscopic studies.

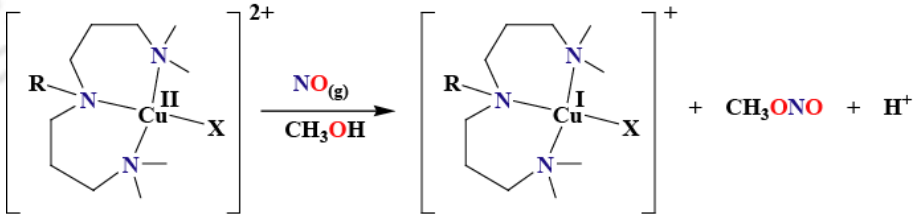

R = Dansyl group; X = CH_3OH

Scheme 5.3

The *d-d* band at 720 nm of complex **5.1** in the electronic spectrum in methanol was found to disappear after addition of NO into the solution (Figure 5.3). This is attributed to the complete reduction of Cu(II) centre to Cu(I).[15] The reduction of Cu(II) centre by NO has been reported to proceed though the formation of [Cu^{II}-NO] intermediate in

various examples.[15, 20b] However, no indication of formation of the [Cu^{II}-NO] intermediate in the present case was observed in UV-visible study. Even in solution FT-IR studies, no stretching band corresponding to ν_{NO} was observed.[15]

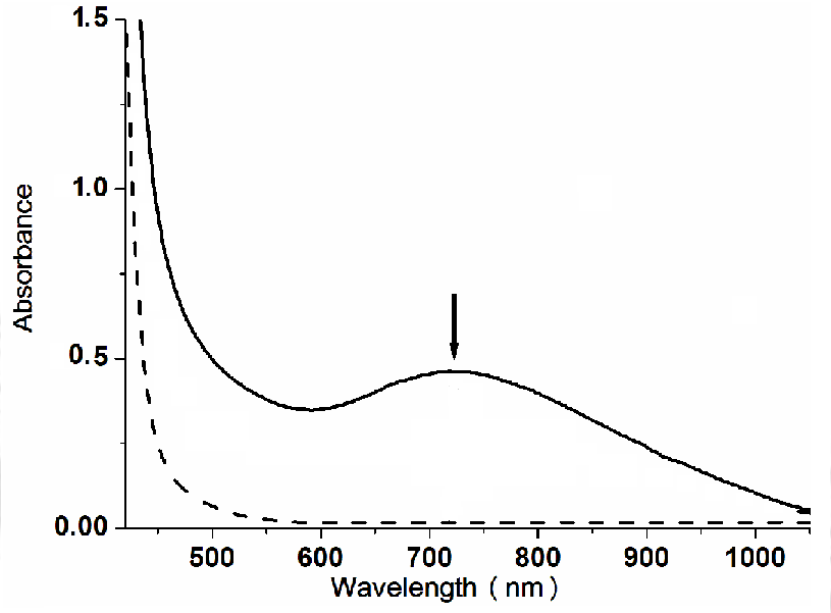

Figure 5.3 UV-visible spectra of complex **5.1** in methanol before (solid line) and after purging NO (dashed line) indicating reduction of Cu(II) to Cu(I).

With $[Cu(dmp)_2(H_2O)]^{2+}$ and $[Cu(phen)_2(H_2O)]^{2+}$, even at the early stage of mixing no spectral change for the inner-sphere complex formation was reported.[23] In cases of $[Cu(Ds\text{-}mpea)(X)]^{2+}$ and $[Cu(Ds\text{-}pepm)(X)]^{2+}$ also, the inner-sphere complex formation was not found.[20] These are attributed to the very less equilibrium constant, K_{NO} values. The complete reduction of Cu(II) in presence of NO has been further supported by the EPR silent nature of the reaction mixture in the X-band EPR study at room temperature (Figure 5.4).[15] The appearance of sharp signal in the ^{1}H-NMR spectrum after the reaction of complex **5.1** with NO also in agreement with the reduction of Cu(II) centre to Cu(I) (Appendix IV, Figure A4.28).

In case of complex **5.2**, the *d-d* band at 758 nm was found to diminished after addition of NO (Appendix IV, Figure A4.29) which is an indication of the reduction of Cu(II)

center to Cu(I) by NO. X-band EPR and ^{1}H-NMR spectroscopic studies also suggest the reduction (Appendix IV, Figures A4.30 and A4.32).

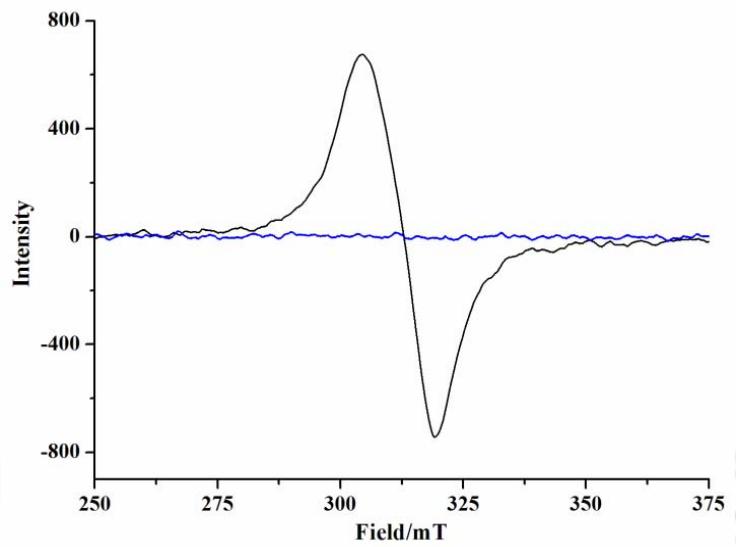

Figure 5.4 X-band EPR spectra of complex **5.1** before (black) and after (blue) purging NO in methanol at room temperature.

Lippard's group reported that in case of Ds-HAMP ligand, the fluorescence enhancement is essentially because of both the formation of Cu(I) species and dissociation of the sulphonamide functionality following protonation by H^+ formed in the reaction (Scheme 5.3).[11b]

They observed the presence of sulphonamide group ($\nu_{N\text{-}H} \approx 3083$ cm^{-1} in KBr) in the FT-IR spectrum of the reaction product which indicates that ligand protonation also occurs. It has been anticipated that the protonated sulfonamide group may be contributing to the fluorescence intensity.[11b] In cases of $[Cu(Ds\text{-}mpea)(X)]^{2+}$ and $[Cu(Ds\text{-}pepm)(X)]^{2+}$, we have not observed the dissociation of sulphonamide group. In the present case also, there was no indication of the dissociation of sulphonamide group in the FT-IR spectrum of the reaction mixture (Appendix IV, Figures A4.33 and A4.34). Hence, the reappearance of the fluorescence intensity is attributed only to the reduction of Cu(II) center to the diamagnetic Cu(I) by NO. It is also important to note

that no N-nitrosamine or [Cu^{II}-NO] frequency was observed in the FT-IR spectrum of the reaction mixture which can be attributed to the reaction of NO^+, formed during the reaction of Cu(II) with NO, with methanol solvent to form CH_3ONO and H^+.[11b,23] In fact, the formation of the CH_3ONO has been observed GC-Mass spectral studies (Appendix IV, Figure A4.36). ^{1}H-NMR spectral studies revealed that after reduction the Cu(I) remains coordinated to the ligand (Appendix IV, Figures A4.28 and A4.32). However, in earlier examples because of geometrical constrain most of the cases, the Cu(I) centres were found to be separated from the ligand frameworks.

It would be worth mentioning here that the quenched fluorescence intensity of complexes **5.1** and **5.2** in an aqueous solution buffered at pH ~7.2 by TRIS-HCl buffer was found to restore upon addition of 10 equivalent NO within 10 minutes (Figure 5.5 and Appendix IV, Figure A4.35). The intensity of the restored emission, in both the cases, was found to be less compared to that in methanol. In cases of [Cu(Ds-mpea)(X)]$^{2+}$ and [Cu(Ds-pepm)(X)]$^{2+}$, similar results were reported.[20]

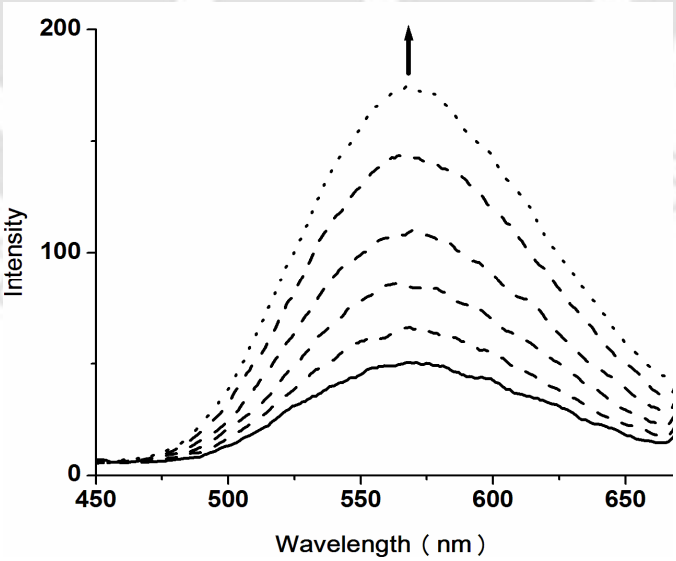

Figure 5.5 Fluorescence responses (λ_{ex}, 340 nm) of 20μM of complex **5.1** in aqueous (pH 7.2; tris-buffer) before (solid line) and after purging of 10 equivalent of NO (doted lines) at 1, 2, 3, 5 and 10 minutes, respectively, at 298 K.

The reappearance of the fluorescence intensity in the buffered aqueous solution is attributed to both the reduction of Cu(II) to Cu(I) as no dissociation of the sulphonamide group following protonation by H^+ formed in the reactions was evidenced from the FT-IR spectrum of the reaction mixture.[20] The ESI-mass of the reaction mixtures also suggest the presence of $\mathbf{L_{14}}$ and $\mathbf{L_{15}}$ in un-dissociated form (Appendix IV, Figures A4.37 and A4.38).

5.3 Conclusion

In conclusion, two Cu(II) complexes, **5.1** and **5.2** have been prepared with a tridentate N-donor ligands having a pendant dansyl fluorophore. Addition of NO to methanol solution of the complexes resulted in the reduction of Cu(II) centre to Cu(I) with a substantial increase in fluorescence intensity. Thus the complexes can act as fluorescence-based NO sensor in methanol. In aqueous solutions (buffered at pH ~7.2) of complexes **5.1** and **5.2**, the quenched fluorescence intensity was observed to be restored upon addition of NO. The reappearance of the fluorescence intensity in both the cases were attributed to the reduction of Cu(II) to diamagnetic Cu(I).

5.4 Experimental Section

5.4.1 Materials and methods

All reagents and solvents were purchased from commercial sources and were of reagent grade. Acetonitrile was distilled from calcium hydride. Deoxygenation of the solvent and solutions were effected by repeated vacuum/purge cycles or bubbling with N_2 for 30 minutes. NO gas was purified by passing through KOH and P_2O_5 column. UV-visible spectra were recorded on a Perkin Elmer Lambda 25 spectrophotometer. FT-IR spectra of the solid samples were taken on a Perkin Elmer spectrophotometer with samples prepared as KBr pellets. The fluorescence spectra were recorded in solution in Varian Cary Eclipse Fluorescence Spectrophotometer at room temperature. Quinine sulfate in acidic medium

was used as the reference compound for the determination of fluorescence quantum yield. Solution electrical conductivity was checked using a Systronic 305 conductivity bridge. ^{1}H-NMR spectra were obtained with a 400 MHz Varian FT spectrometer. Chemical shifts (ppm) were referenced either with an internal standard (Me_4Si) or to the residual solvent peaks. The X-band Electron Paramagnetic Resonance (EPR) spectra were recorded on a JES-FA200 ESR spectrometer, at room temperature. Elemental analyses were obtained from a Perkin Elmer Series II Analyzer. The magnetic moment of complexes is measured on a Cambridge Magnetic Balance.

5.4.2. Synthesis of ligands

Synthesis of L_{14}

The fluorescent ligand **L_{14}** was prepared by the incorporation of the dansyl group in *bis*-{3-(dimethylamino)-propyl}amine. This has been effected by stirring an equimolar mixture of *bis*-{3-(dimethylamino)-propyl}amine (1.87 g, 10 mmol) and dansyl chloride (2.69 g, 10 mmol) in presence of 1.5 equivalent of triethylamine in distilled chloroform (20 ml) for 5 h at room temperature. The resulting solution was then dried under reduced pressure in rotavapour and the greenish yellow fluorescent mass thus obtained was subjected to column chromatographic purification to result into the pure greenish yellow fluorescent ligand, **L_{14}**. Yield: 3.25 g, ~78%. Elemental analyses for $C_{22}H_{36}N_4O_2S$: Calcd. (%): C, 62.82; H, 8.63; N, 13.23. Found (%): C, 62.80, H 8.63, N, 13.18. FT-IR in KBr: 2944, 2829, 1464, 1310, 1140, 789 cm^{-1}. ^{1}H-NMR (400 MHz, $CDCl_3$) δ_{ppm}: 1.69-1.76 (4H), 2.18 (12H), 2.23-2.27 (4H), 2.83 (6H), 3.31-3.34 (4H), 7.12-1.14 (1H), 7.45-7.53 (2H), 8.12-8.13 (1H), 8.19-8.21 (1H), 8.48-8.50 (1H). ^{13}C-NMR (100 MHz, $CDCl_3$) δ_{ppm}: 26.2, 45.1, 45.2, 45.3, 56.6, 115.0, 119.5, 123.0, 127.8, 129.5, 129.9, 130.1, 135.1 and 151.6. ESI-Mass (m+1): Calcd. 421.26; Found, 421.13. Quantum yield of **L_{14}** is 0.1845 at 298 K in methanol.

Synthesis of L_{15}

The ligand **L_{15}** has been synthesized from the parent dipropylenetriamine in a three step process described below (Scheme 5.3).

Step I: Synthesis of 1,7-phthalimido-4-azaheptane ($L_{15}^{/}$)

1,7-phthalimido-4-azaheptane was prepared from the reaction of dipropylenetriamine (2.62 g, 0.02 mol) and phthalic anhydride (6.0 g, 0.04 mol) following the reported procedure.[24] Yield: 6.24 g, ~80%. Elemental analyses for $C_{22}H_{21}N_3O_4$: Calcd. (%): C, 67.51; H, 5.41; N, 10.73. Found (%): C, 67.55; H, 5.40; N, 10.80. FT-IR in KBr: 2932, 1710, 1404, 1039, 730 cm^{-1}. ^{1}H-NMR (400 MHz, $CDCl_3$) δ_{ppm}: 1.89-1.95(4H), 2.70-2.73 (4H), 3.73-3.76 (4H), 7.67-7.70 (4H) and 7.77-7.81 (4H). ^{13}C-NMR: (100 MHz, $CDCl_3$) δ_{ppm}: 31.0, 35.5, 46.0, 123.4, 132.1, 134.1 and 168.5. ESI-Mass (m+1): Calcd. 392.13; Found, 392.15.

Step II: Synthesis of 4-dansyl-1,7- diphthalimido-4-azaheptane ($L_{15}^{//}$)

A mixture of 1,7-phthalimido-4-azaheptane (0.782 g, 2 mmol), dansyl chloride (0.624 g, 2.3 mmol) and K_2CO_3 (0.313 g, 2.4 mmol) was dissolved in 50 ml of dry acetonitrile. The mixture was refluxed for 24 h under a nitrogen atmosphere. After filtration, the solvent was removed on a rotary evaporator under reduced pressure. The resulting residue was mixed with 15 ml of water and extracted with chloroform (20 ml × 3 portions). The organic phase was dried with anhydrous sodium sulfate and evaporation of the solvent on rotary evaporator resulted in light yellow oil. 4-dansyl-1,7- diphthalimido-4-azaheptane was obtained as precipitate on stirring the light yellow oil with 10 ml cold ethanol. The precipitated product was filtered and washed with cold ethanol (10 ml). Yield: 0.562 g, ~45%. Elemental analyses for $C_{34}H_{32}N_4SO_6$: Calcd. (%): C, 65.37; H, 5.16; N, 8.97. Found (%): C, 65.33; H, 5.16; N, 9.03. FT-IR in KBr: 2938, 1712, 1398, 1137, 720 cm^{-1}. ^{1}H-

NMR (400 MHz, $CDCl_3$) δ_{ppm}: 1.82-1.89(4H), 2.83 (6H), 3.33-3.37 (4H), 3.53- 3.57 (4H), 7.10-1.12 (1H), 7.32-7.36(1H), 7.48-7.52(1H) , 7.65-7.69(4H), 7.74-7.79(4H), 8.07-8.09(1H), 8.21-8.23(1H), 8.42-8.44(1H). ^{13}C-NMR (100 MHz, $CDCl_3$) δ_{ppm}: 27.4, 35.5, 44.9, 45.4, 115.3, 119.4, 123.0, 123.3, 128.3, 129.8, 130.0, 130.5, 132.1, 134.0, 134.5, 151.8 and 168.1. ESI-Mass (m+1): Calcd. 625.20; Found, 625.04.

Step III: Hydrolysis of 4-dansyl-1,7- diphthalimido-4-azaheptane to yield ligand L_{15}

A mixture of 4-dansyl-1,7- diphthalimido-4-azaheptane (0.5 g, 0.8 mmol) and hydrazine monohydrate (0.8 g, 16 mmol) was dissolved in 40 ml of ethanol. The mixture was refluxed for 24 h under a nitrogen atmosphere. The mixture was filtered and the filtrate was dried to crude mass. This was dissolved in 50 ml of water and extracted with chloroform (3 × 50 ml portions). The collected organic layer was dried to get the crude product which upon purification by column chromatography yields **L_{15}**. Yield: 0.160 g, ~55%. Elemental analyses for $C_{18}H_{28}N_4SO_2$: Calcd. (%): C, 59.31; H, 7.74; N, 15.37. Found (%): C, 59.36; H, 7.73; N, 15.44. FT-IR in KBr: 2931, 1572, 1315, 1138, 791, 623, 570 cm^{-1}. ^{1}H-NMR (400 MHz, CD_3OD) δ_{ppm}: 1.55-1.62(4H) 2.58-2.62 (4H), 2.82 (6H), 3.27-3.31 (4H), 7.17-7.19 (1H), 7.48-7.52 (2H), 8.06-8.08 (1H) , 8.18-8.20 (1H), 8.48-8.50 (1H). ^{13}C-NMR (100 MHz, $CDCl_3$) δ_{ppm}: 31.4, 38.8, 44.7, 45.3, 115.1, 119.3, 123.0, 127.9 129.1, 129.9, 130.0, 130.1, 135.1 and 151.6. ESI-mass (m+1): Calcd. 365.19; Found, 365.10. Quantum yield of **L_{15}** is 0.1731 in methanol at 298 K.

5.4.3. Synthesis of complexes:

Complexes **5.1** and **5.2** were synthesized using same experimental protocol. The details are given for complex **5.1**.

Synthesis of complex 5.1:

Copper(II) chloride dihydrate, $[Cu(H_2O)_2]Cl_2$ (0.065 g, 0.5 mmol) was dissolved in 10 ml of freshly distilled methanol and to this light blue solution, the ligand **L_{14}**, (0.210 g, 0.5 mmol), was added. The color of the solution was changed to light green. The resulting mixture was stirred for 3 h. The volume of the solution was reduced to 5 ml under reduced pressure and diethyl ether (10 ml) was added and kept at -20 °C for 12 h to afford complex **5.1** as light green precipitate. Yield: 0.225 g, ~80%. Elemental analyses for $\{[(L_{14})Cu(CH_3OH)]Cl_2.2H_2O\}$, $CuC_{23}H_{44}N_4SO_5Cl_2$: Calcd. (%): C, 44.33; H, 7.11; N, 8.99. Found (%): C, 44.37, H 7.10, N, 9.06. UV-vis. (methanol): λ_{max}, 720 nm (ε, 40 M^{-1} cm^{-1}). X-band EPR: g_{av}, 2.21. FT-IR in KBr: 2961, 1319, 1150, 714 cm^{-1}. Molar conductance in methanol: Λ_M ($\Omega^{-1}M^{-1}cm^2$), 212. μ_{obs}, 1.66 BM.

Synthesis of complex 5.2:

It has been synthesised from Cu(II)chloride dihydrate (0.085 g, 0.5 mmol) and **L_{15}** (0.183 g, 0.5 mmol). Yield: 212, mg ~85%. Elemental analyses for $[(L_{15})Cu(CH_3OH)]Cl_2.H_2O$, $CuC_{19}H_{34}N_4SO_4Cl_2$: Cacld. (%): C, 41.56; H, 6.24; N, 10.20. Found (%): C, 41.52; H, 6.24; N, 10.24. UV-vis. (methanol): λ_{max}, 758 nm (ε, 47 M^{-1} cm^{-1}). X-band EPR: g_{av}, 2.18. FT-IR in KBr: 1323, 1137, 781, 3110, 2961 cm^{-1}. Molar conductance in methanol: Λ_M ($\Omega^{-1}M^{-1}cm^2$), 223. μ_{obs}, 1.49 BM.

5.5 References

1. a) Furchgott, R. F. *Angew. Chem. Int. Ed.* **1999**, *38*, 1870. b) Ignarro, L. J.; Buga, G. M.; Wood, K. S.; Byrns, R. E.; Chaudhuri, G. *Proc. Natl. Acad. Sci. U. S. A.* **1987**, *84*, 9265. c) Palmer, R. M. J.; Ferrige, A. G.; Moncada, S. *Nature.* **1987**, *327*, 524.
2. a) *Nitric Oxide: Biology and Pathobiology*, Ed: Ignarro, L. J. Academic Press, San Diego, **2000**. b) Moncada, S.; Palmer, R. M. J.; Higgs, E. A. *Pharmacol. Rev*. **1991**, *43*, 109. c) Butler, A. R.; Williams, D. L. *Chem. Soc. Rev*. **1993**, *22*, 233.
3. a) *Methods in Nitric Oxide Research*, Eds: Feelisch, M.; Stamler, J. S., John Wiley and Sons; Chichester, England, **1996**. b) Jia, L.; Bonaventura, C.; Bonaventura, J.; Stamler, J. S. *Nature*. **1996**, *380*, 221. c) Galdwin, M. T.; Lancaster, Jr., J. R.; Freeman, B. A.; Schechter, A. N. *Nat. Med*. **2003**, *9*, 496.
4. a) Nagano, T.; Yoshimura, T. *Chem. Rev*. **2002**, *102*, 1235. b) Hilderbrand, S. A.; Lim, M.-H.; Lippard, S. J. In *Topics in Fluorescence Spectroscopy*, Eds: Geddes, C. D.; Lakowicz, J. R. Spinger: Berlin, **2005**, 163.
5. Sasaki, E.; Kojima, H.; Nishimatsu, H.; Urano, Y.; Kikuchi, K.; Hirata, Y.; Nagano, T. *J. Am. Chem. Soc.* **2005**, *127*, 3684.
6. a) Katayama, Y.; Takahashi, S.; Maeda, M. *Anal. Chim. Acta.* **1998**, *365*, 159. b) Katayama, Y.; Soh, N.; Koide, K.; Maeda, M. *Chem. Lett.* **2000**, 1152.
7. Soh, N.; Imato, T.; Kawamura, K.; Maeda, M.; Katayama, Y. *Chem. Commun.* **2002**, 2650.
8. a) Franz, K. J.; Singh, N.; Lippard, S. J. *Angew. Chem. Int. Ed.* **2000**, *39*, 2120. b) Franz, K. J.; Singh, N.; Spingler, B.; Lippard S. J. *Inorg. Chem.* **2000**, *39*, 4081.
9. a) Hilderbrand, S. A.; Lippard S. J. *Inorg. Chem.* **2004**, *43*, 4674. b) Lim, M. H.; Lippard S. J. *Inorg. Chem.* **2004**, *43*, 6366.

10. a) Hilderbrand, S. A.; Lim, M. H.; Lippard, S. J. *J. Am. Chem. Soc.* **2004**, *126*, 4972. b) Hilderbrand, S. A.; Lippard, S. J. *Inorg. Chem.* **2004**, *43,* 5294.

11. a) Lim, M. H.; Kuang, C.; Lippard, S. J. *Chem. Bio. Chem.* **2006**, *7*, 1571. b) Lim, M. H.; Lippard, S. J. *J. Am. Chem. Soc.* **2005**, *127*, 12170.

12. a) Smith, R. C.; Tennyson, A. G.; Lim, M. H.; Lippard, S. J. *Org. Lett.* **2005**, *7*, 3573. b) Lim, M. H.; Xu, D.; Lippard, S. J. *Nat. Chem. Biol.* **2006**, *2*, 375. c) McQuade, L. E.; Ma, J.; Lowe, G.; Ghatpande, A.; Gelperin, A.; Lippard, S. J. *Proc. Natl. Acad. Sci. USA*, **2010**, *107*, 8525.

13. Lim, M. H.; Wong, B. A.; Pitcock, Jr., W. H.; Mokshagundam, D.; Baik, M.; Lippard, S. J. *J. Am. Chem. Soc*. **2006**, *128*, 14364.

14. a) Dıaz, A.; Ortiz, M.; Sanchez, I.; Cao, R.; Mederos, A.; Sanchiz, J.; Brito, F. *J. Inorg*. *Biochem.* **2003**, *95*, 283. b) Tran, D.; Skelton, B. W.; White, A. H.; Laverman, L. E.; Ford, P. C. *Inorg. Chem.* **1998**, *37*, 2505.

15. a) Sarma, M.; Singh, A.; Gupta, S. G.; Das G.; Mondal, B. *Inorg. Chim. Acta*, **2010**, *363*, 63. b) Sarma, M.; Kalita, A.; Kumar, P.; Singh, A.; Mondal, B. *J. Am. Chem. Soc*. **2010**, *132*, 7846. c) Sarma, M.; Mondal, B. *Inorg. Chem*. **2011**, *50*, 3206. d) Kalita, A.; Kumar, P.; Deka, R. C.; Mondal, B. *Inorg. Chem.*, **2011**, *50*, 11868. e) Sarma, M.; Mondal, B. *Dalton Trans*. **2012**, *41*, 2927.

16. Riklin, M.; Tran, D.; Bu, X.; Laverman, L. E.; Ford, P. C. *Dalton Trans*. **2001**, 1813.

17. a) Tsuge, K.; DeRosa, F.; Lim, M. D.; Ford, P. C. *J. Am. Chem. Soc*. **2004**, *126*, 6564. b) Khin, C.; Lim, M. D.; Tsuge, K.; Iretskii, A.; Wu, G.; Ford, P. C. *Inorg. Chem*. **2007**, *46*, 9323.

18. Lim, M. H.; Lippard, S. J. *Inorg. Chem*. **2006**, *45*, 8980.

19. Xing, C.; Wang, M.; Yu, S.; Shi, Z.; Li, Y.; Zhu, D. *Macromol. Rapid Commun.* **2007**, *28*, 241.

20. a) Mondal, B., Kumar, P.; Ghosh, P.; Kalita, A. *Chem. Commun*. **2011**, *47*, 2964. b) Kumar, P.; Kalita, A.; Mondal, B. *Dalton Trans.* **2011**, *40*, 8656.

21. a) Halfen, J. A.; Mahapatra, S.; Wilkinson, E. C.; Kaderli, S.; Young, Jr., V. G.; Que, Jr., L.; A. Zuberbhler, D.; Tolman, W. B. *Science.* **1996**, *271*, 1397. b) Holland, P. L.; Tolman, W. B. *Coord. Chem. Rev*. **1999**, *190-192*, 855. c) Mahadevan, V.; Henson, M. J.; Solomon, E. I.; Stack, T. D. P. *J. Am. Chem. Soc.* **2000**, *122*, 10249. d) Mahadevan, V.; Hou, Z.; Cole, A. P.; Root, D. E.; Lal, T. K.; Solomon, E. I.; Stack, T. D. P. *J. Am. Chem. Soc.* **1997**, *119*, 11996.

22. Liang, H. C.; Zhang, C. X.; Henson, M. J.; Sommer, R. D.; Hatwell, K. R.; Kaderli, S.; Zuberbuhler, A. D.; Rheingold, A. L.; Solomon, E. I.; Karlin, K. D. *J. Am. Chem. Soc*. **2002**, *124*, 4170.

23. Searle, G. H.; Lincoln, S. F.; Teague, S. G.; Rowe, D. G. *Aust, J. Chem*. **1979**, *32*, 519.

24. Tran, D.; Skelton, B. W.; White, A. H.; Laverman, L. E.; Ford, P. C. *Inorg. Chem.* **1998**, *37*, 2505.

Lists of publications

1. **'Nitric oxide reactivity of Cu(II) complexes of tetra- and pentadentate ligands: structural influence in deciding the reduction pathway.**

Kumar, P.; Kalita, A.; Mondal, B. *Dalton Trans.* **2013**, DOI:10.1039/C3DT32580F.

2. **Copper(II) complexes as turn on fluorescent sensors for nitric oxide**

Kumar, P.; Kalita, A.; Mondal, B. *Dalton Trans*. **2012**, *41*, 10543.

3. **DNA binding, nuclease activity and cytotoxicity studies of Cu(II) complexes of tridentate ligands**

Kumar, P.; Gorai, S.; Santra, M. K.; Mondal, B.; Manna, D. *Dalton Trans.* **2012**, *41*, 7573.

4. **Reaction of a copper(II)–nitrosyl complex with hydrogen peroxide: putative formation of a copper(I)–peroxynitrite intermediate**

Kalita, A.; Kumar, P.; Mondal, B. *Chem. Commun*. **2012**, *48*, 4636.

5. **First example of a Cu(I)–(η^2-O,O)nitrite complex derived from Cu(II)–nitrosyl**

Kalita, A.; Kumar, P.; Deka, R. C.; Mondal, B. *Chem. Commun*. **2012**, *48*, 1251.

6. **Role of ligand to control the mechanism of nitric oxide reduction of copper(II) complexes and ligand nitrosation**

Kalita, A.; Kumar, P.; Deka, R. C.; Mondal, B. *Inorg. Chem.* **2011**, *50*, 11868.

7. **DNA binding and nuclease activity of copper(II) complexes of tridented type ligands**

Kumar, P.; Baidya, B.; Chaturvedi, S. K.; Khan, R.H.; Manna, D.; Mondal, B. *Inorg. Chim. Acta*. **2011**, *376*, 264.

8. **Fluorescence-based detection of nitric oxide in methanol and aqueous media using**

copper(II) complex.

Mondal, B.; Kumar, P.; Ghosh, P.; Kalita, A. *Chem. Commun.* **2011**, *47*, 2964.

9. **Reduction of copper(II) complexes of tridentate ligands by nitric oxide and fluorescent detection of NO in methanol and water media**

Kumar, P.; Kalita, A.; Mondal, B. *Dalton Trans*. **2011**, *40*, 8656.

10. **An asymmetric dinuclear copper(II) complex with phenoxo and acetate bridge: synthesis, structure and magnetic studies.**

Dutta, G.; Debnath, R. K.; Kalita, A.; Kumar, P.; Sarma, M.; Shankar, R. B.; Mondal, B. *Polyhedron*. **2011**, *30*, 293.

11. **Reduction of copper(II) complexes of tripodal ligands by nitric oxide and trinitrosation of the ligands.**

Sarma, M.; Kalita, A.; Kumar, P.; Singh, A.; Mondal, B. *J. Am. Chem. Soc*. **2010**, *132*, 7846.